Localization of the Mechanism of pH-Dependent Non-Photochemical Fluorescence Quenching in Thylakoid Membranes

by

Scott Christopher Wiebe, B.Sc. (Hon)
Department of Biological Sciences

Submitted to the Department of Biological Sciences
in partial fulfilment of the requirements for the degree of
Master of Science

Brock University
St. Catharines, Ontario

Table of Contents

Table of Figures

Figure L - Literature Review

Figure M - Materials and Methods

Figures 1-53 and Tables 1- 20 - Results

qE induction in thylakoids

PSII Absorption cross-sections

Acknowledgements

First of all, I would like to thank Prof. Doug Bruce for encouraging me to continue in research, at least for the time being. Being "chained to the lab" turned out to be a pretty good choice. Your faith in my scientific abilities and your encouragement, especially during the mysterious disappearance of all qE response, helped to motivate me. I am also thankful that you were around enough to at least attempt to solve my experimental problems despite your heavy involvement in NSERC committees, and that you got me involved in the conferences. Your clear interest in your students was much appreciated. Thank you for helping make my Brock experience as valuable as it was - I learned a lot. After all, I never would have learned to juggle if it hadn't been for you.

To Sergei I would like to say thanks for the immediate improvements in the quality of our lab that you brought with you. Your technical expertise and patient willingness to share that with me helped a great deal. Without you, the validity of our data, strange as it became at times, could not even be half of what it is now. I have enjoyed getting to know you in the last year-and-a-half.

Randy, you were also a large part of the last few years. Thank you for answering my persistent questions about theses in general, and for showing an interest in my work while valuing my opinions of your results at the same time. Reminiscing about the good old days, lab baseball, working on (or watching you and Sergei work on) small electronics projects, and general chatter also helped make my time in the lab enjoyable. Good luck with the teaching career.

I would like to thank Brock University, especially the Department of Biological Sciences, for running good Honours and Masters programs that allow students full access to research and to the expertise of the faculty, and the opportunity to get involved in teaching and lab demonstration. Brock and OGS also deserve thanks for the financial support that saw me through this degree.

Finally, a special acknowledgement goes out to my parents and to Heidi who encouraged and supported me for most of the past 3 years in the lab, while enduring the occasional lab-induced frustration. All of your belief in me was very important. Heidi, thank you for all the patience you could muster while I worked on trying to finish writing, no matter how many times I claimed I could be finished "in the next few weeks" or it seemed to you that I wasn't working hard enough. I'm finally finished.

Abstract

Higher plants have evolved a well-conserved set of photoprotective mechanisms, collectively designated Non-Photochemical Quenching of chlorophyll fluorescence (qN), to deal with the inhibitory absorption of excess light energy by the photosystems. Their main contribution originates from safe thermal deactivation of excited states promoted by a highly-energized thylakoid membrane, detected via lumen acidification. The precise origins of this energy- or ΔpH-dependent quenching (qE), arising from either decreased energy transfer efficiency in PSII antennae (eg Young & Frank, 1996; Gilmore & Yamamoto, 1992; Ruban et al., 1992), from alternative electron transfer pathways in PSII reaction centres (eg Schreiber & Neubauer, 1990; Thompson & Brudvig, 1988; Klimov et al., 1977), or from both (Wagner et al., 1996; Walters & Horton, 1993), are a source of considerable controversy. In this study, the origins of qE were investigated in spinach thylakoids using a combination of fluorescence spectroscopic techniques: Pulse Amplitude Modulated (PAM) fluorimetry, pump-probe fluorimetry for the measurement of PSII absorption cross-sections, and picosecond fluorescence decay curves fit to a kinetic model for PSII. Quenching by qE (~60% of maximal fluorescence, F_m) was light-induced in circulating samples and the resulting pH gradient maintained during a dark delay by the lumen-acidifying capabilities of thylakoid membrane H^+ ATPases. Results for qE were compared to those for the addition of a known antenna quencher, 5-hydroxy-1,4-naphthoquinone (5-OH-NQ), titrated to achieve the same degree of F_m quenching as for qE. Quenching of the minimal fluorescence yield, F_o, was clear (8 to 13%) during formation of qE, indicative of classical antenna quenching (Butler, 1984), although the degree was significantly less than that achieved by addition of 5-OH-NQ. Although qE induction resulted in an overall increase in absorption cross-section, unlike the decrease expected for antenna quenchers like the quinone, a larger increase in cross-section was observed when qE induction was attempted in thylakoids with collapsed pH gradients (uncoupled by nigericin), in the absence of xanthophyll cycle operation (inhibited by DTT), or in the absence of quenching (ΔpH not maintained in the dark due to omission of ATP). Fluorescence decay curves exhibited a similar disparity between qE-quenched and 5-OH-NQ-quenched thylakoids, although both sets

showed accelerated kinetics in the fastest decay components at both F_o and F_m. In addition, the kinetics of dark-adapted thylakoids were nearly identical to those in qE-quenched samples at F_o, both accelerated in comparison with thylakoids in which the redox poise of the Oxygen-Evolving Complex was randomized by exposure to low levels of background light (which allowed appropriate comparison with F_o yields from quenched samples). When modelled with the Reversible Radical Pair model for PSII (Schatz et al., 1988), quinone quenching could be sufficiently described by increasing only the rate constant for decay in the antenna (as in Vasil'ev et al., 1998), whereas modelling of data from qE-quenched thylakoids required changes in both the antenna rate constant and in rate constants for the reaction centre. The clear differences between qE and 5-OH-NQ quenching demonstrated that qE could not have its origins in the antenna alone, but is rather accompanied by reaction centre quenching. Defined mechanisms of reaction centre quenching are discussed, also in relation to the observed post-quenching depression in F_m associated with photoinhibition.

Introduction

Life on earth depends on photosynthesis for the fixation of light energy into the biosphere in the form of chemical food energy and for the release of oxygen. Plants must absorb light from the sun and convert it into the chemical energy of organic molecular bonds. However, because of its integration with other metabolic processes like carbon dioxide fixation, the light reactions of photosynthesis are subject to inhibition should those other processes become rate-limiting due to environmental conditions, such as nutrient limitations, drought, and extremes of temperature.

Inhibition can arise because absorption of light energy is effectively linear in the physiological range of light intensity, while use of that energy saturates at a finite rate. The surplus of energy becomes a potential source of damage to the plant, as it may form destructive oxidative molecules such as singlet oxygen and free. Oxidative molecules can degrade macromolecules of the photosynthetic apparatus in a process called photoinhibition. (Aro et al., 1993; Krause, 1988)

In order to avoid photoinhibition, plants must precisely regulate the safe dissipation of excess energy as heat. The photoprotective processes responsible are called non-photochemical quenching (qN) of excited states because they decrease excited state energy in competition with photochemistry (primary electron transport at Photosystem II). They promote the dissipation of energy through heat loss, also in competition with fluorescence, thereby quenching the yield of chlorophyll a fluorescence from PSII. (Briantais et al., 1986; Butler, 1984)

There are 3 components to photoprotective qN, distinguishable by differing sensitivity to uncoupling of electron transport from proton pumping, and by distinct timescales of onset and reversibility: qI, photoinhibition; qT, the state transitions; and qE, energy-dependent quenching. The latter is believed to be the largest component of qN. It is initiated by an increased size of the pH gradient across the thylakoid membrane compared to optimal, unquenched conditions (Krause & Behrend, 1986), resulting from reduced recycling rates of ADP and $NADP^+$ between the light and dark reactions, which 'energizes' the membrane. One hypothesis states that lumen acidification stimulates proton binding to LHCII proteins, triggering qE events (Horton et al., 1994).

Mechanisms proposed to account for this energy- or pH-dependent quenching involve either the PSII antenna complex, the PSII reaction centre, or a complex heterogeneous combination of the two. The location of the mechanism of qE within PSII is one of the major unresolved questions in photosynthesis research. Thus far, there is no unifying model of the location of qE.

One of the main concepts for reaction centre-based quenching is charge recombination, a reversal of electron transport from an electron acceptor back to $P680^+$. Low lumen pH inhibits the electron donor side of PSII, rendering long-lived charge-separated states when Q_A is reduced, allowing time for the electron to pass backward to $P680^+$ (Klimov et al., 1977). The redox potential of Q_A may also increase, conferring a smaller affinity for electrons and promoting charge recombination (Horton et al., 1994; Krieger et al., 1992), or a futile cycle in which an electron can be passed from the reduced quinone acceptor back to $P680^+$ through a special chlorophyll molecule (Chl_Z) or cytochrome b_{559} (Rees & Horton, 1990; Thompson & Brudvig, 1988). It has also been suggested that $P680^+$ may itself directly quench excited states (Bruce et al., 1997).

Mechanisms proposed for antenna quenching focus on the xanthophyll cycle (Young & Frank, 1996; Yamamoto & Mohanty, 1995;Crofts & Yerkes, 1994; Horton et al., 1994; Demmig-Adams & Adams, 1992) Considerable work has been completed on the xanthophyll cycle, a light-induced, pH gradient-dependent process that de-epoxidizes carotenoid. Two de-epoxidation reactions convert the carotenoid violaxanthin to zeaxanthin, which is more likely to directly thermally deactivate excited states and release heat (Gilmore et al., 1995). However, it has been shown that antenna qE may not be completely dependent on the de-epoxidation state of the xanthophyll cycle (Horton & Ruban, 1995). Instead, it has been proposed that zeaxanthin is a promoter of chlorophyll-binding protein aggregations that decrease the efficiency of energy transfer in the antenna. Zeaxanthin-mediated antenna protein aggregations would alter the spectral overlap of energy-transferring chlorophyll molecules, decreasing the energy transfer efficiency in the antenna. (Härtel et al., 1996; Ruban et al., 1994, 1995, 1997; Mullineaux et al., 1993).

Does pH-dependent fluorescence quenching (qE) occur in the antenna or in the reaction centre, or both? Can the contribution of each mechanism be quantified?

The main focus of this research project is to localize the mechanism of pH-dependent fluorescence quenching in spinach thylakoids. The most common method to identify the presence of qE in either location is to observe the yields of minimum fluorescence (F_o) and maximum fluorescence (F_m). Quenching in both the reaction centre and in the antenna is accompanied by a quenching of F_m, but only quenching in the antenna decreases F_o and the absorption cross-section of PSII. Many previous studies have included analysis of fluorescence parameters and have inferred cross-section changes from measures of F_o. In this study, direct measurement of PSII absorption cross-sections are combined with detailed kinetic modelling of picosecond fluorescence decays from an ideal, well-characterized qE preparation in spinach thylakoids to localize the mechanism of qE. By comparison with a less-detailed kinetic study (Wagner et al., 1996) and with a model for antenna quenching (5-OH-NQ, Vasil'ev et al., 1998), qE is clearly defined as a heterogeneous combination of both antenna- and reaction centre-based mechanisms.

Literature Review

Life on earth depends on the process of oxygenic photosynthesis. Without it most of the light energy received from the sun would be remitted as waste heat. Oxygenic photosynthesis is important both because it yields oxygen for release to the biosphere and because it absorbs and successfully incorporates incoming light energy into the chemical bonds of organic molecules. The oxygen is breathed in by respiratory organisms and the organic molecules are made available for consumption by heterotrophic organisms, subsequently passing through the food web. This chemical energy can then be used to power cellular processes in the plant and in the higher-order organisms which consume it. (Taiz & Zeiger, 1991; Zubay, 1993)

Oxygenic photosynthesis takes place in many algal species and in green plants. The occurrences of this process in algae and green plants follow the same general scheme and with the same reduced chemical equation:

$$CO_2 + H_2O \xrightarrow{\text{Light}} (CH_2O) + O_2$$

where CH_2O represents a carbohydrate molecule. However, in higher plants it occurs in a specialized organelle called a chloroplast, on both sides of an inner membrane termed the thylakoid membrane (see Figure L1). The thylakoid membrane, existing in both stacked (grana) and unstacked (lamella) structures, contains all of the molecular machinery required to trap light energy and to accomplish the initial reactions that fix the energy into the chemical bonds of ATP and NADPH. These primary reactions are designated the light reactions, because of their dependence on incident light. Further integration of this chemical energy into carbohydrate molecules is achieved by enzymatic reactions in the stroma surrounding the thylakoid membrane. These are called the dark reactions, including carbon dioxide fixation, because they do not directly require the input of light energy. The dark reactions form a basic point of metabolic integration with other biochemical pathways in the plant, since their products, simple carbohydrates, are used elsewhere for production of energy or other macromolecules. (Taiz & Zeiger, 1991; Zubay, 1993)

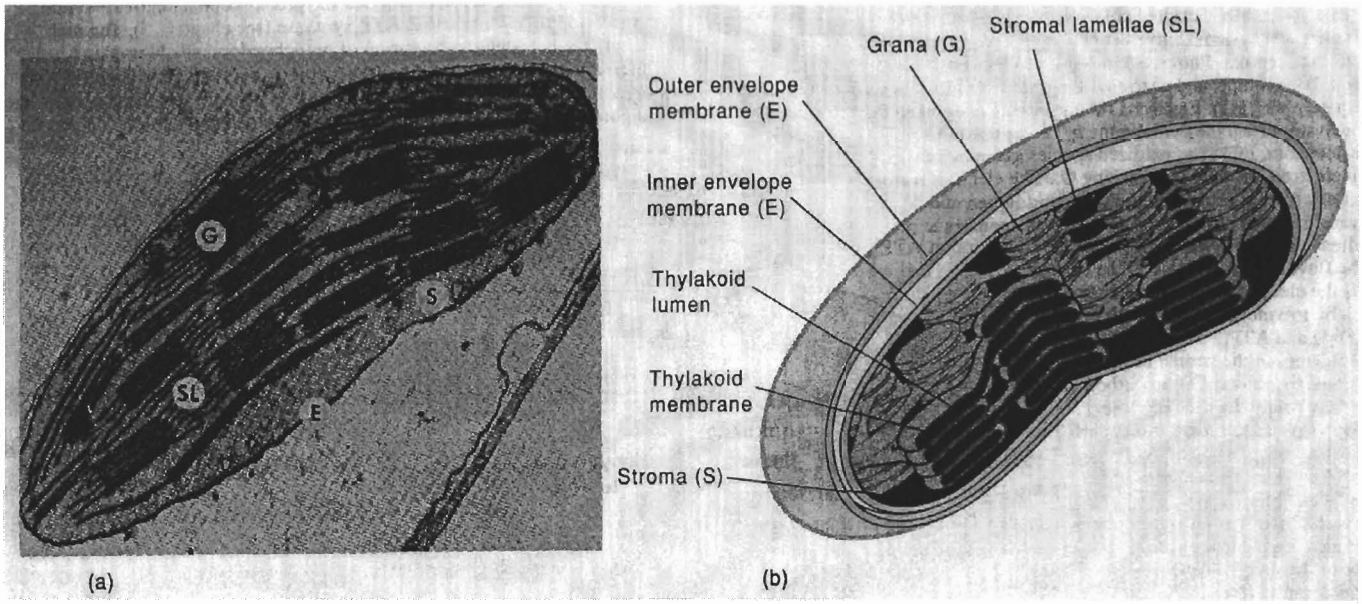

Figure L1: Electron micrograph and schematic drawing of the photosynthetic organelle of green plant leaf cells, the chloroplast. Note the stacked (grana) and unstacked (lamellae) regions of the innermost membrane, the thylakoid membrane, on which all of the light reactions take place. The dark reactions occur within the stroma. (from Zubay, 1993)

The Light Reactions

The successful capture of light by plants takes advantage of the photo-sensitive reactivity of pigment molecules embedded in the thylakoid membrane. These "antenna" pigments are bound by chlorophyll-binding proteins (CPs) or light-harvesting complex proteins (LHCs) (Horton et al., 1994) in two photosystems that work in series along an electron transport chain. In higher plants, the main pigment is chlorophyll a with chlorophyll b and carotenoids acting as accessory pigments. (Taiz & Zeiger,1991; Zubay, 1993)

Incident light can be harvested by chlorophyll molecules because of their complex porphyrin ring structure. The Pi (π) electron orbitals of double bonds exist above and below the flat plane of the molecule and allow an incoming photon of light to excite them to an energy level exactly equal to the energy of the striking photon. This excited singlet state of chlorophyll is extremely short-lived, on the order of nanoseconds (10^{-9}sec), so its energy must be displaced upon the molecule's return to ground state. (Taiz & Zeiger, 1991)

There are five possible, competing fates of the excited singlet state, four of which are shown in Figure L2. The first three of these are waste processes that release energy back to the surroundings: heat loss, fluorescence, and intersystem crossing to the triplet state (Figure L4). Both heat loss and fluorescence, the emission of a photon of light, occur just nanoseconds after excitation so that for any process to successfully in use the energy before decay to the ground state, it must take place on a faster time scale. Intersystem crossing occurs when the singlet excited chlorophyll experiences a spin reversal, making the excited electron spin parallel to that of the ground state electron. This triplet state of chlorophyll has a relatively long lifetime compared to the singlet excited state, and may react with molecular oxygen to create the singlet state of oxygen, decaying the chlorophyll excited state back to ground.

One process that can make use of the excited state energy is the fourth fate of the excited state, the resonance energy transfer. Resonance energy transfer is the result of a close arrangement of chlorophyll molecules such that the energy lost from one pigment molecule is absorbed by an adjacent pigment molecule. This excitation transfer can pass excitons around the antenna bed of the photosystems on a

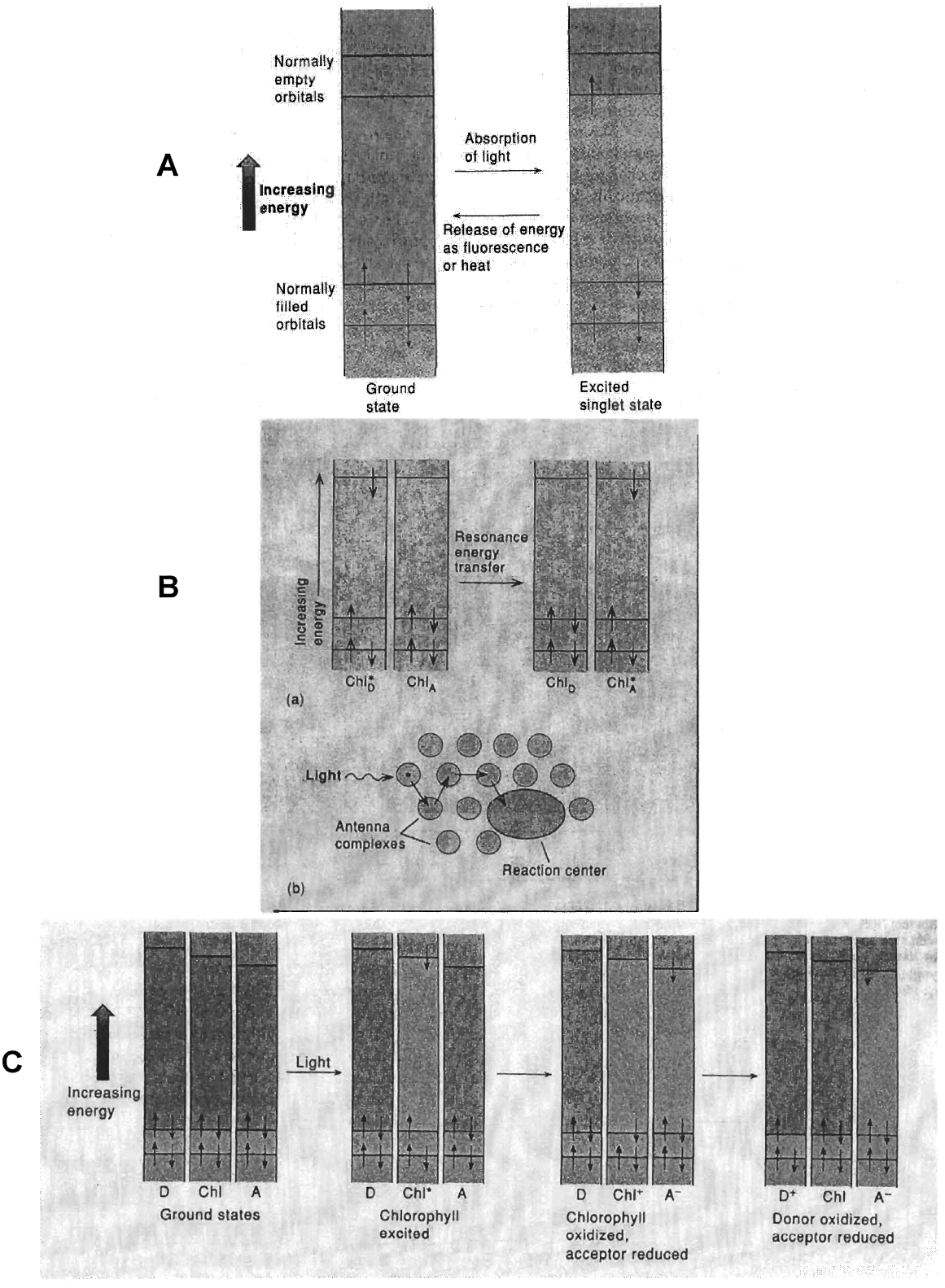

Figure L2: Four of the competing fates of the excited singlet state of antenna chlorophyll molecules. **A**; Waste processes of fluorescence and heat loss **B**; the resonance energy transfer responsible for passage of the excited state through the antenna **C**; photochemical electron transfer in the reaction centre, where D is the donor (Y_Z at PSII), A the acceptor (Pheophytin at PSII), and Chl the P680 chlorophyll molecule (special pair). (Zubay, 1993)

picosecond timescale (10^{-12}sec), potentially in the direction of the reaction centre. There can be hundreds of chlorophylls in the antenna complex, serving to increase the effective area for absorption of photons. (Alberts et al., 1989)

The final possible fate for the excited states occurs when the antenna complex chlorophylls pass the energy to the reaction centre. There, the "special pair" of chlorophylls (P680) can accept excitation by energy transfer. The excitation may be trapped by passing the excited electron to an acceptor molecule: in the case of Photosystem II (PSII, the first photosystem in the series of two), that acceptor is a chlorophyll analog without the central cation, called pheophytin. The loss of electrons by the reaction centre chlorophylls ($P680^+$) is subsequently alleviated by the donation of an electron from an adjacent donor molecule, a tyrosine residue within PSII. The chlorophyll is ready to be excited again. This productive use of the excited state is called photochemistry, or charge separation, and may also occur within a few picoseconds. (Alberts et al., 1989; Zubay, 1993)

The efficiency of light harvesting is due to the rapidity of energy transfer between adjacent chlorophyll pigment molecules in competition with decay processes. In fact, the efficiency of photochemical energy capture under optimum environmental conditions can be as much as 82-85% of the photon energy absorbed in the antenna. Therefore, decay of excited states accounts for just 15% of absorbed energy, in competition with photochemistry.

Representation of the electron transport process is given by the Z-scheme (Figure L3) Each participating molecule is assigned a redox potential, where molecules relatively low on the y-axis more readily accept electrons and those that are higher more readily donate electrons. The ultimate electron donor to PSII, or $P680^+$, is water, which is split by a membrane-bound enzyme yielding protons and oxygen. Electrons are made available to a manganese cluster and are passed via a tyrosine residue (Y_Z) to the $P680^+$. Upon excitation of P680, photochemical charge separation takes place to pheophytin, where the electron is passed along to the primary quinone acceptor, Q_A, also part of the PSII complex. A second quinone, plastoquinone (PQ), is mobile in the membrane. It accepts double reduction by electrons from Q_A and transports them to cytochrome b_6/f, carrying protons from the stroma and releasing them in the thylakoid lumen. Further transport brings electrons to PSI, where they are

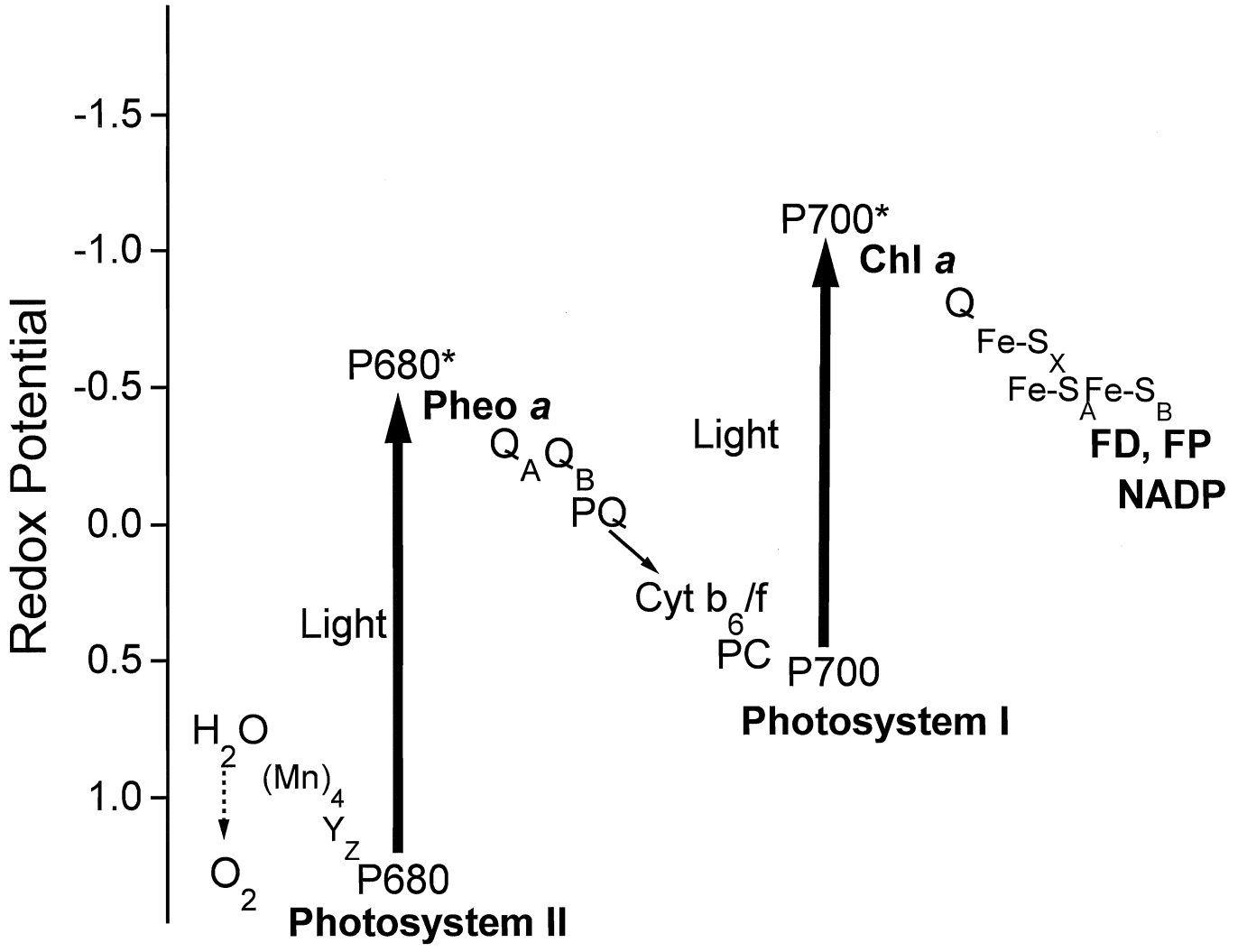

Figure L3: The Z-scheme of photosynthetic electron transfer. The x-axis represents the redox potential of the molecules involved, with more positive values indicating higher affinity for electrons. (redrawn from Zubay, 1993)

energized in the same manner as in PSII, transferring to the eventual acceptor, $NADP^+$. (Taiz & Zeiger, 1991; Zubay, 1993)

Energetically, proton translocation acidifies the lumen within the thylakoid and creates a gradient for the outward movement of protons, driving an ATP synthase located in the membrane. In addition, $NADP^+$ is reduced to NADPH. Both ATP and NADPH are used by the carbon dioxide fixation cycle (the "dark" reactions) to build the carbohydrates necessary for normal cell functioning. Recycling of the oxidized forms (ADP, P_i, $NADP^+$) of these molecules allows further production of ATP and NADPH by the photosynthetic light reactions. (Taiz & Zeiger, 1991; Zubay et al., 1993)

Chlorophyll a Fluorescence

Though fluorescence from chlorophyll molecules in the antenna is actually a waste product for the plant, it gives researchers a powerful and noninvasive assay for monitoring photosynthetic efficiency. At room temperature, the fluorescence yield from photosynthetic preparations is dominated by emissions from chlorophyll a of PSII, because PSII is significantly less efficient at trapping energy than PSI.

Briantais et al. (1986) submitted an explanation of the variability in chlorophyll fluorescence which makes it useful as a photosynthetic indicator. Light-induced photochemistry, or charge separation, occurs as follows at PSII:

$$Y_Z - P680 - Pheo - Q_A \xleftrightarrow{\text{Light}} Y_Z - P680^* - Pheo - Q_A \xleftrightarrow{\text{charge separation}}$$
$$Y_Z - P680^+ - Pheo^- - Q_A \xrightarrow[\text{charge stabilization}]{} Y_Z^+ - P680 - Pheo - Q_A^-$$

where Y_Z is the donor side tyrosine residue and the * designates an excited state (see also Reversible Radical Pair model, Figure L7). The final state in this scheme is relatively long-lived with reduced Q_A awaiting oxidation by a mobile PQ molecule. At saturation of electron flow, further excitation of P680 chlorophyll will not result in electron transport because reduced Q_A cannot accept another electron. Reoxidation of the PQ pool is a rate-limiting factor - a saturated pool of reduced PQ has a decreased rate at which it can re-oxidize Q_A. Excess excitation energy trapped at the

reaction centre in the presence of Q_A^- will decay to the ground state either as fluorescence after returning the excited state to the antenna (note the equilibria indicated in the above equation) where it has further chance to decay (Lee et al., 1992). There will be a proportional rise in the fluorescence yield. In fact, any process which affects the rate of photosynthesis will be detected as an change in the fluorescence emission of the system. Photosynthetic performance can thus be monitored with the use of fluorescence emission.

Fluorescence parameters resulting from the above property can be defined. The first is the minimal fluorescence yield, F_o. This is the dark-adapted state where all reaction centres are "open" (Q_A oxidized, ready to accept an electron). It is the fluorescence yield emitted without the input of actinic light. Maximum fluorescence, F_m, is the yield when all reaction centres are "closed" (Q_A reduced, electron transport minimal). In this situation, all excitation results in non-photochemical decay of the excited states and fluorescence emission reaches its maximum. Variable fluorescence, F_v, is equal to the difference between F_m and F_o, corresponding to varying proportions of trap closure within the population of PSIIs. Two ratios are also important. F_v/F_o is a measure of the activity of the particular preparation employed in an experiment, while F_v/F_m can be used as an estimation of the quantum yield of photochemistry (the fraction of energy trapped by the antenna that successfully induces photochemistry). (Briantais et al., 1986; Krause, 1988)

Fluorescence Quenching

Any process that potentially decreases the fluorescence yield of a system is said to "quench" the fluorescence. In PSII, fluorescence yield remains less than 5% of the absorbed photon energy because of the high efficiency of successful induction of photochemistry. For this reason, charge separation and subsequent stabilization is said to photochemically quench fluorescence. The resulting term is Photochemical Quenching (qP) of chlorophyll fluorescence.

There are other processes that compete with qP to dissipate energy that are not photochemical. The broad category of Non-photochemical Quenching (qN) generally refers to energetic loss that depletes excited state energy but is not the result of normal photochemical electron transfer and subsequent transport. Even

under optimum conditions, some heat loss competes with fluorescence, thereby acting as a non-photochemical quencher.

Processes of qN are also associated with photoprotective mechanisms in the plant because light is a major stress factor that can cause a loss in productivity. Light energy absorption by chlorophyll pigments in the photosystem antennae occurs linearly with light incident intensity even up to extremely high photon fluxes. But at the same time, utilization of that energy by the photosynthetic apparatus is finite due to electron transport and enzymatic reaction rates, even at optimum efficiency. The rate of use is easily saturated. Thus there exists an excess of absorbed light energy which can be a source of harm for the plant. To compound the problem, the metabolic integration of photosynthesis makes it susceptible to environmental conditions. If stresses like water depletion, low carbon dioxide concentration, or other limiting conditions for coordinated pathways decrease the photosynthetic rate, there is an even greater excess of energy absorption and a greater risk of photodamage to the plant. It becomes a problem for the plant to seek a balance between capturing energy for conversion to chemical potential, and minimizing the risk of photodamage.

Non-Photochemical Quenching (qN)

Non-photochemical quenching comes to the rescue. Plants have evolved photoprotective mechanisms, that are well-conserved across plant species, which allow safe dissipation of the excess energy as heat. Since such mechanisms increase heat emission in competition with photochemistry, they contribute to qN (energy quenching), quenching fluorescence emissions in the process. Precise sensing and dissipation of the imbalance of energy must ensue, effectively depleting only that fraction of energy that is in excess of photosynthetic capacity.

Recently, substantial research has gone into revealing the processes of qN that contribute to the safe dissipation of energy in green plants and many algae. The focus has exposed three main categories of qN, distinguishable by different time-scales of onset and recovery, and by differential sensitivity to uncouplers:

1- qI, photoinhibitory - response time in minutes, relaxation time in hours

2- qT, state transitions - response and relaxation time in minutes

3- qE, high-energy or pH-dependent - response and relaxation time in seconds

qI - Photoinhibitory qN

Photoinhibition is the realization of damaging effects from the absorption of excess energy by plant cells. Under conditions of excess light intensity it may dominate qN, but even under very low light conditions qI can become quite dominant should other environmental stresses decrease photosynthetic activity (Huner et al., 1991). Photoinhibition falls under qN because the damage it does to the photosynthetic apparatus results in a decrease in fluorescence that accompanies a reduction in the quantum yield of photochemistry, although it is reversible if it is not allowed to proceed too far (Huner et al., 1991). There are 2 components to qI: 1 - oxidative damage to PSII, and 2 - a slowly-relaxing, photoprotective, pH-independent component, part of which involves the recycling and *de novo* synthesis of damaged PSII proteins.

The cause of photoinhibition is the production of strong oxidizing agents resulting from a surplus of excited states. Allowed to linger, the chlorophyll singlet excited state may experience a spin reversal so that the electron spin of the excited electron is parallel with the spin of the ground state electron in its orbital. This is called the triplet state of chlorophyll, and it is relatively long-lived because of its inability to decay without undergoing reversal of the electronic spin again, which does not readily come about. Triplet state chlorophyll reacts with the triplet state of molecular oxygen to create the singlet state of oxygen (Figure L4). Singlet oxygen is an extremely reactive oxidant that may readily and irreversibly react with other molecules, thereby damaging the structural and functional integrity of important molecules like lipids and proteins on the thylakoid membrane.

There is controversy over the site of the damage within PSII. It may originate with either acceptor-side or donor-side inhibition, and either with or without subsequent degradation of the 32-kDa D1 protein of PSII (Kyle, 1987). The D1 protein binds PQ to PSII for electron transport. Others think that the D1 protein is destroyed and that there is a great turnover of that protein.

Demeter et al. (1987) reported an impairment in the amplitude of absorbance changes at 685 nm under photoinhibitory conditions. These changes reflect a decrease in the extent of photoreduction of pheophytin. Their interpretation was that the primary site of photoinhibition is in the vicinity of the radical pair within the PSII

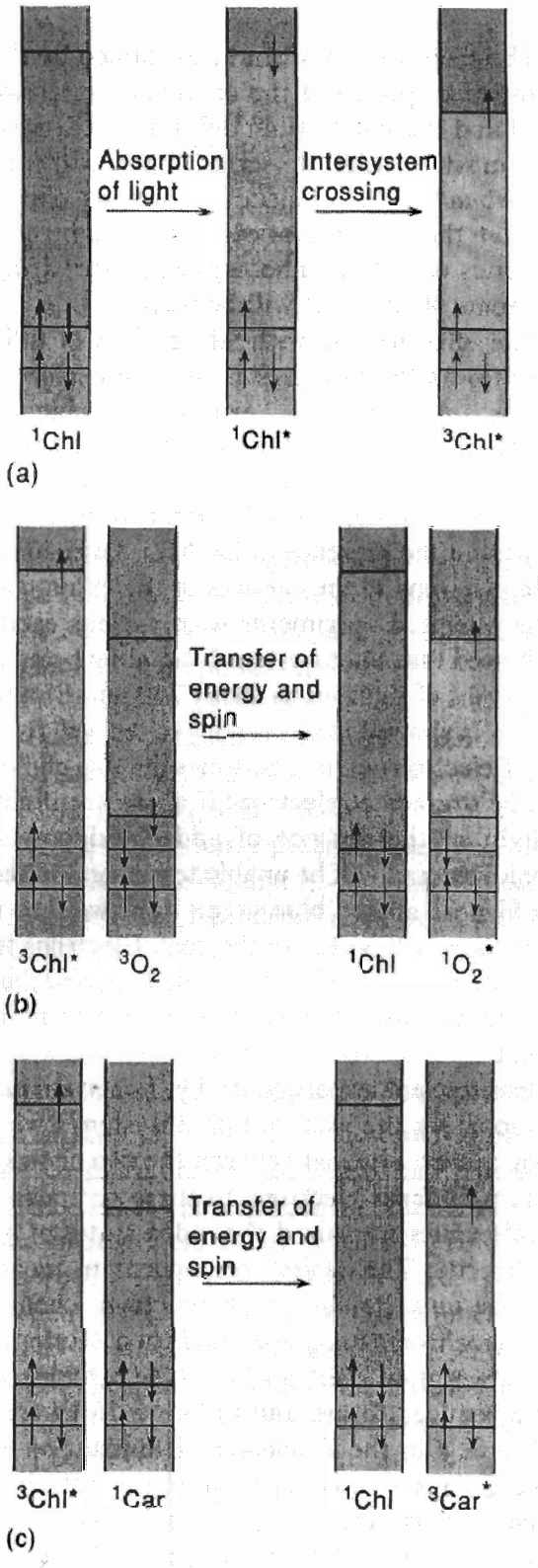

Figure L4: The singlet oxygen scavenging ability of antenna carotenoids. Triplet chlorophylls formed in the antenna by intersystem crossing during excess illumination can transfer their excited state to triplet oxygen, forming the singlet oxygen state, a destructive molecule. The carotenoids can accept this transfer of energy as well, decaying either triplet chlorophyll or singlet oxygen to their respective ground states, expelling the exciton harmlessly through loss of heat.

reaction centre, and was not due to protein destruction.

The other position is held by Aro et al. (1993). They implied that the toxic oxygen species irreversibly oxidizes and degrades the D1 protein. They contend that inhibition of electron transport is due to the inability to bind PQ and pass the electrons to it. Aro and co-workers have also seen *de novo* synthesis of the D1 protein that can promote recovery from photo-induced PSII protein damage. It is the fact that the rate of repair is slower than the rate of damage that aggravates the pathway, and they propose that other qN responses act to decrease the rate of damage so that D1 repair can overtake it. Anderson and Aro (1994) further supported this hypothesis when they investigated PSII movements under prolonged inhibitory light conditions. They observed an accumulation of inhibited PSII in the stacked region of the thylakoid where D1 degradation and turnover is limited by structural constraints. This may confer protection on the functional PSII centres, decreasing the rate of damage.

Besides synthesis of new polypeptides, other indirect ways to deal with photoinhibition by the singlet oxygen species involve oxygen scavengers that could potentially steal away the excited state. One example of a scavenger is carotenoid molecules in the antenna bed, whose excited state energy level lies below triplet chlorophyll and singlet oxygen (Figure L4). This allows carotenoids to be elevated to their excited states without generating singlet oxygen. Thus, they may quench excitation from chlorophyll or from oxygen before it begins to degrade proteins (Huner et al., 1991). Chlorophyll or oxygen harmlessly decay to the ground state, while the carotenoid does the same with a release of heat.

However, limiting the production of destructive species would be a much more efficient method of stopping photoinhibition. It was observed by Kyle (1987) that photoinhibition was often preceded by more readily reversible forms of quenching that helped protect against it. This is the proposed role of the other 2 components of qN, the state transitions, qT, and energy-dependent quenching, qE.

qT - State Transitions

The state transition, qT, is another non-photochemical quenching strategy implemented by plants to promote the safe dissipation of energy from PSII. State transitions involve a phosphorylation-induced redistribution of portions of the LHCII antenna between the stacked and unstacked regions of the thylakoid membrane. This physical displacement of PSII antenna chlorophylls facilitates complementary increases in apparent antenna size of PSI particles. There is still some debate about whether this indicates an actual binding of the phosphorylated LHCIIs to the PSI antenna or whether it entails spillover of energy to the PSI particle through connectivity. In either case, the effect is to decrease the energy absorbed by PSII.

In general, the state transitions are the result of preferential excitation of one of the photosystems. The probable sensing point for the state transitions is the plastoquinone pool that acts as a shuttle of electrons between the photosystems. Upon excessive reduction of the PQ pool (rate of reduction by PSII > rate of oxidation by PSI), the activity of a protein kinase attached to the cytochrome b_6/f complex is enhanced (Frank & Trebst, 1995). Frid et al. (1992) were able to show that various substituted quinones (PQ analogs) bound to the cytochrome complex and altered its interaction with the kinase, such that phosphorylation events were inhibited. It is suggested that the PQ binding domain at the cytochrome may change conformation depending upon the redox state of PQ, thereby activating the kinase system which eventually phosphorylates the LHCII proteins (Bracht & Trebst, 1994). Phosphorylated LHCII particles have less affinity for PSII and the granal regions than for the stromal regions and PSI.

McCormac et al. (1994) have recently demonstrated strong support for the state transitions using 77K fluorescence methods. Complementary changes in emission bands from the photosystems showed that LHCII undergoes phosphorylation and can then migrate between the photosystems. A sequence of events can be deduced in which the phosphorylated LHCII species appears first in the PSII-enriched granal regions of the thylakoid, prior to its appearance in the PSI-enriched stromal regions. This group confirmed the role of phosphorylation to the complementary state shifts by blocking dephosphorylation with NaF. Without dephosphorylation, the state 2 to state 1 transition could not proceed. In addition,

they used a LHCII-kinase deactivator, DCMU, to block the original phosphorylation responsible for the transition from state 1 to state 2.

The state transitions are convincingly verified in work done by Samson and Bruce (1995). Complementary changes in absorption cross-section were observed through modulated fluorescence, picosecond fluorescence decay, photoacoustic experiments, and pump-probe techniques. In studies involving magnesium depletion, which increases the amount of membrane destacking in the marginal region between the grana and lamellae, Samson and Bruce showed that the probability of energy donation by PSII to PSI also increased. It appeared that LHCII migrates from the granal to the less stacked outer regions of the grana where it meets the lamellae. Here, LHCII particles may be able to interact with PSI in either a physical manner or by spillover of excitation energy to PSI antenna chlorophylls.

Though it is quite well elucidated, qT is a minor quenching mechanism compared to the third component of qN, which can operate down to submicrosecond time scales (Krause & Behrend, 1986). This form of qN is called qE.

qE - High energy-dependent Quenching

Energy-dependent, or ΔpH-dependent, quenching (qE) is the form of qN believed to be dominant in the plant system (Horton et al., 1994). Its precise method of induction is based upon the extent to which the thylakoid membrane is energized for ATP synthesis. What this entails is tight feedback regulation of the excess energy through dissipative processes correlated with the light-induced chemiosmotic pH gradient across the thylakoid membrane.

This is a logical recognition point because of the integration of common intermediates between the light reactions and other metabolic processes. Intermediates of special importance here are ATP and NADPH formed by the light reactions. If the rates of absorption of light energy and the ensuing production of ATP and NADPH are greater than the capacity of other processes like the dark reactions to utilize these valuable products, then their oxidized forms will not be returned fast enough to reform ATP and NADPH. This results in reduced effectiveness of the ATPase to make use of the pH gradient. Protons will not diffuse energetically downhill through the coupled ATPases because little ADP and inorganic phosphate

is available for ATP synthesis. Therefore, the pH continues to decrease in the lumen as it is acidified by electron transport-coupled proton pumping. An relative increase in the pH gradient compared to conditions of optimum energy use is the starting point for qE.

Linearity of the relationship between qE quenching and pH was demonstrated by Krause and Behrend (1986). Acidification of the lumen was shown to correlate directly with the thermal deactivation of excited states in the photosynthetic apparatus. They further showed that under photoinhibitory light conditions with limiting carbon dioxide concentrations (dark reaction slows and delays ADP, $NADP^+$ recycling), the high pH gradient allowed quenching of excited state energy, decreasing the contribution of photoinhibition in the sample. A second approach by the same group used the uncoupler nigericin to disintegrate the pH gradient while being subjected to light. The result was a significant increase in photoinhibition compared to chloroplasts with an intact pH gradient.

Mechanistically, the increase in lumen acidification invokes a response through proton binding somewhere in the membrane. Evidence in support of this comes from Horton et al. (1994) who subjected the thylakoid membrane to DCCD, a strong binder of aspartate and glutamate residues. Upon its addition, qE formation was blocked because DCCD bound in positions on LHCII proteins where protons would normally bind under qE-eliciting conditions.

Sites of protonation aside, the actual location of qE effects is a topic of considerable controversy. Some researchers believe it occurs in the reaction centre of PSII while others maintain that its primary effects are in the antenna system. While heterogeneous redundancy of qE mechanisms is almost sure to exist depending upon phenotypic and genotypic factors of different species, localization has become a major source of debate.

Reaction Centre qE

Existence of quenching activity in the reaction centre was already hypothesized in the 1970s. Wraight et al. (1972) observed that extremes of pH caused the inhibition of photochemistry and induction of heat-releasing qN processes. Since low pH inhibits the water-splitting enzyme and thus the electron flow from water through

PSII, a reaction centre mechanism was submitted. Weis and Berry (1987) also hypothesized an inactive, dissipative form of the reaction centre in the presence of low pH.

In terms of the mechanism for reaction centre energy dissipation, Klimov et al. (1977) observed photoaccumulation of reduced pheophytin based on its absorbance pattern when Q_A is reduced to Q_A^-. From this relatively long-lived state ($P680^+$-$Pheo^-$) came the concept of charge recombination. Charge recombination occurs when the electron is passed backward from the unstable radical pair, from either pheophytin or from the long-lived reduced Q_A, to the special pair of chlorophylls (P680). Recombination of the electron to P680 is believed to accomplish one of two things: either to re-excite the special pair but lose the energy to the antenna where it can be safely dissipated; or else the transfer to P680 allows decay directly to the ground state, the energy lost as heat (Schreiber & Neubauer, 1990). (Figure L5)

Another piece of evidence for the reaction centre charge recombination mechanism of qE is given by Krieger et al. (1992). Looking at the kinetics of fluorescence relaxation they noted that a 2 ns component, associated with the reduction of Q_A, was significantly quenched. Moreover, that fluorescence component could be recovered using an electron donor, indicating a role for inactive water-splitting reactions in the reaction centre. The fact that $P680^+$ must then be a longer lived species permits its re-reduction by the reduced quinone acceptor, also oxidizing the quinone and opening the reaction centre.

A model of the low lumen pH requirement for qE, as related to a reaction centre mechanism, has been proposed (Horton et al., 1994; Pospíšil, 1997). In this model, acidification of the lumen accommodates the release of bound calcium. The freed Ca^{2+} ions inhibit the donor side by preventing the Mn cluster from moving to higher S-states of electron transfer. Inhibited electron donation induces conditions that are suitable for alternative pathways of $P680^+$ reduction, since the lifetime of the oxidized $P680^+$ is greatly increased. Ca^{2+} also shifts the redox potential of the acceptor side Q_A (Krieger et al., 1995). An increase in the redox potential of Q_A confers a smaller probability of electron transfer to Q_B (Andréasson et al., 1995), promoting accumulation of the radical pairs, $P680^+Pheo^-$ and $P680^+Q_A^-$, and dramatically increasing the probability of charge recombination back to $P680^+$.

Further evidence in support of a reaction centre charge recombination or cycling of electrons came from Rees and Horton (1990). They found discrepancies between their experimentation with fluorescence quenching and the expected quantum yield predicted by the models set forth by Butler (1984). The fluorescence emission was less than expected from an antenna-based fluorescence quenching. Therefore they suggested that a non-radiative dissipation of energy in the reaction centre should account for this disparity.

What they consequently set forth was a cycling of electrons including the constituents of the PSII reaction centre. They also showed evidence of rapid P680 reduction by adjacent chlorophylls, lending support for a futile cycle in which an electron can be passed from the reduced quinone acceptor back to P680 through a special chlorophyll molecule (Chl_Z). The role of the accessory Chl_Z in this cyclic electron transport was also demonstrated by Buser et al. (1992). This sort of heat-releasing cycle could also operate through the cytochrome b_{559} of the reaction centre. It has been shown that $P680^+$ can be reduced by cytochrome b_{559} when it is converted to a low potential form of about 60 mV (Misuzawa et al., 1995), which is low enough to accept an electron from pheophytin or quinone (Barber & De Las Rivas, 1993; Thompson & Brudvig, 1988). The reduced cytochrome could then donate the electron to $P680^+$ via the tyrosine Y_Z (Falkowski et al., 1986), or via the accessory Chl_Z (Buser et al., 1992). Fluorescence would be quenched because Q_A remains oxidized by the passage of the extraneous electron, not allowing the system to get backed up there (Krause & Behrend, 1986). However, the turnover times for Chl_Z and cytochrome b_{559} are on the order of seconds, much too slow to account for the quenching under most circumstances.

However, some evidence reported by Krieger et al. (1992) could not be fully explained by reaction centre qE. Apparent decreases in F_o normally associated with affected antennae were more consistent with quenching within the antenna complex.

Antenna Complex qE

It is possible to distinguish between fluorescence quenching occurring in the reaction centre versus that occurring in the antenna. Theoretically, the most direct way to do so is to observe the F_o and F_m values stimulated in the system being

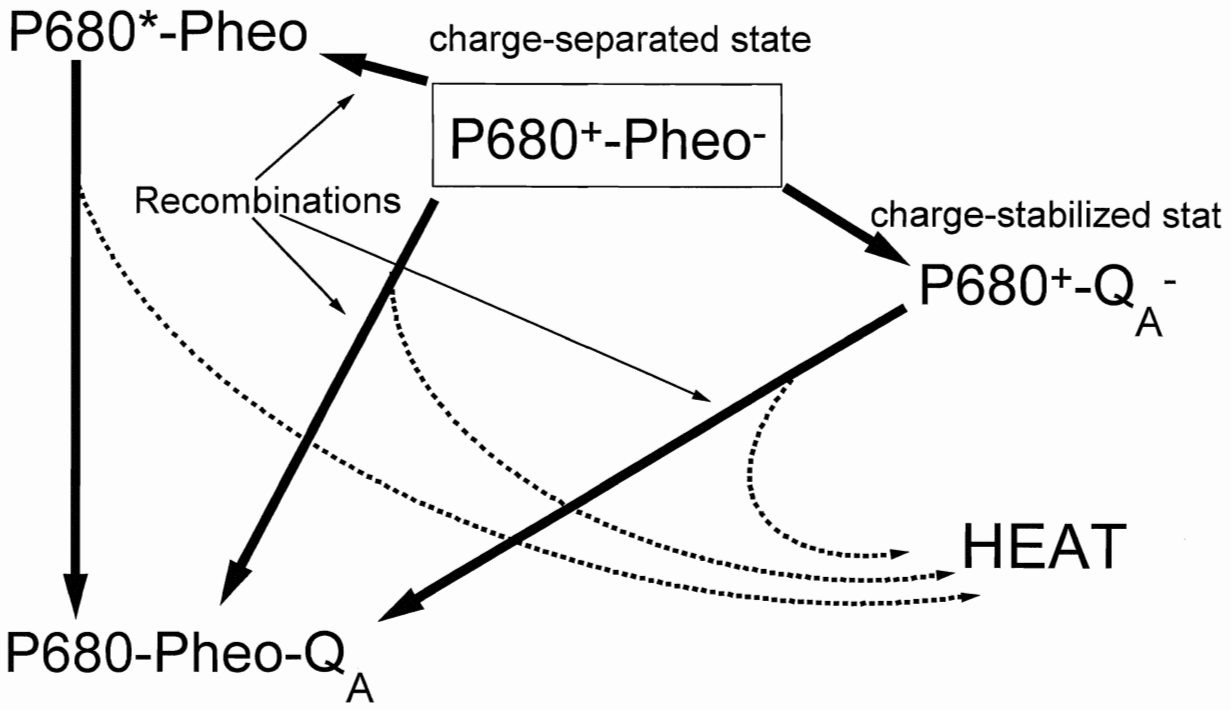

Figure L5: The charge recombination reactions proposed to elicit non-photochemical quenching in thylakoid membranes. The charge-separated state formed in the boxed arrangement allows for a back transfer of charge to $P680^+$ or for the normal charge stabilization through the reduction of Q_A. From any of these states, P680 may be re-excited or simply re-reduced, simultaneously losing the energy of excitation as heat. Note that should these recombination reactions ever become a dominant force, productive passage of an electron to PQ would be significantly reduced, even under optimum photosynthetic conditions.

studied. As related by Butler (1984) and Krause (1988), an indication of either location of qN can be observed in quenching of F_m and of the quantum yield of photochemistry, expressed by the ratio F_v/F_m. However, F_o occurs in the absence of photochemical activity in the reaction centre, as a function of fluorescence given off in the antenna. Thus, a depression in the value of F_o upon non-photochemical quenching can only be the result of quenching in the antenna. Related to this effect, quenching within the antenna bed would also dampen the effective absorption cross-section, as excited states are dissipated prior to trapping by the reaction centre (Horton & Ruban, 1994). Antenna quenching thus renders some portion of the antenna's light-capturing activity useless. Reaction centre quenching does not effect the excited state transfer within the antenna and so could not decrease the effective area of photon absorption (Bruce et al., 1997; Samson & Bruce, 1996; Horton & Ruban, 1994).

Different time scales of heat release are also predicted by the two locations of qE quenching. Even the fastest component of heat release by the reaction centre would be beyond 10 μs after light-induced qE, with the bulk occurring on the order of 100 to 200 μs after excitation. This accounts for the time it requires to transfer energy through the antenna to the centre and then for the charge separation reactions to take place. Antenna quenching, on the other hand, should release heat on the order of a few hundred picoseconds, closer to the time scale of energy transfer through the antenna. Mullineaux et al. (1994) used Laser-induced Optoacoustic Spectroscopy (LIOAS) to measure the qE-induced heat release, as sensed by piezoelectric transducers. Their work indicated that all of the heat release associated with qE was complete within 1.4 μs, leading them to propose that quenching occurred in the antenna and did not involve charge recombination. However, they could not demonstrate that the qN they observed accounted for all of the quenching in their samples. It could have been only a small portion of the quenching.

Specific mechanisms proposed to account for antenna quenching include the xanthophyll cycle and LHCII antenna protein aggregations. The xanthophyll cycle operates to form zeaxanthin, which may either deactivate excitons directly or may facilitate the aggregation of the LHCII proteins, forming quenching complexes that increase the probability of thermal deactivation of excited states. A third alternative

was proposed by Delrieu (1998), who reported a 2-fold decrease in absorption cross-sections during exposure to photoinhibitory light, suggested to be the result of monomerization of PSII dimers, which could be restored after removal of the light.

By far the most studied mechanism of antenna non-photochemical quenching is the xanthophyll cycle. Xanthophylls are part of the carotenoid family of accessory antenna pigments. Many carotenoids are very efficient at light harvesting and successful resonant energy transfer in the antenna (Young & Frank, 1996). In addition to this light-harvesting function, they may also be effective at scavenging the energy from the triplet excited state of chlorophyll or from destructive active radicals like the singlet oxygen species (Krause, 1988) (Figure L4). A second photoprotective role for the carotenoid family comes from the xanthophyll cycle, which uses the enzyme Violaxanthin De-epoxidase to convert violaxanthin into zeaxanthin through a 2-step de-epoxidation reaction via the intermediate xanthophyll, antheraxanthin.

The xanthophyll cycle has been extensively shown to exist in higher plants (Niyogi et al., 1998; Verhoeven et al., 1997;Johnson et al., 1993a,b), while a parallel cycle has also been shown in diatoms to act as a dissipative qN mechanism (Olaizda et al., 1994). Johnson et al. (1993a,b) demonstrated that the capacity for qN was strongly correlated with shade or open field tolerance in British plant species. Sun-adapted plants had much higher levels of zeaxanthin as a percent of the total xanthophyll cycle pigments and showed a greater capacity for qN. In addition, nitrogen-stressed spinach plants exhibited a higher capacity for qN owing to a higher de-epoxidation state (DEPS = (Zeaxanthin + 0.5Antheraxanthin)/(Zeaxanthin + Antheraxanthin + Violaxanthin)) in high light conditions. Mutants deficient in a structural gene for violaxanthin de-epoxidase (VDE) in both *Arabidopsis* leaves and in single-celled *Chlamydomonas* accomplished very little qE and possessed greater sensitivity to photoinhibition due to their inability to produce zeaxanthin (Niyogi et al., 1998, 1997). Similarly, Niyogi et al. (1998, 1997) found that mutants that could not accomplish epoxidation, but instead accumulated zeaxanthin constitutively, displayed accelerated kinetics of qE formation, although the extent of qE was not altered. The xanthophyll cycle appears to be a conserved photoprotective mechanism in the plant kingdom.

The xanthophyll cycle's dependence on the pH gradient was demonstrated in

experiments by Yamamoto and Mohanty (1995), who subjected thylakoids to dibucaine. The resulting inhibition of the pH gradient inhibited zeaxanthin formation and thus its ability to contribute to qN effects. Under pre-illumination conditions, the concentrations of zeaxanthin and antheraxanthin increased compared to the condition without pre-illumination, which had an elevated concentration of violaxanthin. The pre-illuminated thylakoids were able to quench further in the presence of a pH gradient than thylakoids without pre-illumination, indicating the necessity for the de-epoxidized forms of the xanthophylls and a low pH. Delayed fluorescence decays established that not only was energy quenching manifested in the fastest decay times indicating antenna quenching, but also that the absence of a pH gradient (in the presence of DCMU) yielded the same kinetics as in thylakoids in the absence of zeaxanthin (presence of DTT) (Terjung & Maier, 1998). This work pointed to an obligatory role for pH and zeaxanthin in qE. The pH optimum for VDE activity has been determined to be 5.2 in spinach enzyme, while also requiring ascorbate as a co-factor, and experiencing strong inhibition by the sulfhydryl reductant, Dithiothreitol (DTT) (Havir et al., 1997). (see Figure L6)

De-epoxidation of violaxanthin to zeaxanthin may facilitate fluorescence quenching due to differential abilities to accept singlet energy transfer from chlorophyll and then to transfer it back to antenna chlorophylls. Young and Frank (1996) estimated the lowest excited singlet states (S_1) of the xanthophylls and determined that this level is lower in chlorophyll *a* than for violaxanthin, but higher in chlorophyll than in zeaxanthin. Zeaxanthin contains more conjugated double bonds which serves to decrease the energy of its S_1 excited state. Energetically, this low energy state makes it possible for zeaxanthin to accept energy transfer and quench chlorophyll singlet excited states, but relinquishes its ability to pass it along, instead thermally de-activating the excitation. Violaxanthin, on the other hand, has a higher energy excited state than the chlorophyll S_1, allowing transfer, making violaxanthin only good for light harvesting function. They also demonstrated direct quenching of chlorophyll excitons by zeaxanthin in organic solvents. However, there is still no direct, *in vivo* evidence of this "Molecular Gear Shift" model, the thermal deactivation by zeaxanthin - although there is also no evidence that direct thermal deactivation does not occur.

Reactions of this cycle have been observed by various other research groups

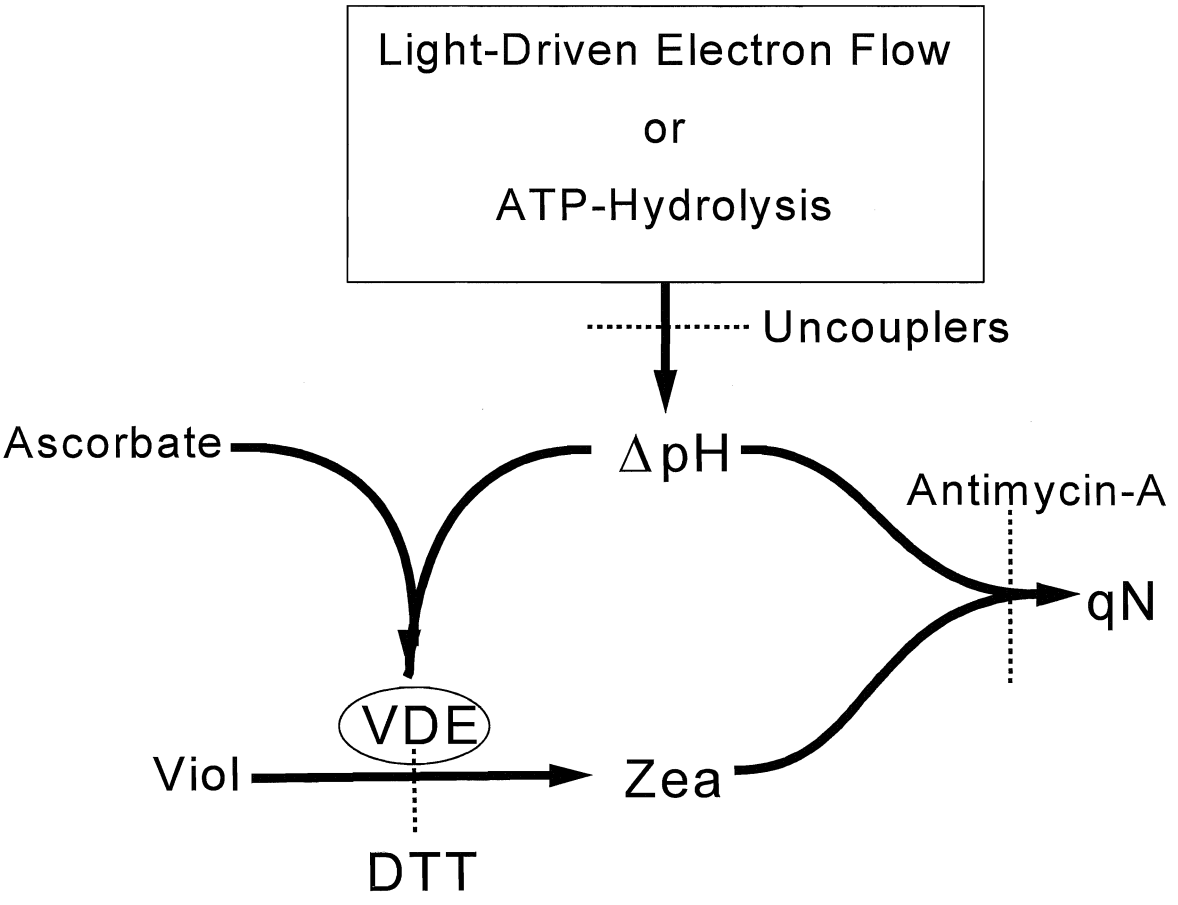

Figure L6: Schematic of zeaxanthin-dependent non-photochemical quenching. Low lumen pH and ascorbate are required for activation of the violaxanthin de-epoxidase enzyme (VDE), which converts violaxanthin to zeaxanthin. Zeaxanthin, along with another pH-dependent factor, contribute to induction of non-photochemical quenching. DTT inhibits zeaxanthin formation, while Antimycin-A and uncouplers such as nigericin or dibucaine can inhibit qE formation. Zeaxanthin formation is not reversed by uncouplers, in contrast with qE itself. Note that some quenching may form in the absence of zeaxanthin formation, so long as a pH gradient is generated (from Gilmore & Yamamoto, 1992)

(Demmig-Adams & Adams, 1992; Horton & Ruban, 1995). Some evidence has shown, however, that quenching in the antenna can still be observed without initiation of the xanthophyll cycle (Figure L6) (Niyogi et al., 1998; Wagner et al., 1996; Young & Frank, 1996; Horton & Ruban, 1995). First, quenching by xanthophylls is not inhibited at low temperatures, indicating a non-collisional, non-diffusion effect attributed to a 'quenching complex' (Gilmore et al., 1995). Second, some zeaxanthin-independent, DTT-insensitive quenching is also often observed, although at least one group has explained this by constitutive presence of zeaxanthin in the LHCII proteins (Gilmore, 1997). Third, inhibition by antimycin A occurs without inhibiting either formation of a ΔpH or zeaxanthin formation, so the relationship is not so simple. In fact, generation of a ΔpH has faster kinetics than the formation of qE, even in the presence of pre-formed zeaxanthin, providing a lag time during which some critical change occurs in the system (Gilmore & Yamamoto, 1992). Finally, Hurry et al. (1997) reported that leaves from abscisic acid mutants of *Arabidopsis*, which cannot synthesize any xanthophylls except zeaxanthin, and therefore accumulate the latter, were sensitized to qE, but did not accomplish a greater overall degree of quenching with respect to wild-type leaves. So although a correlation has been found for qE and the xanthophyll cycle over a wide range of environmental conditions, it is still unknown whether qE is the direct or indirect result of zeaxanthin formation.

What has been deduced from observations like these is a mechanism that controls LHCII protein aggregation and structure within the antenna, the "Allosteric LHCII" model. Such an aggregation could alter the interactions between excited state pigments. If this is not in fact the direct result of deactivation by zeaxanthin, the xanthophylls could have a promotional role in the physical aggregation of the protein complexes. (see Figure L7)

Spectral analyses performed on the antenna complex and its constituents illustrate the connection between qE and LHCII aggregation. Ruban et al. (1992) explored absorbance spectra of systems undergoing qE and compared them to LHCII aggregate absorbance spectra. They were remarkably similar. When antimycin A, a compound believed to inhibit aggregation, was added, formation of qE was also inhibited. Thylakoid conformation-specific light-scattering effects observed at 535 nm were suggested to originate in this aggregation of proteins (Ruban et al., 1993).

Ruban and Horton (1994) also contributed 77K fluorescence emission spectra comparing photochemical fluorescence quenching versus non-photochemical fluorescence quenching. qP had an emission peak at 688 nm while qN had peaks at 683 nm and 698 nm. Differences indicate that qN does not have reaction centre-like emission, supporting antenna quenching. Most importantly, though, was the observation that qN spectra closely resembled those of an aggregated LHCII isolated from leaves with an enhanced emission peak at 700 nm. Ruban et al. (1995) added Resonance Raman Spectroscopy of LHCII which showed structural changes upon formation of qE, accompanied by conformational alterations in the carotenoid population and hydrogen-bonding interactions of the chlorophyll a population.

Picosecond time-resolved fluorescence emission studies performed with spinach LHCII particles (Mullineaux et al., 1993) exposed decay lifetimes in LHCII trimers of 4 ns, while decay lifetimes of LHCII in the aggregated state were about 100 ps. This evidence shows that a highly efficient energy dissipater is formed upon LHCII aggregation, independent of the violaxanthin-to-zeaxanthin ratio. This group suggested that creation of red-shifted non-fluorescent chlorophyll species in this state explains the quenching of fluorescence by qE. In particular, four red-shifted chlorophyll species were later identified, with dramatically-accelerated fluorescence decay kinetics belonging to the longest wavelength species (Vasil'ev et al., 1997). It was proposed that each chlorophyll species is associated with aggregates possessing different qE quenching properties. Similar pronounced aggregations were observed in the 700 nm 77K fluorescence emission band in tobacco LHCIIs stressed by CO_2 deficit and in tobacco LHCIIs aggregated due to exposure to high light stress (Šiffel & Vàcha, 1998).

Independence of the protein aggregations from the zeaxanthin concentration suggested by Mullineaux et al. (1993) is disputed by data to the contrary from Gilmore et al. (1995). Increased de-epoxidation increased the energy dissipation centred around a 0.4 ns lifetime proposed to represent a fast, dissipative quenching complex. Further evidence of xanthophyll cycle-dependent aggregations came from kinetic studies (Härtel et al., 1996) in which LHC proteins known to harbor de-epoxidase activity could only aggregate upon accumulation of zeaxanthin. Zeaxanthin was not sufficient to elicit the response, but was required, implying that a major proportion of

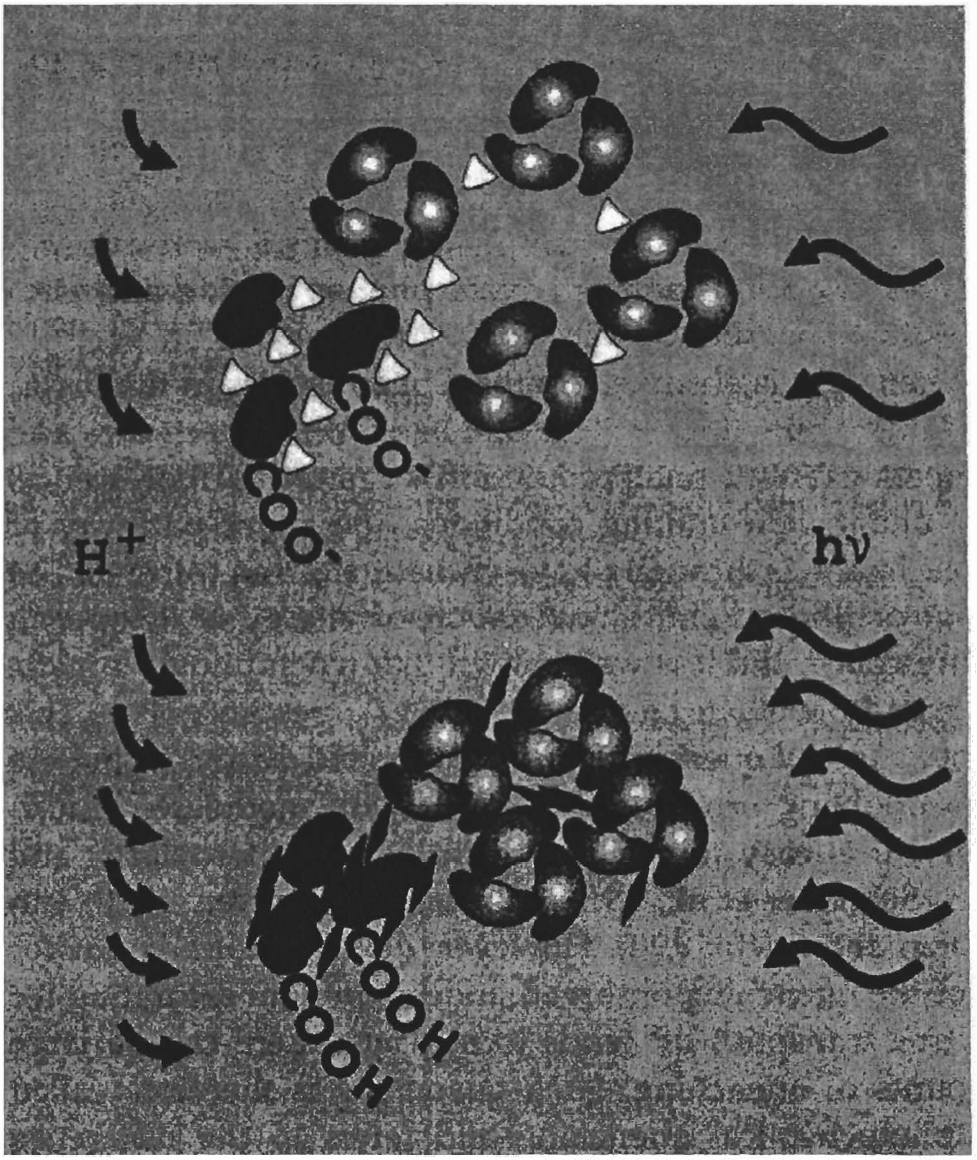

Figure L7: Schematic representation of the xanthophyll cycle and LHCII aggregations. The excess of incident light causes the qE response, allowing protons to induce the structural changes envisaged by LHCII aggregations by protonation of the LHCII carboxylate residues. These have been called "quenching centres", where fluorescence is quenched (represented by the darker shade of the quenched portion of the model). Note here that the xanthophylls are triangles in the top state (violaxanthin), flattened in the bottom state (zeaxanthin). The LHCIIs are the kidney-shaped bodies. (from Horton et al., 1994)

qE is the result of zeaxanthin-mediated LHCII aggregations.

What precisely is the role that zeaxanthin plays in LHCII aggregations? In its absence, some groups have reported formation of qE, so it is not the sole driving force. However, it must play a role as an activator (Young & Frank, 1996). Experiments have illustrated that qE quenching occurred at a lower ΔpH in the presence of zeaxanthin than in its absence (Young et al., 1997), inferring a possible role for zeaxanthin in stimulation of protein aggregations. Zeaxanthin has been shown to stimulate formation of LHCIIb aggregates on sucrose gradients, with little or no difference in quenching ability from aggregates that contained no xanthophylls. This indicated a lack of direct quenching by the zeaxanthin apart from its aggregating influence (Ruban et al., 1997). Additionally, Ruban et al. (1997) demonstrated an 'anti-quenching' effect of adding violaxanthin. Violaxanthin inhibited aggregation and elevated fluorescence yield, probably stabilizing the LHCs in their photosynthetically competent state. The effect of the xanthophylls thus appears to involve finetuning the degree of quenching by increasing or decreasing the de-epoxidation state, indirectly quenching fluorescence through allosteric mediation of protein aggregations.

There is evidence that some portion of the effect of the xanthophyll cycle is independent of S_1 energies and direct de-excitation, yet there remains some debate about whether zeaxanthin amplifies the quenching in this way (Young et al., 1997). In fact, some groups (Gilmore, 1997; Pospíšil, 1997) believe that quenching associated with aggregations have the opposite causality: that pH gradient-induced structural aggregations in the LHCs strengthen energetic associations between chlorophyll and zeaxanthin by activating binding sites for zeaxanthin, allowing direct singlet-singlet energy transfer and quenching. However, aggregation-mediated direct thermal deactivation by zeaxanthin cannot account for most of the data to the contrary already described.

Localization of the pH-dependent aggregation site has been narrowed down to the minor chlorophyll-protein complexes of the peripheral antenna, since xanthophylls have not been identified in the PSII core antenna complex. Specifically, binding of DCCD at proton-binding residues of CP29, CP26, and CP24 (LHCIIa, LHCIIc, and LHCIId, respectively) inhibited qE responsiveness and inferred pH sensitivity in these proteins (Bassi et al., 1997; Walters et al., 1994). In light of the

fact that relatively high xanthophyll concentrations have been found in these proteins, and that xanthophylls in these proteins are readily de-epoxidized, it could be concluded that aggregation originates with them. However, while the highest ratios of xanthophyll-to-chlorophyll are located there, the lowest occurs in LHCIIb (Crofts & Yerkes,1994; Young et al., 1997), but only in unquenched samples. Färber et al. (1997) and Gilmore (1997) demonstrated that de-epoxidation of the xanthophylls substantially strengthens their interaction with LHCIIb subcomplexes. Zeaxanthin may be formed by de-epoxidation in the former LHCs, thereby increasing its affinity for LHCIIb, where it initiates the quenching-induced aggregations.

Heterogeneous qE

While considerable evidence has been collected to support both reaction centre and antenna-based quenching mechanisms for pH-dependent non-photochemical quenching, it is still unclear which mechanisms operate in *in vivo* systems. There is almost certain to be heterogeneity of photoprotective mechanisms in chloroplasts, depending upon various environmental and genetic factors. A complex mixture of processes is likely the source of qE.

Wagner et al. (1996) presented the results of a powerful approach to the investigation of heterogeneity in qE. From picosecond fluorescence decay kinetics, they modelled the qE responses in thylakoids using a global target fitting analysis. This analysis fit the decay data to a model for primary processes in PSII, the Reversible Radical Pair Model from Schatz et al. (1988) and Wasielewski et al. (1989) (Figure L8). The RRP model takes into account the equilibrium of the primary charge separation and the excited state of P680 which makes PSII 'trap-limited'. It also relates decay of fluorescence in the antenna complex and each of the PSII electron transport processes to rate constants (ns^{-1}). Wagner et al. (1996) applied this model to qE to determine which rate constants required changing to make the qE-quenched data fit best.

They attempted to separate the effects of zeaxanthin from the effect of the ΔpH. More generally, they showed that fluorescence lifetimes were markedly decreased at both F_m and F_o during formation of qE, while only F_m decreased when zeaxanthin formation was blocked with DTT. Zeaxanthin and a pH gradient were

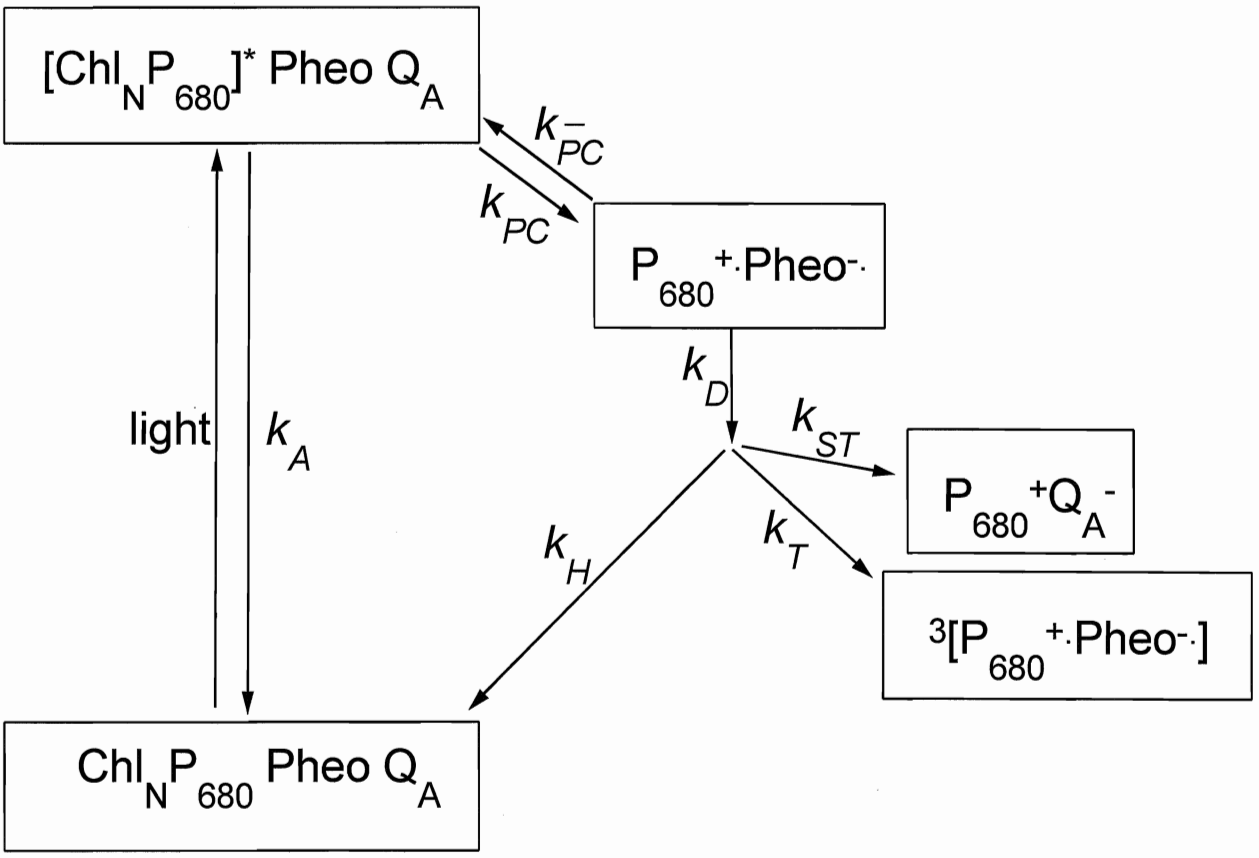

Figure L8: The Reversible Radical Pair Model for primary processes in PSII (Schatz et al., 1988; Wasielewski et al., 1989). $[Chl_N P_{680}]^*$ symbolizes the exciton equilibration among N antenna Chl molecules and P680. The rate constants describe excitation decay from the antenna (k_A), primary charge separation (k_{PC}), and its reversal (k_{PC}^-). Because this reversal is possible, the electron able to return an excited state to the antenna, it is considered a "trap-limited". The rate constant for decay of the primary radical pair (k_D) is the sum of the rate constants of charge stabilization by electron transfer from $Pheo^-$ to Q_A (k_{ST}), triplet formation (k_T), and heat loss (k_H).

clearly necessary for F_o-related antenna quenching. More importantly, there was a decrease in F_m in the absence of zeaxanthin that indicated a pH-dependent reaction centre-based fluorescence quenching. In terms of the kinetic model, they found that the best fits for the data involved increasing the rate constant for antenna decay (k_A) and that for the decay of the radical pair (k_D), the latter of which indicates enhanced recombination or cyclic electron transport in the reaction centre. Also, the quenching observed in the absence of zeaxanthin could only be modelled by an increase in k_D, with no changes in k_A. This work clearly demonstrated a separation of antenna and reaction centre quenching in the same sample.

Consideration of even more complex models is also reasonable. Partially because it is unknown whether quenching is delocalized (all PSIIs are quenched) or restricted to sites which have undergone a transition to a quenched state, 3- and 4-state models complete with complex forms of energetic connectivity and cooperativity cannot be ruled out. Figure L9 illustrates a few of the possibilities. Walters and Horton (1993) have concluded that a 2-state model best describes antenna quenching, in which there exists a decrease in connectivity between antennae, energetically isolating quenched centres from unquenched centres due to LHCII aggregations within the quenched centres. The present study will attempt to distinguish some of these heterogeneous mechanisms of qE, using a powerful combination of absorption cross-sections, picosecond decay kinetics, and kinetic modelling as previously performed (Wagner et al., 1996). This will be accomplished in an well-characterized, light-induced qE preparation in thylakoids, to be compared with strict antenna quenching given by 5-OH-NQ (Vasil'ev et al., 1998).

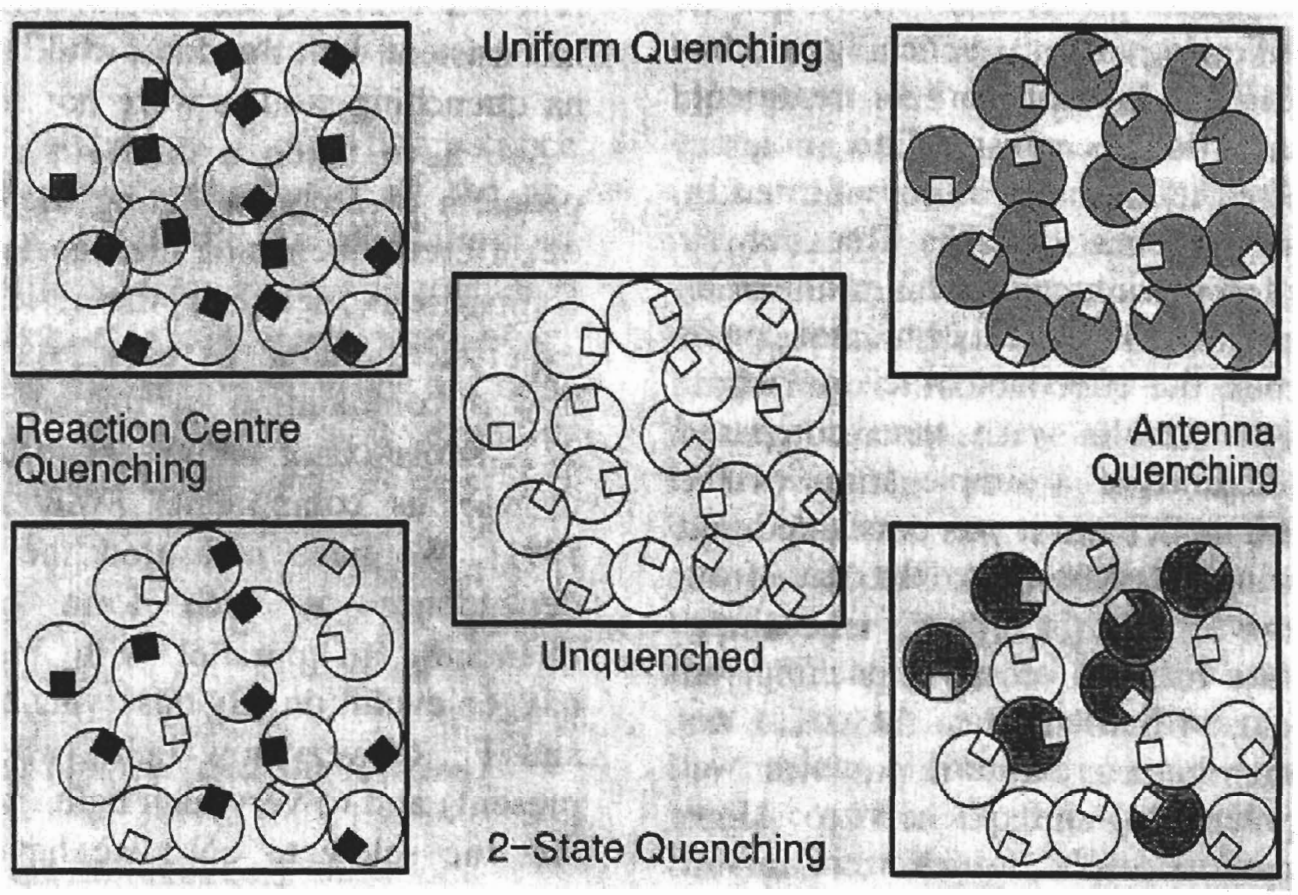

Figure L9: The alternative models for the localization of qE quenching. Panels each represent a set of PSII units on the thylakoid membrane. Antennae are shown as circles, with their associated reaction centres as squares. Shading shows the location of quenching, while its intensity indicates the extent of changes in thermal dissipation. Uniform quenching implies homogeneous populations that all react in the same way to quenching, while 2-state quenching implies only certain centres react to qE. (from Walters & Horton, 1993)

Materials and Methods

Solutions

Grinding Medium

NaCl	0.3 M
Tricine buffer, pH 7.8 KOH	30 mM
$MgCl_2$	3 mM
Na_2EDTA	0.5 mM
Ascorbic Acid	2 mM
Bovine Serum Albumin (BSA)	0.5 mg/ml

Thylakoid Resuspension Medium

D-Sorbitol	0.33 M
Hepes buffer, pH 7.8 KOH	10 mM
$MgCl_2$	15 mM
Ascorbic Acid	30 mM
BSA	0.5 mg/ml

Thylakoid Isolation

Thylakoids were isolated from fresh market spinach as previously described by Whitmarsh and Ort (1984) with minor modifications to preparation and suspension media (above). Fresh, fully developed, and undamaged spinach leaves were picked from the head, which was dark-adapted for 24 hours prior to isolation, and washed 3 times in double distilled water. The midribs were removed from the leaves, which were snipped into smaller pieces and loosely packed in a chilled blender (Osterizer) with cold grinding medium. Leaves were broken by 3- 1 second grinds on the highest setting. The resulting liquid was filtered through cheesecloth soaked in ice-cold double distilled water and divided equally between 4 to 6 250-ml centrifuge bottles in the dark on ice. These bottles were centrifuged at 4200 rpm for 2 minutes in a Beckman J-25 centrifuge. Supernatants were discarded, pellets were resuspended gently using a small paint brush in a few millilitres of resuspension medium, and were transferred to 4 to 6 centrifuge tubes. The tubes were filled with resuspension medium to balance and then centrifuged by accelerating to 4000 rpm and then stopping quickly with the brake. The supernatant was filtered through 2 layers of Kimwipes into centrifuge tubes. These suspensions, again balanced, were centrifuged for 3 min at 4000 rpm. Again the supernatant was discarded and the

pellets resuspended in resuspension medium. The tubes were filled and balanced again and centrifuged once more at 4000 rpm for 3 min, discarding the supernatant in between. The last time they were combined to give a high concentration thylakoid suspension, to be kept on ice and in the dark before use, or to be stored at -80°C with 20% glycerol.

Determination of Chlorophyll Concentration

Thylakoids were stirred carefully and 0.1 ml of the suspension was placed by Hamilton syringe into 80% acetone (by volume in water) and filled to 10 ml. After being shaken vigorously, the solution was poured through #1 Whatman filter paper into a 1 cm cuvette. Absorbance of the solution was determined by a Beckman 7400 Diode Array Spectrophotometer at 664 nm, 647 nm, and 700 nm, after blanking with a cuvette containing 80% acetone alone. The following equation was then employed to determine the concentration of chlorophyll in the dilution (Zeigler & Egle, 1965):

$$[\text{chl } \underline{a} + \underline{b}] = 0.793\ (A_{664}-A_{700}) + 1.953\ (A_{647}-A_{700}) \quad \text{(mM)}$$

Typical thylakoid isolations prepared to yield 60 to 80 ml of suspension contained 400 to 800 mM chlorophyll (~400-800 mg/L). Thylakoid preparations were removed from the freezer to thaw slowly on ice just before use. After gentle mixing by inversion, thylakoid suspension was diluted to 6 mM chlorophyll in resuspension medium, with 100 µM Methyl Viologen as an electron acceptor, for all following experiments. Other additions (DTT, ATP) were as noted in Results.

Quinone Recrystallization

About 50 ml of absolute ethanol were heated to 40°C over a low Bunsen burner flame and then about 0.5 g of quinone (5-hydroxy-1,4-naphthoquinone) crystal were added to saturation. The ethanol was heated further to 60°C before another saturating amount of quinone was added. The solution was allowed to cool slowly to -20°C by transition from room temperature to refrigerator to freezer. Crystals having formed in the flask, the mixture was poured through a cold Büchner funnel with a paper filter. The crystals were vacuum dried overnight. A 4 mM quinone solution was made by dissolution in absolute ethanol and was stored at 4°C.

Sample Circulation System

For experiments with circulating thylakoid samples, Masterflex pump controllers were used to pump 60 ml of thylakoid suspension through an illumination reservoir built in the lab. This reservoir consisted of Pyrex pipettes heated and drawn into short tubes (about 10 cm), and connected by short plastic tubing to achieve a flow-through effect for the chamber. From out of the chamber, sample ran through a dark delay period of 21 seconds before the tubing led into the detection portion of the cycle. Total time for an entire cycle was 90 seconds, about 60 of which were accounted for by the illumination reservoir (42 ml). This small version was used for PAM and pump-probe measurements (0.7 ml/sec pumping rate), while a larger version (360 ml) was used for picosecond decay collection so that samples could be pumped at faster (4.2 ml/sec) without losing the same proportions of dark and light periods in the full cycle.

Both variations of the reservoir were mounted on a 'stage' with a backdrop of reflective aluminum foil, and were covered with a black cloth so that only sample within the reservoirs was exposed to the qE-inducing actinic light source illuminating the reservoir. The smaller variant was illuminated with heat-filtered halogen light fitted with a red filter and a dispersion lens for uniform illumination of the sample area. The lamp was kept under black cardboard to reduce light leakage. For the picosecond kinetic version, uniform illumination was achieved with a slide projector, the qE-inducing red filter slid into the transparency projection slot. For S state randomization in both versions, the reservoir was masked with black cardboard except for a 5 to 8 second window allowing exposure to background light.

PAM Fluorimeter

Pulse Amplitude Modulated (PAM) fluorescence traces were obtained from a Model 101 PAM Chlorophyll Fluorimeter (Walz, Effeltrich, Germany). Fluorescence was excited by 1 µsec pulses from a light-emitting diode (655 nm excitation) at a frequency of 1.6 kHz, with an integrated intensity low enough to keep reaction centres open (F_o). (9-aa fluorescence detection utilized a 450 nm LED and 100 kHz frequency, with a filter combination described in Results.) White actinic illumination (>3000 µE/m^2/sec, 1 second duration) from a halogen lamp was triggered by the PAM-103 timer every 40 seconds to saturate reaction centres and induce F_m.

A right-angled excitation emission-detector-cuvette assembly was used that allowed sensitive measurements of fluorescence from relatively dilute thylakoid samples. This geometry allowed it to be connected to a variety of actinic light sources via fibre optics from different angles, for the application of different quenching conditions. To ensure accurate fluorescence measurements, the emitter was fitted with a 695 short-pass filter, while the detector photodiode was protected by a far-red cut-off filter (Schott RG 9, >710 nm). The modulated nature of the measuring beam allowed reliable detection of the signal against a background of continuous illumination.

All fluorescence signals were registered on a computer data collection system (Brock University Electronics Shop) that was also used for the collection of millisecond timescale decays after single and multiple turnover flashes.

Other Spectrophotometry

Other spectrophotometric assays were accomplished with various spectrophotometers and fluorimeters in the lab. As for the determination of chlorophyll concentration, the transmittance spectra and the effects of pH on 5-OH-NQ absorbance spectra were completed with a Beckman DU-7400 Diode Array Spectrophotometer. The absorbance changes ($\Delta A_{505/565}$) associated with zeaxanthin formation (Niyogi et al., 1998) were measured with a DW-2 UV/VIS spectrophotometer. Room temperature fluorescence spectra of chlorophyll were performed as previously described (McCormac et al., 1994) on a 77K spectrofluorimeter.

Determination of Relative PSII Absorption Cross-sections

The pump-probe method of fluorimetry was used in this study for the determination of relative absorption cross-sections of PSII, as previously described in Vasil'ev et al. (1998) (see Figure M1). Non-actinic probe pulses of light were supplied by low intensity light-emitting diodes (450 nm excitation) focussed onto a 1 mm capillary tube masked to expose a narrow band of detection for an optically-thin, circulated thylakoid sample. Fluorescence was measured from this narrow detection band (~ 3 mm) at 90° to the direction of the incident pump-and-probe flashes using

a fibre optic leading to a Hamamatsu RG967 photomultiplier tube protected with a 690 nm long pass filter. When fired at a dark-adapted sample of thylakoids, the value obtained from LED flashes alone represented F_o. When fired 100 µs after a 300 ps saturating actinic flash of light energy delivered by fibre optic cable from a Nitrogen-pumped dye laser (Photon Technologies International, GL-3300) set at 650 nm wavelength, the data generated represented F_{sat}. F_{sat} is the saturating level of fluorescence induced by a single-turnover pulse of light. It is different from F_m for reasons still under investigation (eg Vasil'ev & Bruce, 1998). Relative intensities of each pump laser flash were quantified from scattered light by a photodiode connected to a 9-Volt biassing battery. Data were collected by a Tectronics TD 540 digital storage oscilloscope and uploaded to a computer data collection program, which also triggered both the laser flashes and the probe LEDs via an adjustable trigger delay box built in the lab. Each data point consisted of an average of 10 signals at a flash frequency of 2 Hz. Flash saturation curves were acquired using various pump flash energies controlled by 2 graduated neutral density filters positioned in the path of the pump pulse.

Data Fitting

Origin 4.0, a commercial curve-fitting program, was used to plot the data obtained. Flash energies remained as relative light intensities. Data were fit with the cumulative Poisson single-hit probability distribution (as described by Mauzerall & Greenbaum, 1989):

$$\Phi(I) = \Phi_{max} (1 - e^{-I \times \sigma}) \quad ; \text{alternatively: } F(I) = F_o + F_m (1 - e^{-I \times \sigma})$$

where I is the flash intensity, $\Phi(I)$ is the yield of photoproduct measured (fluorescence), Φ_{max} is the maximum yield (F_m), and σ is the effective absorption cross-section ($Å^2$). This equation gives a single component sigmoidal fit for cross-section, representing a homogeneous population of photosystems ie the parameters generated can be applied to 100% of the photosystems in question.

Determination of Picosecond Fluorescence Lifetimes

A picosecond pulsed laser diode with single photon timing apparatus (Bruce & Miners, 1993; Vasil'ev & Bruce, 1998) (Figure M2) was employed to determine the picosecond fluorescence decay kinetics of the thylakoid preparation under various

quenched and unquenched states.

Excitation pulses were supplied at 667 nm by a Hamamatsu Picosecond Light Pulser (PLP-01) at 10 MHz with a pulse width of 60 ps. The laser output was polarized and 10% of the excitation pulse was reflected off a neutral density filter and focussed onto a fast avalanche photodiode used as the timing reference. Fluorescence emission was detected from the sample by a Hamamatsu R-2809 microchannel plate photomultiplier screened by a double monochromator at a 90° angle to the incident laser light, yielding an instrument response function (IRF) of about 70 ps. Instrument response functions (IRFs) were collected as background decay from cold, circulating sample at 667 nm. Pulses from the photomultiplier and the reference photodiode were input to two channels of a constant fraction discriminator. There, photomultiplier-detected, fluorescence-induced pulses were counted and timed in reverse timing mode to the stop signal from the timing reference photodiode. Data obtained represent the lifetime of the excited state within the photosynthetic apparatus before emission as a photon of light. Data was collected by a multichannel pulse height analyzer (Nucleus PCAII board) mounted in a personal computer.

Samples were circulated through a 360-ml illumination reservoir system (described above) with a flow speed of 4.2 ml/sec. For detection, the sample flowed through a laboratory built nozzle forming a 1 mm diameter jet used as the measurement area for detection of fluorescence. In the dark, this allowed the measurement of F_o with open reaction centres. The F_m state was achieved by illuminating the sample in a 2-ml pre-illumination chamber located just before the sample jet, exposing thylakoids to saturating light for about 400 ms just prior to measurement (<1 ms). The rate of sample flow through the jet ensured that the time delay between saturation and detection was less than 1 ms, an important point considering that no chemical modifying agents were used to stabilize the F_m state. In all experiments, the bulk of data collection was completed within 20 minutes of removal of samples from ice storage to avoid the effects of destabilization of thylakoid membranes over time.

Fluorescence decay data were collected for 8 detection wavelengths between 680 and 730 nm with 20 000 counts in the peak channel of 512, each representing

a certain length of time in picoseconds. Data were fit by modelling with a convolution of the IRF to a sum of 5 exponential decay components associated with different elements of the photosynthetic apparatus. Fluorescence decay curves from all detection wavelengths were fit simultaneously on an interactive program using global model functions: a sum of 5 exponential decay components or the Reversible Radical Pair model of PSII (Schatz et al., 1988). Complete programming information can be obtained from S. Vasil'ev.

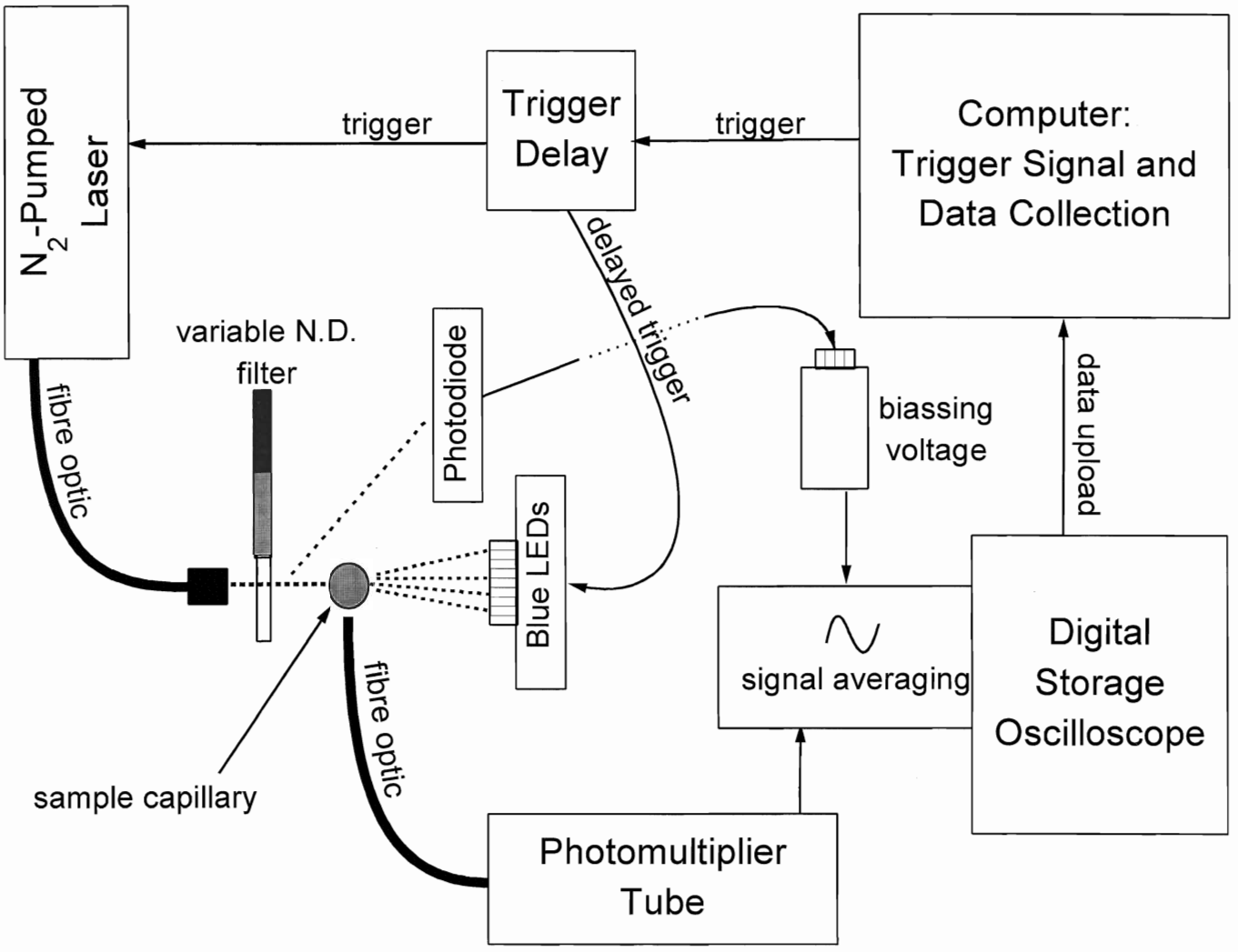

Figure M1: Schematic representation of the apparatus used to determine the optical cross-section of PSII. The 300 ps laser pulse was supplied by a Nitrogen-pumped dye laser. Relative light intensity of the pump pulses was measured from light scattered onto a photodiode connected to a 9-V battery for biassing voltage. Four blue LEDs (450 nm) focussed onto a narrow portion of the circulated sample, supplied as probe flashes, were triggered 100 µs after the laser pump flashes. Fluorescence was received by a second fibre optic cable leading to a photomultiplier tube. All data were collected on a digital oscilloscope and uploaded into a computer data collection program (Brock University Electronics Shop).

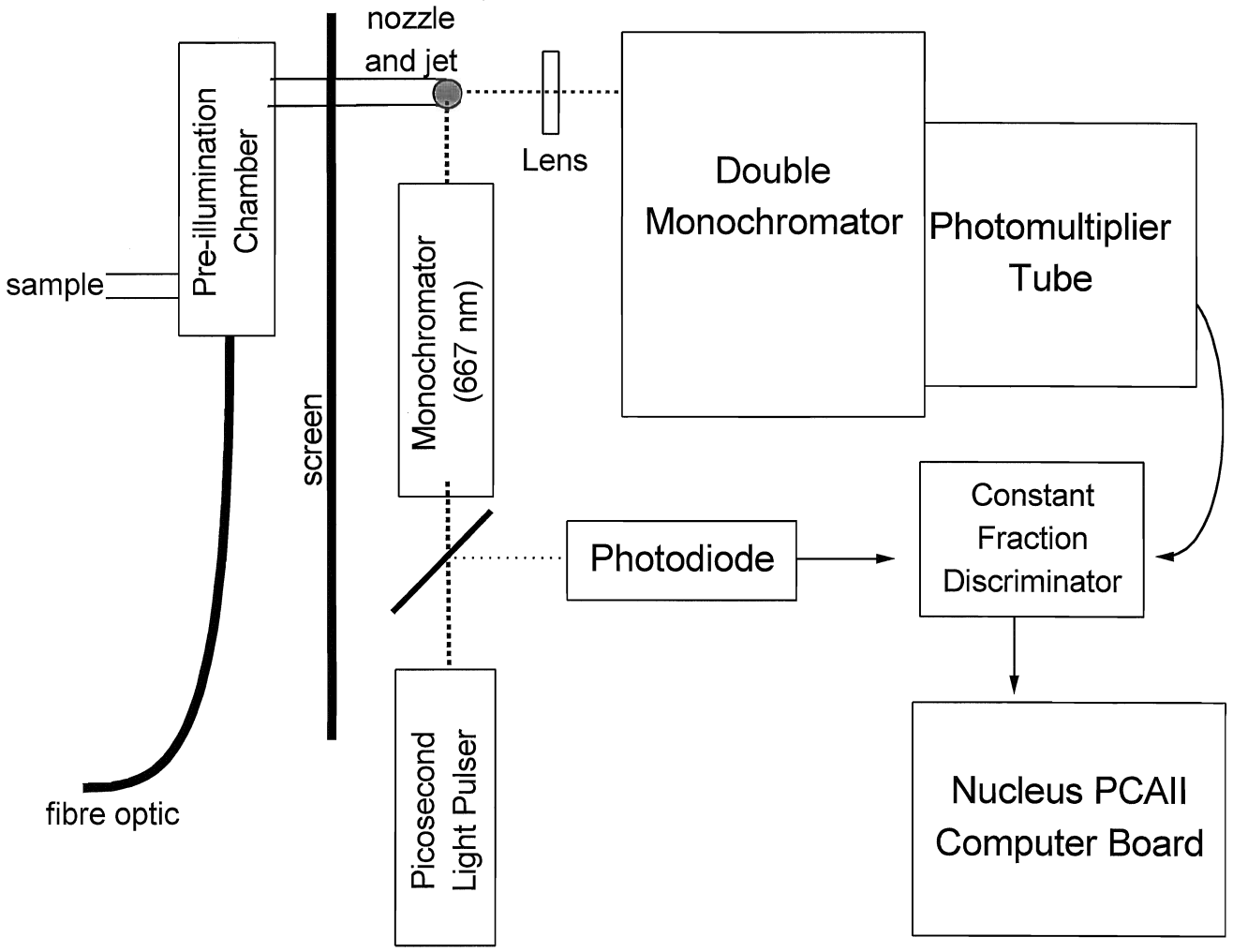

Figure M2: Schematic representation of the single photon timing apparatus used for the collection of picosecond fluorescence decays. A Picosecond Light Pulser laser operating at 10 MHz supplies excitation energy of 667 nm to a circulated thylakoid sample delivered by a nozzle that forms a 1 mm jet. A portion of the excitation pulse is deflected onto a fast avalanche photodiode used as the timing reference for comparison to photons of fluorescence detected by a photomultiplier protected by a double monochromator set alternatively at 8 detection wavelengths between 680 and 730 nm. After input into a constant fraction discriminator, signals are collected by a Nucleus PCAII board mounted in a personal computer. For measurements at F_m, thylakoids are exposed to saturating white light in the pre-illumination chamber, delivered via fibre optic cable from a halogen lamp.

Results

Results from the experiments performed are divided into 3 parts.

The first section, taking into account Figures 1 to 22 and Table 1, deals with the development and characterization of an appropriate protocol for the induction and measurement of pH-dependent quenching in isolated spinach thylakoids. It contains primarily pulse-amplitude modulated (PAM) fluorescence measurements in both centimetre cuvettes and in a pump-circulated, illumination reservoir system developed for this purpose. The 2 subsequent sections use the final form of this circulated qE preparation.

The second part contains data pertaining mainly to pump-probe fluorimetry used to measure effective absorption cross-sections (σ) of PSII under various quenched and unquenched conditions related to qE. Absorption cross-sections, a measure of the probability of photon capture and trapping by PSII, are valuable in ascertaining the involvement of PSII antenna processes in fluorescence quenching. This section encompasses Figures 23 to 36 and Tables 2 to 5.

The final part illustrates the results from picosecond time-resolved fluorescence decay kinetic experiments performed on spinach thylakoids in quenched and unquenched states at both F_o and F_m. Fluorescence decays are fit to a deconvolution of 5 components associated with different processes within the photosynthetic light reactions, especially at PSII. Kinetics are further modelled to an applicable model that contains 4 rate constants related to reversible charge separation and stabilization in PSII. This final section consists of Figures 37 to 53 and Tables 6 to 20.

qE Induction in Thylakoids

Figures 1 through 25 illustrate the development of a protocol for the induction of qE in isolated spinach thylakoid membranes at room temperature. Most of these measurements were completed using a PAM fluorimeter.

Figure 1 shows PAM traces of chlorophyll a fluorescence from thylakoids exposed to red actinic light for 10 minutes with a photon flux density of 200 $\mu E/m^2/sec$. The sample was placed in a 3 ml cuvette for these measurements. Fluorescence is normalized to the maximal pre-illumination fluorescence level, F_m, which is reached by the application of saturating flashes (>3000 $\mu E/m^2/sec$) for 1 second every 40 seconds, which results in full reduction of Q_A and therefore a lack of ability to do further photochemistry. The minimum fluorescence level, F_o, was measured between these flashes using only the application of the PAM fluorimeter's pulsed non-actinic measuring beam, operated at 1.6 kHz and 650 nm (both the excitation and detection sides were filtered accordingly, so that chlorophyll fluorescence and excitation wavelengths did not overlap). The F_o value was typically around 0.20 with F_m normalized to 1.0, giving the thylakoids an F_v/F_o ratio of 4.0 and a quantum yield, F_v/F_m, of 0.8. Both of these ratios indicate that the thylakoid preparations were healthy, despite storage at -80°C for up to 6 weeks after the isolation procedure was completed.

Treatment of thylakoids with actinic light caused dramatic quenching of F_m within a minute, levelling at approximately 37% of pre-illumination F_m. In Figure 1A, simple removal of the actinic light source was enough to release most of the fluorescence quenching. In Figure 1B, the uncoupler nigericin was used to dissipate the pH gradient that was formed by electron transport during light application, while the light source was still on. This was equally effective in relieving the quenching caused by the actinic light, indicating that not only was light required to drive the quenching, but that a pH gradient was also necessary, as is expected for qE quenching. Note that additions of ethanol alone did not change the fluorescence level either at F_m or during quenching (nigericin stock, 2 mg/ml in absolute ethanol added to a final ethanol content of <1%). The small change in fluorescence in Figure 2 upon the first addition of 1% ethanol was created by mistakenly bumping the cuvette with

the Hamilton syringe used to administer the ethanol. Ethanol is also important for Figures 33 to 35, since 5-OH-NQ is also dissolved in absolute ethanol.

Does the wavelength of light used to induce quenching affect the extent of quenching or the recovery of fluorescence from the quenched state? White light was not used because it was thought likely to cause more photoinhibition, and because red light might excite at PSI (>695 nm) more effectively, assisting the efficiency of electron transport. Three different red filters were used to investigate this question - long-pass filters with half-maximal transmittance at 600 nm, 630 nm, and 670 nm (Figure 3A). F_m quenching had an average magnitude of 67.2%, 66.3%, and 66.2% for these filters, respectively, after 10 minutes of light exposure (200 $\mu E/m^2/sec$) (Figure 3B). Though the 600 nm filter appears to quench more, it is doubtful that this difference was significant considering the standard deviations, which indicate a very reproducible degree of quenching in independent trials. Fluorescence recovery (Figure 3C) after removal of the quenching light showed that there was more efficient recovery of fluorescence following exposure to light at the longer 2 wavelengths, although statistically the difference is almost negligible. Nevertheless, the 630 nm long pass filter was chosen for all subsequent experiments due to its ability to saturate quenching and its maximized recovery of F_m. The 670 nm filter was ruled out because of its reduced transmittance of visible light (<700 nm). A maximum of intensity was important for producing enough light to uniformly illuminate the reservoir used during pump-circulated experiments.

The quenching that is demonstrated in Figures 1 and 2 is quite dramatic even though the quench-inducing light could have been 3 or 4 times more intense with the light source used. But how much light was required to saturate the quenching response? Figure 4A demonstrates that there is no significant difference in the extent of quenching beyond 200 $\mu E/m^2/sec$ (64%). By extrapolation of the data, saturation of quenching occurred beyond just 100 $\mu E/m^2/sec$ incident light. In fact, only 30 $\mu E/m^2/sec$ were required to elicit a significant amount of quenching in the sample. There is, however, a small amount of fluorescence loss without the addition of any light (0 $\mu E/m^2/sec$, 6.5% average loss) that must be related to thylakoid instability over time. This amount of fluorescence loss was typical over the course of 15-20 minutes after the thylakoid samples were removed from temporary storage on ice.

In terms of recovery from this saturated quenching of F_m, Figure 4B illustrates that lower light intensities allowed a higher degree of recovery than did intensities beyond about 150 $\mu E/m^2/sec$. However, this showed that there was a photon flux density dependence inherent in the portion of fluorescence not recovered, indicating a possible origin in photoinhibition.

Two immediate complications arose from the quenching seen in Figures 1 and 2. Most importantly, direct illumination of the cuvette sample elevated the base level of fluorescence beyond an actual measure of F_o, related to PSII trap closure due to Q_A reduction. The ability to measure F_o is essential to localization of fluorescence quenching to the antenna. The second complication was the incomplete post-illumination recovery of F_m, suggesting that there was still quenching of some type in the system, as has been observed many times before (eg Casper-Lindley & Björkman, 1996). If this nigericin-insensitive quenching affected F_o or absorption cross-sections (σ), then the quenching measurements would become experiments on more than qE.

Was it possible to induce fluorescence quenching such that experiments could be achieved in the absence of continuous actinic light, at least in the vicinity of the detection cuvette? To address the problem associated with direct illumination, the thylakoid membrane ATPase was activated using 100 µM dithiothreitol (DTT), a sulfhydryl reducing reagent, and 300 µM ATP was added to take advantage of the reversibility of this enzyme. It was expected that protons would be pumped into the thylakoid lumen, acidifying it and thereby maintaining qE even after light was removed. Figure 5 demonstrates the general applicability of this approach to fluorescence quenching. Once the actinic light was shut off, F_m began to increase, but remained significantly quenched compared to pre-illumination levels, recovering to only 48-55% after 40 seconds to 4 minutes later. Within the first 20 post-illumination seconds, the base fluorescence level decreased to and levelled out at a value that was quenched with respect to the pre-illumination F_o. Addition of hexokinase (15 units/ml) and glucose (10 mM) released the quenching of both F_m and F_o that was maintained by operation of the ATPase. Hexokinase catalyzes the phosphorylation of glucose to glucose-1-phosphate, using up the ATP that had been added to acidify the lumen.

Because maximized quenching was desired, the first 20 seconds post-illumination were of most interest. During this initial period, F_o levelled off and F_m only began to recover. By circulating the sample through the dark 3-ml detection cuvette from an illumination reservoir after a 21 second delay, it was hoped that maximized quenching of both F_m and F_o could be detected during qE. Figure 6 illustrates that F_m remained quenched by more than 60%, while a reduction in F_o could also be detected. Figure 7 demonstrates the effect of quenching on F_o in a circulated sample. Note that the exposure to the light still produced an initial rise in base fluorescence.

To address the second complication, in which the post-quenching fluorescence did not fully return to the original F_m, the PAM fluorimeter was set up to detect 9-amino acridine fluorescence, an assay known to demonstrate the formation and degradation of a transmembrane pH gradient. Chlorophyll and 9-aa fluorescence were not assayed simultaneously, however, exact lengths of time were maintained so that figures could be overlaid for indirect correspondence. Transmittance spectra of the filters used to do so are displayed in Figure 8.

Quenching of 9-aa fluorescence was clearly shown to correspond with the quenching of chlorophyll fluorescence upon exposure to the quench-inducing light (Figures 9 to 12), including a negative control in which omission of ATP from the circulated sample allowed very little significant quenching of 9-aa or chlorophyll fluorescence. The major portion of the quenching is therefore qE. In addition, even though the chlorophyll fluorescence signal did not recover completely, the 9-aa quenching did, indicating that nigericin dissipated the pH gradient completely. Thus, the leftover quenching of chlorophyll fluorescence was not related to qE. The 9-aa response saturates quicker than that of the fluorescence, but both are released immediately upon removal of the actinic light or the addition of nigericin.

The same quenching pattern occurred in non-circulated cuvette samples, in ATP-maintained quenching, and in circulated samples in which quenching was held by ATP. A slight upward drift of the quenched 9-aa signal was noted in some of the trials, but this was never accompanied by a release of qE quenching. Figure 13 shows that the saturation of the 9-aa response was very similar to that of chlorophyll quenching in terms of intensity dependence. Although the response in the absence of ATP in a circulated sample appeared to have some 9-aa quenching, there was no

significant recovery observed when the actinic light was removed (Figure 12). It was unclear whether or not there was any pH gradient detected in these samples, although the lack of qE quenching substantiates the expectation of no gradient. The circulated sample that contained ATP held as much or more of the pH gradient-related 9-aa fluorescence even after the 21 seconds of dark delay.

The major portion of the observed quenching was clearly qE. However, the other 2 forms of quenching, the state transitions (qT) and photoinhibition (qI), could not yet be positively identified within the quenching. Photoinhibition is not expected to change σ because it is proposed to represent complete loss of PSII centres - it would just be observed as a small decrease in F_m. State transitions, however, involve physical changes in antenna sizes and would adversely affect measurements of F_o and σ that were to represent qE by itself.

Figures 14 through 16 and Table 1 rule out the existence of qT in these samples. Two requirements for qT are phosphorylation and PQ pool reduction. The phosphorylation requirement was filled by addition of ATP to maintain the pH gradient, while the observation of increased fluorescence during light exposure (eg Figure 1) indicated that PQ reduction also took place. Since the relaxation kinetics of qT are on the order of many minutes, it could contribute to F_m quenching and would also constitute a portion of the residual post-illumination F_m quenching. However, samples allowed to quench in the presence and absence of ATP show no significant difference in either the extent of quenching or in the recovery (Figure 14, Table 1). Samples that were pre-uncoupled with nigericin and so were unable to qE quench also showed no such difference after 10 minutes of illumination (Figure 15, Table 1). Table 1 also establishes that there was more quenching of F_m remaining in the non-photo-protected sample (+nigericin at t=0) than in the sample that was allowed to quench, leaving F_m open to more photoinhibition in the former. Finally, Figure 16 shows that even after waiting for a period of 20 minutes, there was no further recovery of F_m after the release of qE quenching. Therefore, there is no qT in these quenched samples, and irreversible qI (photoinhibition) probably accounts for the residual quenching of post-illumination or uncoupled F_m, the complete nature of which is still unknown.

Concerning the nature of the elevated F_o at the initial exposure to actinic light, and after quenching in circulated thylakoids, samples were exposed to far-red light,

a treatment that has previously been used to preferentially excite PSI and therefore draw electrons through the transport chain, oxidizing PQ to help keep PSII traps open, with minimum fluorescence yield (eg Wagner et al., 1996). However, far-red light (>700 nm) was unable to reduce F_o below the dark-adapted level, despite inclusion of the electron acceptor methyl viologen, and could not inhibit the elevation of F_o when actinic light was added (Figure 17). Thus, the elevation in F_o could not have its origin in electron transport.

The solution was to illuminate the sample with background light prior to actinic light (<5 $\mu E/m^2/sec$ for 5 seconds out of the 90-second circulation cycle). The effect of this treatment was to all but eliminate the elevation of F_o. F_o is distinctly quenched in the qE-quenched state compared to the background-lit state. Figure 18 illustrates the same point. Exposure to 30 $\mu E/m^2/sec$ of red light was too much because it was enough to cause qE quenching. However, 5 $\mu E/m^2/sec$ elevated F_o enough to eliminate the qE-light-induced elevation, without causing any significant F_m quenching itself (remained >95% of pre-illumination F_m).

The origin of this effect was suggested to be randomization of S states in the oxygen-evolving complex (OEC) of PSII, a necessary step in comparing F_o levels of control and quenched samples, since quenched samples were exposed to enough continuous light to randomize S states (B. Genty, personal communication with D. Bruce). The S states of the OEC are related to the redox state of the manganese cluster that donates electrons to P680+ from the water-splitting reaction. Each of these states is known to have different quenching effects on fluorescence.

To test this hypothesis, thylakoids were exposed to a set of 10 consecutive single-turnover saturating flashes (0.5 Hz) in the dark-adapted state and after exposure to background light. Figures 19 to 21 illustrate the decay of fluorescence following the flashes in this experiment. After just 4 averaged repeats, it was possible to distinguish the kinetics of fluorescence decay in the dark-adapted sample from those of the sample exposed to background light. It was possible to visually differentiate the decay kinetics of the first 4 flashes of the dark-adapted sample (Figure 19), while no discernable differences could be detected in the background-lit sample (Figure 20). The decay rates were more separated from each other in the dark-adapted state. Furthermore, the peak fluorescence amplitudes at the beginning

of the flashes show an oscillation pattern in the dark-adapted samples that cannot be found in the background-lit thylakoids given this treatment (Figure 21). Although not all flashes induced significantly different yields in the dark sample, the low-light-exposed set shows no significant difference between the yields at any flash number. Both the pattern and the range of fluorescence amplitudes found in the dark-adapted sample were gone or reduced in the background-lit sample - the average scatters about the normalized yields were approximately 13% to 6% respectively. These phenomena would be even more obvious given an increased number of trials. This data supports S-state randomization as the origin of the F_o elevation, since randomized S states yield the same amplitudes and kinetics at all flash numbers, whereas the dark-adapted sample shows differences in yield. These differences in yield include a low first flash corresponding to the lower yield of fluorescence in the dark, although the average changes shown in Figure 21 are not as large as those observed during pump-probe experiments (12%; Figure 24, Table 3), owing to Q_A reduction by the actinic light, which would yield a decrease in photochemical quenching and thus a contribution to the elevated base fluorescence level.

Having established the appropriate states for each parameter for correct comparisons, the final preparation looks like the PAM trace in Figure 22. The low background light randomizes the S states of the OEC and elevates F_o to the appropriate level for comparison with quenched F_o, which appears to be quenched by approximately 12%. F_o also returns to the elevated control level after the addition of nigericin, even though the background light is not replaced. This is due to the relatively long decay rate (5-10 minutes) of the randomized S states. F_m consistently remains quenched up to 60% in the circulated system. Furthermore, the only other quenching component involved is photoinhibition, the state transition being completely absent. This well-defined qE-quenched preparation is used throughout the rest of the project, except where otherwise indicated.

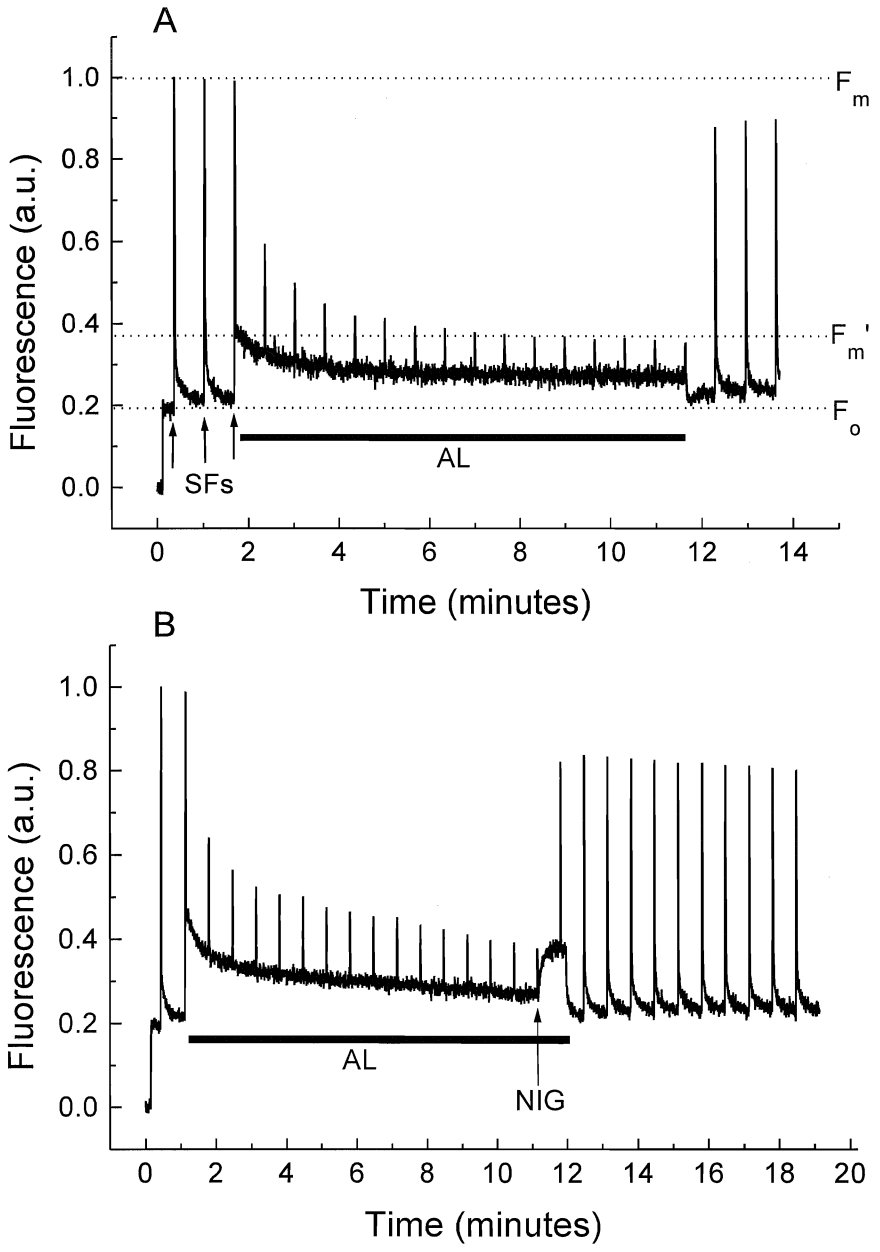

Figure 1: Pulse Amplitude Modulated (PAM) Fluorimeter traces of Chlorophyll a fluorescence from spinach thylakoids (6 µM Chl, 3 ml cuvette) treated with red actinic light (AL, 200 µE/m^2/sec) for 10 minutes. Fluorescence is normalized to the maximal pre-illumination fluorescence level (F_m), reached during saturating flashes of white light (SF, >3000 µE/m^2/sec for 1 sec). F_o is the minimal fluorescence level (~0.20) obtained using only application of a non-actinic measuring beam. F_v/F_o is about 4 in both A and B. In each case, fluorescence is quenched by about 60% of F_m upon addition of actinic light. **A**; Quenching is relieved by removal of the actinic light source. **B**; Quenching relieved by addition of the uncoupler nigericin (NIG, 1 µM), which degenerates the pH gradient. Relaxation of fluorescence is not complete, F_m recovering to approximately 80-85% of pre-illumination values.

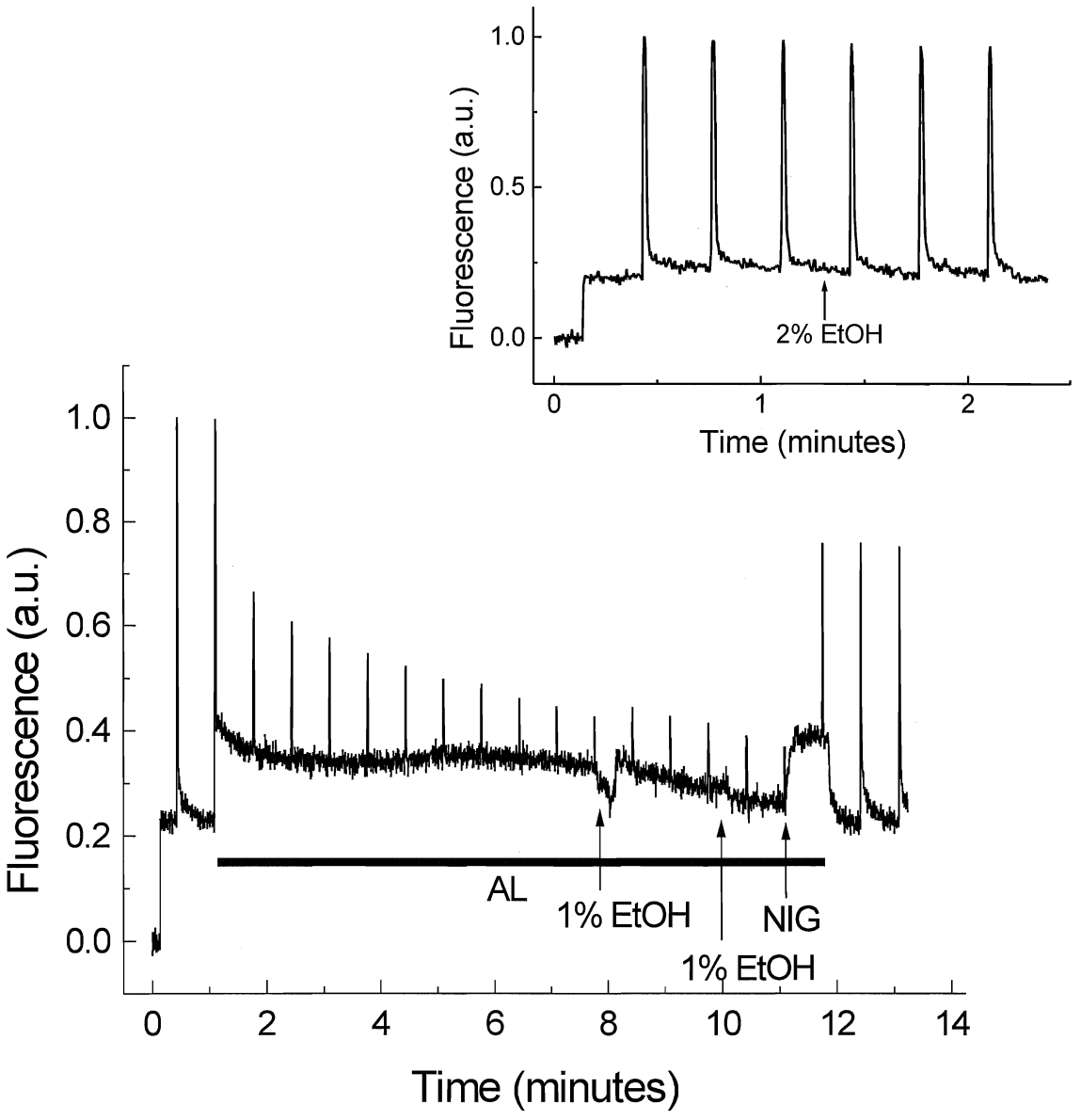

Figure 2: PAM trace of chlorophyll fluorescence from spinach thylakoids treated with 10 minutes of actinic light, with additions of 1% ethanol and 1 µM nigericin (stock 2 mg/ml in absolute ethanol). Addition of ethanol does not affect fluorescence levels by itself, while nigericin dissolved in ethanol causes pH gradient uncoupling, allowing relief of quenching. **Inset**; addition of 2% ethanol to thylakoid sample at F_m. The amplitude of F_m remains unchanged (98 ± 1%).

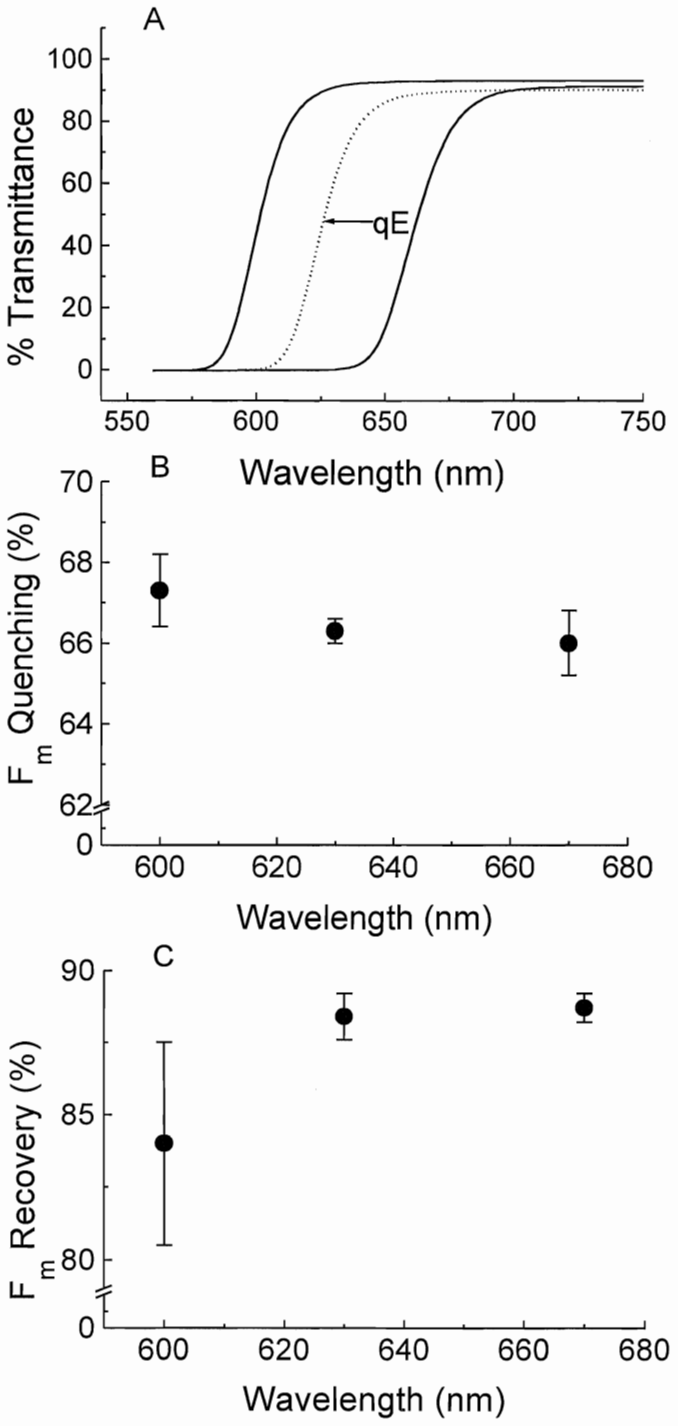

Figure 3: A; Transmittance spectra of 3 red filters used to induce fluorescence quenching in spinach thylakoids. Half-maximal transmittance for the filters occurred at 600 nm, 630 nm, and 670 nm. All experiments beyond Figure 3 use the 630 nm long-pass filter to induce quenching (qE). **B**; Fluorescence quenching of spinach thylakoids using the 3 different filters, with 10 minutes of equal light intensity (200 $\mu E/m^2/sec$). There is no significant difference between the extent of F_m quenching induced by the change in wavelengths. Each point is an average of 3 trials, ± 1 standard deviation. **C**; Recovery of F_m after removal of the actinic light source. There is an approximately 5% increase in recovery at 630 nm and 670 nm compared to that at 600 nm. (n=3, ± 1 S.D.)

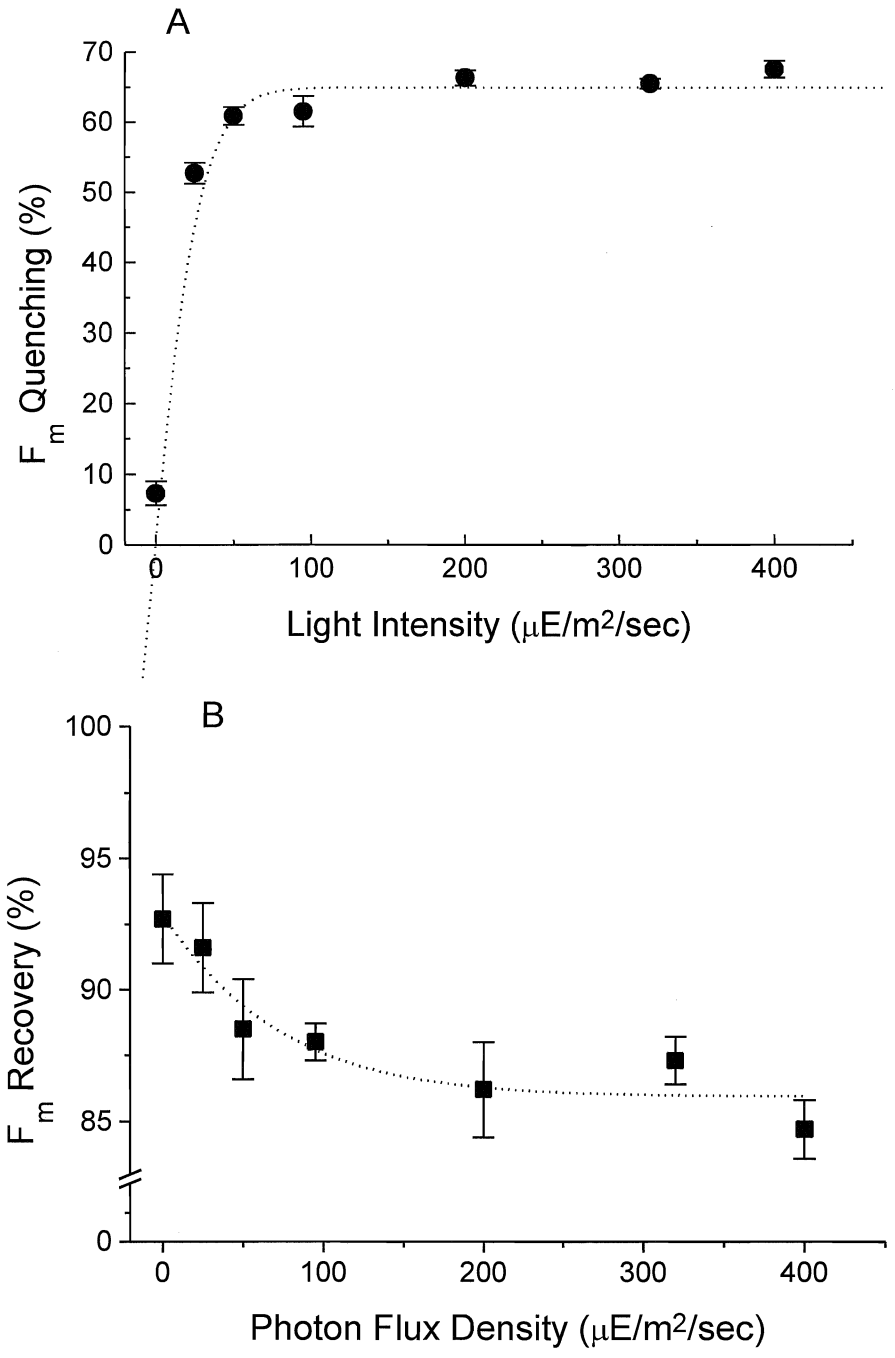

Figure 4: A; Saturation of F_m quenching versus photon flux density (light intensity) between 0 and 400 μE/m^2/sec for thylakoid samples treated with 10 minutes of red actinic light. The quenching response saturates at 64% beyond approximately 150 μE/m^2/sec. F_o could not be monitored from PAM traces as was F_m due to the elevation of base fluorescence during exposure to light. **B**; Recovery of F_m from light-induced quenching of different photon flux densities. The highest extent of recovery from quenching occurred before about 150 μE/m^2/sec, with a low of approximately 85% of pre-illumination F_m. There is little significant difference in recovery beyond 150 μE/m^2/sec.

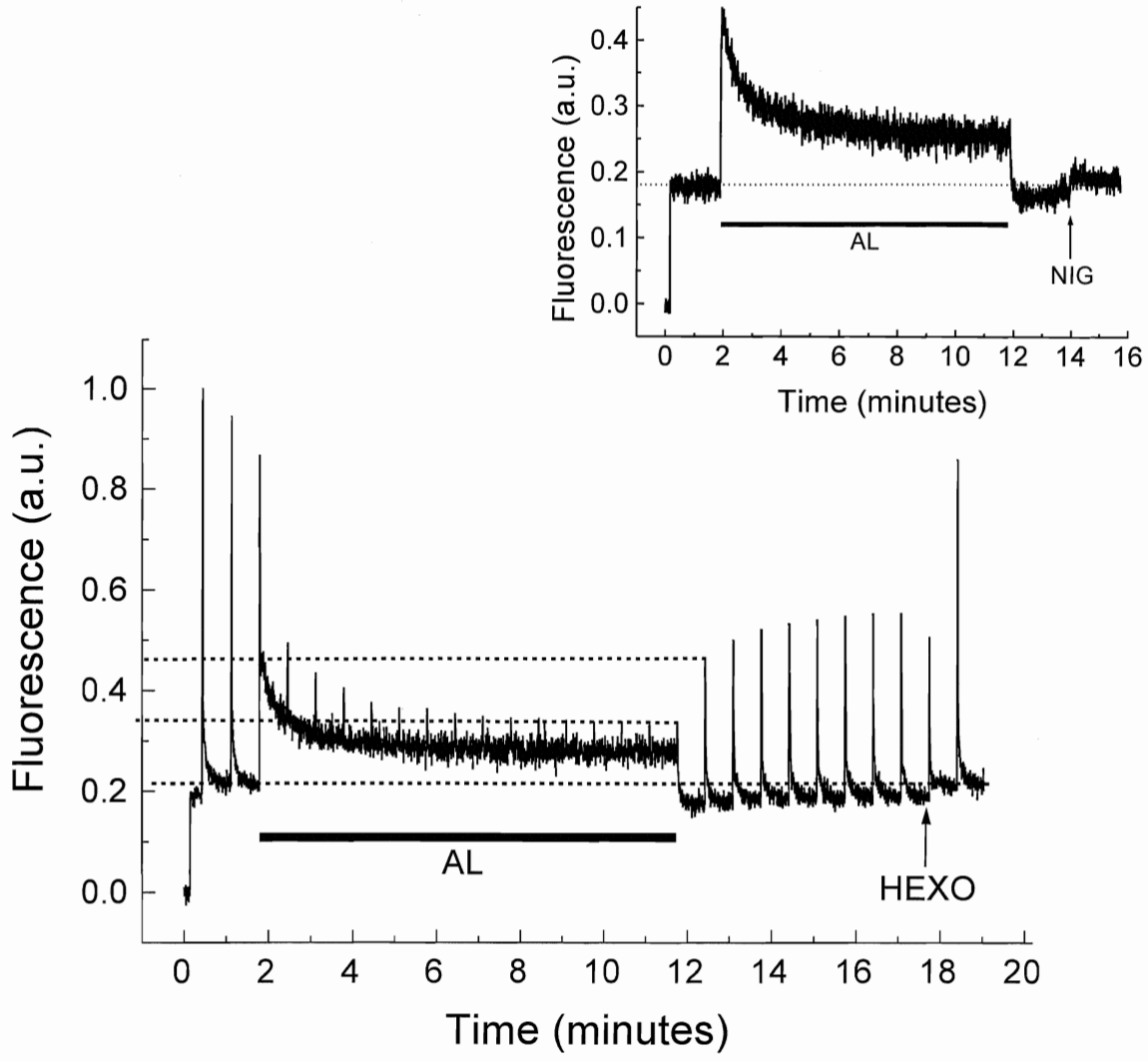

Figure 5: PAM trace of spinach thylakoids treated with 10 minutes of actinic light (>630 nm, 200 μE/m^2/sec), 300 μM ATP and 100 μM DTT. F_m only recovers to approximately 48-55% of pre-illumination values upon removal of the actinic light. HEXO refers to the addition of 15 units of hexokinase/ml and 10 mM glucose. This addition allows the release of quenching. F_o remains significantly quenched during the 6-minute post-illumination period before addition of the hexokinase reactants. Within the first 20 seconds, F_o levels out, while F_m slowly begins to increase.
Inset; PAM trace without use of saturating flashes in order to monitor F_o in thylakoids with 300 μM ATP and 100 μM DTT added. F_o increases during illumination, but removal of the light allows return to a base level that is quenched with respect to pre-illumination F_o. Addition of nigericin relieves this small amount of F_o quenching.

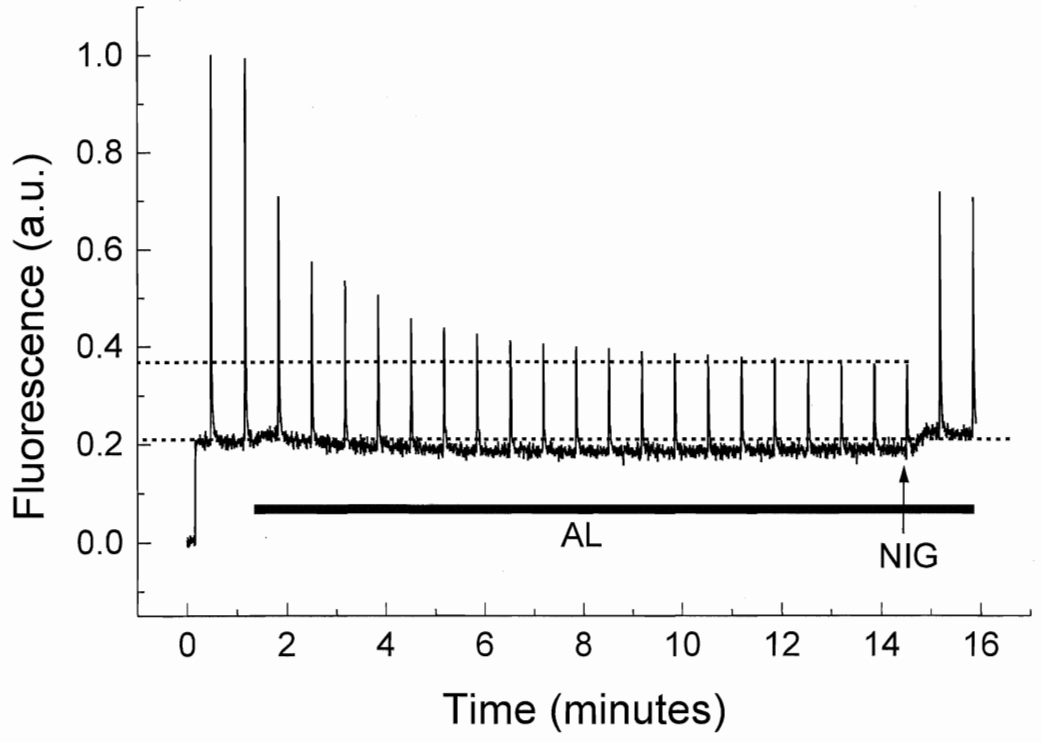

Figure 6: PAM trace of spinach thylakoids treated with almost 15 minutes of actinic light, 300 µM ATP, and 100 µM DTT, and circulated through a 3-ml measurement cuvette in the dark from a 42-ml illumination reservoir with a delay between illumination and measurement of 21 seconds (0.7 ml/sec flow rate). F_m is still quenched by more than 60% despite the delay interval, while F_o decreases by approximately 10% following an initial rise of about 5%. Addition of nigericin before the illumination reservoir, and 1 minute-30 seconds before removal of the light, relieves quenching of both F_m and F_o. The uncoupled F_o value is slightly increased compared to pre-illumination F_o.

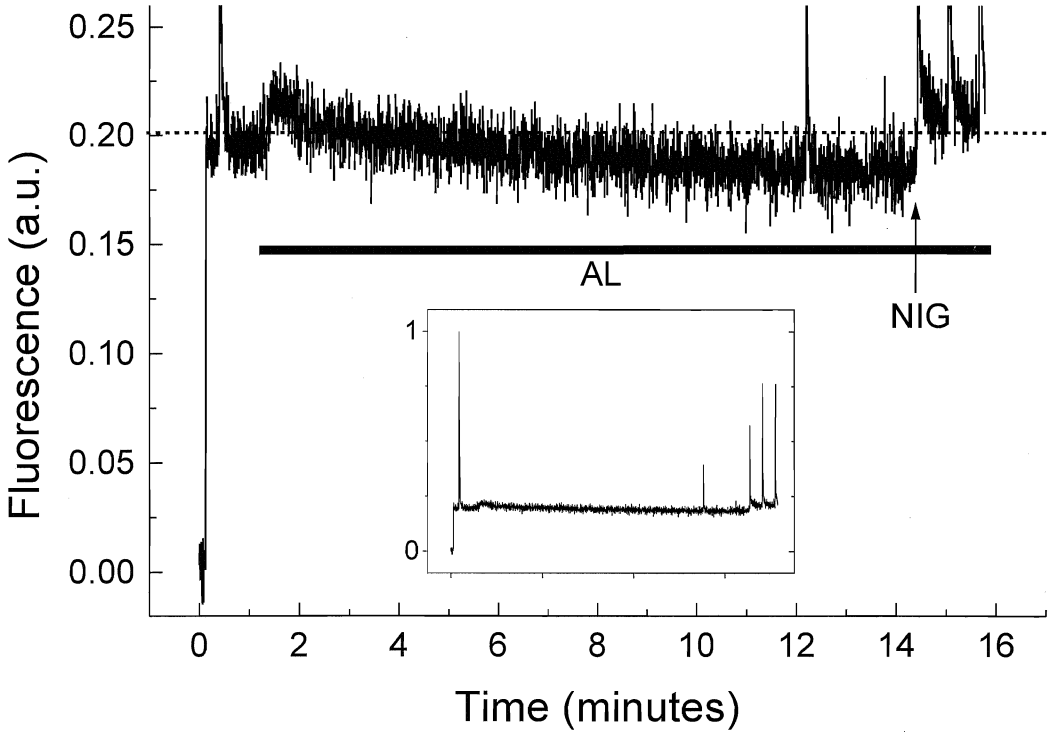

Figure 7: PAM trace of circulated spinach thylakoids treated with 15 minutes of actinic light, 300 µM ATP, and 100 µM DTT, without use of repetitive saturating flashes. F_o is quenched, again after a slight rise at the initial application of actinic light. Nigericin relieves the quenching, increasing F_o slightly beyond the pre-illumination value of F_o. **Inset**; Full PAM trace showing the saturating flashes. During illumination, F_m was quenched, recovering after the addition of nigericin.

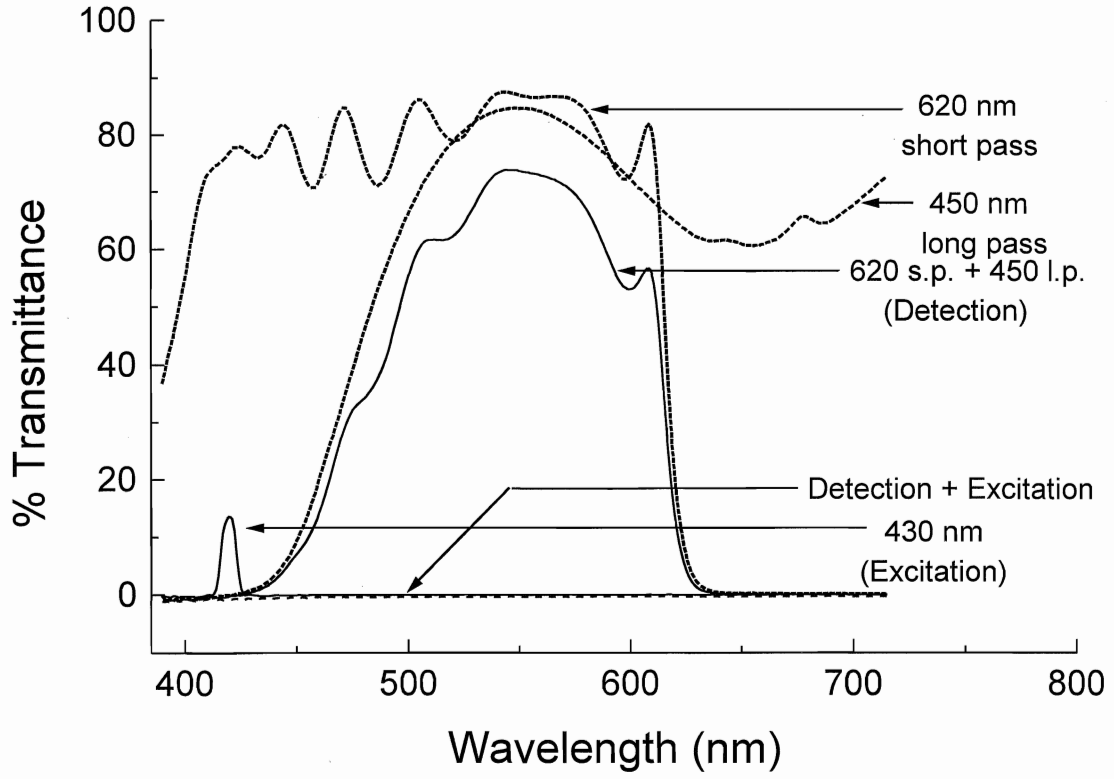

Figure 8: Transmittance spectra of filters used to detect 9-amino acridine (9-aa) fluorescence. 9-aa has absorption at 430 nm and fluoresces at 530 nm. Excitation was accomplished using a 430 nm narrow band filter in front of the PAM 450 nm LED, while fluorescence detection was filtered through a 450 nm long-pass filter coupled with a 620 short-pass filter to remove most of chlorophyll fluorescence. Dotted lines represent individual filters, while the solid lines represent actual filter combinations. The flat dotted line at 0% transmittance across the entire spectrum is the detection and excitation filters placed together.

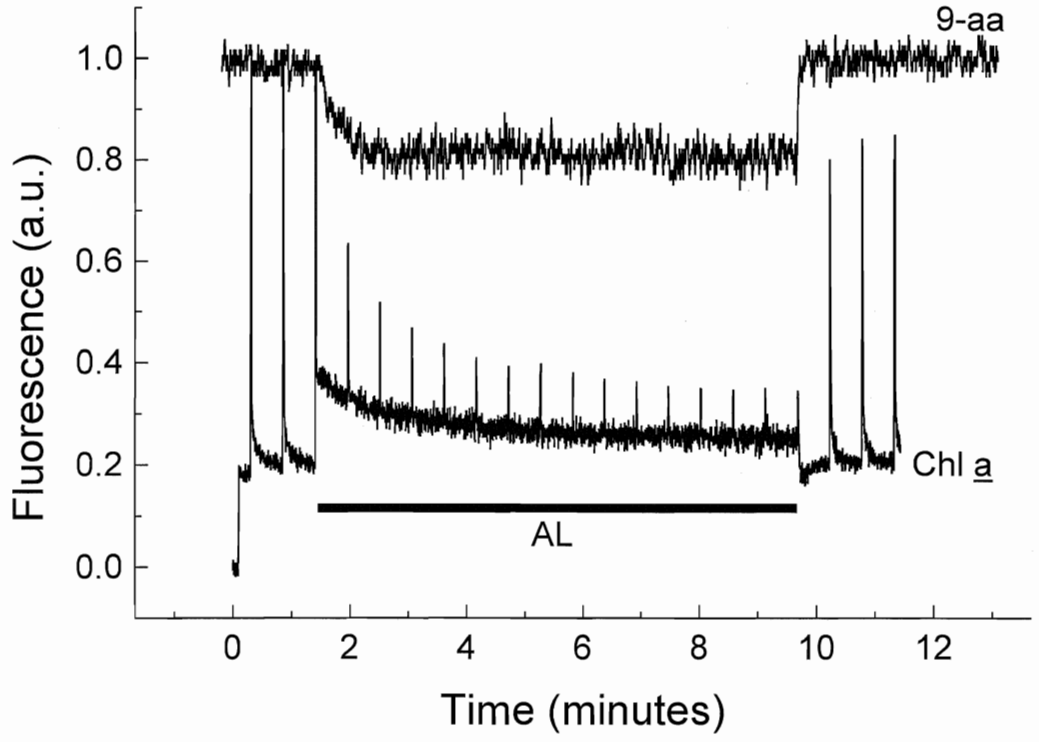

Figure 9: PAM trace of chlorophyll fluorescence overlaid with the 9-aa fluorescence response for spinach thylakoids treated with actinic light. Quenching of 9-aa fluorescence occurs simultaneously with the quenching of chlorophyll fluorescence, though the response saturates quicker for 9-aa than for chlorophyll. Removal of the actinic light allows the immediate release of quenching of both 9-aa and chlorophyll fluorescence.

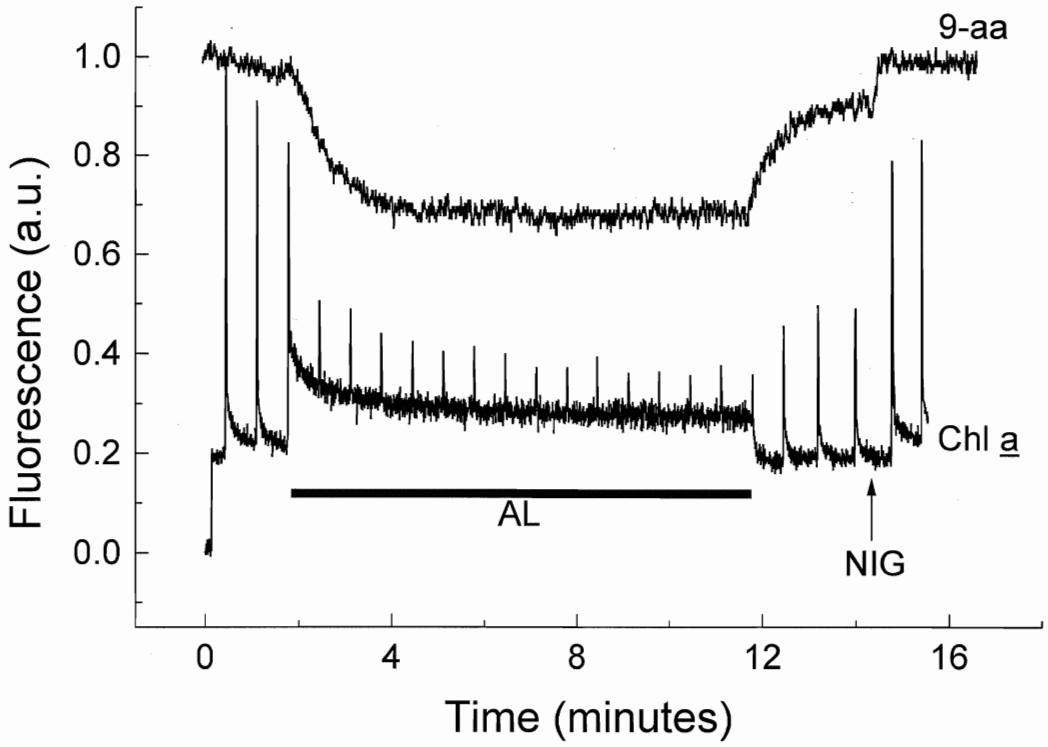

Figure 10: PAM trace of chlorophyll fluorescence overlaid with the 9-aa fluorescence response for spinach thylakoids treated with actinic light, 300 μM ATP, and 100 μM DTT. Quenching of 9-aa and chlorophyll occur simultaneously with the application of light. Upon removal of the actinic light, both begin to recover some of the quenched fluorescence, but some significant portion of each is held quenched until the addition of nigericin to degenerate the pH gradient across the membrane. At a delay of 21 seconds after removal of the actinic light, there is still 23% quenching of the 9-aa signal, with significant quenching of F_m remaining, along with a slight quench of F_o, which can be deduced from the increase in base fluorescence after the addition of nigericin.

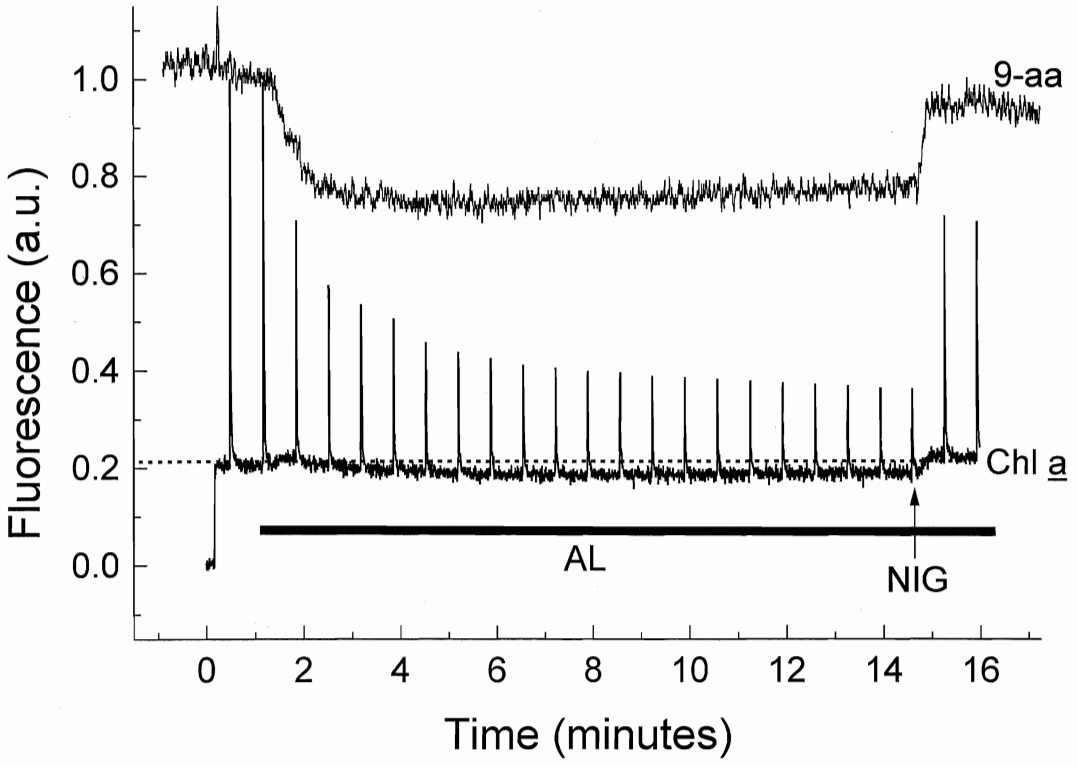

Figure 11: PAM trace of chlorophyll fluorescence overlaid with the 9-aa fluorescence response for spinach thylakoids treated with actinic light, 300 μM ATP, and 100 μM DTT, and circulated in a flow-through reservoir system. Quenching of 9-aa and chlorophyll occurs simultaneously, both remain significantly quenched despite the 21 second delay between illumination and detection, and both are relieved by the addition of nigericin.

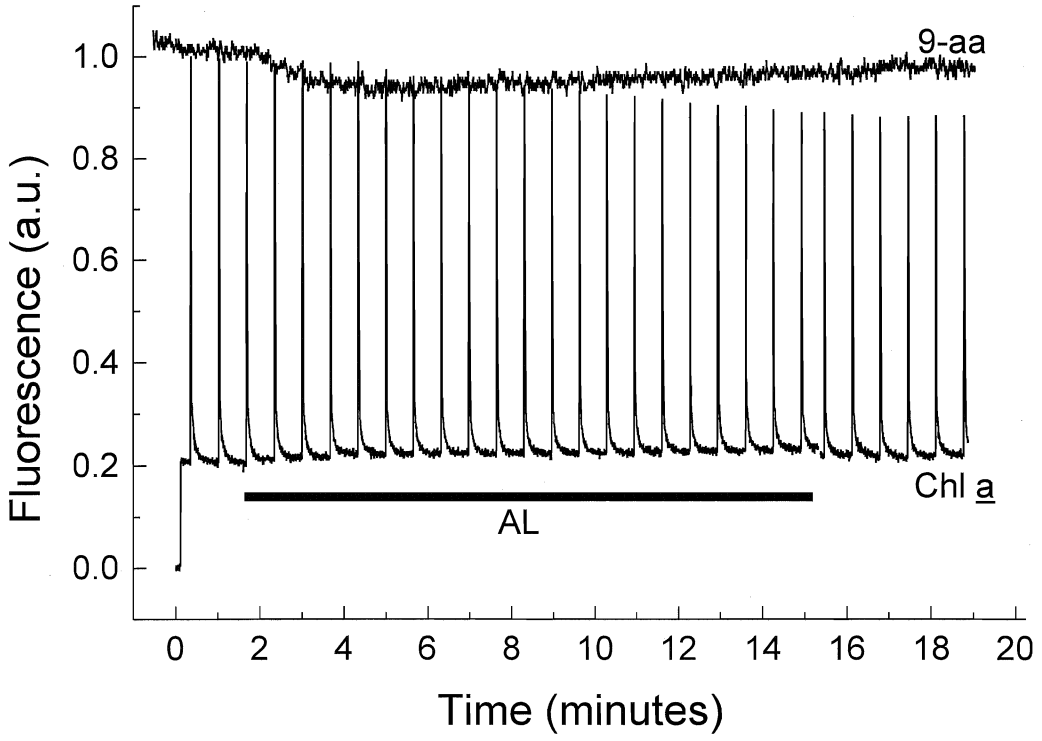

Figure 12: PAM trace of chlorophyll fluorescence overlaid with the 9-aa fluorescence response for circulated spinach thylakoids treated with actinic light and 100 μM DTT, but with the omission of ATP. F_m does not remain quenched any further than is seen after the removal of light or addition of nigericin (Figure 4B). Though 9-aa fluorescence decreases slightly during exposure to actinic light, there is no significant increase in 9-aa fluorescence when that light is removed.

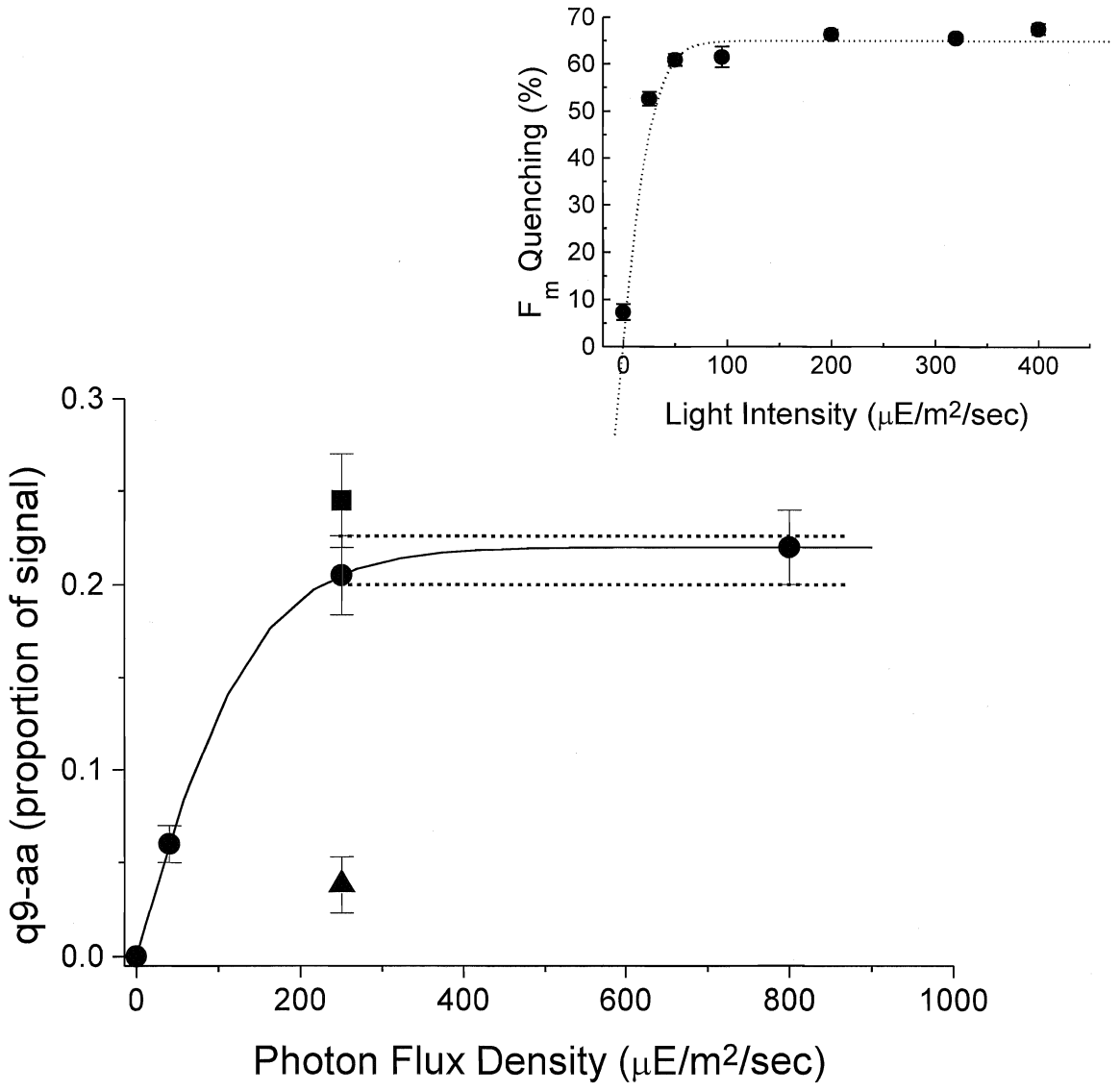

Figure 13: Saturation response of 9-aa quenching (q9-aa) versus photon flux density for spinach thylakoids exposed to actinic light for 14 minutes. Quenching saturates at 22% of the total 9-aa signal at about 200 μE/m^2/sec, similar to the saturation found for quenching of F_m (**inset**). (n=3, ± 1 S.D.)
● - q9-aa saturation for non-circulated samples in 3-ml cuvette
■ - q9-aa for circulated thylakoids ▲ - q9-aa for circulated sample without ATP
The q9-aa signal is approximately equal in the circulated thylakoid sample and non-circulated sample. The q9-aa for the circulated sample without ATP is not 0, although it is significantly smaller than the quenching for the other trials.

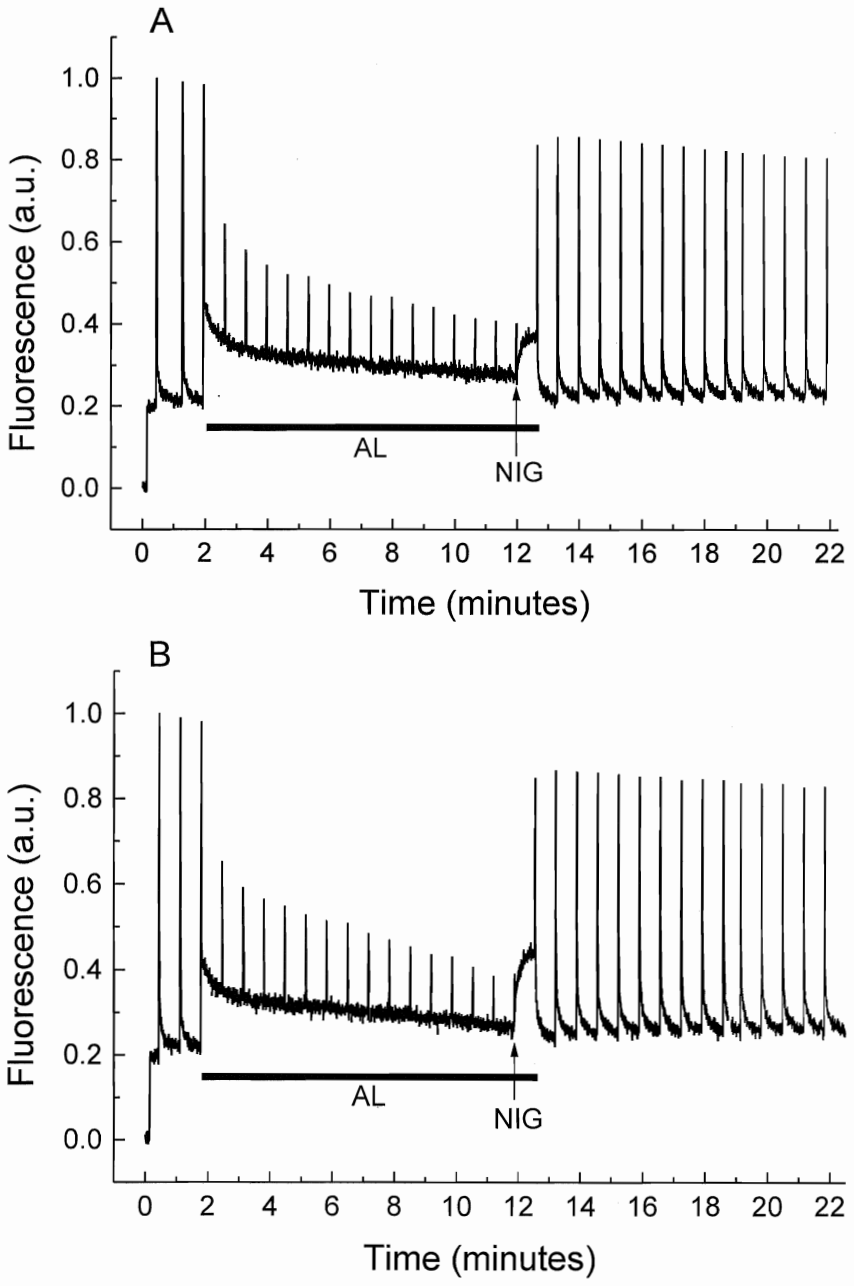

Figure 14: PAM traces of non-circulated thylakoid samples exposed to actinic light. Both figures are the same, except that **A** contains 300 μM ATP and **B** contains no ATP. Neither the extent of F_m quenching (approximately 60%) nor the recovery of fluorescence after the addition of nigericin are significantly different between the 2 cases. (See Table 1)

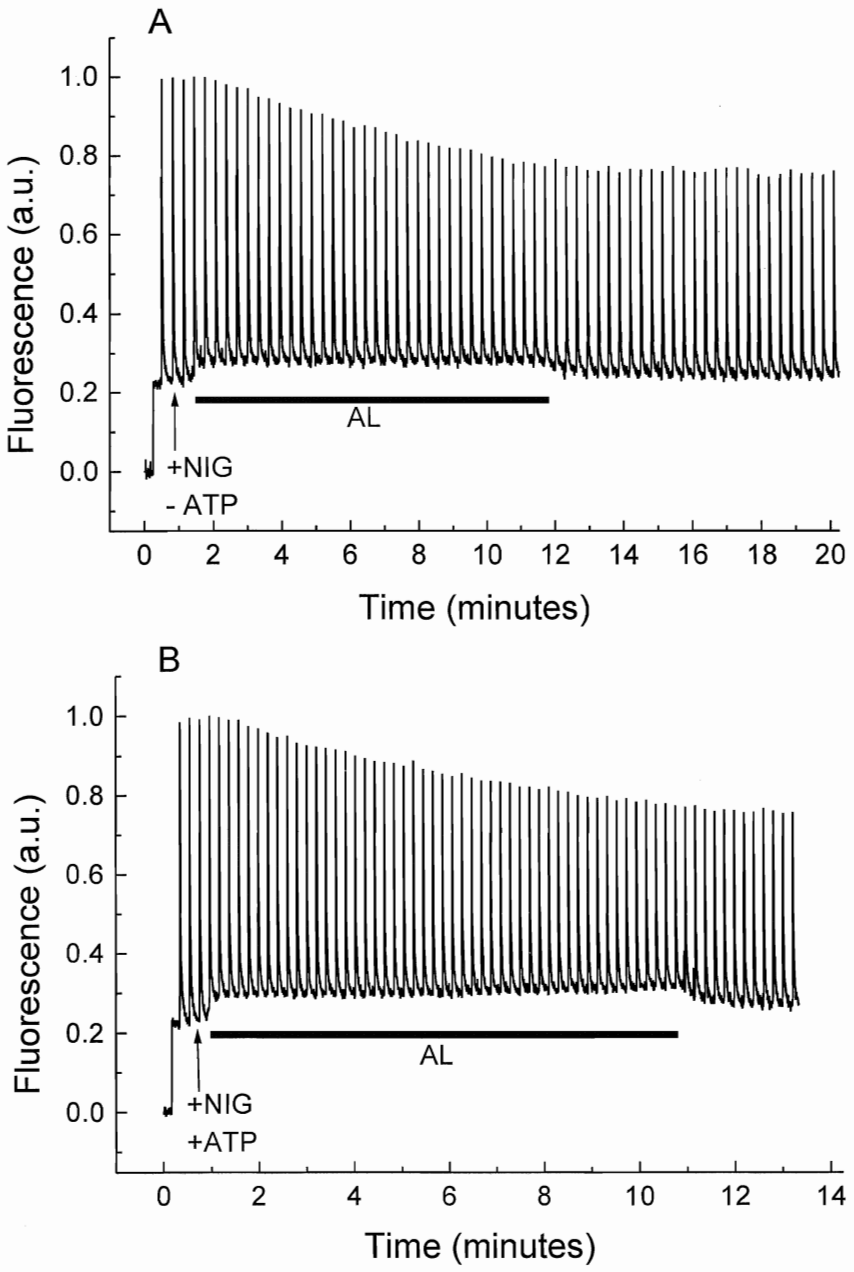

Figure 15: PAM traces of non-circulated spinach thylakoids exposed to actinic light and pre-uncoupled with nigericin. **A**; Thylakoids are treated with nigericin only. **B**; Thylakoids are treated with nigericin and ATP at the beginning of the trial. F_m after the removal of the actinic light source is not significantly difference between these 2 trials. (See Table 1)

Table 1: Post-illumination maximal fluorescence yields (F_m') from thylakoid samples exposed to 10 minutes of red actinic light with various reagent treatments. Values represent the percentage of pre-illumination F_m recovered after removal of the light or the addition of nigericin. (± 1 S.D., n=3)

Reagent additions at t=0		
0.3 mM ATP	1 µM Nigericin	F_m'
No	(at t=10 min)	85.8 ± 0.8
Yes	(at t=10 min)	84.5 ± 0.8
No	Yes	77.2 ± 0.5
Yes	Yes	76.5 ± 0.8

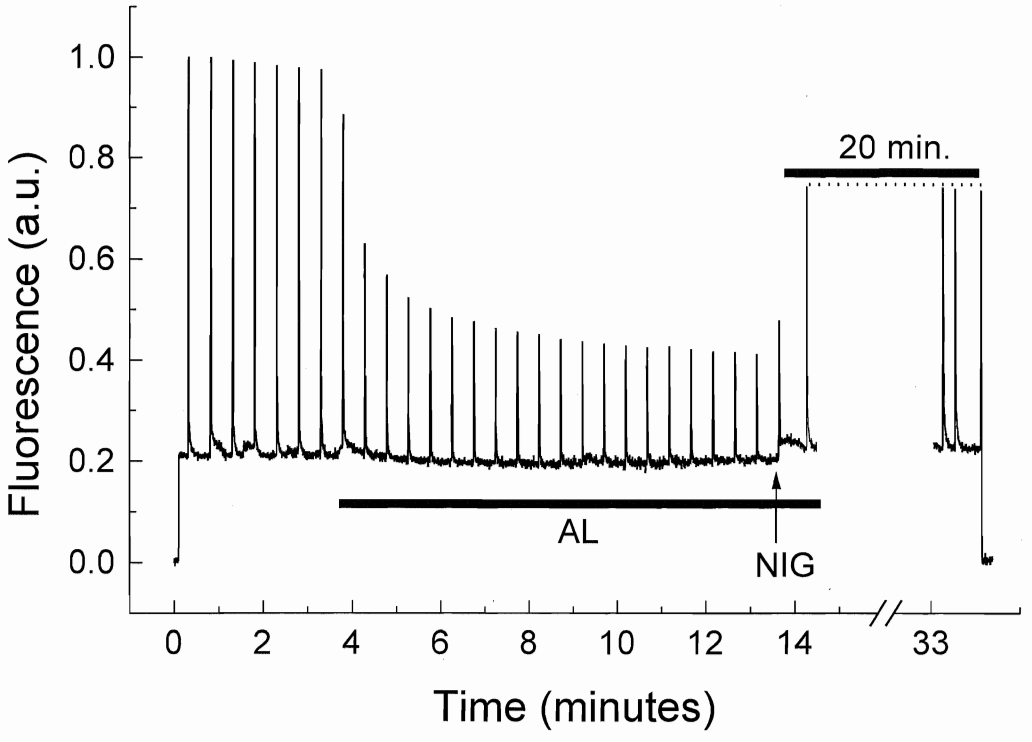

Figure 16: PAM trace of circulated thylakoids exposed to actinic light for about 13 minutes. After the addition of nigericin, F_m recovered to about 75% of its pre-illumination value and remained steady for 20 minutes, without recovering or quenching further.

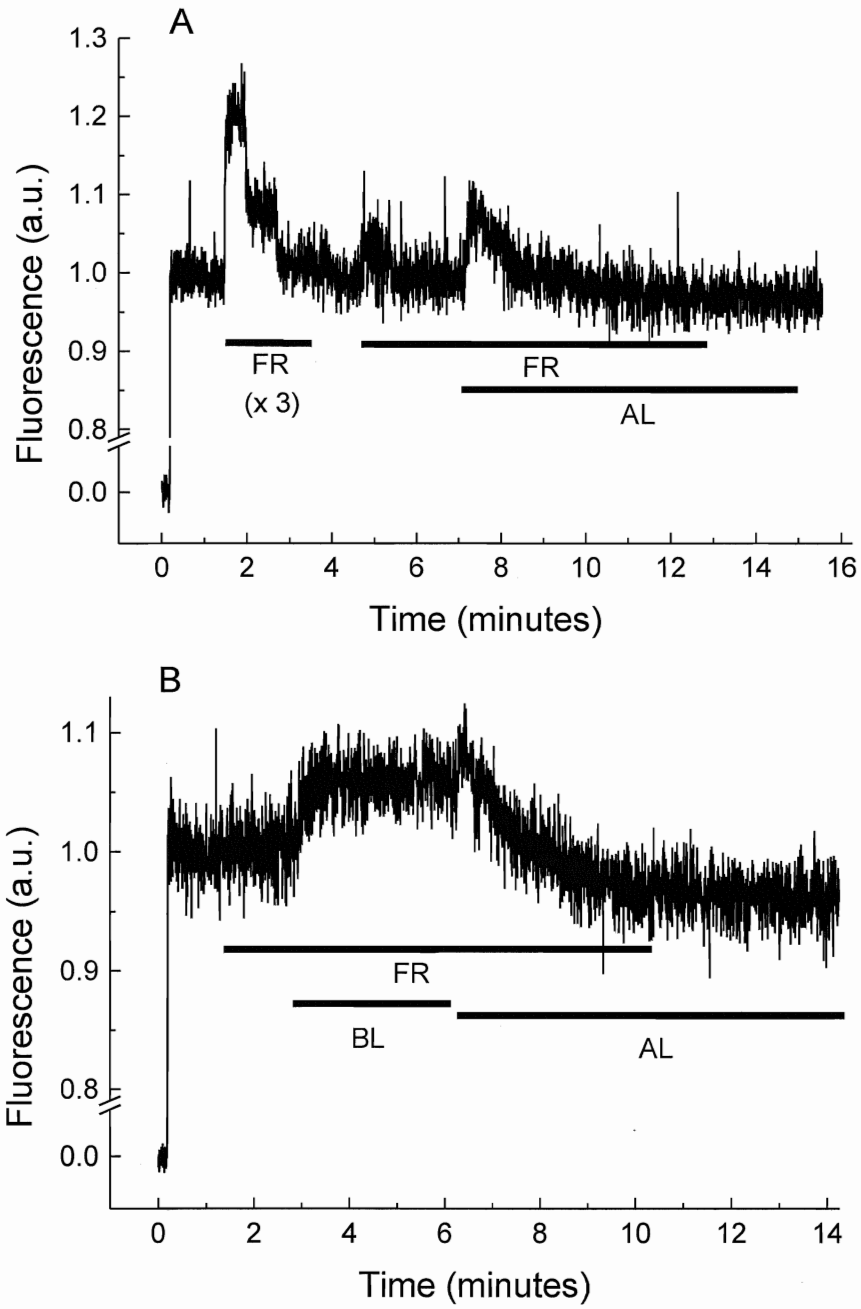

Figure 17: PAM traces from spinach thylakoids exposed to far red light (FR, >695 nm), background light (BL, <5 μE/m^2/sec for 5 seconds per cycle through the 90 second circulation apparatus), and actinic light (AL). F_o is set to 1 for dark-adapted sample. **A**; Exposure to far-red light (×3) does not decrease F_o, rather it increases it due to an excess of light intensity. Exposure to less far-red light does not decrease or elevate it. Furthermore, it was unable to prevent the elevation in fluorescence associated with turning on the actinic light used for qE quenching. **B**; Treatment with far-red light is again unable to affect F_o. However, exposure to background light elevates F_o enough to make the initial rise in base fluorescence upon addition of the actinic light insignificant. F_o clearly decreases during qE.

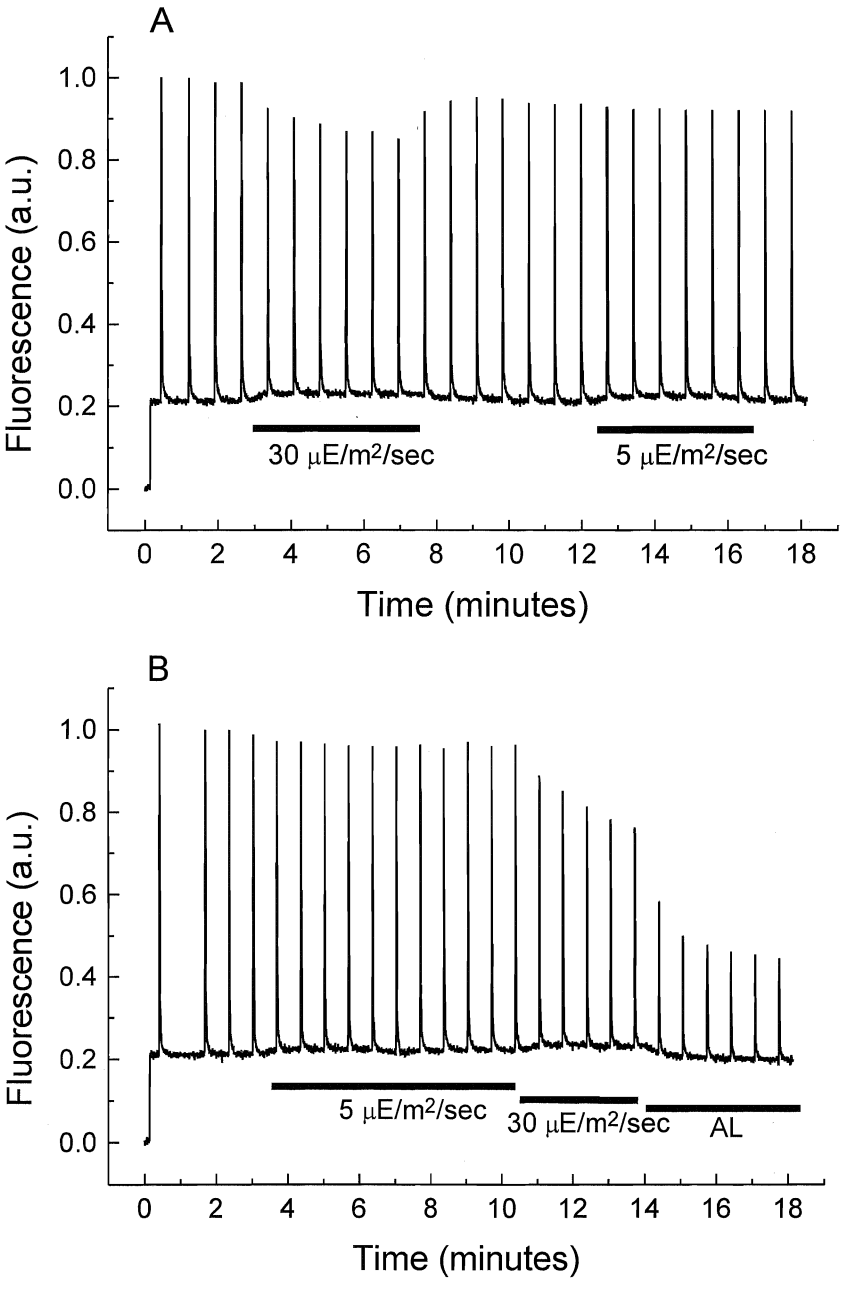

Figure 18: PAM traces from spinach thylakoids exposed to low light intensities through a small exposure window of 5 seconds out of the full 90-second cycle through a flow-through apparatus. **A**; Exposure to 30 μE/m^2/sec of red light elevates base fluorescence, but is intense enough to cause some quenching of F_m. Using only 5 μE/m^2/sec succeeds in elevating base fluorescence about the same amount as using 30, but does not cause any significant qE quenching (F_m>95% pre-illumination value). **B**; As in A, 5 μE/m^2/sec elevates fluorescence without causing qE, while 30 μE/m^2/sec causes qE. Immediate replacement of the background light with qE-inducing actinic light (200 μE/m^2/sec) causes the initial rise in base fluorescence previously seen upon treatment with actinic light is eliminated. F_o clearly decreases during qE.

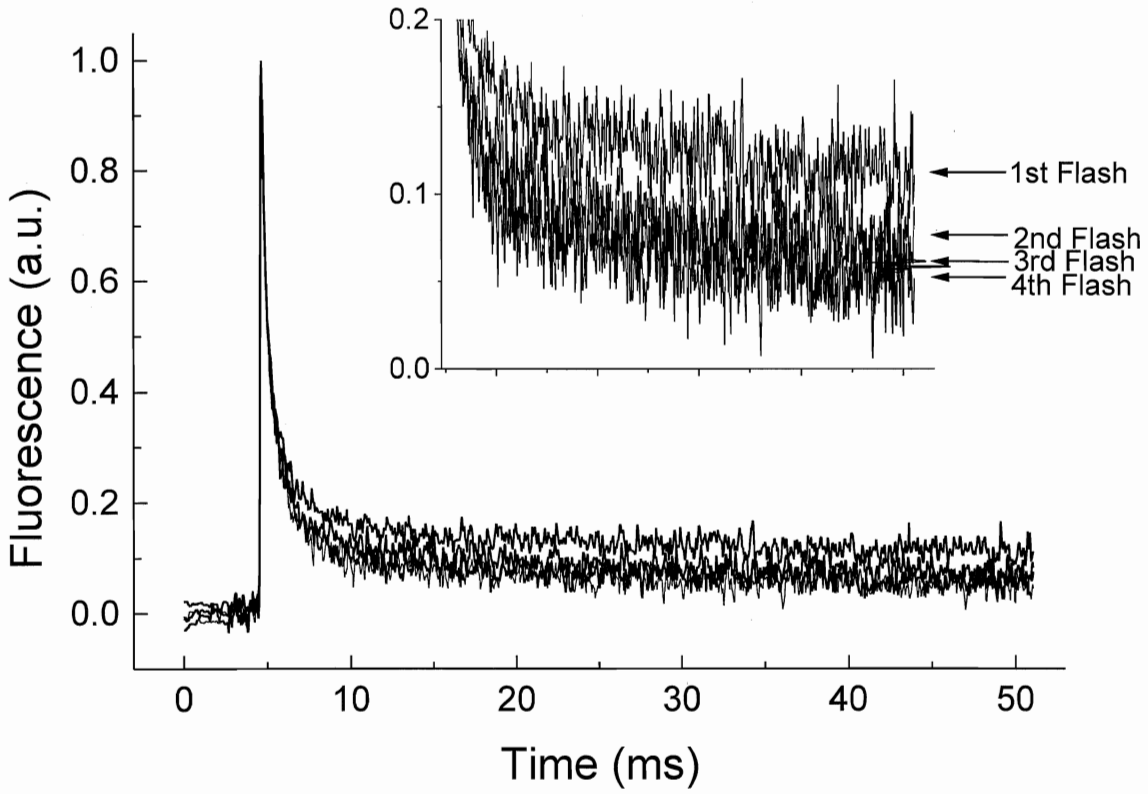

Figure 19: Kinetic traces from dark-adapted spinach thylakoids exposed to a set of 4 consecutive single-turnover saturating flashes (0.5 Hz). **Inset**; Magnification of part of the decay of the 4 flashes. The decay rates of the flashes are clearly different, as are the initial peak amplitudes of each flash (see Figure 24). Each trace is the average of 4 repeats.

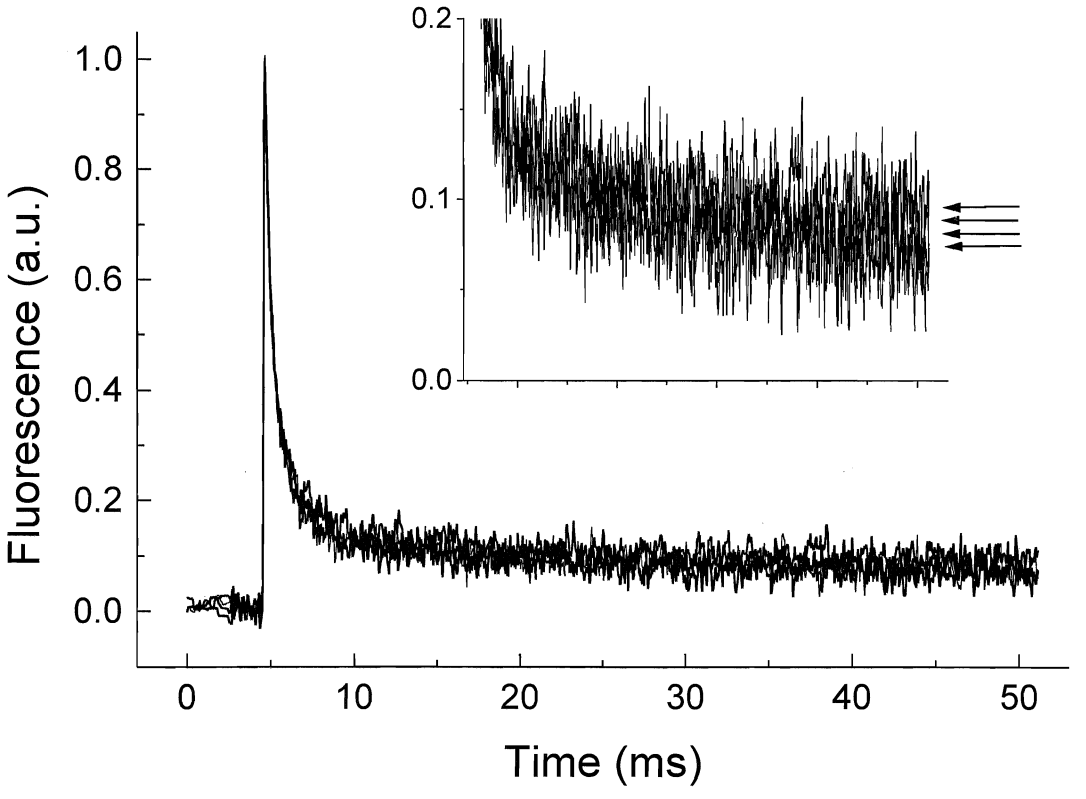

Figure 20: Kinetic traces from spinach thylakoids exposed to a set of 4 consecutive single-turnover saturating flashes (0.5 Hz) after exposure to background light (<5 $\mu E/m^2/sec$ for 5 seconds of 90 sec. total circulation time). **Inset**; Magnification of part of the decay of the 4 flashes. Arrows indicate the 4 flashes. The decay rates of the flashes are very similar, as are the initial peak amplitudes of each flash (see Figure 24). Each trace is the average of 4 repeats.

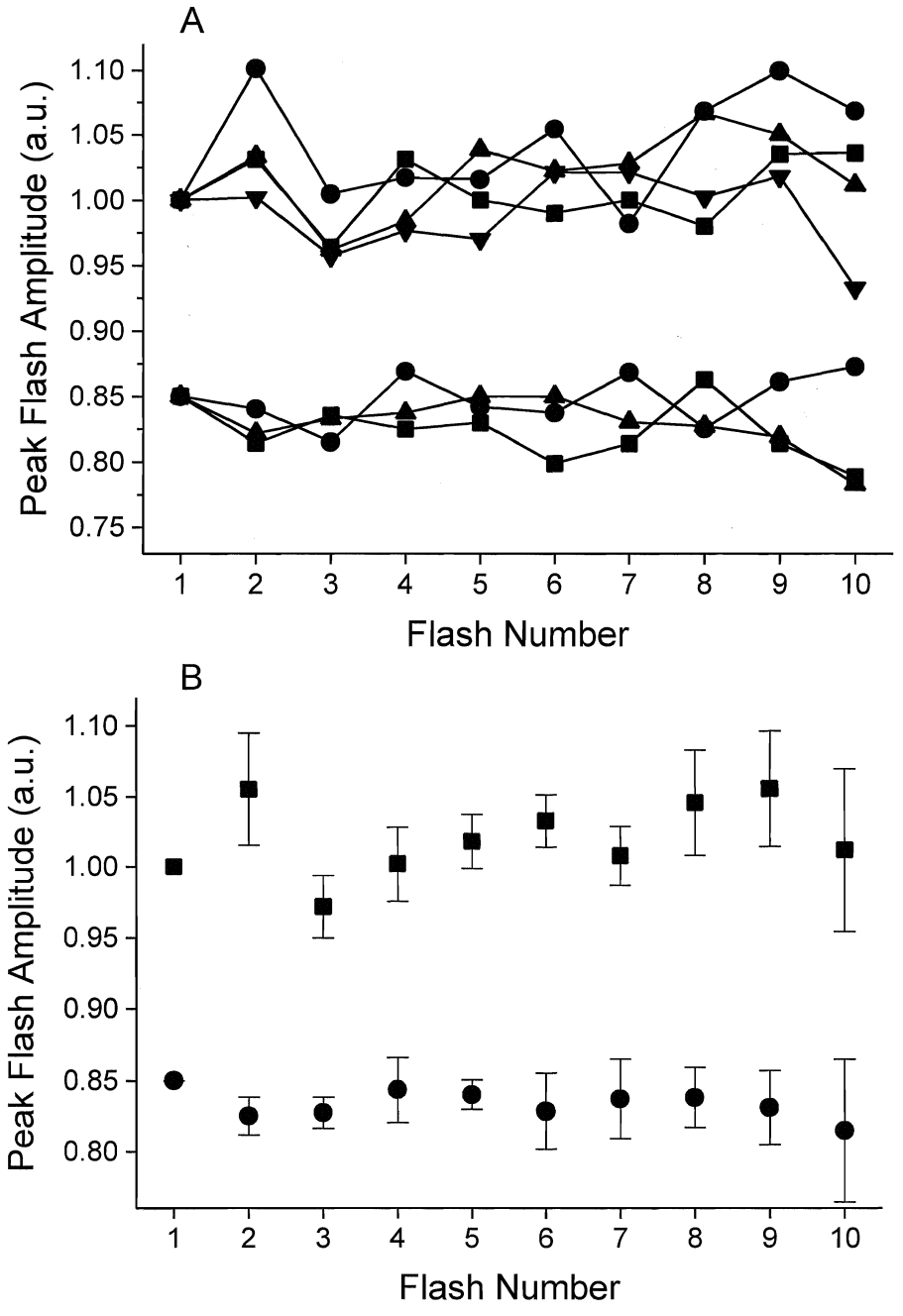

Figure 21: Peak fluorescence amplitudes from spinach thylakoids following consecutive single-turnover saturating flashes (0.5 Hz). In each case, fluorescence is normalized to the amplitude of the first flash, samples exposed to background light being offset by 0.15 (to 0.85). **A**; Individual sets of 10 flashes, with dark-adapted samples on the top. There is a clear pattern in the first 4-5 flashes of the dark-adapted sets, and possibly in the last 2 flashes, while the low-light-exposed samples remain less scattered, over a smaller range of amplitudes. **B**; Average peak amplitudes of fluorescence. ■ - dark-adapted thylakoids ● - thylakoids exposed to background light. There is a significant difference between some of the flash amplitudes in the dark-adapted set that can not be seen in the set exposed to background light.

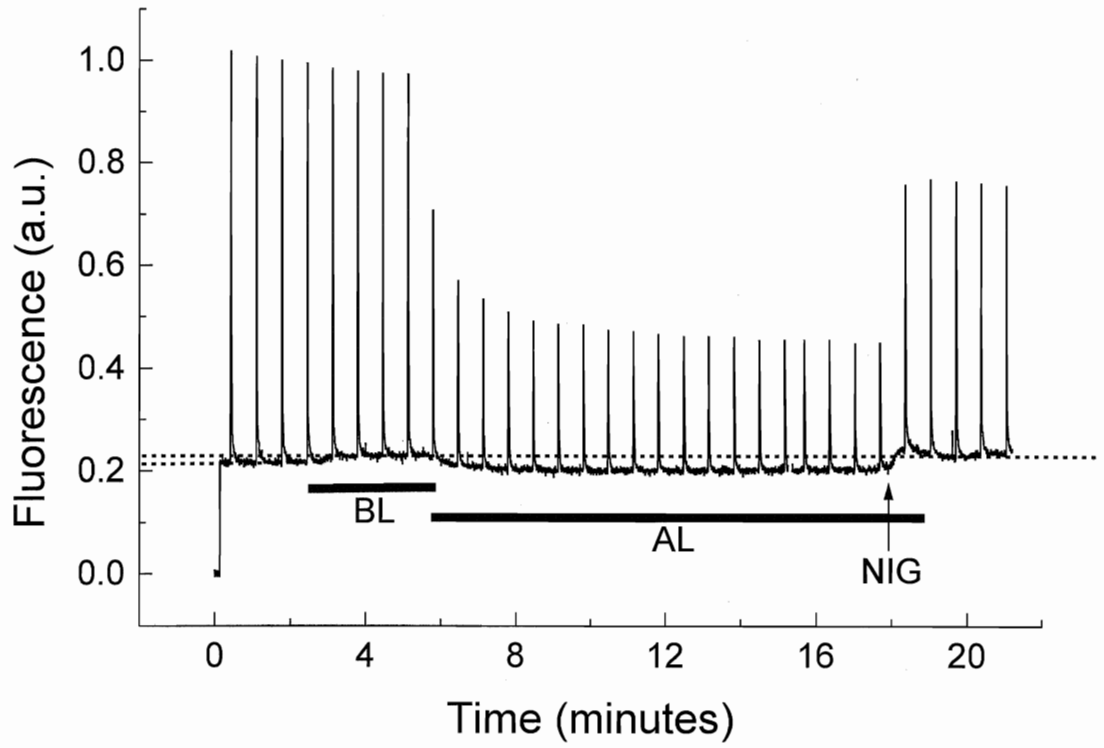

Figure 22: PAM trace of circulated spinach thylakoids exposed to background light previous to exposure to qE-inducing actinic light. The low background light elevates F_o by approximately 10%, such that there is no additional elevation when the actinic light is added. From the elevated F_o level, F_o is quenched by approximately 12%. Addition of nigericin relieves the quenching of both F_m and F_o, which returns to the elevated F_o level reached during exposure to background light, even though it is not turned back on.

Absorption Cross-Sections

Figures 23 through 36 and Tables 2 to 5 describe the results of pump-probe experiments used for the determination of PSII absorption cross-sections (σ) of thylakoid samples under qE conditions. For a complete summary of cross-section data, see Tables 4 and 5.

Figure 23 depicts a PAM trace of the time course of fluorescence and of quenching that is used for the determination of σ. Because the measurement of flash saturation curves required less than 5 minutes each, thylakoid stability had to be considered. Figure 23 shows that there was more than enough time to do a single curve for control, and then a curve for the qE state begun after about 4 minutes of quenching. This was the collection protocol employed for all pump-probe experiments.

Figure 24 shows sample flash saturation curves of a thylakoid sample in the dark and then with randomized S states. Each data point represents the average of 10 individual single-turnover laser flashes from a pump-probe apparatus operated at 1.5 Hz, affording enough time for complete recycling of the sample through the flow-through detection cuvette (no part of the sample was flashed more than once per 90 seconds). The curves were fit using a single-hit Poisson probability distribution after the theory of Mauzerall and Greenbaum (1989) (see Methods). Absorption cross-sections are measured in square Ångströms ($Å^2$), though in this study most are stated in relative terms. Typically, calculated standard errors in cross-section measurements were less than 3% of σ, with single-day variability within control trials of less than 3% (from standard deviations; see Table 2). Similar consistency was found for F_o and F_{sat} in control runs. Note that the saturation level is not equal to F_m due to use of single-turnover flashes, which induce a lower level of fluorescence for reasons that are still under investigation (Vasil'ev & Bruce, 1998; Samson & Bruce, 1995).

In the case of dark-adapted samples compared to those with randomized S states (Figure 24), F_o increased by an average of 12% in the randomized state, while the saturation curve shifted leftward, which yielded an increase in σ of an average of 11%. F_{sat} was hardly significantly quenched (4±3%), as expected (Table 3). There is a close association between the change in F_o and in σ that follows the quantitative model prediction for PSII, where the change in σ is reflected by the same change in

F_o during antenna quenching ($\Delta\sigma_{PSII} \propto \Delta F_o$; Vasil'ev et al., 1998; Butler, 1984), lending credibility to data obtained from our newly-rebuilt pump-probe apparatus. Conceivably, a simple decrease in photochemical quenching (qP) could induce the small increase in yield, due to Q_A reduction. It could then also increase σ. However, this would also be accompanied by an increase in the amplitude of the 3.1 ns PSII reaction centre decay component (Figure 48, decay kinetics) in the randomized state. This is not the case.

Figure 25 represents an example of the first attempt to determine σ from flash saturation curves of qE-treated thylakoids, but without S state randomization. As expected, F_o did not decrease during qE, but did increase to the randomized level after quenching, due to the randomizing effects of the qE-inducing light. The increase upon the addition of nigericin again reflects the Butler model, with F_o and σ increasing by approximately the same proportion (9% and 11% respectively) compared to the dark-adapted control state.

However, flash saturation curves applied to the investigation of qE quenching did not at first appear to adhere to the Butler model of antenna quenching. Flash saturation curves in Figure 25 reflected a σ increase of 53% in the quenched state even though F_o remained the same. Similarly, qE-quenched thylakoids compared to the randomized state showed an average increase of 27% in σ, while F_o decreased an average of 11% (Figure 26). This was certainly an unanticipated observation for the qE-quenched samples, where it was expected that σ would either decrease or remain the same. After uncoupling, however, both F_o and σ recovered to the pre-quenched control levels, establishing that if zeaxanthin were formed during qE, it did not have any direct quenching effect without the presence of a pH gradient, as had been previously reported (Niyogi et al., 1998; Wagner et al., 1996). This point also confirmed that the source of the residual quenching of maximal fluorescence after uncoupling did not involve a change in σ and did not contribute to the measurement of cross-sections. The origin of the residual quenching is probably photoinhibition of PSII, which is supported by increases in F_o observed under qE-inhibited conditions (+Nigericin, Figure 27) and partially-inhibited qE conditions (+DTT, Figure 30A).

The unexpected increase in σ during formation of qE led to the measurement of cross-sections in thylakoids exposed to qE-inducing light, but with alternative

treatments. The first approach to dissecting the increase in σ was to pre-uncouple the samples with nigericin before exposure to the qE-inducing light (Figure 27). In this case, however, F_{sat} increased by 48% during illumination, approaching F_m and yielding F_v/F_o close to 4 as reported during PAM experiments. The origin of this increase will be examined in the discussion. When comparing the qE-quenched samples to the pre-uncoupled 'F_m' (see Table 5), the amount of quenching is 57%, an extent similar to the F_m quenching observed during PAM experiments. The cross section increased by an average of 59% during illumination, but only returned to 29% higher than control after the removal of the actinic light, partly due to a further increase in F_o during re-application of the background light. Despite the higher signal-to-noise ratio and reasonable fit qualities, σ for these samples were less consistent than for other experiments, resulting in a large standard deviation. This approach may not be the most reliable for these reasons.

A second approach to understanding the increase in σ was to inhibit the formation of the pigment zeaxanthin in qE-quenching samples. Zeaxanthin is believed by some to be an explicit requirement for qE formation in the antenna (eg. Gilmore, 1997). Figure 28 confirms that the isolated thylakoids used in this study formed zeaxanthin during exposure to qE-inducing light. The light-induced absorbance change ($\Delta A_{505/565}$) is known to indicate changes in the epoxidation state of the xanthophyll cycle, with the absorbance peak at 505 nm representing an absorbance for zeaxanthin. Figure 28 shows a distinct rise in the absorbance for this peak, on the same order of magnitude as that found by Niyogi et al. (1998) and Ruban and Horton (1998), that saturated within 3 minutes, with a half-time comparable to that seen by Ruban et al. (1993). In the presence of 3 mM DTT, however, no absorbance change occurred. These thylakoid samples exhibit zeaxanthin formation that can be inhibited by DTT. DTT is known to inhibit Violoxanthin De-epoxidase in high enough concentrations, stopping formation of antheraxanthin (an intermediate) and zeaxanthin. Note that this does not mean a complete absence of zeaxanthin in dark-adapted thylakoid samples.

Because DTT was already being used as an activating agent for the ATPase in smaller amounts (100 μM), the same experiment was run in the presence of activating and inhibiting amounts of DTT (Figure 29). The zeaxanthin-related

absorbance change still occurred with the smaller amount of DTT. Note also that in no case did removal of the light result in decreases in the signal, indicating no reversion of zeaxanthin to violaxanthin despite the reversibility of this cycle. Reversal of the xanthophyll cycle is not possible in thylakoids because of the requirement for stromal enzymes and co-factors washed away during isolation.

Zeaxanthin formation is believed to induce formation of antenna quenching and would therefore stimulate a decrease in σ. Addition of DTT to reduce or eliminate its formation should also inhibit any decreases in σ that may have occurred within the observed increase in σ. Figures 30 and 31 illustrates the difference between flash saturation curves obtained in the presence and absence of inhibiting DTT. Thylakoids treated with 3 mM DTT quenched only 25% of F_{sat} compared to 40% quenching in its absence. The decrease in F_o was also eliminated by this treatment. Most interestingly, σ increased by 64% compared to only 34% in the absence of DTT. These data strongly suggest a separation of antenna- and reaction centre-based quenching within qE. Both cases displayed a further decrease in F_{sat} given a longer time to quench, but the sample without DTT appeared to have decreases in σ. These decreases were previously hidden within the overall increase in σ found for the qE samples.

One final approach to the increase was to circulate the sample without the help of ATP to maintain the quenched state (for a PAM trace, see Figure 12). These samples have been quenched, but are not significantly quenched upon reaching the flow-through detection cuvette, leaving only the source of the σ increase, assuming that it does not also require the pH gradient. In the absence of ATP and thus a pH gradient, previously-quenched thylakoids showed a σ increase of 58% compared to 27% with ATP (Figure 32). F_{sat} was only quenched 11% (only 5% of the recovered F_{sat} value). As with each of the other approaches to the observation of an increased σ, F_o was somewhat increased in the alternative approach, an effect that seems to be masked when full qE quenching was allowed to occur. However, each of these approaches also displayed σ increases of approximately the same magnitude (~60%), which was a further increase than that observed during qE. For a summary of all σ data, see Tables 4 and 5.

For a comparison of qE quenching to a known antenna quencher, 5-OH-NQ

was added to thylakoids and measurements repeated (Vasil'ev et al., 1998). Figure 33 represents PAM traces of 5-OH-NQ titrations in 3 different resuspension buffers. In all 3 cases, titration with quinone to 60% quenching of F_m (comparable to the extent of qE) was accompanied by very strong quenching of F_o, more than that for qE. The amount of quinone required to do so was affected by the presence of ascorbate, a reducing agent that could reduce the quinone (which needs to be in oxidized form to quench), and by higher pH, which turned the quinone's colour more pink than the orange-brown stock solution (Figure 35). Ascorbate was removed from the resuspension buffer in all subsequent experiments where quinone is concerned. Figure 34 shows the results of an absorbance assay on the spectral shape of 5-OH-NQ at different pHs. There was a shift in a peak in the visible region, but no effect was apparent in a UV-region peak (252 nm) that is associated with the absorbance of the ringed quinone structure itself. Coupled with the fact that the degree of F_o quenching is similar with respect to a similar degree of F_m quenching from another study (Vasil'ev et al., 1998), the quinone seemed to be alright for use. The higher requirement for 5-OH-NQ to obtain similar extents of quenching to that study may be the result of a higher degree of thylakoid stacking in the present study where 15 mM Mg^{2+} was used (3 mM in Vasil'ev et al., 1998). Thus, although the efficiency of quenching is not as high as in the previous study, the amount added did not exceed a reasonable addition of ethanol (<2%, see Figure 2 also).

Flash saturation curves of samples quenched by 5-OH-NQ displayed a rightward shift of the curves that indicated a smaller σ_{PSII}, along with an 18% decrease in F_o (Figure 36). When compared to a sample curve for qE quenching, it was clear that with a comparable amount of F_{sat} quenching, F_o decreased considerably more in quinone-quenched samples than in qE-quenched samples. There was also a difference in σ changes, indicating differential dependence on antenna processes in the 2 forms of quenching.

A complete summary of pump-probe data can be found in Table 4. Further comparison of the absorption cross-section experiments completed is found in Table 5. Table 5 displays pair-wise comparisons of cross-section data sets resulting from the alternative approaches to the observed increase in σ. These demonstrate that there was a decrease in absorption cross-section hidden within the increase. All 3

approaches taken illustrated the same extent of this decrease in σ during fully-induced qE quenching. Standard deviations of the data in Table 5 are calculated from those in Table 4 by:

$$\frac{\Delta\sigma_{Table5}}{\sigma_{Table5}} = \frac{\Delta\sigma_{A}}{\sigma_{A}} + \frac{\Delta\sigma_{B}}{\sigma_{B}}$$,where A and B are the Table 4 data sets being compared. Additionally, allowing thylakoids to quench for an extra 5 minutes after the first saturation curve was measured revealed a small but significant decrease in σ and F_o. There is some antenna quenching in qE, but it cannot originate solely from an antenna mechanism, based on comparison with 5-OH-NQ quenching, which is all antenna-based.

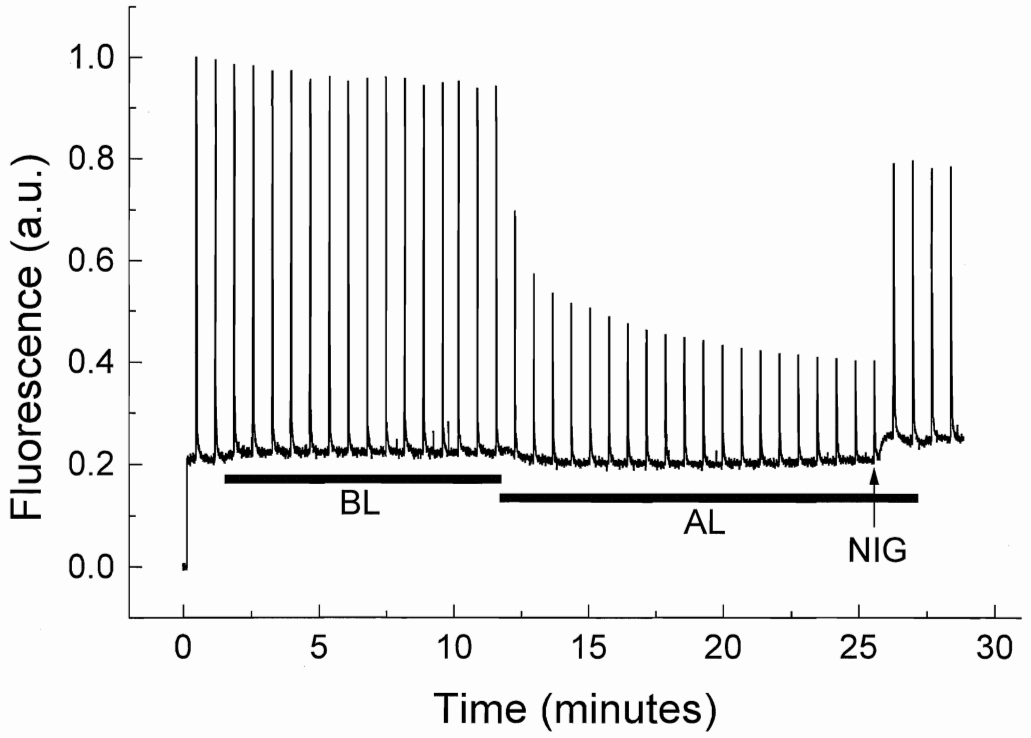

Figure 23: PAM trace from spinach thylakoids exposed to 10 minutes of S-state randomizing background light (qE=0), followed by 13 minutes of qE-inducing light (qE>0) before the addition of nigericin (qE=0 again). F_m and F_o remain stable over those time periods, more than enough time to measure flash saturation curves for absorption cross-sections of PSII.

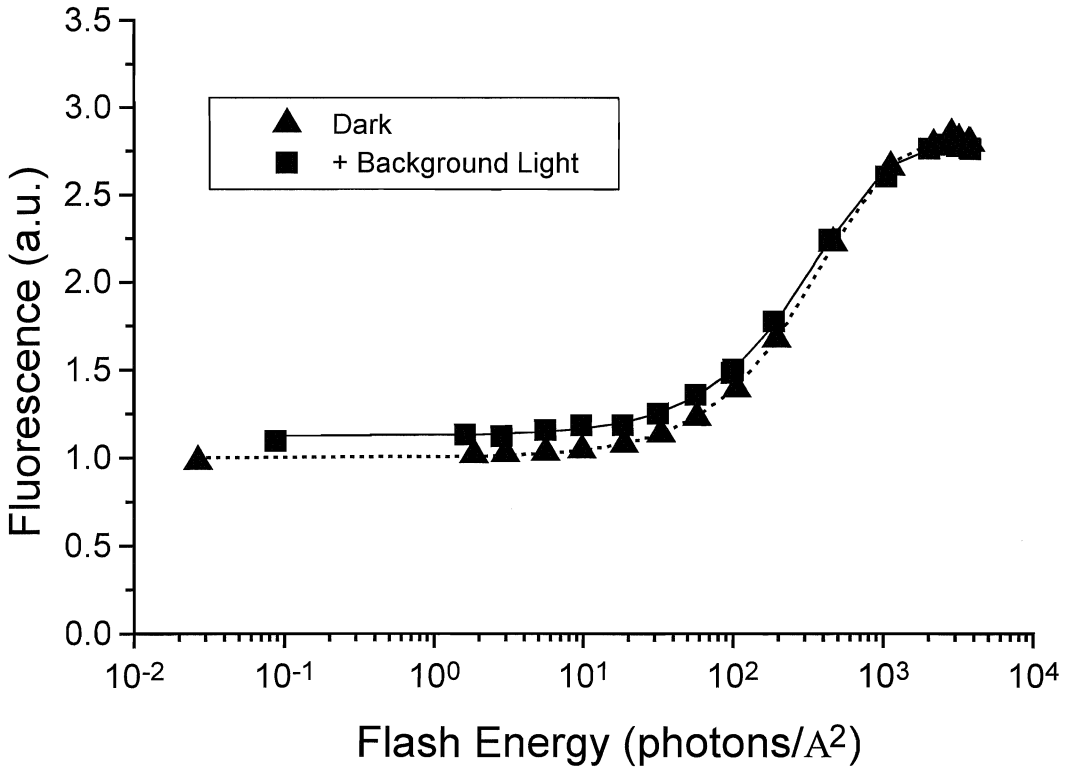

Figure 24: Flash saturation curves of a thylakoid sample in the dark (▲) and then with the S states of PSII randomized (■). Each data point represents the average of 10 individual single-turnover laser flashes from a pump-probe apparatus operated at 1.5 Hz. Fits are accomplished using a single-hit Poisson distribution, typically with computer-generated errors in cross-section measurement of less than 3%. F_o increases by 12% in the randomized sample with respect to the dark-adapted thylakoids, while F_{sat} decreases insignificantly. The absorption cross-section increases by 11% from the dark-adapted state to the randomized state, reflected in a slight leftward shift in the curve. The close association between the change in F_o and that in σ follow the classical model for PSII ($\Delta\sigma_{PSII} \approx \Delta F_o$: Vasil'ev et al., 1998; Butler, 1984).

Table 2: Same-day variability of control fluorescence parameters determined from pump-probe measurements of absorption cross-sections (σ). (± 1 S.D., n=6+)

	F_o	F_{sat}	σ
Absolute value	11.1 ± 0.4 (mV)	28.4 ± 0.7 (mV)	2.04 ± 0.07 (Å^2)
S.D. as a Percent	± 4%	± 3%	± 3%

Table 3: Fluorescence yields (F_o, F_{sat}) and absorption cross-sections (σ) obtained from flash saturation curves of thylakoid samples in the dark or exposed to S-state randomization (BL, <5 μE/m^2/sec). Values represent changes relative to dark-adapted data: F_o and F_{sat} are normalized to $F_{o\ Control}$ equal to 1, while σ control is set to 1. (± 1 S.D., n=4)

Treatment	F_o	F_{sat}	F_{sat} (relative)	σ
Dark	1.00	2.92 ± 0.16	1.00	1.00
Randomized S states	1.12 ± 0.01	2.80 ± 0.05	0.96 ± 0.03	1.11 ± 0.04

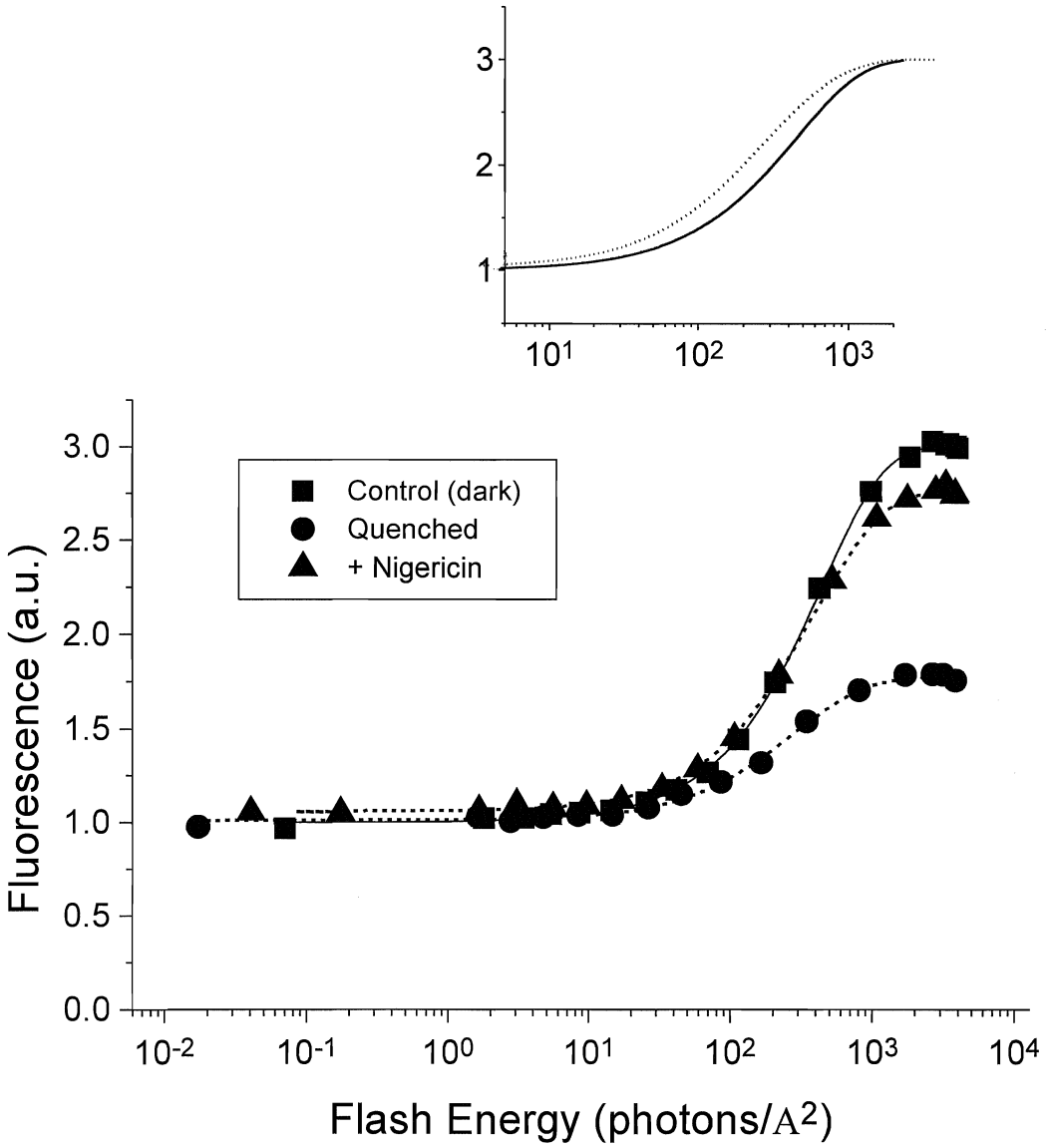

Figure 25: Flash saturation curves of a thylakoid sample in the dark (■), in the qE quenched state (●), and then after the addition of nigericin to relieve the quenching (▲). F_{sat} decreases to 59% in the quenched state, returning to 92% of pre-quenched F_{sat} after uncoupling. F_o does not show any change in the quenched state, even though the absorption cross-section increases by 53%. However, F_o and σ increase by 8% and 11% respectively after uncoupling, similar to what occurs in the case of S-state randomized samples (see Table 3). **Inset**; Normalized flash saturation curves for thylakoids in the dark (solid line) and in the qE-quenched state (dotted line), showing the shift in the curve and thus the change in cross-section.

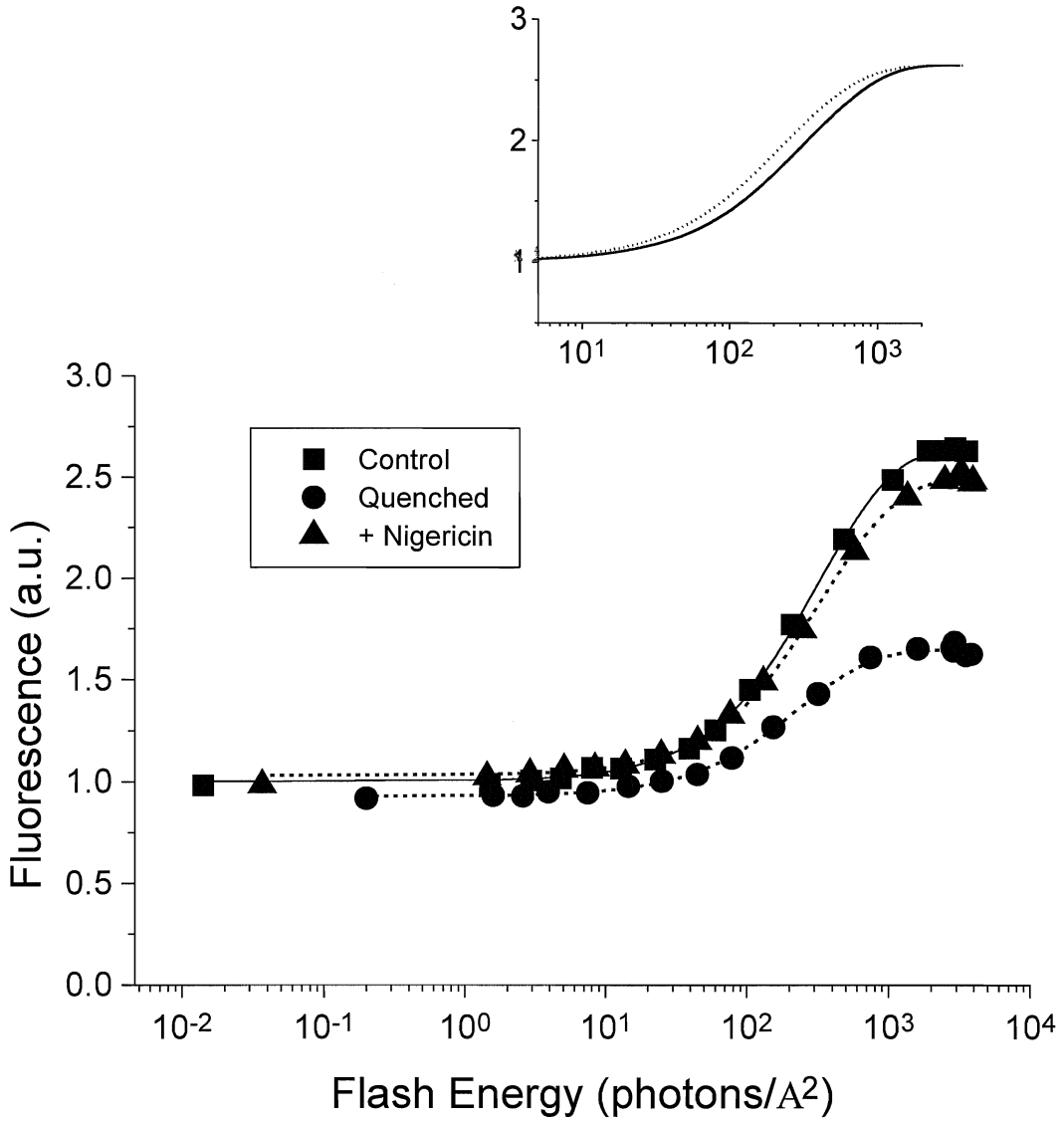

Figure 26: Flash saturation curves of a thylakoid sample with randomized S states (■), qE quenched (●), and then uncoupled by nigericin (▲). F_{sat} decreases 36% in the quenched state before recovering to 98%. F_o decreases 11% during formation of qE and almost fully recovers to the pre-illumination value. Cross-sections do not follow the F_o trend, however, increasing by 27% during qE, while returning to the control value after uncoupling. **Inset**; Normalized flash saturation curves for thylakoids exposed to S state randomizing light (solid line) and in the qE-quenched state (dotted line), showing the shift in the curve and thus the change in cross-section.

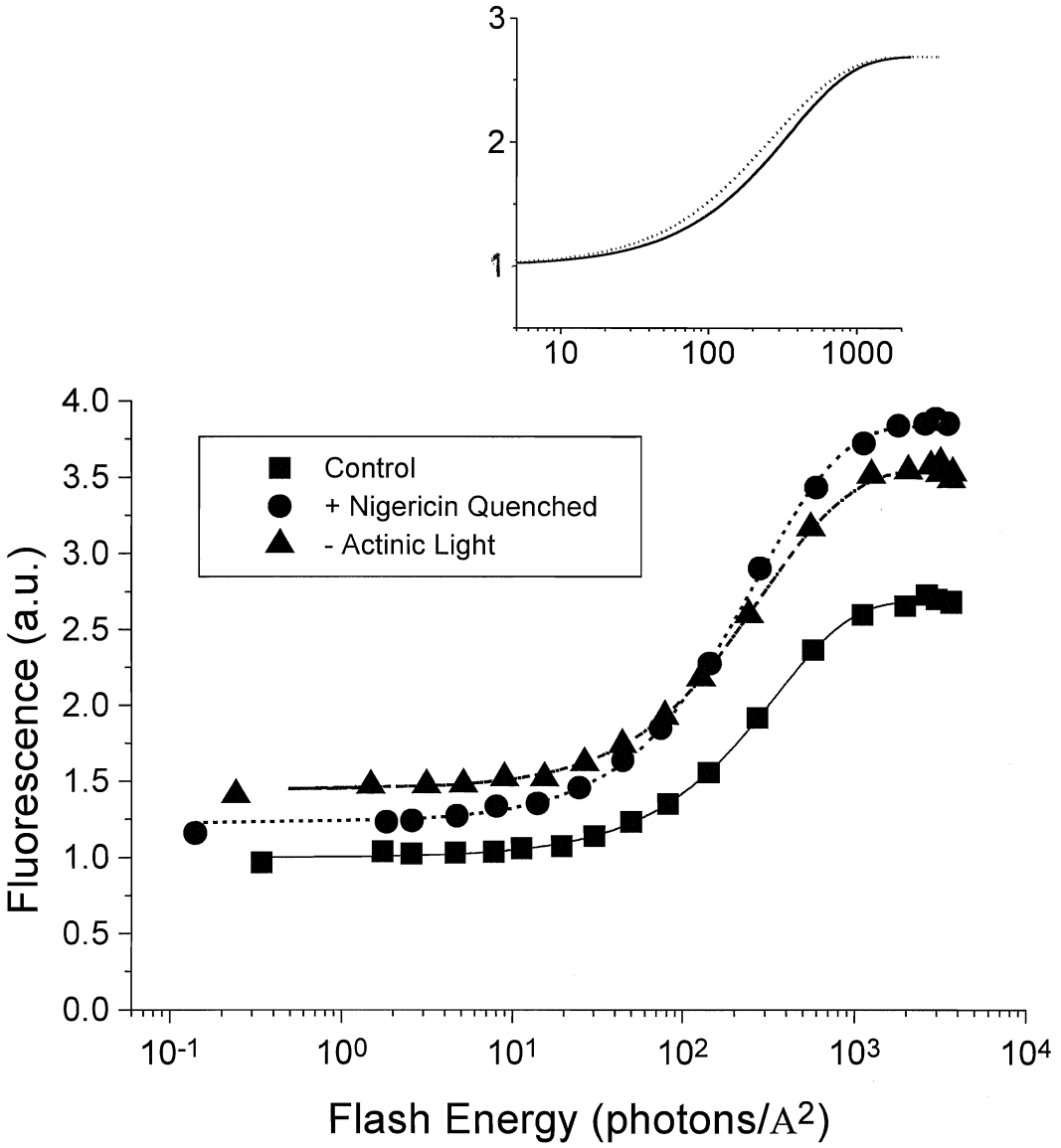

Figure 27: Flash saturation curves of a pre-uncoupled thylakoid sample with randomized S states (■), exposed to qE-inducing light (●), and then removed from exposure to the light (▲). F_{sat} increases during the qE-inducing light, approaching F_m, with F_v/F_o close to 4 as was often observed during PAM experiments. F_o increases 29% while the cross-section goes up by 59%. The post-illumination cross-section remains 29% higher than that of the control (pre-actinic light). **Inset**; Normalized flash saturation curves for pre-uncoupled thylakoids exposed to S state randomization (solid line) and during exposure to qE-quenching light (dotted line), showing the shift in the curve and thus the change in cross-section.

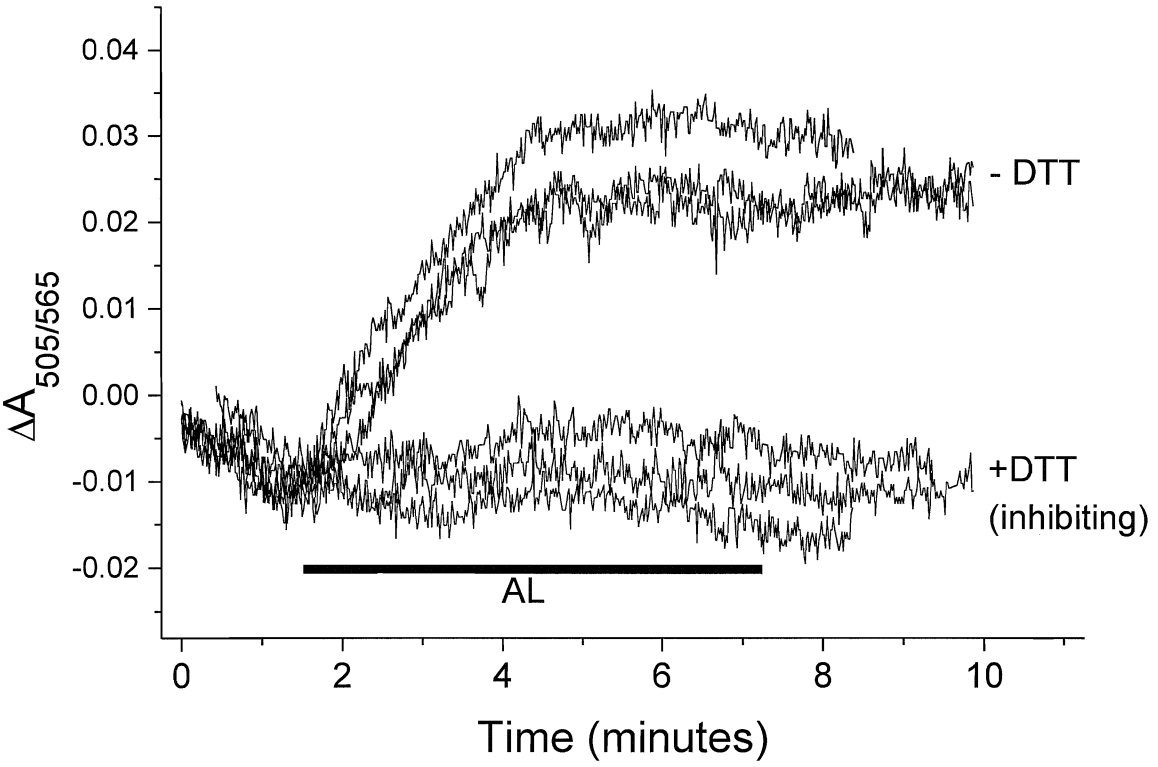

Figure 28: Light-induced absorbance changes ($\Delta A_{505/565}$) in spinach thylakoids exposed to qE-inducing actinic light for about 6 minutes. In the absence of any DTT, which is known to inhibit Violoxanthin De-epoxidase (Xanthophyll Cycle), exposure to light induces an immediate increase in 505 nm absorbance that saturates within about 3 minutes. In the presence of 3 mM DTT, no absorbance change occurs.

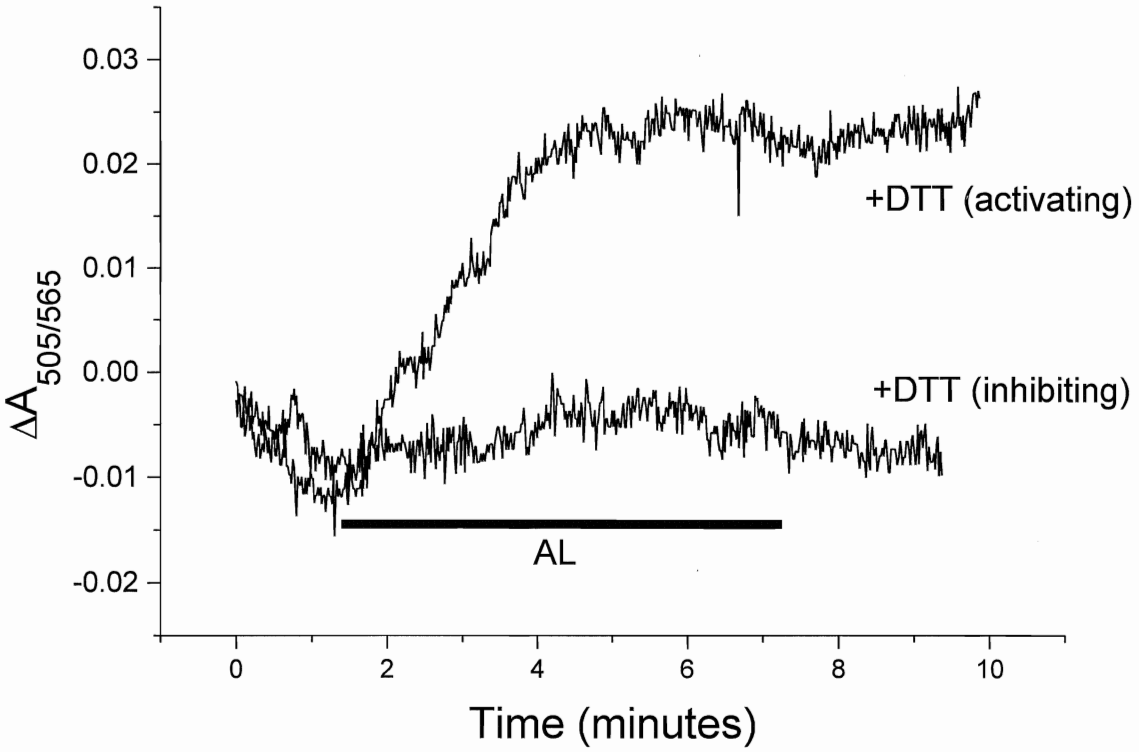

Figure 29: Light-induced absorbance changes ($\Delta A_{505/565}$) in spinach thylakoids exposed to qE-inducing actinic light for about 6 minutes. In the presence of 100 μM DTT, the amount used as a sulfhydryl activating agent for the thylakoid membrane ATPase, exposure to light is able to induce the immediate increase in 505 nm absorbance. In the presence of an inhibiting amount of DTT (3 mM), no absorbance change occurs.

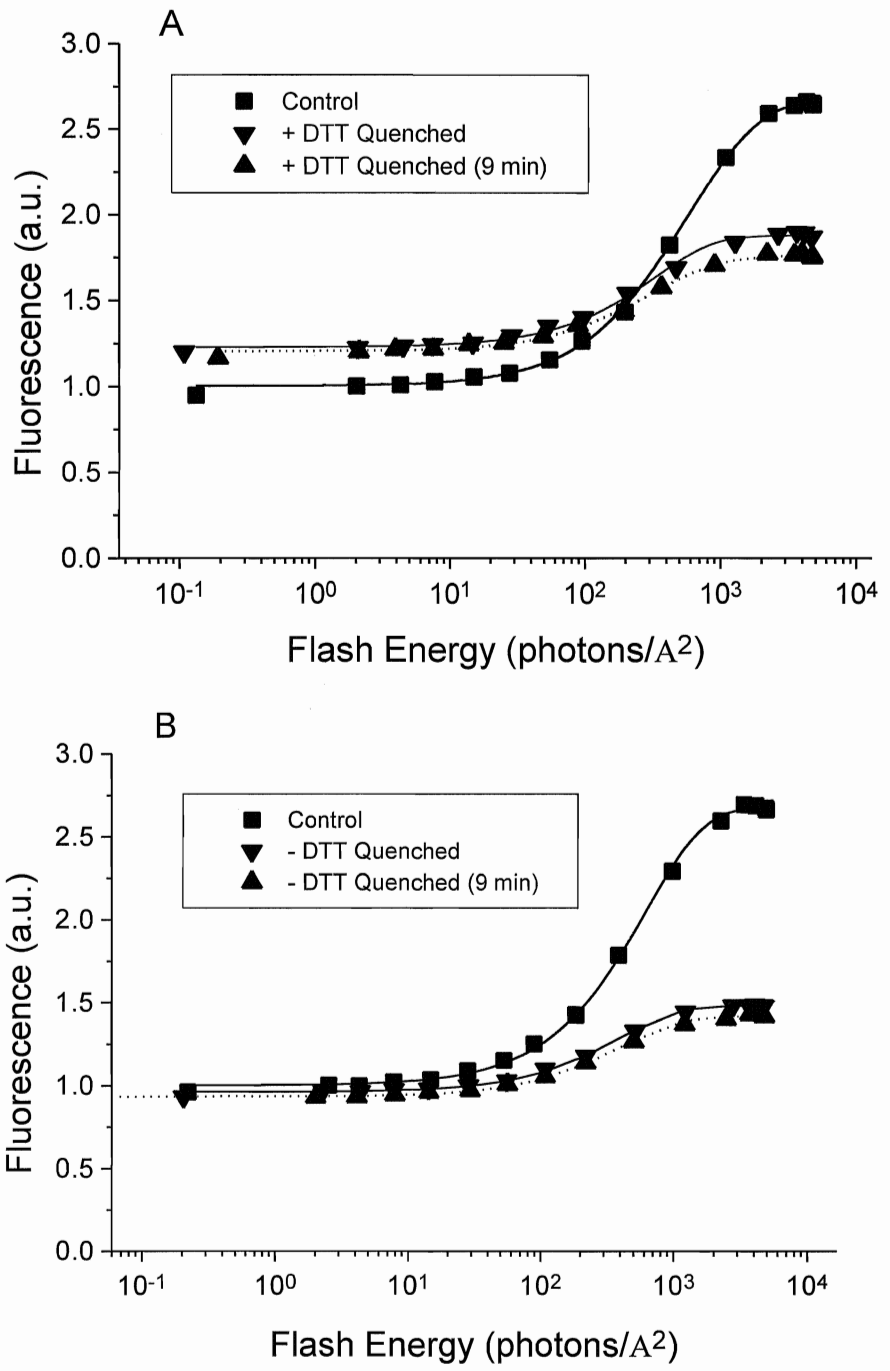

Figure 30: Flash saturation curves of thylakoid samples exposed to 4 minutes and 9 minutes of qE-inducing light in the presence (**A**) and absence (**B**) of 3 mM DTT to inhibit formation of zeaxanthin. The presence of inhibiting DTT limits the effect of qE-inducing light on F_{sat} quenching, which only decreases 25% in the inhibited sample compared to 40% quenching in the absence of DTT (full qE induction). The presence of DTT also eliminates the decrease in F_o that occurs during quenching in its absence. However, the absorption cross-section in the presence of DTT increases by 64% compared to only 34% in the absence of DTT. Given a longer time to quench, only the sample in the absence of DTT appeared to have further quenching of F_o and in fact a decrease in σ, even though both samples had further quenching of F_{sat}.

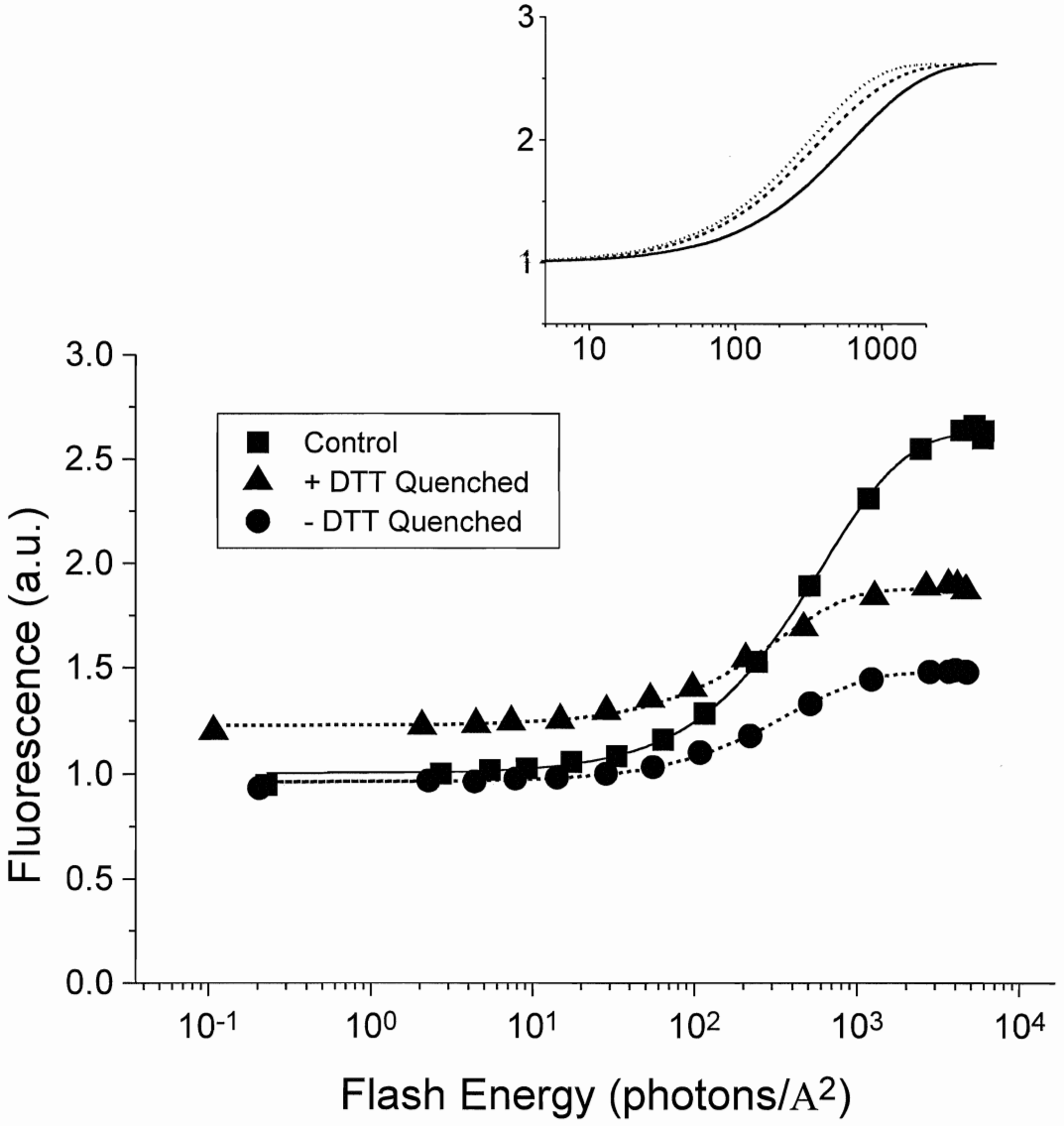

Figure 31: Flash saturation curves of thylakoid samples exposed to qE-inducing light in the absence (●) and presence (▲) of 3 mM DTT to inhibit zeaxanthin formation. There is clearly more quenching of F_{sat} and F_o in the absence of DTT than in its presence. The increase in σ is 64% and 34% in the presence and in the absence of DTT respectively. **Inset**; Normalized flash saturation curves for thylakoids exposed to S state randomizing light (qE=0, solid line), in the qE-quenched state in the presence of DTT (dotted line), and in the qE-quenched state in the absence of DTT (dashed line), showing the shift in the curve and thus the change in cross-section.

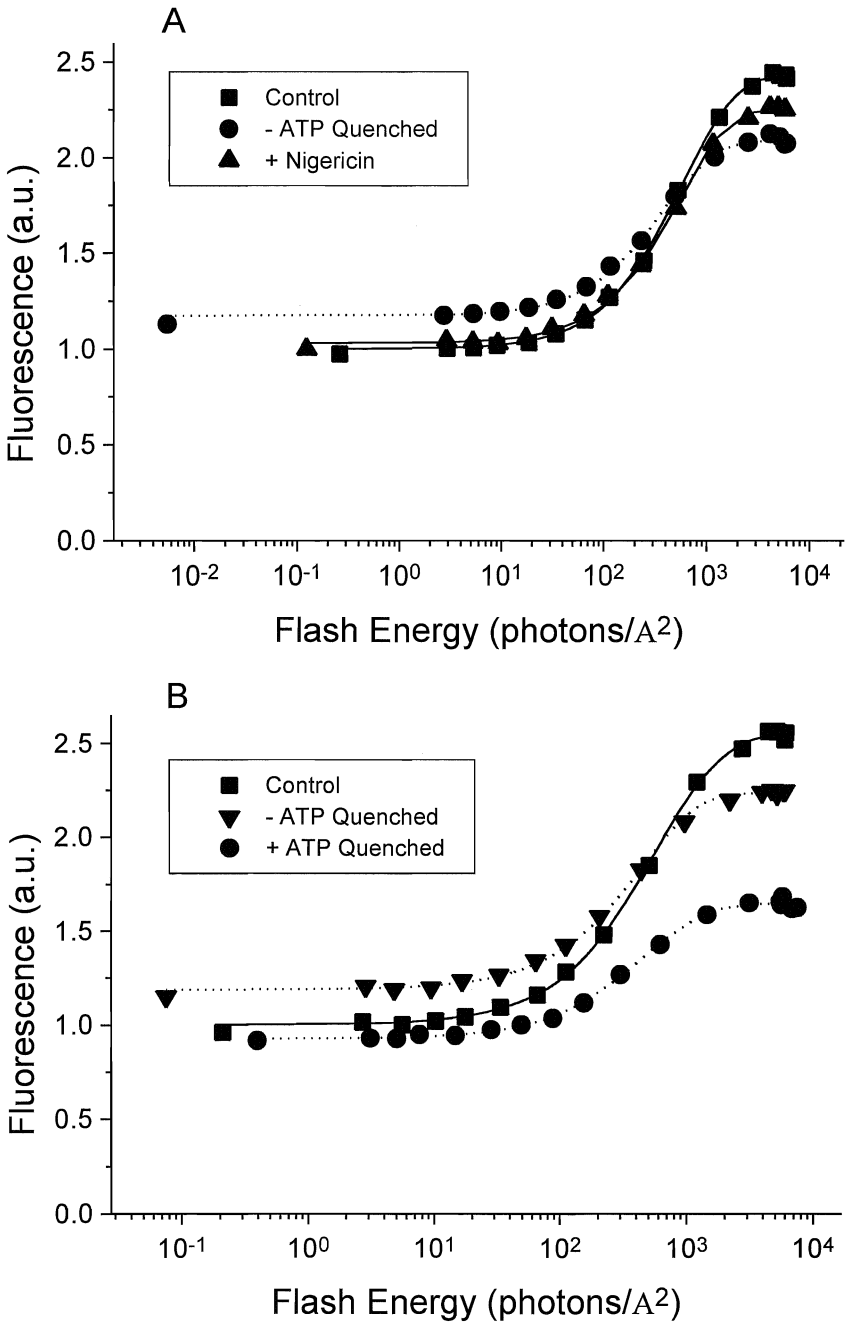

Figure 32: Flash saturation curves of thylakoid samples circulated without ATP, and exposed to qE-inducing light. **A**; Thylakoids without ATP exposed to qE-inducing light. **B**; Direct comparison of flash saturation curves of thylakoids exposed to qE-inducing light with and without ATP added (quench held and not held, respectively). In the absence of ATP to hold a pH gradient across the thylakoid membranes, there is significantly less quenching of F_{sat} (11% of control, 5% of post-illumination F_{sat}) and an elevation of F_o compared to quenched thylakoids with ATP added. The cross-sections increase 58% with no ATP, compared to 27% with ATP, and returned close to the control value once uncoupled by nigericin (shown in **A**).

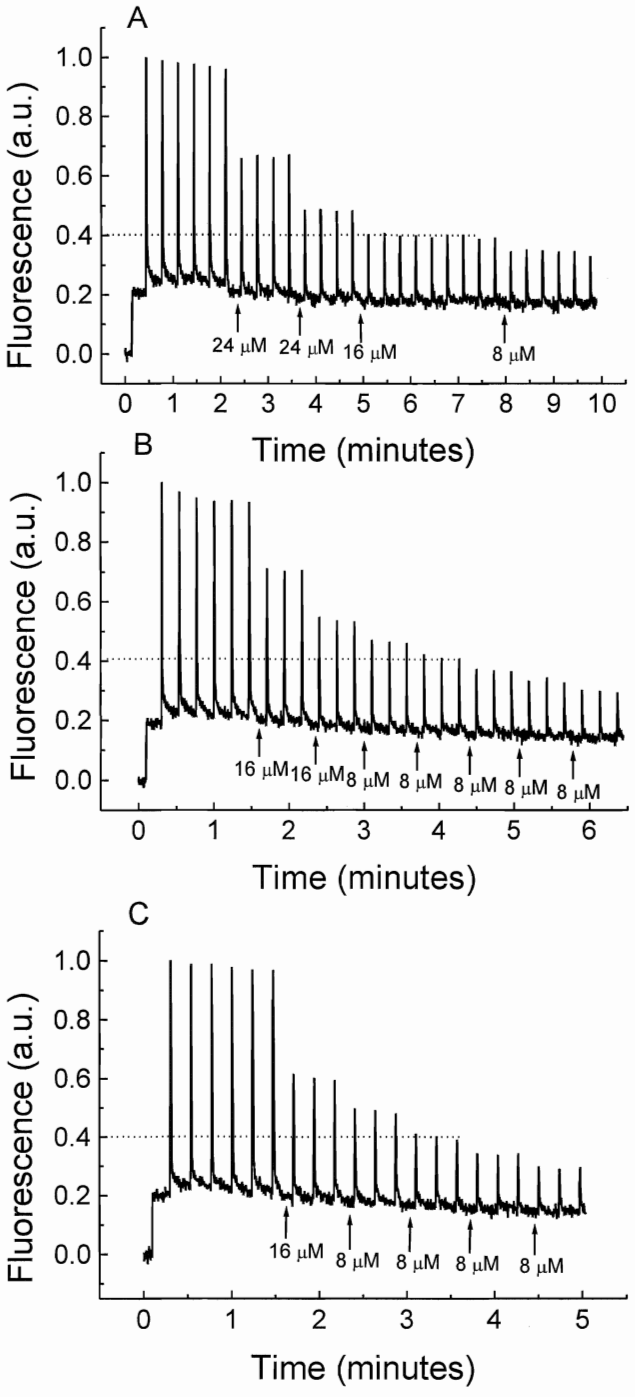

Figure 33: PAM traces of spinach thylakoids titrated with the antenna fluorescence quencher 5-OH-NQ using 3 different resuspension buffers. Along with the quenching of F_m, there is very strong quenching of F_o in all 3 cases. Concentrations refer to additions of 5-OH-NQ at the points indicated. Dotted lines show the titration to 60% F_m quenching.
A; Buffer pH 7.8, with 30 mM ascorbate **B**; Buffer pH 7.8, no ascorbate **C**; Buffer pH 7.0, no ascorbate.

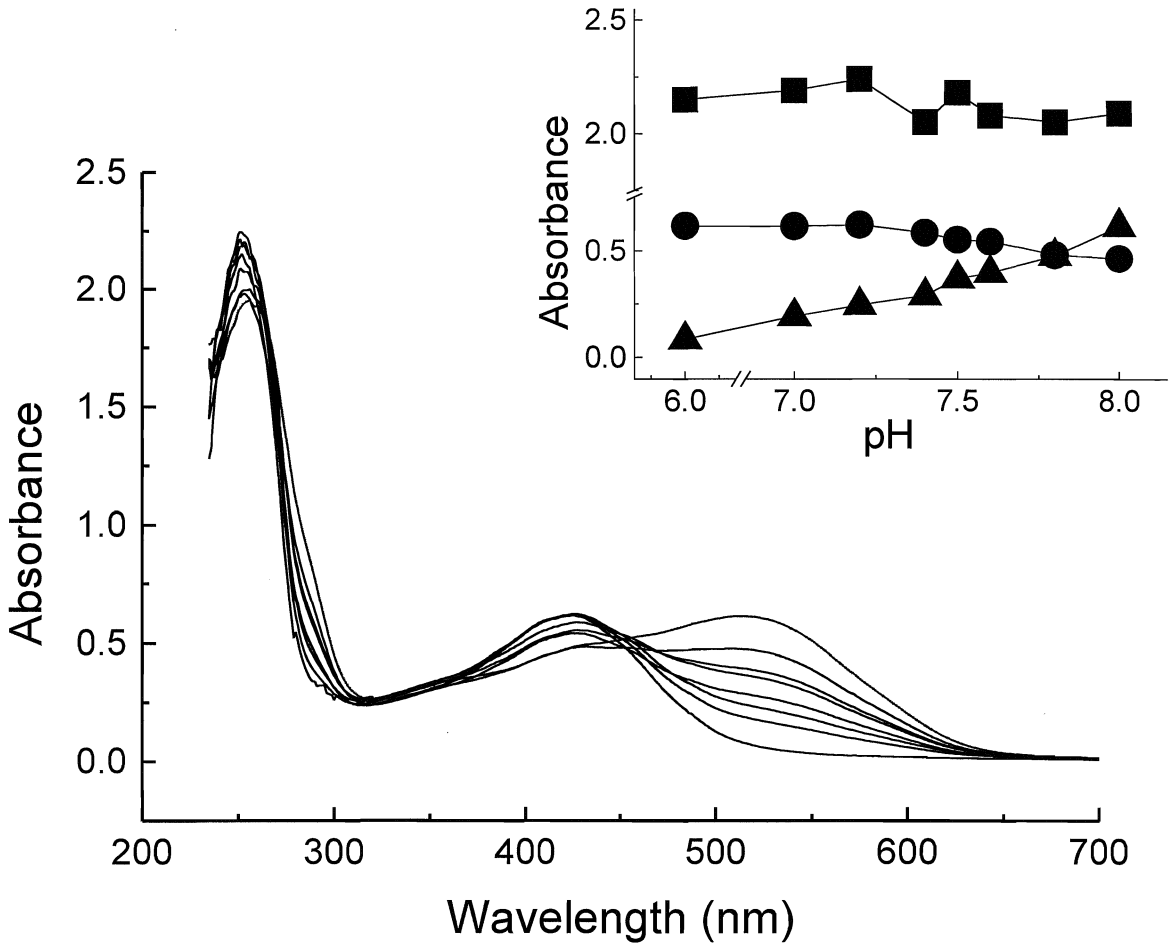

Figure 34: Absorbance spectra of 5-OH-NQ in resuspension buffers of varying pH, from pH 6 to pH 8. **Inset**; Absorbance values of the 3 peak wavelengths seen in the absorbance spectra of 5-OH-NQ versus pH. ▲ - 513 nm peak ● - 425 nm peak ■ - 252 nm peak. The UV peak (252 nm) changes very little as pH changes, but there is a distinct shift from the other narrow peak at 425 nm toward the broader 513 nm peak as pH increases.

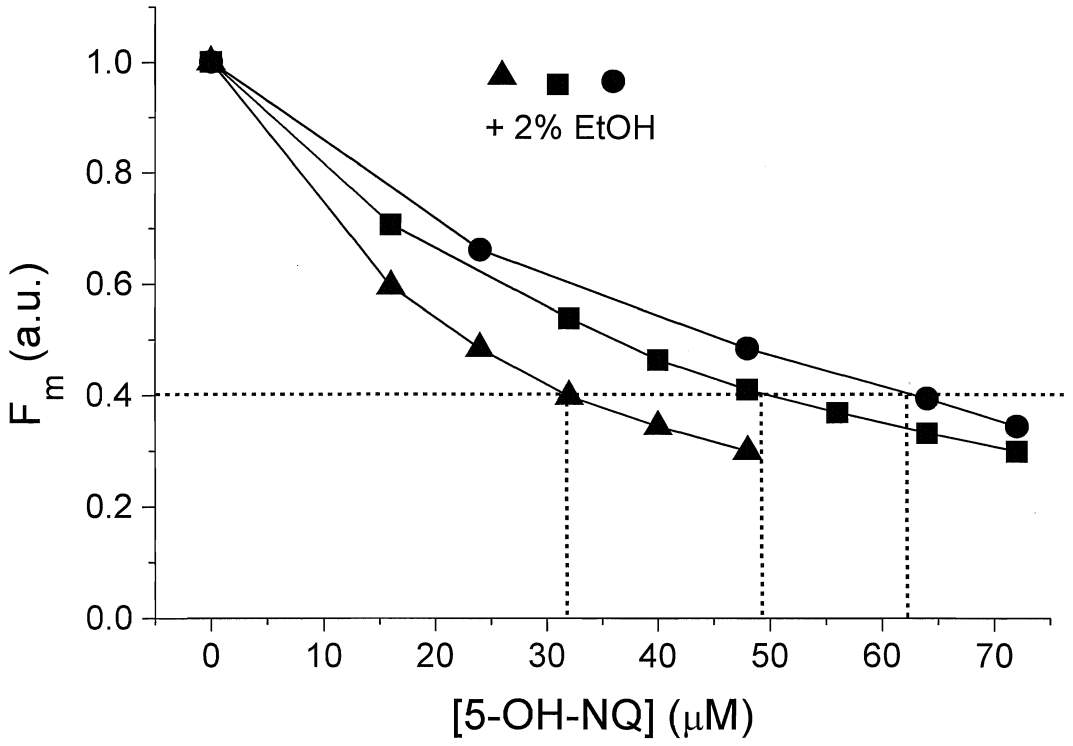

Figure 35: Results of the titration of F_m with 5-OH-NQ using 3 different resuspension buffers. ▲ - pH 7.0, no ascorbate ■ - pH 7.8, no ascorbate ● - pH 7.8 with 30 mM ascorbate. Each titration resulted in a different quinone concentration requirement to reach 60% quenching of F_m. Without ascorbate, it required less than with it, and pH 7.0 required less than pH 7.8. At pH 7.8, about 48 μM was needed, while the addition of ascorbate increased that to 64 μM, and at pH 7.0, only 32 μM was needed. The 3 symbols at the top refer to the addition of 2% ethanol to thylakoids. (5-OH-NQ stock 4 mM in absolute ethanol)

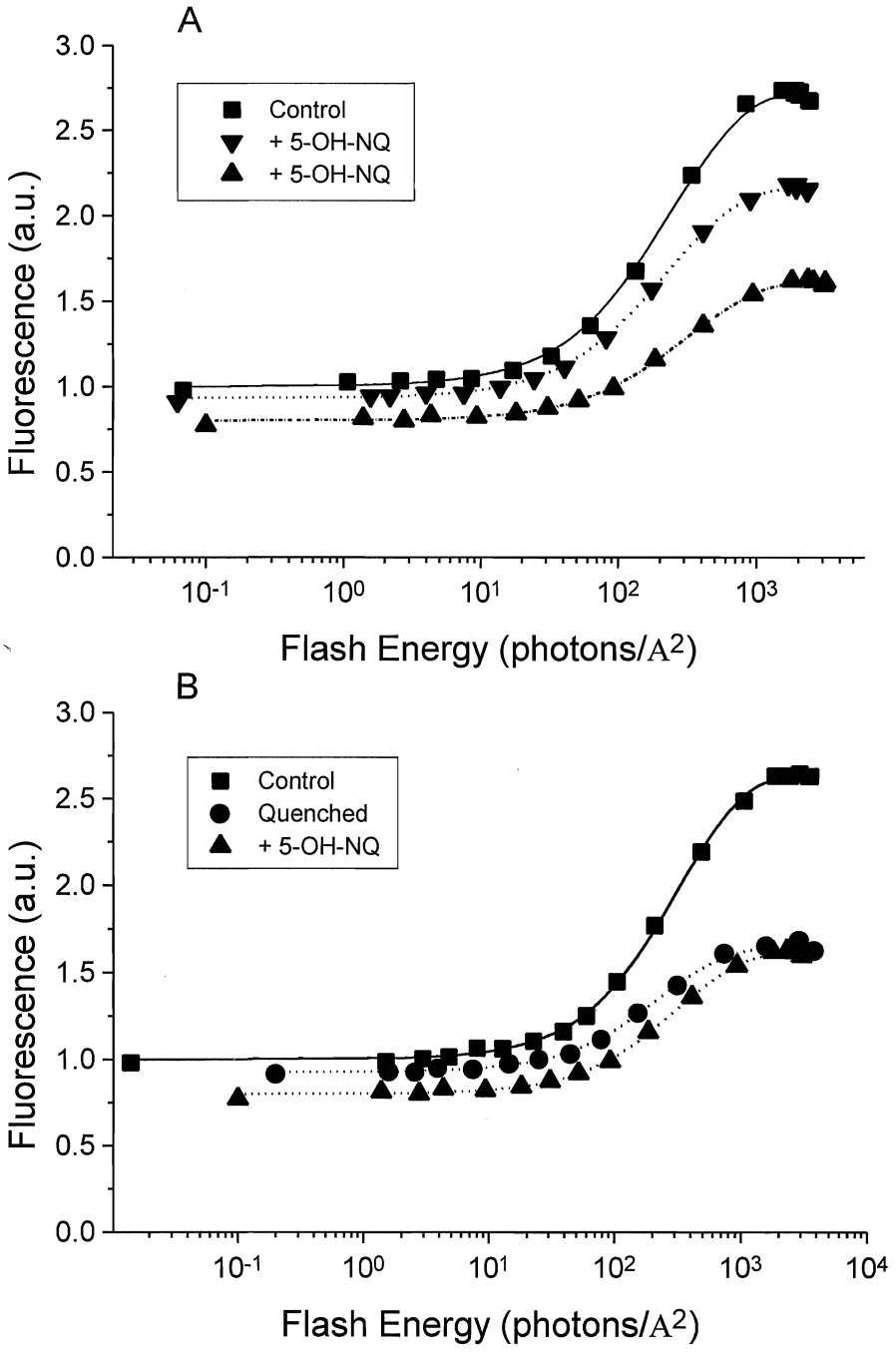

Figure 36: Flash saturation curves of thylakoid samples quenched by the antenna quencher 5-OH-NQ (**A**), and a direct comparison of flash saturation curves for qE-quenched and quinone-quenched thylakoids (**B**). **A**; Quinone-quenched PSII quenches both F_{sat} and F_o effectively. Addition of 24 μM decreases F_o approximately 10%, while addition of another 24 μM to get F_{sat} down to the same level as in qE-quenched thylakoids quenches F_o 18%, along with a decrease in σ of 11%. **B**; Comparison of quinone-quenched and qE-quenched samples reveals that F_o decreases considerably more due to 5-OH-NQ than due to qE when F_{sat} is quenched the same amount. The same is seen for σ.

Table 4: Fluorescence yields (F_o, F_{sat}) and absorption cross-sections (σ) obtained from flash saturation curves of thylakoid samples with various treatments. Except for the addition of 5-OH-NQ, which uses no actinic light, all treatments include exposure to background light (BL, <5 μE/m^2/sec) during the control followed by exposure to the actinic light (AL) used for induction of qE. Uncoupled refers to reversal of qE quenching by the addition of 1 μM Nigericin. Pre-uncoupled refers to addition of 1 μM Nigericin before exposure to actinic light. Values represent changes relative to control data: F_o and F_{sat} are normalized to $F_{o\ Control}$ equal to 1, while the σ control is set to 1. (± 1 S.D., n=3+)

Treatment	F_o	F_{sat}	F_{sat} (relative)	σ
Control (+ BL)	1.00	2.44 ± 0.15	1.00	1.00
qE	0.89 ± 0.04	1.56 ± 0.07	0.64 ± 0.03	1.27 ± 0.08
Uncoupled	1.04 ± 0.03	2.39 ± 0.12	0.98 ± 0.05	1.04 ± 0.08
+ 5-OH-NQ	0.82 ± 0.01	1.49 ± 0.07	0.61 ± 0.03	0.89 ± 0.06
Pre-uncoupled	1.29 ± 0.06	3.61 ± 0.04	1.48 ± 0.04	1.59 ± 0.13
- AL	1.42 ± 0.03	3.17 ± 0.06	1.30 ± 0.02	1.29 ± 0.06
- $DTT_{activating}$	0.88 ± 0.02	1.44 ± 0.03	0.59 ± 0.01	1.34 ± 0.08
+ $DTT_{inhibiting}$	1.16 ± 0.04	1.83 ± 0.07	0.75 ± 0.03	1.64 ± 0.07
- ATP	1.19 ± 0.03	2.17 ± 0.03	0.89 ± 0.01	1.58 ± 0.11
- AL	1.05 ± 0.05	2.29 ± 0.06	0.94 ± 0.02	1.09 ± 0.12

Table 5: Pair-wise comparisons of related data sets from pump-probe measurements of fluorescence yields and absorption cross-sections (from Table 4). Values shown represent the second data set of the paired treatments relative to the first data set (2nd set value divided by the 1st set). Numbers in the brackets represent F_{sat} compared to the control value for unquenched F_{sat} (2.44). (± 1 S.D., n=3+)

Treatment Pair	F_{sat} (relative)	σ
Pre-uncoupled → qE	0.43 ± 0.02 (1.05)	0.80 ± 0.12
- ATP → qE	0.68 ± 0.04 (1.66)	0.81 ± 0.11
+ $DTT_{inhibiting}$ → - $DTT_{activating}$	0.79 ± 0.05 (1.93)	0.82 ± 0.08
+ $DTT_{inhibiting}$ → qE	0.85 ± 0.07 (2.07)	0.77 ± 0.08
4 min qE → 9 min qE	0.97 ± 0.02 (2.37)	0.94 ± 0.04

Picosecond Decay Kinetics and Kinetic Modelling

Figures 37 to 53 and Tables 6 to 20 describe the results of picosecond fluorescence decay kinetics experiments, global fitting analysis, and global target analysis on decay data obtained from spinach thylakoids under various quenched and unquenched conditions.

Global lifetime analysis

Typical fluorescence decay curves for thylakoids in the F_o state measured at 685 nm are shown in Figure 37A. Fluorescence decay curves were recorded for 8 detection wavelengths between 680 and 730 nm. The data were analyzed by global fitting to the instrument response function (IRF), taken at the beginning and end of each sample set of 4 decay wavelengths, with a sum of 5 exponential decays to obtain fluorescence lifetimes and amplitudes that give corresponding decay-associated spectra (DAS, Figure 37B). As previous studies have shown, weighted residuals (Figure 38 for F_o and 44 for F_m) and χ^2 values demonstrated that 5 components are necessary in order to fit this data at both F_o and F_m (Vasil'ev & Bruce, 1998; Wagner et al., 1996; Roelofs et al., 1992). Some shift of the IRF was required to fit many of the decay curves due to random instrument drift with respect to the time reference, so they were modelled in this way during fitting. There was also a small amount of background observed before the excitation pulse, due to light scattering, that was modelled by allowing the background to fit as a constant over the entire time window of measurement. Figure 46 possesses a little bit of this background for F_m compared to the IRF, but it amounts to just 0.01% of total fluorescence emission.

The DAS shown in Figure 37 (F_o) and Figure 43 (F_m) help to assign identities to the components. In all of the conditions, the fastest component had a lifetime of 11 ps and was identified as exciton equilibration within the antenna complexes of PSII and PSI. The second fastest lifetime component (100 to 110 ps) had a red-shifted amplitude peak around 720 nm in all states and could thus be assigned to emission from PSI, although at F_o a second peak around 685 nm suggested incomplete component separation and thus a partial origin in PSII. The third and fourth decay components (τ_3 and τ_4) in both states had similar spectral shapes with peaks at 685

nm and very little emission in the longer wavelengths, and so were assigned to PSII. The slowest component, τ_5 (3.1 ns), which had negligible presence at F_o and appeared much stronger at F_m was assigned to the closure of PSII traps, as Q_A became saturated.

Qualitatively, the DAS were almost identical to those in Vasil'ev and Bruce (1998), including the DAS for the addition of 5-OH-NQ to F_m, despite running experiments at room temperature in the present study compared to 0°C for the previous study. Two major differences were a relatively large amplitude for the exciton equilibration component, and a smaller amplitude for the PSI component, the latter possibly related to the higher degree of thylakoid stacking in the present study ($[Mg^{2+}]$ >3 times higher) or a poorer separation of this component from the fastest PSII component. The lifetimes obtained for the present study were also consistent with those found in the previous study despite the alterations in resuspension and temperature (Table 7).

Figures 37, 39, 43, and 45 demonstrate the reproducibility of decay kinetics obtained independently at 685 nm. With the exception of dark-adapted F_o (Figure 37), repeats at each state appeared identical across the entire collection time-frame. The main differences in the F_o repeats occurred in the slower region, beyond 4 ns, where the difference on the logarithmic scale is limited to approximately 100 counts in 20 000 for the peak channel (<2% of total fluorescence yield). In addition, all repeats fit well to the excitation pulse front indicated by the IRF. From here, discussion is limited to individual repeats that were completely fit and modelled by the global target analysis.

Figures 38 and 44 illustrate the weighted residuals generated from global analysis of decay kinetics from spinach thylakoids at F_o and F_m. There is random distribution about the median at every wavelength, except for some extra noise below 1.5 ns that corresponds to a region before the actual beginning of the decays. Allowing that region to fit, the global χ^2 was 1.14 at F_o and 1.34 at F_m. Substantial improvement in the fit quality was achieved by cutting some of this pre-decay noise from the fitting. At F_o, the improvement was to a χ^2 of 1.11, while the effect was more pronounced at F_m where the χ^2 improved to 1.21 from 1.34. The decays from all other states investigated were fit with this is mind. A summary of DAS normalized to

fluorescence spectra for all states, including the χ^2, is given in Table 8.

With respect to the quinone-quenched decay kinetics, the decay was taken from a solution of 5-OH-NQ in pH 7.8 resuspension buffer as a control (Figure 40). Quinone did not have any decay of its own, with a slight hint of the IRF appearing in its decay, amounting to less than 0.5% of the counts in its peak channel compared to the peak number of counts for the IRF.

Figure 41 illustrates the typical decay kinetics for the 4 states collected from F_o (F_o dark, F_{RS}, F_o' with qE quenching, F_o' with 5-OH-NQ). Compared to F_{RS} (randomized S states), F_o has an accelerated decay in the fast components but nearly the same decay in the longer components. The qE-quenched sample is also faster in the fastest components than F_{RS}, although the 2 converge in the slowest components. The decay of the qE-quenched sample was nearly identical to that of F_o. This indicates that the poise of the S states when PSII is dark-adapted (F_o in the dark) had a quenching effect, with respect to the randomized S state, which was similar to that observed for qE - that is, both are antenna quenched compared to the randomized S states (see discussion). The antenna-quenched state where 5-OH-NQ was added is clearly the most accelerated, especially in the fast components, remaining approximately parallel to F_o in the slower region. Even though 5-OH-NQ was titrated to give the same fluorescence yield from the system and each set of data was collected up to 20 000 counts, quinone-quenched and qE-quenched samples had clearly different kinetics.

The overall yield of fluorescence at F_o was also calculated from the single photon counting apparatus (decay kinetics). Table 6 shows how changes in fluorescence parameters appeared in the 3 types of data collected. For comparable degrees of saturation quenching (F_m or F_{sat}), F_o was quenched significantly more by addition of the antenna quencher 5-OH-NQ than by induction of qE. This simple analysis of yields from all 3 methods demonstrates that qE cannot be the result of only antenna quenching.

Because no chemical modification of PSII reaction centres was used to stabilize F_m, such as DCMU, the relaxation kinetics of variable fluorescence were measured after saturating multiple turnover light of about 2 seconds duration (PAM) to be sure that F_m was being reached and maintained during circulation through the

single photon counting apparatus' detection zone. The millisecond time course of F_m decay is shown in Figure 42 (composite of 10 individual decays), where the saturating actinic light is removed by closing of a shutter at 29.4 ms on the x-axis. In the case of this saturation, the decrease in the fluorescence yield from its maximum value to that at the moment of measurement (750 µsec after the saturating pulse) was less than 3%. This is considerably more loss than that reported for this apparatus by Vasil'ev and Bruce (1998), however, the presence of the electron acceptor methyl viologen in the present study produced this faster re-oxidation of the PQ pool and of Q_A. Nevertheless, fluorescence decays collected at F_m are assured to be at least 97% of actual F_m yield.

Figure 46 illustrates the typical decay kinetics for the 3 states collected at F_m (unquenched, qE-quenched, and quinone-quenched). The F_m condition had much slower kinetics than did F_o, taking more than 5 times longer to decay 90% of fluorescence, since approximately 4 times as much fluorescence was emitted at F_m ($F_v/F_o \approx 3$), originating from the dramatic increase in both lifetimes and amplitudes for the 3 PSII components due to trap closure (Table 7). With trap closure, much more decay is associated with longer lifetime reaction centre components. Both quinone-quenched and qE-quenched kinetics were considerably accelerated compared to the F_m condition. However, addition of 5-OH-NQ to thylakoids did not succeed in approximating the qE-quenched kinetics. The qE kinetics were faster than quinone in the fastest components, but became considerably slower in the longer components of the curve, becoming slower than even the slow components of the unquenched control curve, converging toward it. The quinone-quenched kinetics, on the other hand, appeared to be mainly quenched in the fast components, remaining more parallel to the F_m control in the slower region.

Since the exciton equilibration component remained essentially the same in all states, it could be removed from the DAS before normalizing the sum of all decay components to the room temperature fluorescence spectra from spinach thylakoids. Normalization gives a relative amplitude to all components and allows direct comparison of components in different states. The fluorescence spectra from chlorophyll a with and without 5-OH-NQ added are shown in Figure 47. There was clear quenching of fluorescence with quinone, but the spectral shape did not change,

with a peak at 682 nm and a shoulder around 720 to 740 nm. Figures 48 and 49 are the normalized forms of DAS at F_o and F_m. Table 8 also summarizes the resulting DAS and gives the χ^2 values, which ranged from 1.09 to 1.18 for measurements taken at F_o and from 1.12 to 1.21 for F_m.

Analysis of the normalized DAS at F_o reveals that the longest component (3.1 ns) is negligible in all cases, all but completely disappearing in the quinone-treated kinetic. The removal of the long component by quinone may be due to a lack of resolution within the tiny amplitude of that component. What little was there can be attributed to a limited number of closed centres. Very little effect is exhibited in the PSI component in any state, except that its PSII-associated peak is mildly quenched in a few cases, and the quinone-quenched sample showed a slight decrease in the PSI peak, since 5-OH-NQ quenches in the antenna of PSI as well (Lee et al., 1992). The 2 intermediate PSII components were affected the most. The fast PSII component dominated all states, although it was less affected by quenching than was the slower PSII component, an effect very similar to that observed in a previous study for quinone at F_o (Vasil'ev et al., 1998). However, the smaller effect on the faster component may be the result of incomplete resolution of the PSI component from PSII, since there is considerable quenching in the PSII-associated portion of the PSI component. Quinone quenches the longer PSII antenna component more than qE, while the faster PSII antenna component remains more dominant in the quinone-quenched sample. Thus, the DAS for additions of quinone and for qE-quenched thylakoids are qualitatively and quantitatively different.

Inspection of the normalized DAS at F_m similarly demonstrates a difference in DAS between qE- and 5-OH-NQ-treated thylakoids. Compared to F_o, the longest 2 PSII components became dominant (3.1 ns PSII closed, 1.5 ns PSII), as expected when Q_A becomes saturated (fully reduced). The PSI component exhibited a similar effect in both qE and quinone kinetics, while the closed PSII component almost completely disappeared, especially in the quinone example. The intermediate PSII components were affected most, exchanging dominance in the qE-quenched sample, but not in the 5-OH-NQ kinetics. The slower PSII kinetic decreased in both lifetime and amplitude for both quenched states compared to F_m while the opposite was true for the faster PSII decay component (both increased in lifetime and amplitude).

Kinetic Analysis

Relying on the DAS to provide mechanistic information is unreasonable due to the variety of factors that may affect each lifetime component. To reveal more specifically the molecular mechanisms which might explain qE quenching in thylakoids, kinetic modelling was completed using global target analysis with the Reversible Radical Pair model (Figure L8, Schatz et al., 1988). According to this model, PSII can be defined by a set of rate constants (k_A, k_{PC}, k_{PC}^-, k_D) and by an amplitude related to the relative amounts of the total chlorophyll content that can be attributed to PSII. At F_m, kinetics must be described by a heterogeneous model containing 2 distinct populations of PSII, PSIIα and PSIIβ (Vasil'ev & Bruce, 1998; Roelofs et al., 1992). However, the exact nature of the PSIIβ centres is unclear. Some suggestions involve inactive electron transport to PQ (Chylla & Whitmarsh, 1987), differences in antenna size and protein composition (Jansson et al., 1998), or it could be both. Two additional components were added to the model to account for the non-PSII-associated decay components (PSI and exciton equilibration).

Only three of the four rate constants for the model can be determined independently with any accuracy because of the large number of variables available to fit. Better separation of the PSII components was expected given minimal constraints placed on the data. First, the exciton equilibration component was fixed to reflect its unchanging kinetic contribution to each state measured in the present study. Second, the component for PSI emission was fixed to the lifetimes and amplitudes previously calculated by the global lifetime analysis for each state. The compound nature of this component (PSII peak included) at first seems to complicate this restriction. However, it is reasonable because the 3 PSII components are replaced by 4 rate constants, resulting in improved separation from the PSI emission. Figure 50 illustrates that the RRP model applied to fitting qE-quenched samples at F_m reduced the PSII emission within the 100 ps component by approximately 75%, separating it out of the DAS so that the quenched state looks more like the well-resolved F_m state. Finally, k_A was set to constant values in the controls at F_o and F_m, corresponding to the fluorescence lifetime of isolated light-harvesting antennae of 3.3 ns (0.3 ns^{-1} at F_m, Hodges et al., 1987), and to the rate constant at F_o and F_{sat} (0.83 ns^{-1}, Vasil'ev & Bruce, 1998). All of these constraints have previously been shown to

be reasonable (Vasil'ev & Bruce, 1998).

The values of the rate constants obtained for F_o and F_m in the absence of qE are shown in Table 9, as compared to those obtained by Vasil'ev and Bruce (1998). The values for the rate constants are in reasonable agreement with the previous study. As expected, the rate of the primary charge separation was high and its reversal was low at F_o owing to the open reaction centre, which allows efficient electron transport to Q_A. At F_m, k_{PC} decreased significantly while k_{PC}^- increased, indicating limited affinity for the electron at saturated Q_A^-. The only difference from the pattern displayed by the previous study was a slight increase in the k_D upon closure of the reaction centres. The k_D is expected to decrease due to limited transfer to Q_A. However, note that the PSIIα/PSIIβ ratio used in Table 9 was 1.0, an unlikely equality for the PSIIα and PSIIβ subpopulations. More generally-accepted ratios of 2- or 3-to-1 (~20-30% PSIIβ; Melis, 1985), exhibited in Table 14, displayed the expected decrease in k_D. It should also be noted that in the case of the higher ratios, the PSIIβ obtained very low values for charge separation (k_{PC}), and extremely high values for its reversal, k_{PC}^-. This might be expected in closed PSII if the nature of β centres were inactivity in PQ reduction, and should appear as a monoexponential component at F_m, like the 3.1 ns component that did not have any significant contribution at F_o, but dominated at F_m.

Kinetic modelling of qE at F_o

Having determined the PSII rate constants for the control states, it was possible to test the kinetic model with respect to the effects of the different states for which decay kinetics were collected. The rate constants for the control states were linked in various combinations to those from other conditions, fixing some rate constants to the control value while allowing others to change. At minimum, one rate constant was fixed (single link), at maximum 3 (triple link). In addition, a predicted change in absorption cross-section could be calculated from the rate constants, according to Vasil'ev et al. (1998):

$$\frac{\sigma}{\sigma_{\text{Quenched}}} = \frac{\Phi}{\Phi_{\text{Quenched}}} = \frac{k_{A,\text{Quenched}} + k_{PC} - k_{PC}^-}{k_A + k_{PC,\text{Quenched}} - k^-_{PC,\text{Quenched}}}$$

This procedure permitted the modelling of what rate constants were most likely to require changing in order to produce the quenched states from the control states.

Table 10 shows the results of the global target analysis of F_o linked with the kinetics for randomized S states. Allowing only one constant to change with respect to the independent analysis of F_o, some noticeably poorer fits were obtained, especially where k_{PC} and k_D were free, in which χ^2 values were 1.31 and 1.90, respectively. More reasonable fits were secured when either of the other 2 constants were free. Fits were considered significantly better when χ^2 values changed by more than 0.05. Changing k_A alone could nearly account for the full extent of the change to randomized S states, with a reasonable fit of 1.21, although it decreased below the value for that rate constant at F_m and overestimated the increase in σ. When 3 constants were free and only one was linked, there was an expected increase in fit quality over that from changing only 1 constant (χ^2 values ranged from 1.16 to 1.20). However, none of the quantitative predictions for cross-section even closely approximated the 11% increase found during pump-probe determinations of σ, except when modelling with a double link. When only 2 constants were free to change, fit qualities remained reasonable, while some of the predicted σ changes were close to the observed 11%. Any example where k_A remained fixed predicted σ changes in the wrong direction. But for example, allowing k_A and k_D to change resulted in a cross-section increase of 18%, while that from setting k_A and k_{PC}^- free was 14%. Of these 2 solutions, either one would suffice because the decreases in k_{PC}^- or k_D that were required to improve the σ prediction were not significant changes considering the relatively large error associated with them (Vasil'ev & Bruce, 1998). Neither was the effect on the value of k_A significant when examining these alternative results, which only yielded the difference from 0.44 to 0.42. Freedom of k_A and k_D together yielded a χ^2 value of 1.18, better than that for the other combination.

The similarity in the decay kinetics of F_o and the qE-quenched state at F_o (Figure 41) was reflected in the linked kinetic modelling (Table 11). All of the single linkage combinations (3 free constants) predicted considerable changes in σ that were not expected given the similarity in F_o yields observed at F_o and F_o' (+qE). Given the presumed equality of σ and F_o yield changes from the equation used to predict changes in σ, evaluation of the unchanged F_o was of interest, even though σ for this

combination increased by 53%. Thus, the most probable predicted σ change should be 0%, or some other insignificant change. While a couple of results in the triple-linked samples remained essentially unchanged, only that from releasing k_D had a reasonable χ^2 value (1.25). A similar situation occurred with the double-linked examples. Only 1 of these yielded an acceptable fit with k_A free, but the extent of that change is unexpected considering the near complete identity between the decay curves. Allowing k_D alone to change appears to be the best model fit -- that change was nearly insignificant, and could be explained by a small increase in the number of traps closed by the use of qE-inducing light (k_{PC}^- was also free, but did not change). The poise of the S states in dark-adapted thylakoids thus appears to quench fluorescence with the same changes in rate constants as occurs during qE quenching.

Also contained in Table 11 is the confirmation that quenching by 5-OH-NQ could be modelled sufficiently by letting free only the rate constant for the antenna, k_A, yielding a dramatic increase to 1.6 ns^{-1}. This increase fits almost perfectly with the degree of k_A change found with the same amount of quenching in Vasil'ev et al. (1998). The fit came out with a χ^2 of 1.20 and a prediction for the σ change that closely mirrored what was found for F_o and σ (Tables 4 and 6).

Randomization of S states in the OEC was necessary for a true modelling of qE at F_o. To do this, the rate constants obtained from the combined global target analysis of F_o and so-called F_{RS} were linked with the kinetics from the qE-quenched thylakoids. Fixed constants for F_{RS} were taken from example solutions where k_A remained fixed or where it was unconstrained. The former solution was again shown to be less likely than one in which k_A changed due to the limited number of quality fits obtained from such a combined analysis (Table 12). Only 4 results had χ^2 less than 1.30, and each of those predicted σ changes of clearly incorrect magnitudes (each had increases, when they should exhibit decreases). One such solution predicted a σ increase of 54% that might help explain the overall increase in pump-probe cross-sections, but this was due to a two-fold decrease in k_A. It was expected that qE quenching would rather yield an increase in k_A due to the clear decrease in F_o that was observed during data acquisition using all 3 techniques, so the role of the predicted σ increase can here be discounted.

The more likely solution for the randomized S states, which included a change

in k_A and k_D, was applied to a linked analysis with qE as well (Table 13). In general, the quality of fits generated was better than for the above attempt to model qE. With k_A constrained at 0.42, again the predicted σ changes were in the wrong direction. If qE was modelled by only a change in antenna quenching like for 5-OH-NQ, k_A increased to 0.63 (↑50%) -- quinone almost doubled the antenna rate constant when it was unrestricted. Although its fit was quite reasonable, a homogeneous mechanism of qE is not expected in light of the clear differences in the decay kinetics observed for qE and 5-OH-NQ. The solution that better approximated this expectation was the release of 2 rate constants, including k_A and either of k_{PC}^- or k_D, which yielded χ^2 values of 1.26 and 1.24, respectively. Both results fairly predicted the quenching of F_o and of σ.

Quenching in the antenna was apparently a necessary part of the model for qE kinetics, although it appeared to significantly depart from the mechanism of a pure antenna quencher. Part of the problem with attempting to define any molecular mechanism for qE in reaction centre rate constants is that, by definition, qE occurs during exposure to light. Reaction centres would not remain open in this state. Thus, F_o modelling is unreliable for detection of changes in electron transport processes during formation of qE. Many of the reported variations in k_{PC}, k_{PC}^-, and k_D were very small, and quite probably insignificant considering the relatively large error that are associated with them (10%, 25%, and 15%, respectively; Vasil'ev et al., 1998). The strength of the forward reactions (k_{PC} and k_D) at F_o could preclude reaction centre limitations imposed by a pH gradient. There were very few cases in which the quality of fit was greatly reduced by modelling with any particular combination of rate constant constraints, indicating that not only were the changes small (reflecting the small yield change at F_o), but that they also had considerable tolerance for changes in the rate constant for antenna processes. Clarification of the mechanism behind the quenching effects of the S states would also have been affected by these complications. These patterns could potentially be overcome by modelling the kinetics at F_m, with closed reaction centres.

Kinetic modelling of qE at F_m

A different complication accompanied the kinetic modelling at F_m. PSII must be modelled by a heterogeneous population of PSII (the α and β centres), as

described above. Table 14 shows that it was possible to model the rate constants with 3 different PSIIα/PSIIβ ratios almost independently from fit quality. This may indicate a requirement for ratios greater than 3:1. At 1:1 α-to-β, the fit was best, but as previously mentioned, such a high PSIIβ fraction is unlikely. At 2:1 or 3:1, the rate constants began to look more like those from a PQ-nonreducing population of PSIIβ with little ability to do charge separation, but with lots of charge recombination (k_{PC}^-), as has been suggested before.

To be independent of the assumption of a particular PSIIβ content in the thylakoid samples, modelling was examined with selected combinations of fixed rate constants for both quinone-quenched and qE-quenched samples (Tables 15 and 16) while varying the α/β ratio. Table 15 demonstrates that the decays of 5-OH-NQ were adequately modelled with variability in only k_A, which increased in α particles to 0.83, identical to the observations of Vasil'ev and Bruce (1998). The β particles were slightly less affected by quinone, which is not illogical considering the proposed differences in antenna size and composition (Jansson et al., 1998). Modelling quinone quenching with variable k_A also established that neither the pattern nor the extent of change in the rate constants were substantially affected by altering the ratio of PSIIα and PSIIβ particles. This point was further supported when the same approach was taken for a triple link of qE (k_A free) or a double link of qE (k_A and k_D free) (Table 16). Each rate constant that was permitted to change closely approximated the effects observed at the other 2 PSII ratios employed. However, in the selected qE trials of Table 16, a value of 3:1 substantially improved the fit quality compared to smaller ratios. A preference for a larger ratio was mirrored in the quinone-quenched modelling where PSIIα/PSIIβ ratios of 2- or 3:1 improved the fit with respect to the control values, while 1:1 made no such improvement on the control χ^2. Global target analysis at F_m was continued assuming a PSIIα/PSIIβ of 3 (~25% β-centres), which is within the range previously reported (Melis, 1985).

With the PSIIα/β subpopulations set to 3:1, global target analysis was performed for all combinations of fixed rate constants (Tables 17 to 19). When only one constant was free (Table 19), all of the fits were very poor, ranging from 1.74 to almost 7. Allowing k_A to change was closest to being able to account for the quenching, with the best fit of the 4 combinations (χ^2=1.74). The other 3 rendered

unlikely solutions, either due to poor fits or simply because the changes were improbable. For example, the increase in k_{PC} alone for α and β centres should be physically impossible, since it is unconvincing to conceive that an appreciable increase in charge separation could account for pH-dependent quenching. When k_{PC}^- was set free, the α and β centres went in opposite directions, with a huge magnitude change. Permitting k_D to change seemed a little bit more sensible with a large increase to about 12 ns^{-1}, which could represent addition of a recombination reaction, triplet formation, or cyclic electron transport through Chl_Z or cytochrome b_{559}. However, its fit was also very poor (χ^2=4.80). In any case, it was clearly insufficient to model qE on the basis of a homogeneous mechanism involving a modification of only 1 PSII rate constant.

Modelling with at least one more degree of freedom was certainly essential to understanding a heterogeneous mechanism of qE. The qualities of fit for the double-linked modelling of qE (Table 18) were substantially improved compared to those for triple links. Even so, none were better than a χ^2 of 1.33, and 5 of the 6 had changes in at least 1 rate constant that went in opposite directions for α and β centres. For example, one of the better combinations involving changes in k_A yielded a χ^2 of 1.33, but its k_D went up for α centres and virtually disappeared for β centres. This is indicative of a lack of resolving power between the effects of qE on a heterogeneous population of PSIIs. However, of the attempts to model qE with a combination of 2 free rate constants, variable k_A and k_D appear to work the best.

Modelling with a third degree of freedom (Table 17) provided some of the better fits found at F_m. All were better than χ^2 of 1.37, although 1 clearly stood out, with χ^2 of 1.24. This solution contained only a fixed k_{PC} while k_A, k_{PC}^- and k_D were allowed to vary. While k_A increased significantly only in α centres, k_{PC}^- and k_D changed only in β centres, with a large increase in both reaction centre constants. Changes in k_{PC}^- and k_D in α centres can not be considered significant. Like in most F_m trials in which it was unrestricted, the k_A constant of PSIIα centres was significantly more sensitive to qE, a 9-fold greater increase in antenna quenching than in β centres.

It is not simple to understand how k_{PC}^- and k_D could shift in the same direction, since one of these electron transport processes could compensate when the other

increases. For instance, augmentation of transport to Chl_Z would increase k_D, while affecting an opposite decrease in recombination to the antenna (k_{PC}-). Because of the lack of a convincing solution from a heterogeneous population of PSII centres, the tendency for some solutions to affect opposite directionality in α and β rate constants, and the fact that the quenched states tended toward higher and higher PSIIα/PSIIβ ratios when they were not fully restricted (data not shown), there appears to be an inability to resolve the heterogeneity of PSII. This is supported by the disappearance of the 3.1 ns component that is suggested to have at least partial origin in a monoexponential kinetic from β centres (F_m DAS, Figure 49). Its absence was nearly complete under both quinone and qE conditions. It is possible that both of these conditions could be modelled adequately with a homogeneous population of PSIIs, as was the case in the quinone-quenched sample in Vasil'ev and Bruce (1998).

Kinetic modelling was repeated at F_m assuming a homogeneous population of PSII centres, for those solutions that included unrestricted k_A (Table 20). Inspection of the results readily shows that, in the case of antenna quenching by the quinone, a homogeneous model of PSII was at least as good as a heterogeneous fit. The χ^2 value improved slightly to 1.22 from 1.27, and the increase in k_A was again the same as that reported by Vasil'ev and Bruce (1998). A similar effect was observed for qE-quenched thylakoids that were modelled with only the release of k_A, where the fit was drastically improved to 1.39 from 1.74 for the heterogeneous fit. In the double- and single-linked sets fit with this homogeneous model, there was little change in fit quality, and in fact there was a slight decrease for the outcome of fixing only k_{PC}. It was clearly possible to model the data as a homogeneous population of PSIIs as opposed to a heterogeneous one in the quenched samples. This accounts for the discrepancies between the effects of qE on the rate constants for reaction centre processes in PSIIα and β centres.

As a final step toward successful modelling of qE with a model for PSII, PSII decay curves were recalculated from the parameterized curves fit independently to the Reversible Radical Pair Model. These curves were then compared with simulated decays constructed from the linked fitting procedure exhibited in Tables 9 to 20. In other words, PSII fluorescence time courses were computed from the kinetic model by adjusting one or more of the rate constants -- what rate constant changes were

required to make the unquenched data simulate the quenched data?. The simulations for the randomized state, for qE at Fo, for qE at Fm, and for 5-OH-NQ are shown in Figures 51 and 52, respectively. A more detailed visualization of the differences between the independently-fit and simulated curves can be found in Figure 53.

Figure 52 demonstrates again that quenching by 5-OH-NQ can be fit successfully with a change in only k_A. At F_m, the simulation achieved near unity with the independent fit. In fact, the difference over the entire timeframe is better than all fits for qE, even those with more degrees of freedom (ie 2 or more rate constants variable). The difference is more pronounced for quinone at F_o, probably originating from higher sensitivity owing to the small change in fluorescence yield at F_o, although its fit is also better than some of the qE simulations employing multiple changes in rate constants.

On the contrary, it is demonstrated in the F_m simulations that, again, it was insufficient to model qE with only a change in k_A (Figures 51 and 53), an observation that could not be confirmed at F_o because of the aforementioned requirement for PSII closure in order to observe reaction centre changes -- by definition, qE occurs during reaction centre closure, not in open reaction centres as are found at F_o. Modelling with a change in k_A was, however, a better fit than modelling with a fixed k_A, despite 2 more degrees of freedom in the latter, illustrating the importance of varying k_A in the qE fit. Simulations including variable k_A were the only ones that correctly approximated the fastest region of the decays. To fit the data most successfully, variable reaction centre rate constants were necessary. Freeing k_{PC}- and k_D along with k_A clearly yielded the best fit to the data, achieving a nearly identical curve to the simulation of the independent data qE fit.

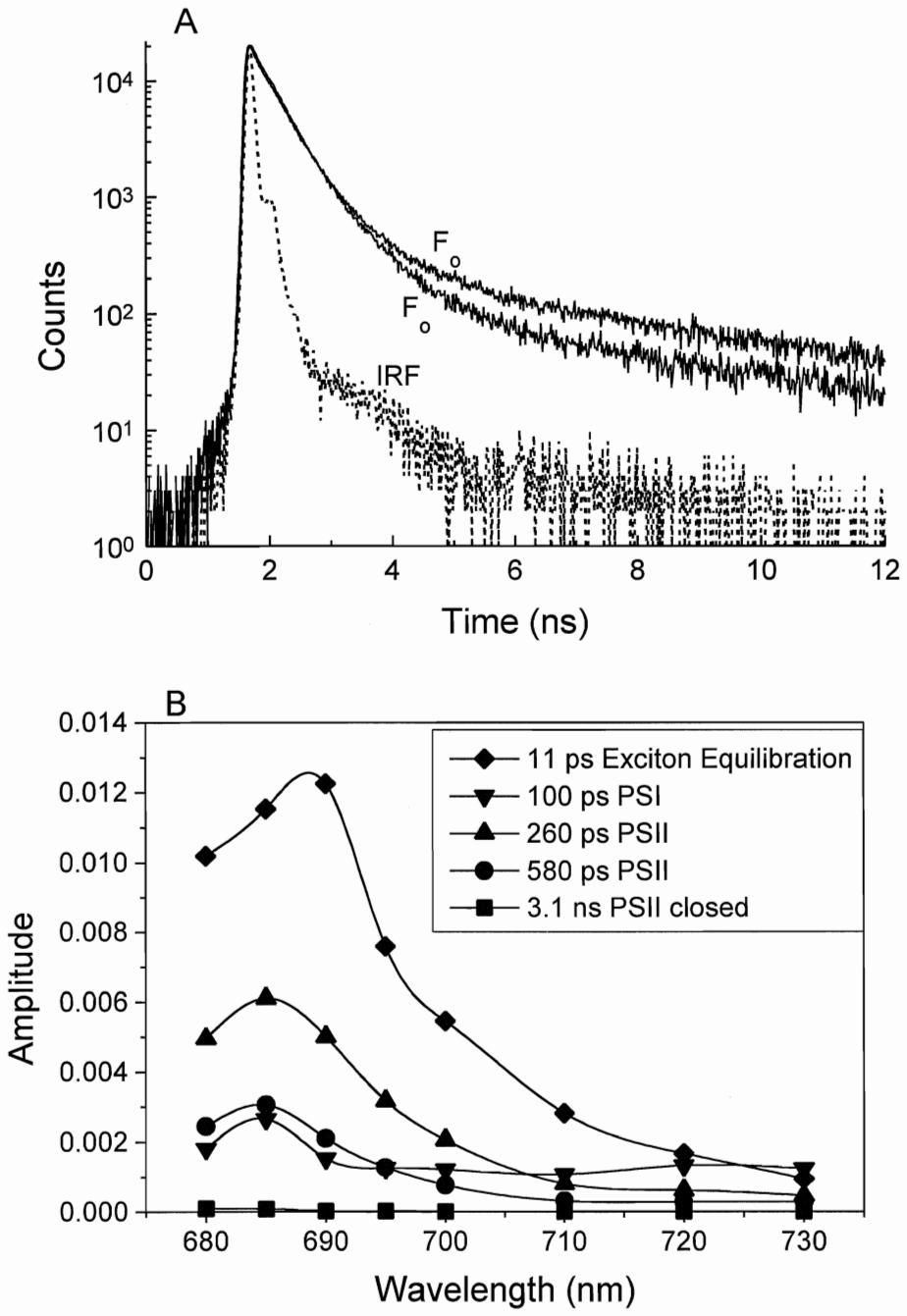

Figure 37: Picosecond fluorescence decay kinetics of dark-adapted spinach thylakoids at F_o. **A**; Two repeats of picosecond decay curves for F_o at 685 nm. Data were fit by modelling with a convolution of the instrument response function (IRF) to a sum of 5 decay components. The 2 samples are reasonable repeats especially in the fast components, with the least agreement occurring in the slower components (>4 ns). **B**; Decay-associated spectra (DAS) from globally-fitted data at F_o. Fits separate into 5 components related to different processes in the light reactions. There is an extremely fast component at 11 ps, a relatively slow component at 3.1 ns that has negligible amplitude, and 3 intermediate components, one of which has a red shift with a peak at about 720 nm (100 ps).

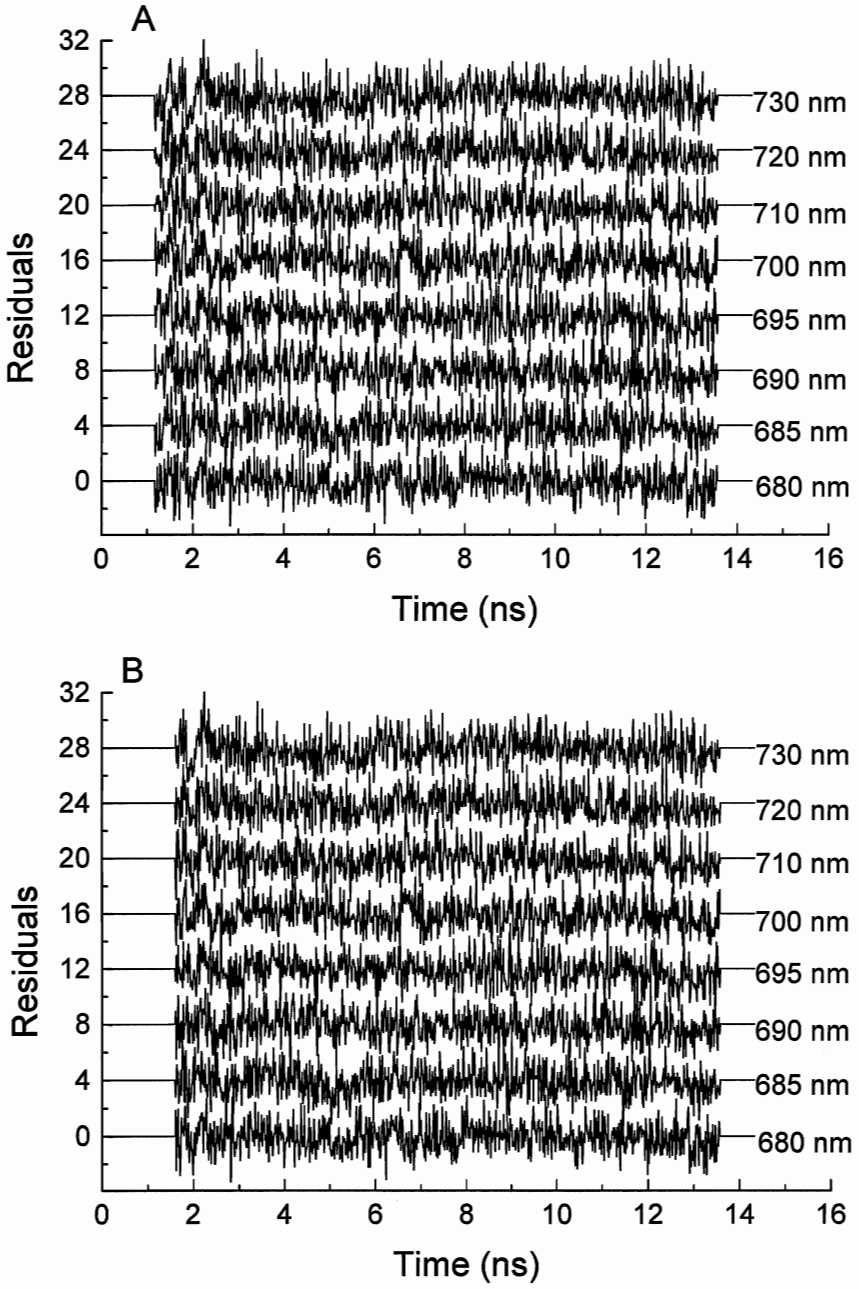

Figure 38: Residuals generated from global analysis of decay kinetics of spinach thylakoids at F_o. **A**; Residuals generated from the fit of the entire curve. There is good distribution about the median in every wavelength, except for some extra noise <1.5 ns that is before the beginning of the actual decay. χ^2=1.14. **B**; Residuals generated from a fit of the curve with some of the pre-decay curve left unfit. The χ^2 improves to 1.11 in this case. This effect is more pronounced at F_m, and all subsequent decays are analyzed with this in mind.

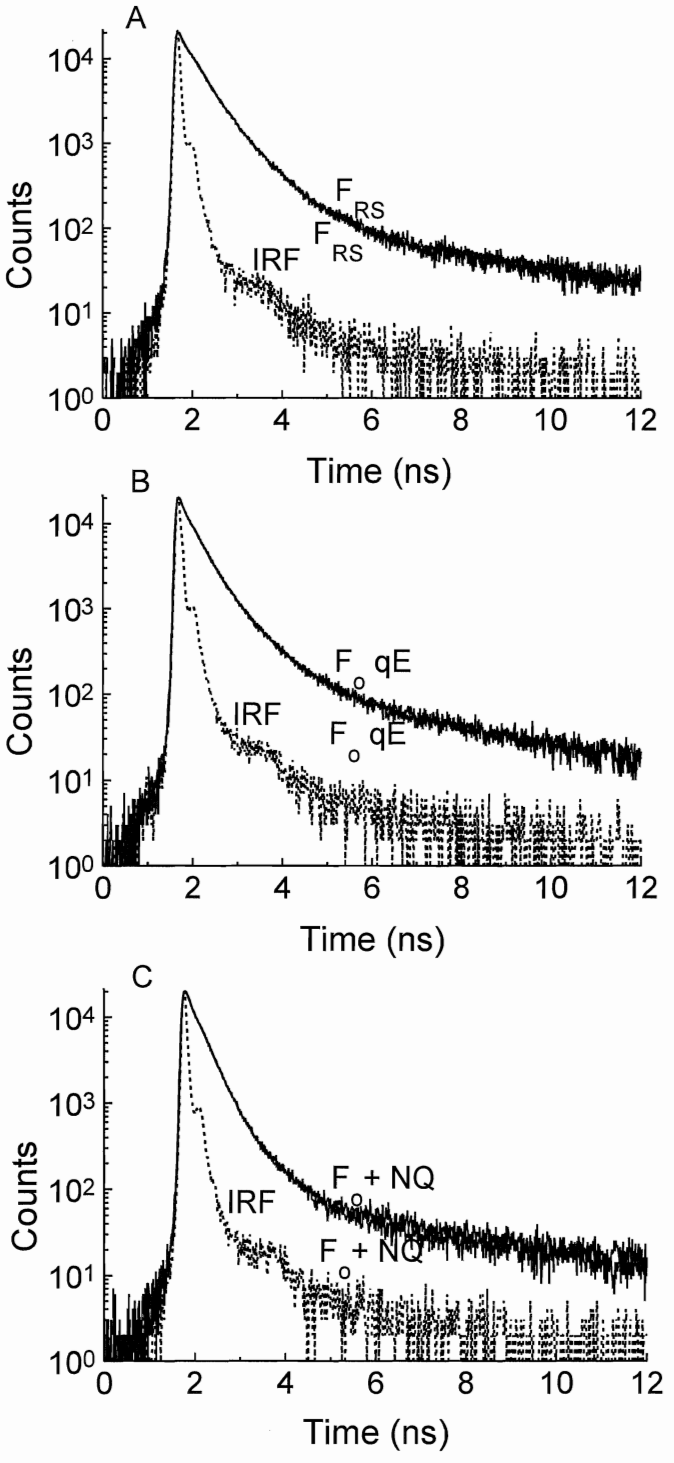

Figure 39: Picosecond fluorescence decay kinetics of spinach thylakoids at F_o with randomized S states (**A**), qE quenched (**B**), and quenched by 5-OH-NQ (**C**). Each figure depicts 2 repeats of the state, with an associated IRF. The decay kinetics are very reproducible.

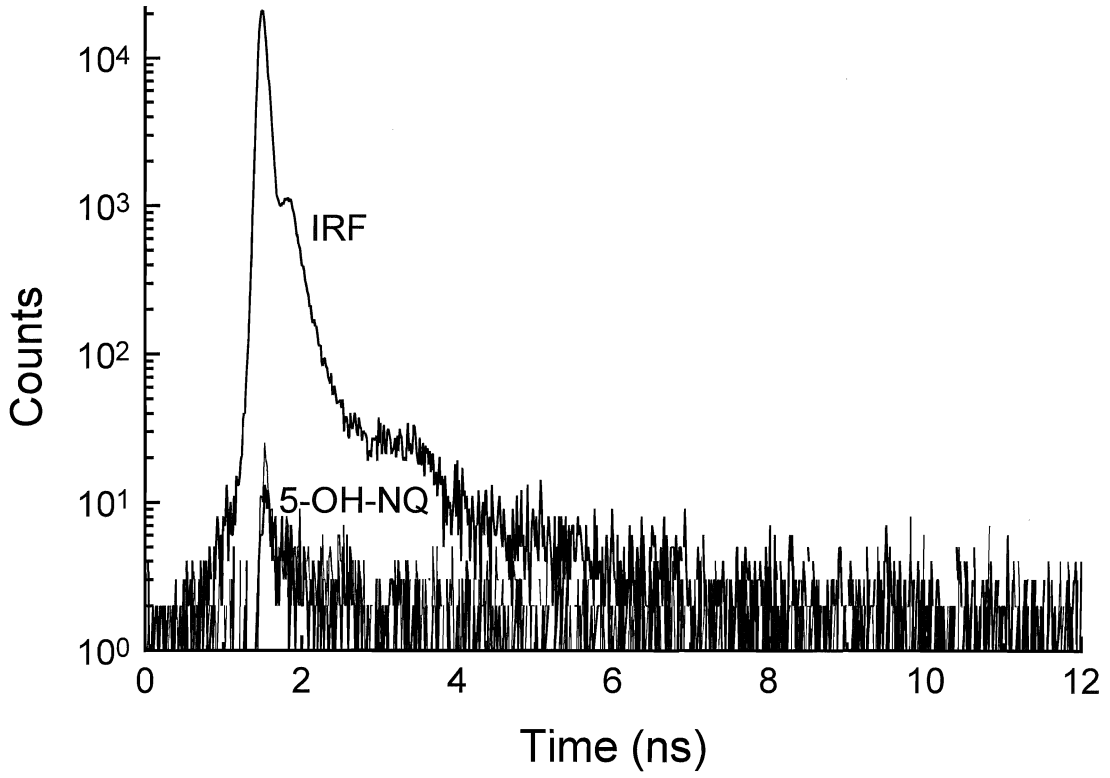

Figure 40: Decay kinetics of a solution of 5-OH-NQ in pH 7.8 resuspension buffer as a control. Quinone does not have any decay of its own, with only a slight hint of the IRF turning up in its decay (<0.5% of total counts for the IRF).

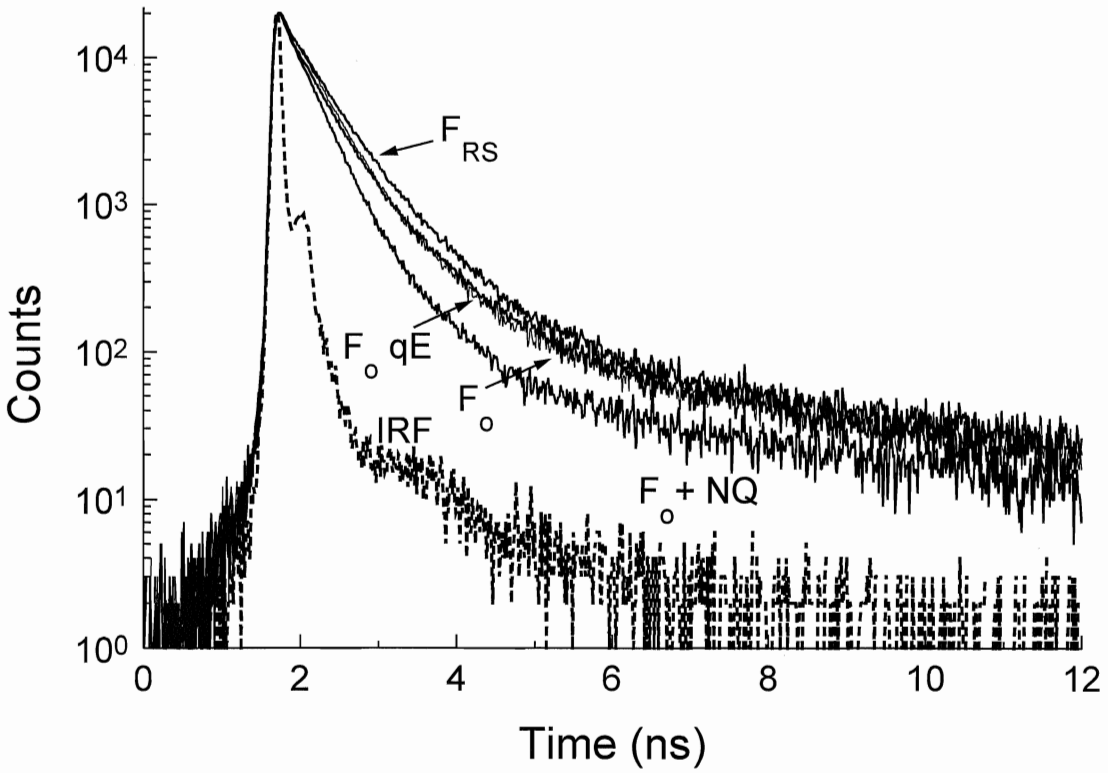

Figure 41: Picosecond fluorescence decay kinetics of spinach thylakoids at F_o under different quenching conditions: in the dark (F_o), with randomized S states (F_{RS}), qE-quenched (F_o qE), and 5-OH-NQ-quenched (F_o + NQ). F_o decays faster in the fast components, but is slower in the long components than F_{RS}. The qE-quenched sample is also faster in the fastest components than F_{RS}, but the 2 converge in the slower components, and is nearly identical to F_o up to about 4 ns. The antenna-quenched 5-OH-NQ sample is clearly the fastest, but remains approximately parallel to F_o in the slow components. Quinone-quenched and qE-quenched have clearly different kinetics.

Table 6: Changes in fluorescence yields from thylakoid samples after quenching with either actinic light (qE) or with quinone (5-OH-NQ), as obtained from PAM fluorimetry, pump-probe fluorimetry, or single photon counting (SPC) measurements. Values represent the amount of fluorescence quenching as a percentage of pre-quenched control levels. (± 1 S.D., n=3+)

Quenching Condition	PAM		Pump-probe		SPC	
	F_o	F_m	F_o	F_{sat} *	F_o	F_m
qE	13 ± 3	61 ± 3	11 ± 4	36 ± 3	8**	49
5-OH-NQ	28 ± 2	60 ± 1	18 ± 1	39 ± 3	25	46

* F_m was not determined during pump-probe measurements due to the single-turnover flashes used for cross-section measurements. F_{sat} is the yield of fluorescence at saturation for these flashes.

** Single photon counting values represent the data set completely fit and modelled; thus yields shown have no standard deviations.

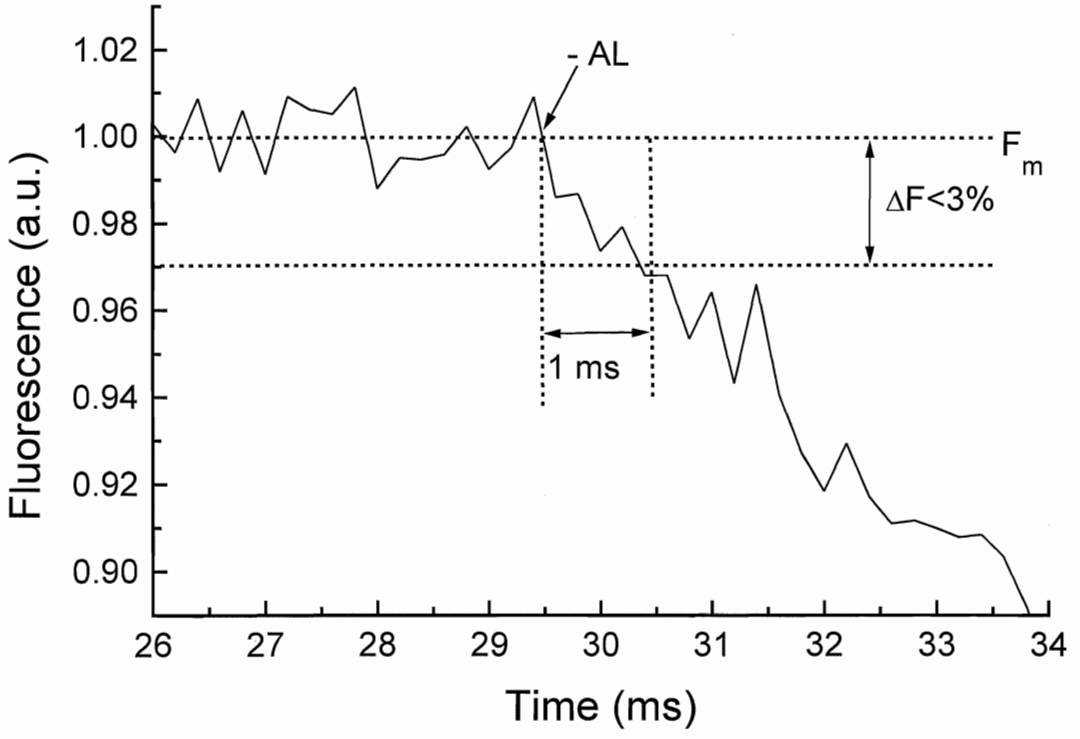

Figure 42: Magnification of the decay from F_m after 2 seconds of saturating white light. Removal of the light occurs at -AL. In 1 ms, less than 3% of fluorescence is lost. Picosecond kinetic measurements at F_m are accomplished using high-speed circulation of thylakoids through an illumination chamber before entering the excitation/detection zone, with a delay of approximately 750 µs. Fluorescence decays collected in this state are at least 97% of F_m. Decay shown here is a composite average of 10 trials.

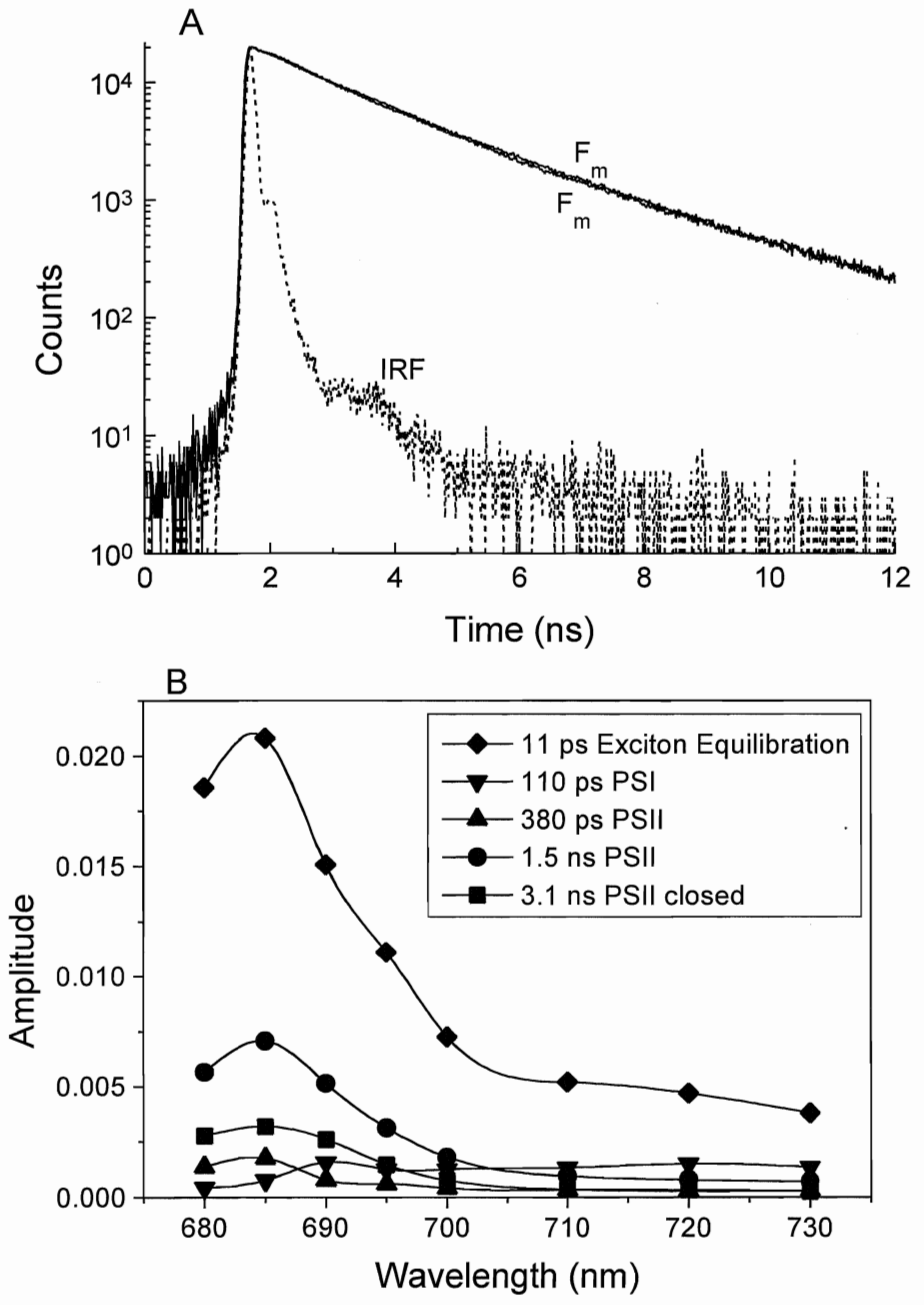

Figure 43: Picosecond fluorescence decay kinetics of dark-adapted spinach thylakoids at F_m. **A**; Two repeats of picosecond decay curves for F_m at 685 nm. Data were fit by modelling with a convolution of the instrument response function (IRF) to a sum of 5 decay components. The 2 samples are very good repeats through the whole decay. **B**; Decay-associated spectra (DAS) from globally-fitted data at F_m. Fits separate into 5 components related to different processes in the light reactions. There is an extremely fast component at 11 ps that is found also at F_o, a relatively slow component at 3.1 ns that has more amplitude than the same component at F_o, and 3 intermediate components, one of which has a slight red shift with a peak at about 720 nm as at F_o (110 ps).

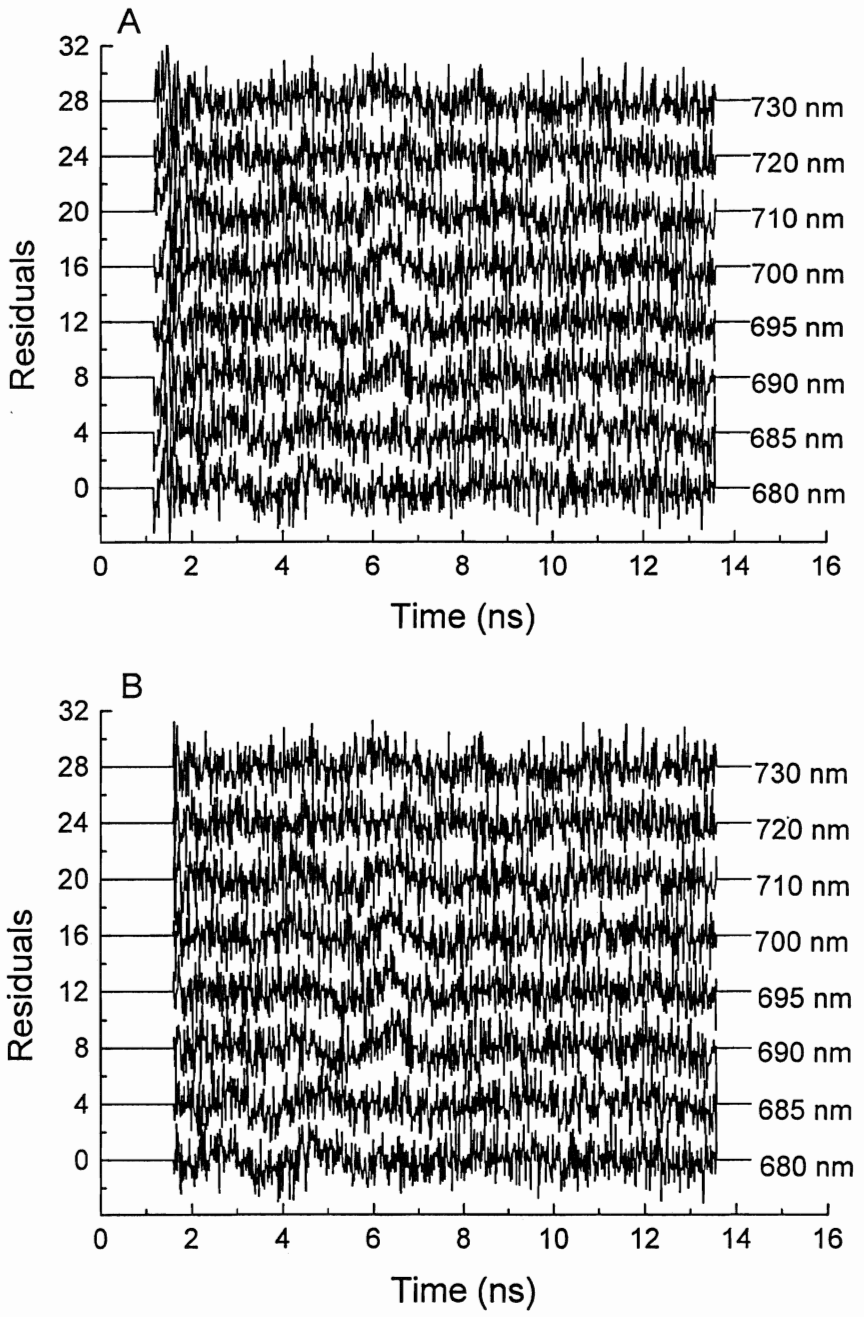

Figure 44: Residuals generated from global analysis of decay kinetics of spinach thylakoids at F_m. **A**; Residuals generated from the fit of the entire curve. There is good distribution about the median in every wavelength, except for some extra noise <1.5 ns that is before the beginning of the actual decay, and a bit of electrical noise around 5-7 ns that was less pronounced at F_o. χ^2=1.34. **B**; Residuals generated from a fit of the curve with some of the pre-decay curve left unfit. The χ^2 improves to 1.21 in this case.

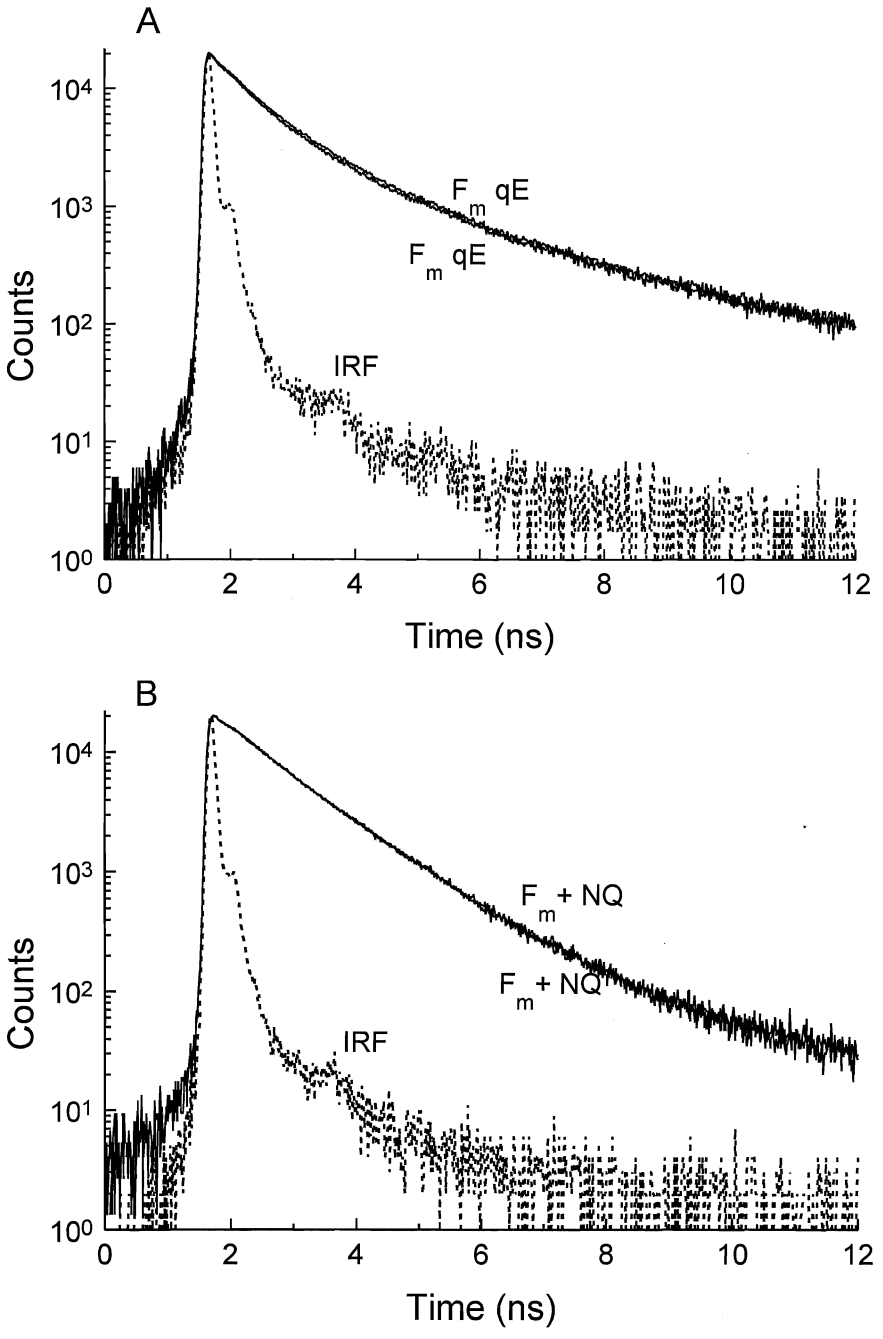

Figure 45: Picosecond fluorescence decay kinetics of spinach thylakoids at F_m with qE quenching (**A**), and quenched by 5-OH-NQ (**B**). Each figure depicts 2 repeats of the state, with an associated IRF. The decay kinetics are very reproducible.

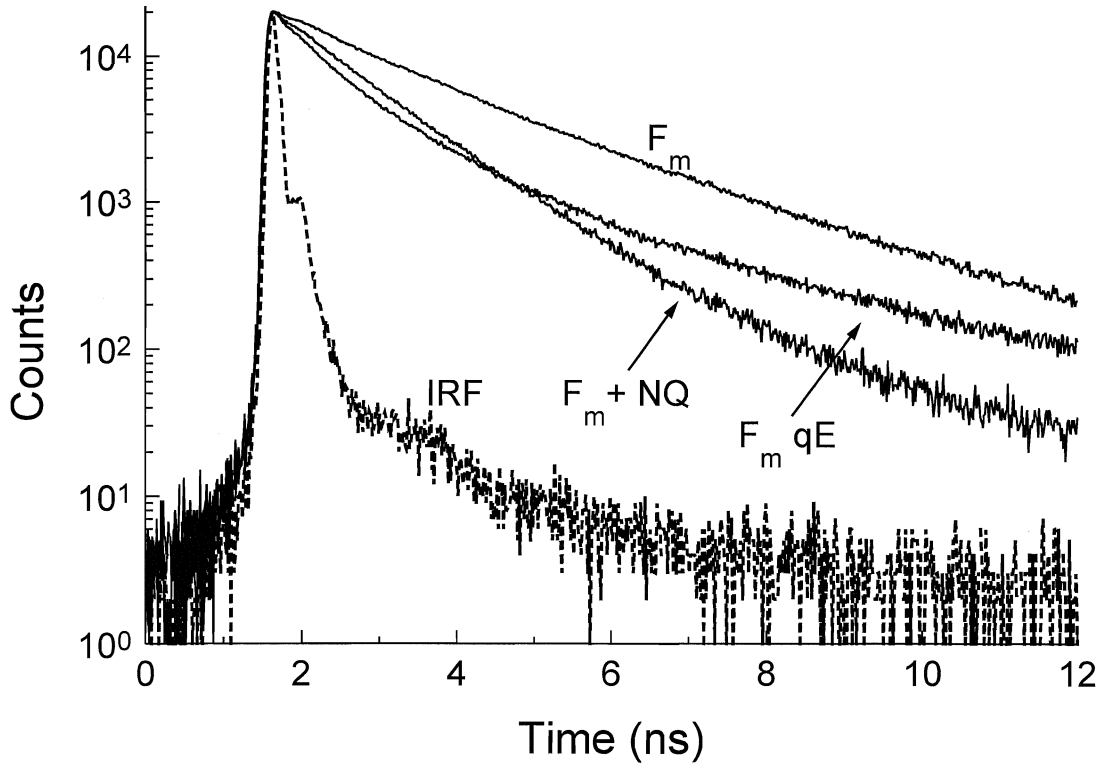

Figure 46: Picosecond fluorescence decay kinetics of spinach thylakoids at F_m under different quenching conditions: control (F_m), with qE quenching (F_m qE), and 5-OH-NQ-quenched (F_m + NQ). F_m decays slower throughout the entire decay. Quinone-quenched and qE-quenched have clearly different kinetics. The qE-quenched sample is faster than quinone-quenched in the fastest components, but becomes considerably slower in the slower components of the curve, even beginning to converge toward the control. The quinone-quenched curve appears to be mainly quenched in the fast components and more parallel to F_m control in the slower ones.

Table 7: Lifetimes for the F_o and F_m states of thylakoid samples measured by picosecond fluorescence decay kinetics. Data represent kinetics obtained from global fitting during this study compared with Vasil'ev and Bruce (1998). Lifetimes are given by τ_x. Uncertainty in lifetimes is approximately 10%.

State		Lifetimes (ps)				
		τ_1	τ_2	τ_3	τ_4	τ_5
F_o	present study	11	100	260	580	3100
	Vasil'ev	11	70	245	515	4000
F_m	present study	11	110	380	1500	3100
	Vasil'ev	11	104	350	1200	4100

Table 8: Results from the global fitting of picosecond fluorescence decay kinetics of spinach thylakoids in various quenched and unquenched states. The sum of the relative amplitudes of each component are given in parentheses. The uncertainty in both lifetimes and amplitudes is approximately 10%. (See also Decay Associated Spectra, DAS)

State		Lifetimes (ps)				
		PSI	$PSII_{fast}$	$PSII_{slow}$	PSII closed	χ^2
F_o	Dark	100 (1.1)	260 (2.0)	580 (0.92)	3100 (0.046)	1.12
	Random-ized	120 (1.6)	390 (2.1)	770 (0.74)	3100 (0.032)	1.09
	qE	120 (1.3)	360 (2.1)	840 (0.38)	3100 (0.051)	1.18
	Quinone	100 (1.0)	300 (1.6)	580 (0.19)	3100 (0.010)	1.14
F_m	Control	110 (0.84)	380 (0.49)	1500 (2.05)	3100 (0.95)	1.21
	qE	130 (0.63)	520 (0.87)	1400 (0.52)	4600 (0.060)	1.15
	Quinone	130 (0.53)	700 (0.75)	1200 (0.95)	4100 (0.012)	1.12

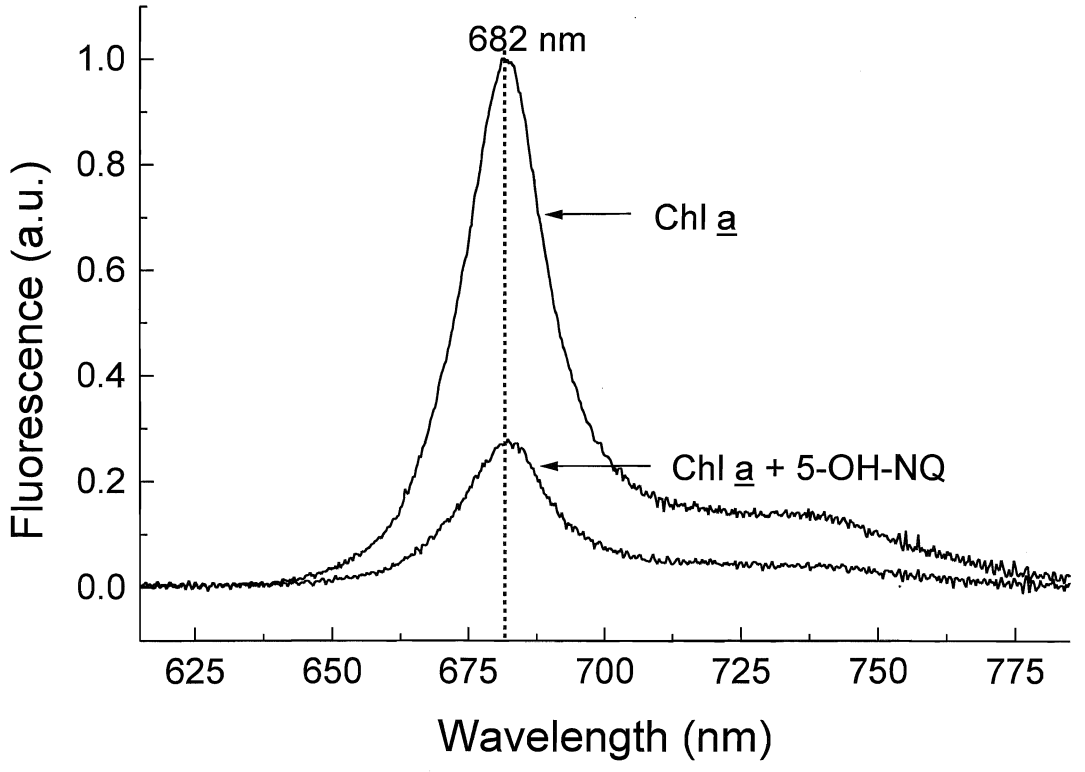

Figure 47: Room temperature fluorescence spectra from spinach thylakoid chlorophyll a with and without the addition of 5-OH-NQ. There is a clear quenching of fluorescence upon the addition of quinone, but the spectral shape does not change, with a peak at 682 nm and a shoulder around 720-740 nm. Global analysis of picosecond decay kinetics employs these curves as references for normalizing the relative amplitudes in decay-associated spectra (DAS) without the exciton equilibration component, which is essentially the same in all kinetics and can be removed for more detailed analyses. Figures 48 and 49 have this normalization applied to DAS.

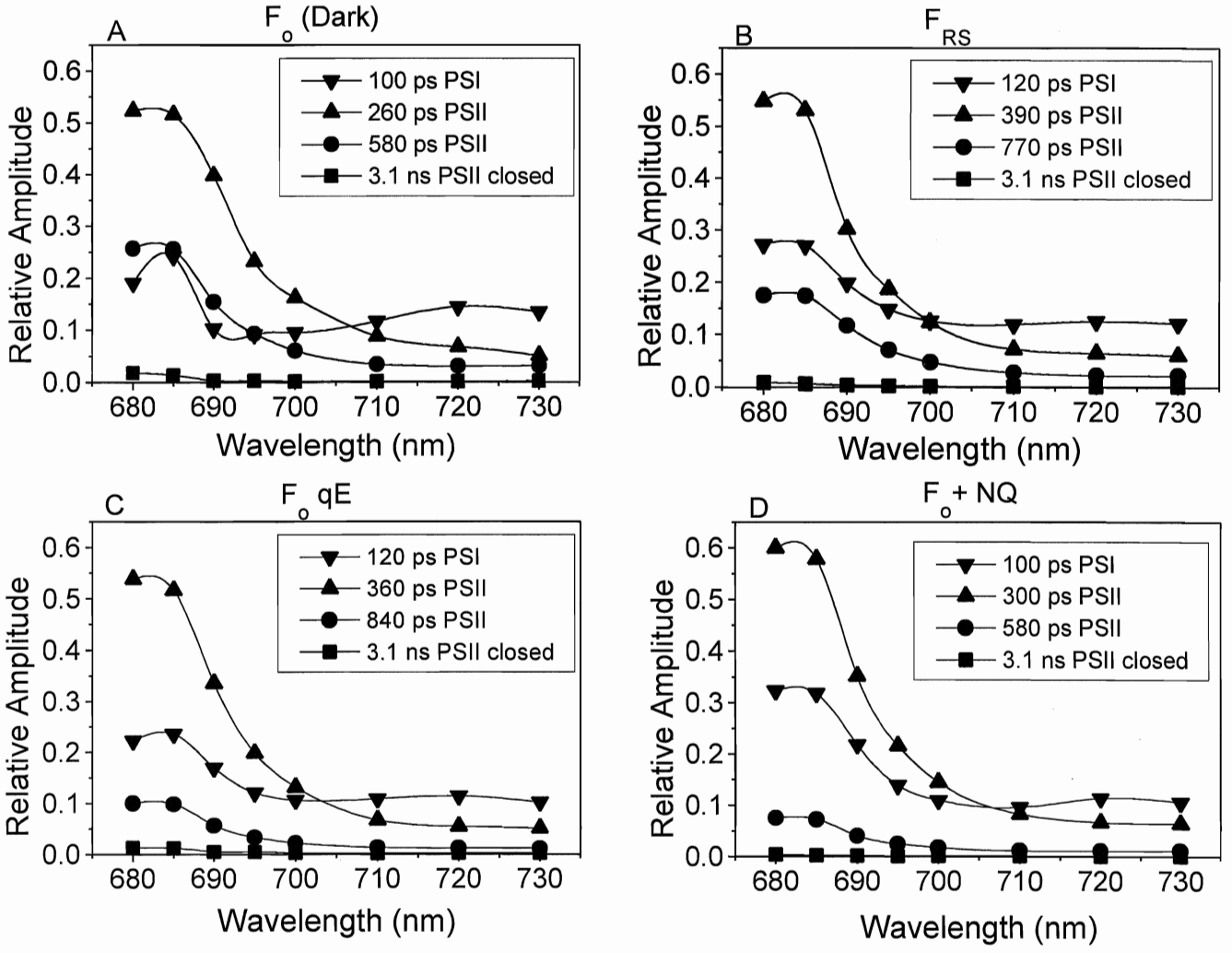

Figure 48: Decay-associated spectra of spinach thylakoids at F_o under various quenched and unquenched conditions: **A**; dark-adapted F_o **B**; with randomized S states **C**; qE-quenched **D**; 5-OH-NQ-quenched. DAS are normalized at 685 nm to the sum of all decay components, except exciton equilibration, allowing direct comparison of amplitudes. χ^2 values generated for fits ranged between 1.09 and 1.18. The longest component is negligible in all cases, all but completely disappearing in the quinone-treated DAS, corresponding to a limited number of closed centres, as expected at F_o. Very little effect is exhibited in the PSI component, except in its PSII-associated peak (685 nm), and in the quinone-quenched sample. The 2 intermediate PSII components are affected most. The fast PSII component is dominant in all states, although it is less affected by quenching than is the slower PSII component. The DAS for addition of quinone and for qE-quenched thylakoids are considerably different.

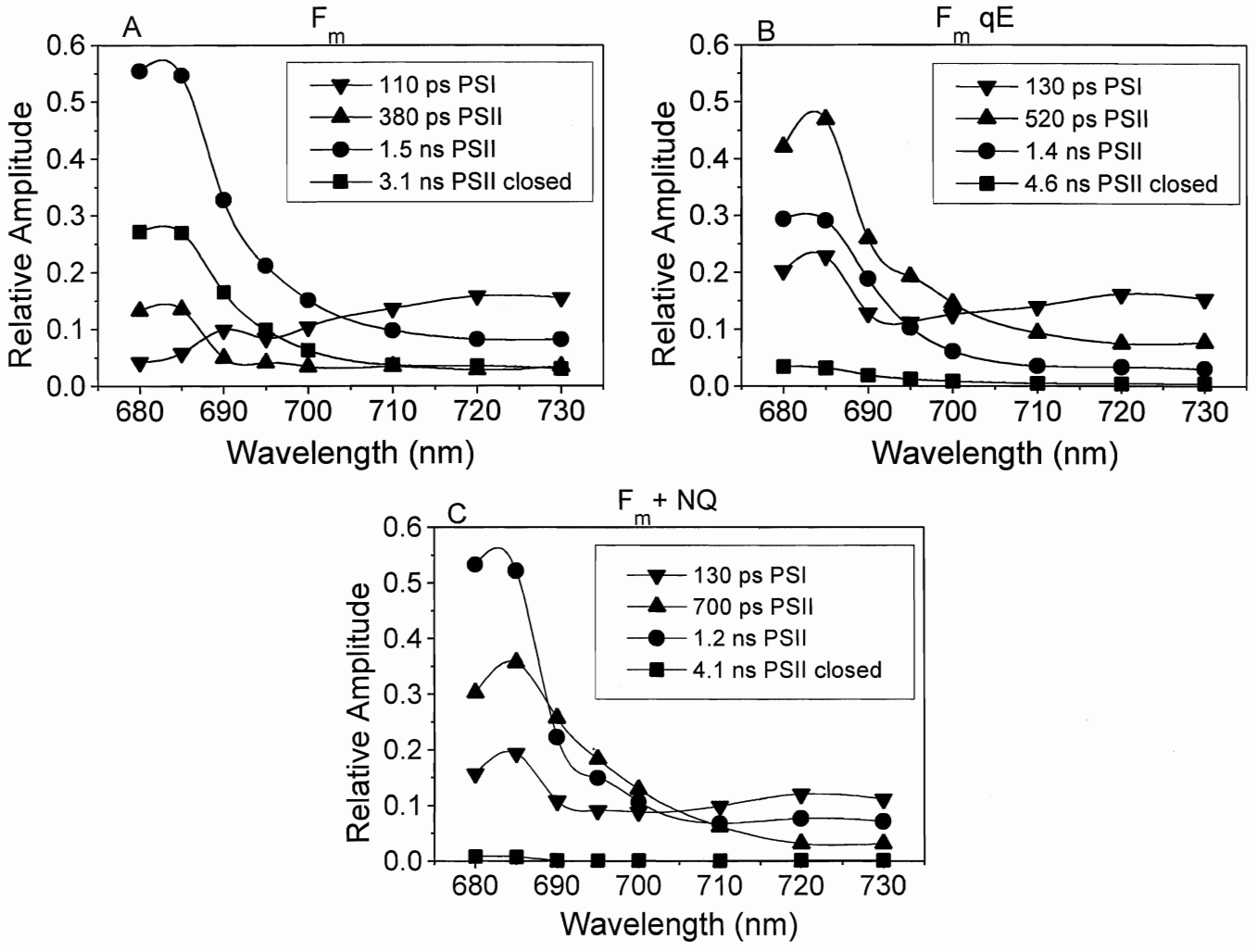

Figure 49: Decay-associated spectra of spinach thylakoids at F_m under various quenched and unquenched conditions: **A**; F_m **B**; qE-quenched **C**; 5-OH-NQ-quenched. DAS are normalized at 685 nm to the sum of all decay components, except exciton equilibration, allowing direct comparison of amplitudes. χ^2 values generated for fits ranged between 1.11 and 1.21. The quinone-quenched DAS is qualitatively similar to that from Vasil'ev and Bruce (1998). Compared to F_o, the longer PSII and the closed PSII components now dominate, as expected when Q_A becomes saturated (fully reduced). The PSI component exhibits a similar effect in both qE and quinone samples, while the closed PSII component almost completely disappears. The intermediate PSII components are affected the most, flipping dominance in the qE-quenched example, but not in the naphthoquinone sample. The slower PSII decreases in both lifetime and amplitude for both quenched states compared to F_m, while the opposite is true for the faster PSII decay component (both increase in lifetime and amplitude).

Table 9: Rate constants for the F_o and F_m states of thylakoid samples measured by picosecond fluorescence decay kinetics. Data represent kinetics obtained from global target analysis during this study compared with Vasil'ev and Bruce (1998). Rate constants are given by k_A (antenna), k_{PC} (primary charge separation), k^-_{PC} (reversal of PC), and k_D (sum of other electron transport processes, including charge stabilization at Q_A), as modelled by the Exciton/Radical Pair Equilibrium Model for PSII (Schatz et al., 1988). Uncertainty in k_A and k_{PC} are approximately 10%, while that for k_{PC}^- and k_D are about 25% and 15% respectively. For F_m, the PSII α/β ratio=1, assuming a heterogeneous population of PSII centres.

	State	Rate constants (ns^{-1})			
		k_A	k_{PC}	k_{PC}^-	k_D
F_o	present study	0.83*	2.3	0.40	2.0
	Vasil'ev	0.83	2.6	0.35	2.2
F_m					
α	present study	0.3**	1.0	1.3	2.2
β		0.3	0.79	3.0	0.86
α	Vasil'ev	0.3	0.7	1.6	1.9
β		0.3	0.5	2.6	0.46

* k_A is set to experimental values derived from fluorescence lifetimes of thylakoids (*, Vasil'ev and Bruce, 1998) and isolated LHCII particles (**, Hodges et al., 1987)

Table 10: Rate constants as calculated by global target analysis of fluorescence decay kinetics from thylakoid samples at F_o. The rate constants for F_o in the dark are linked in various combinations to the rate constants for F_o with the addition of background light (F_{RS}), which was used to randomize the S states of the Oxygen-Evolving Complex. Numbers in boldface represent linked, or fixed, rate constants: those in normal face are free to change. At F_o, the Exciton/Radical Pair Equilibrium Model (Reversible Radical Pair) can be used to quantitatively predict the change in absorption cross-section (σ) from the set of rate constants (see text; Vasil'ev et al., 1998).

	Linked State	Rate constants (ns^{-1})					
		k_A	k_{PC}	k_{PC}^-	k_D	χ^2	Δ σ (%)
F_o	independent analysis	**0.83**	**2.3**	**0.40**	**2.0**	1.17	--
F_{RS}	single link	**0.83**	1.6	0.29	1.5	1.16	- 21
		0.16	**2.3**	0.22	1.6	1.16	41
		1.3	1.2	**0.40**	1.4	1.17	- 100
		0.22	2.5	0.42	**2.0**	1.20	39
F_{RS}	double link	**0.83**	**2.3**	0.70	1.8	1.22	- 11
		0.83	1.8	**0.40**	1.6	1.17	- 20
		0.83	2.0	0.66	**2.0**	1.23	- 20
		0.42	**2.3**	**0.40**	1.8	1.18	18
		0.44	**2.3**	0.47	**2.0**	1.21	14
		0.16	2.6	**0.40**	**2.0**	1.20	45
F_{RS}	triple link	0.21	**2.3**	**0.40**	**2.0**	1.21	30
		0.83	1.5	**0.40**	**2.0**	1.31	- 28
		0.83	**2.3**	0.79	**2.0**	1.23	- 14
		0.83	**2.3**	**0.40**	1.4	1.90	0

Table 11: Rate constants as calculated by global target analysis of fluorescence decay kinetics from thylakoid samples at F_o. The rate constants for F_o in the dark are linked in various combinations to the rate constants for F_o exposed to pH-dependent quenching (+ AL, qE). Also included is a confirmation of the dependence on k_A for 5-OH-NQ quenching, as seen in Vasil'ev et al. (1998). Numbers in boldface represent linked, or fixed, rate constants: those in normal face are free to change. At F_o, the Exciton/Radical Pair Equilibrium Model can be used to quantitatively predict the change in absorption cross-section (σ) from the set of rate constants (see text; Vasil'ev et al., 1998).

	Linked State	Rate constants (ns^{-1})					
		k_A	k_{PC}	k_{PC}^-	k_D	χ^2	Δ σ (%)
F_o	independent	**0.83**	**2.3**	**0.40**	**2.0**	1.17	--
qE	single link	**0.83**	1.8	0.25	1.4	1.21	- 13
		0.48	**2.3**	0.25	1.5	1.20	20
		1.2	1.6	**0.40**	1.4	1.21	- 34
		0.51	2.4	0.44	**2.0**	1.27	17
qE	double link	**0.83**	**2.3**	0.41	1.6	1.24	0
		0.83	1.9	**0.40**	1.7	1.26	- 16
		0.83	1.8	0.39	**2.0**	1.35	- 20
		0.69	**2.3**	**0.40**	1.7	1.23	0
		0.78	**2.3**	0.57	**2.0**	1.31	- 4
		0.60	2.1	**0.40**	**2.0**	1.32	0
qE	triple link	0.51	**2.3**	**0.40**	**2.0**	1.27	13
		0.83	1.7	**0.40**	**2.0**	1.36	- 21
		0.83	**2.3**	0.59	**2.0**	1.32	- 7
		0.83	**2.3**	**0.40**	1.6	1.25	0
+5-OH-NQ		1.6	**2.3**	**0.40**	**2.0**	1.20	- 20

Table 12: Rate constants as calculated by global target analysis of fluorescence decay kinetics from thylakoid samples at F_{RS}. The rate constants for F_{RS} in the presence of S-state randomizing background light are linked in various combinations to the rate constants for F_o exposed to pH-dependent quenching (+ AL, qE). The F_o-F_{RS} linked solution used to obtain the set of fixed F_{RS} constants is one in which k_A remained fixed. Numbers in boldface represent linked, or fixed, rate constants: those in normal face are free to change. For F_o experiments, the Exciton/Radical Pair Equilibrium Model can be used to quantitatively predict the change in absorption cross-section (σ) from the set of rate constants (see text; Vasil'ev et al., 1998).

	Linked State	Rate constants (ns^{-1})					
		k_A	k_{PC}	k_{PC}^-	k_D	χ^2	Δ σ (%)
F_{RS}	from F_o link	**0.83**	**2.0**	**0.66**	**2.0**	1.23	--
qE	single link	**0.83**	1.9	0.30	1.5	1.24	14
		0.42	**2.0**	0.12	1.1	1.21	54
		2.1	0.4	**0.66**	0.59	1.21	- 84
		1.1	1.6	0.55	**2.0**	1.40	- 26
qE	double link	**0.83**	**2.0**	0.32	1.5	1.24	16
		0.83	2.4	**0.66**	2.0	1.35	16
		0.83	1.6	0.35	**2.0**	1.40	0
		1.3	**2.0**	**0.66**	1.6	1.30	- 19
		0.86	**2.0**	0.52	**2.0**	1.35	5
		1.2	1.7	**0.66**	**2.0**	1.38	- 25
qE	triple link	1.0	**2.0**	**0.66**	**2.0**	1.33	- 9
		0.83	2.4	**0.66**	**2.0**	1.33	20
		0.83	**2.0**	0.50	**2.0**	1.34	7
		0.83	**2.0**	**0.66**	2.3	1.44	0

Table 13: Rate constants as calculated by global target analysis of fluorescence decay kinetics from thylakoid samples at F_{RS}. The rate constants for F_{RS} in the presence of S-state randomizing background light are linked in various combinations to the rate constants for F_o exposed to pH-dependent quenching (+ AL, qE). The F_o-F_{RS} linked solution used to obtain the set of fixed F_{RS} constants is one in which k_A was free to change. Numbers in boldface represent linked, or fixed, rate constants: those in normal face are free to change. For F_o experiments, the Exciton/Radical Pair Equilibrium Model can be used to quantitatively predict the change in absorption cross-section (σ) from the set of rate constants (see text; Vasil'ev et al., 1998).

	Linked State	Rate constants (ns^{-1})					
		k_A	k_{PC}	k_{PC}^-	k_D	χ^2	$\Delta\sigma$ (%)
F_{RS}	from F_o link	**0.42**	**2.3**	**0.40**	**1.8**	1.18	--
qE	single link	**0.42**	2.2	0.18	1.4	1.22	5
		0.13	**2.3**	0.11	1.1	1.20	29
		1.3	1.4	**0.40**	1.4	1.22	- 55
		1.1	1.7	0.49	**1.8**	1.29	- 45
qE	double link	**0.42**	**2.3**	0.23	1.5	1.22	7
		0.42	2.6	**0.40**	1.8	1.26	15
		0.42	2.3	0.30	**1.8**	1.26	4
		0.72	**2.3**	**0.40**	1.7	1.24	- 12
		0.74	**2.3**	0.45	**1.8**	1.26	- 14
		0.74	2.1	**0.40**	**1.8**	1.27	- 20
qE	triple link	0.63	**2.3**	**0.40**	**1.8**	1.25	- 8
		0.42	2.6	**0.40**	**1.8**	1.26	15
		0.42	**2.3**	0.31	**1.8**	1.26	4
		0.42	**2.3**	**0.40**	2.0	1.34	0

Table 14: Rate constants as calculated by global target analysis of fluorescence decay kinetics from thylakoid samples at F_m. Target analysis for the F_m condition assumed a heterogeneous PSII model, so that 2 sets of rate constants are shown. The rate constants for F_m are determined for 3 different PSII α/β ratios.

PSII α/β Ratio		Rate constants (ns^{-1})				
		k_A	k_{PC}	k_{PC}^-	k_D	χ^2
1	α	0.3	1.0	1.3	2.2	1.24
	β	0.3	0.79	3.0	0.86	
2	α	0.3	0.90	1.0	1.6	1.26
	β	0.3	0.29	3.0	1.3	
3	α	0.3	0.79	0.91	1.4	1.28
	β	0.3	0.19	4.4	1.5	

Table 15: Rate constants as calculated by global target analysis of fluorescence decay kinetics from thylakoid samples at F_m as a function of 3 different PSII α/β ratios. The rate constants for F_m are linked to the rate constants for F_m exposed to 5-OH-NQ quenching. Numbers in boldface represent linked, or fixed, rate constants: those in normal face are free to change.

State	PSII α/β Ratio		Rate constants (ns^{-1})				
			k_A	k_{PC}	k_{PC}^-	k_D	χ^2
F_m	1	α	**0.3**	**1.0**	**1.3**	**2.2**	1.24
		β	**0.3**	**0.79**	**3.0**	**0.86**	
	2	α	**0.3**	**0.90**	**1.0**	**1.6**	1.26
		β	**0.3**	**0.29**	**3.0**	**1.3**	
	3	α	**0.3**	**0.79**	**0.91**	**1.4**	1.28
		β	**0.3**	**0.19**	**4.4**	**1.5**	
+5-OH-NQ							
	1	α	0.83	**1.0**	**1.3**	**2.2**	1.24
		β	0.70	**0.79**	**3.0**	**0.86**	
	2	α	0.83	**0.90**	**1.0**	**1.6**	1.24
		β	0.65	**0.29**	**3.0**	**1.3**	
	3	α	0.83	**0.79**	**0.91**	**1.4**	1.27
		β	0.64	**0.19**	**4.4**	**1.5**	

Table 16: Rate constants as calculated by global target analysis of fluorescence decay kinetics from thylakoid samples at F_m for 3 different PSII α/β ratios. The rate constants for F_m are linked to the rate constants for F_m exposed to pH-dependent quenching (+AL, qE). Numbers in boldface represent linked, or fixed, rate constants: those in normal face are free to change.

State	PSII α/β Ratio		Rate constants (ns^{-1})				
			k_A	k_{PC}	k_{PC}^-	k_D	χ^2
F_m	1	α	**0.3**	**1.0**	**1.3**	**2.2**	1.24
		β	**0.3**	**0.79**	**3.0**	**0.86**	
	2	α	**0.3**	**0.90**	**1.0**	**1.6**	1.26
		β	**0.3**	**0.29**	**3.0**	**1.3**	
	3	α	**0.3**	**0.79**	**0.91**	**1.4**	1.28
		β	**0.3**	**0.19**	**4.4**	**1.5**	
qE	1	α	1.2	**1.0**	**1.3**	**2.2**	2.76
		β	0.52	**0.79**	**3.0**	**0.86**	
	2	α	1.2	**0.90**	**1.0**	**1.6**	2.16
		β	0.48	**0.29**	**3.0**	**1.3**	
	3	α	1.2	**0.79**	**0.91**	**1.4**	1.74
		β	0.47	**0.19**	**4.4**	**1.5**	
qE	1	α	0.90	**1.0**	**1.3**	6.1	2.33
		β	0.77	**0.79**	**3.0**	0.002	
	2	α	0.77	**0.90**	**1.0**	7.5	1.54
		β	0.57	**0.29**	**3.0**	0.001	
	3	α	0.85	**0.79**	**0.91**	6.2	1.33
		β	0.49	**0.19**	**4.4**	0.001	

Table 17: Rate constants as calculated by global target analysis of fluorescence decay kinetics from thylakoid samples at F_m with PSII α/β equalling 3. The rate constants for F_m are linked in various combinations to the rate constants for F_m exposed to pH-dependent quenching (+AL, qE). Numbers in boldface represent linked, or fixed, rate constants: those in normal face are free to change. One constant is fixed in each case.

	Linked State		Rate constants (ns^{-1})				
			k_A	k_{PC}	k_{PC}^-	k_D	χ^2
F_m	independent	α	**0.3**	**0.79**	**0.91**	**1.4**	1.28
		β	**0.3**	**0.19**	**4.4**	**1.5**	
qE	single link	α	**0.3**	1.3	0.31	1.9	1.34
		β	**0.3**	1.2	1.1	0.51	
		α	0.97	**0.79**	0.85	1.61	1.24
		β	0.36	**0.19**	5.89	2.30	
		α	1.4	0.07	**0.91**	0.80	1.35
		β	0.50	1.1	**4.4**	0.24	
		α	0.42	1.1	0.001	**1.4**	1.37
		β	0.26	0.61	1.9	**1.5**	

Table 18: Rate constants as calculated by global target analysis of fluorescence decay kinetics from thylakoid samples at F_m with PSII α/β equalling 3. The rate constants for F_m are linked in various combinations to the rate constants for F_m exposed to pH-dependent quenching (+AL, qE). Numbers in boldface represent linked, or fixed, rate constants: those in normal face are free to change. Two constants are fixed in each case.

	Linked State		Rate constants (ns^{-1})				
			k_A	k_{PC}	k_{PC}^-	k_D	χ^2
F_m	independent	α	**0.3**	**0.79**	**0.91**	**1.4**	1.28
		β	**0.3**	**0.19**	**4.4**	**1.5**	
qE	double link	α	**0.3**	**0.79**	0.0002	1.1	3.64
		β	**0.3**	**0.19**	0.17	1.7	
		α	**0.3**	1.4	**0.91**	7.3	1.40
		β	**0.3**	0.87	**4.4**	1.5	
		α	**0.3**	1.2	0.002	**1.4**	1.33
		β	**0.3**	0.92	5.1	**1.5**	
		α	0.85	**0.79**	**0.91**	6.2	1.33
		β	0.49	**0.19**	**4.4**	0.001	
		α	0.72	**0.79**	0.001	**1.4**	1.40
		β	0.45	**0.19**	6.7	**1.5**	
		α	1.5	0.0001	**0.91**	**1.4**	1.39
		β	0.3	0.87	**4.4**	**1.5**	

Table 19: Rate constants as calculated by global target analysis of fluorescence decay kinetics from thylakoid samples at F_m with PSII α/β equalling 3. The rate constants for F_m are linked in various combinations to the rate constants for F_m exposed to pH-dependent quenching (+AL, qE). Numbers in boldface represent linked, or fixed, rate constants: those in normal face are free to change. Three constants are fixed in each case.

	Linked State		Rate constants (ns^{-1})				
			k_A	k_{PC}	k_{PC}^-	k_D	χ^2
F_m	independent	α	**0.3**	**0.79**	**0.91**	**1.4**	1.28
		β	**0.3**	**0.19**	**4.4**	**1.5**	
qE	triple link	α	1.2	**0.79**	**0.91**	**1.4**	1.74
		β	0.47	**0.19**	**4.4**	**1.5**	
		α	**0.3**	2.3	**0.91**	**1.4**	3.34
		β	**0.3**	1.4	**4.4**	**1.5**	
		α	**0.3**	**0.79**	0.0003	**1.4**	6.98
		β	**0.3**	**0.19**	17.8	**1.5**	
		α	**0.3**	**0.79**	**0.91**	12.1	4.80
		β	**0.3**	**0.19**	**4.4**	12.5	

Table 20: Rate constants as calculated by global target analysis of fluorescence decay kinetics from thylakoid samples at F_m assuming a homogeneous model of PSII. The rate constants for PSIIα centres at F_m are linked in various combinations to the rate constants for F_m exposed to pH-dependent quenching (+AL, qE) or to 5-OH-NQ quenching. Numbers in boldface represent fixed rate constants: those in normal face are free to change.

Linked State		Rate constants (ns^{-1})				
		k_A	k_{PC}	k_{PC}^-	k_D	χ^2
F_m	PSIIα (independent)	**0.3**	**0.79**	**0.91**	**1.4**	--
+5-OH-NQ		0.83	**0.79**	**0.91**	**1.4**	1.22
qE	linked	0.86	**0.79**	**0.91**	**1.4**	1.39
		0.69	**0.79**	0.48	**1.4**	1.39
		1.0	**0.79**	**0.91**	0.92	1.31
		0.77	**0.79**	0.45	0.91	1.28

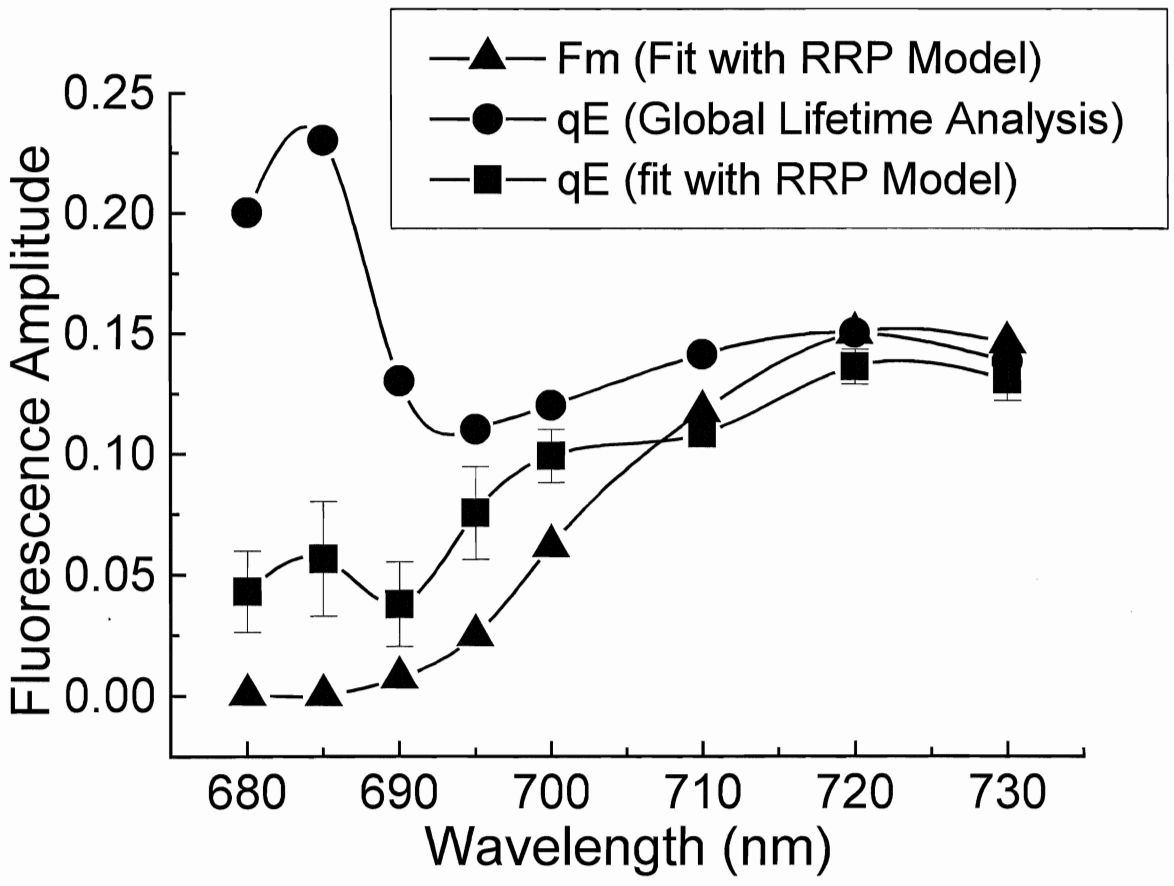

Figure 50: DAS of the 100 ps PSI decay component before and after its application to the RRP model of PSII. There is better separation of the PSII-associated peak in the quenched (■) and the unquenched (▲) spectra after fitting with the RRP model compared to the global analysis of qE quenching (●). The qE-quenched RRP spectrum represents the average and standard deviations of 5 different linked fits, using the same constraints placed on the link as in Figure 51.

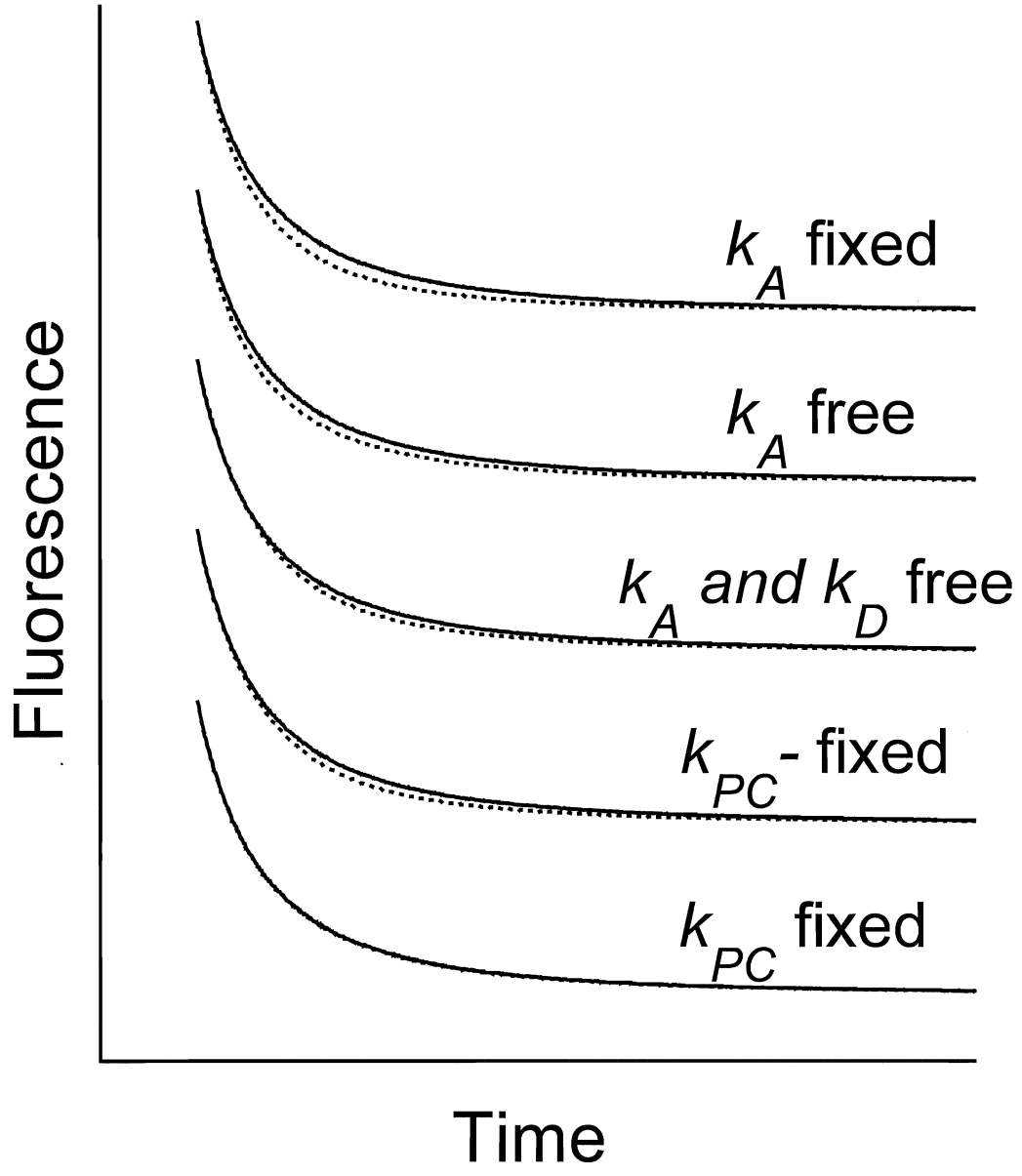

Figure 51: Simulated fluorescence decay curves of thylakoids at F_m in the qE-quenched state, generated from the Reversible Radical Pair Model represented by the PSII rate constants. Solid lines represent decays derived from simulation of an independent fit of the F_m quenched data, while dotted lines represent decay curves from simulations of the fits as they were linked to F_m under various constraints on the rate constants, as labelled on the figure.

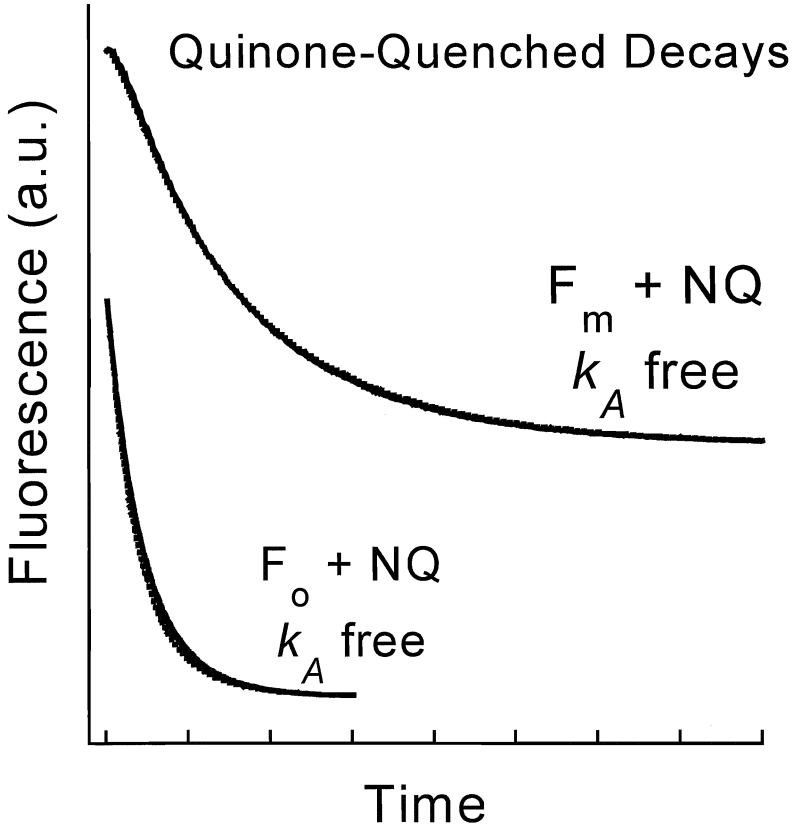

Figure 52: Simulated fluorescence decay curves of thylakoids quenched by 5-OH-NQ, generated from the Reversible Radical Pair Model represented by the PSII rate constants. Solid lines represent decays derived from simulation of an independent fit of the F_o and F_m quinone-quenched data, while dotted lines represent decay curves from simulation of the fits as they were linked to the control curves with only k_A free to vary. This confirmed that only this change was necessary to fit the quinone data.

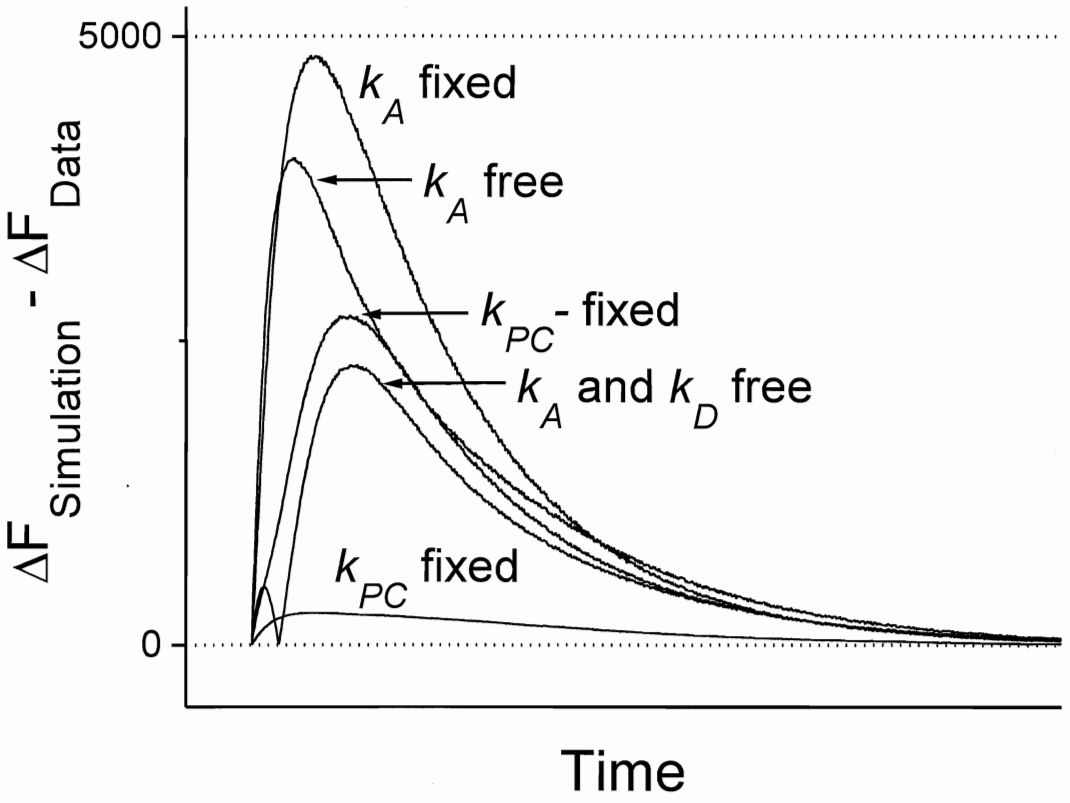

Figure 53: Plots of the absolute value of the difference between the independent data fitting and the simulated data generated from the linked-state analysis (ie absolute value of the differences between paired curves in Figure 51).

Discussion

The results reported in the present study point to some definite conclusions concerning the localization of the mechanisms of photoprotective ΔpH-dependent quenching (qE) in spinach thylakoids. A well-characterized qE preparation was developed for this purpose and was applied effectively to the powerful combination of fluorescence spectroscopic techniques used: PAM fluorimetry, direct measurements of PSII absorption cross-sections, and picosecond decay kinetics.

The thylakoid isolations used were clearly robust and efficient, despite storage at -80EC for upwards of 6 weeks. The F_v/F_o ratios obtained were typically at or above 4, with quantum yields (F_v/F_m) of about 0.8, indicating PSII efficiency that held steady during PAM experiments for upwards of 30 minutes per sample. In addition, attempts to induce qE in samples throughout the time span of storage proved to be equally successful, with consistent extents of quenching that reached approximately 60% of F_m. Along with the fact that activated thylakoid membrane ATPases could maintain a high degree of qE quenching, this suggests intact membranes capable of holding a pH gradient for extended periods of time. Compared to the quenching held by dark activation of ATPase H^+ pumping from another study (Gilmore & Yamamoto, 1992), qE maintenance reported in this study was slightly less effective pointing to lower ATPase activity or membranes that were slightly more leaky to protons. However, the circulated thylakoids could maintain as much chlorophyll and 9-aminoacridine fluorescence quenching as was observed in a stationary 10 mm cuvette, in spite of the dark delay of 21 seconds. Quenched samples also possessed significant response in the DTT-sensitive absorbance change at 505 nm, indicating active de-epoxidase enzymes and formation of zeaxanthin, which could not be epoxidated. Lack of epoxidation is expected since NADPH or FAD are required in the stroma for the reaction to take place: these were not supplied in the resuspension buffer.

The quenching that was observed is definitively identified as qE. First, the majority of the quenching could be immediately reversed upon degeneration of the pH gradient by the uncoupler nigericin. Also, due to the clear quenching response of the ΔpH indicator, 9-aminoacridine, it can be positively concluded that the major portion of the quenching was pH dependent.

In this respect, the post-illumination, nigericin-insensitive F_m quenching was of some concern, since it implies that another form of qN was induced during exposure to light. The state transitions, qT, can be ruled out since provision of the required phosphorylation source (ATP) did not increase the extent of quenching either during or after illumination when compared to thylakoids not supplied with ATP. There was also no discernable quenching of F_o in the post-illumination period, as might be expected in the presence of the slowly-reversible state transition. A high degree of thylakoid membrane stacking resulting from the high concentration of Mg^{2+} in the buffer probably contributed, since the timescale of experiments would have been too short to realize migration of phosphorylated LHCs to the non-appressed regions to join PSI (Walters & Horton, 1993). The alternative to qT is a contribution from photoinhibition (qI) to quenching. This is likely the source of the nigericin-insensitive F_m quenching.

Photoinhibition is not expected to affect the measurements of F_o and absorption cross-sections (σ) that are so interesting to the study of qE. Indeed, uncoupling of thylakoids by nigericin after measurement of cross-sections in the qE state revealed complete recovery of both F_o and σ, even while qI-related F_m quenching remained. Since uncoupling by nigericin proved to completely degenerate the pH gradient, this eliminates the assertion that sustained levels of ATP hydrolysis delay the relaxation of qE in the dark and cause misinterpretation of F_m quenching as qI (Wagner et al., 1996; Gilmore & Yamamoto, 1992). It also precludes a role for residual zeaxanthin quenching, implied by Färber et al. (1997) when they observed drastically reduced epoxidation rates in LHCIIb subcomplexes exposed to photoinhibitory light conditions. The qI component detected in the present study can not be related to the de-epoxidation state, even though zeaxanthin was apparently not re-epoxidized, nor could it be in the timescale of nigericin uncoupling. There is no indication of antenna quenching without the presence of qE. The proposition offered by Laisk et al. (1997) seems more reasonable: that qI may be a long-lived reaction centre-based quenching. However, even their proposal requires a sustained ΔpH, which is absent in uncoupled thylakoids. The qI seen here is more consistent with damage to the reaction centre. Both damaging and non-damaging qE are pH-independent.

Thus, the circulating thylakoids achieve a high level of qE quenching without interference from qT. However, the qE preparation used is most effective in part because of the dark delay between qE-inducing light exposure and instrument detection, as well as the application of low-level background light for a short time period to induce the randomization of S states in the Oxygen-Evolving Complex (OEC). Both of these features served to eliminate problems associated with accurate measurements and comparisons of F_o, a very important parameter in these experiments. The dark delay provided sufficient time for complete reoxidation of the plastoquinone pool, opening PSII centres to permit a more accurate representation of F_o. Randomization of the S states was also necessary because of the clear distinction between the F_o level attained in dark-adapted thylakoids and that reached in thylakoids exposed to light, even when the latter were returned to the dark. Relaxation of S states in the dark takes a few minutes, whereas reoxidation of PQ was more or less complete in less than 20 seconds. Since thylakoids exposed to the qE-inducing light would be detected in the randomized state, control measurements also required randomization in order to make valid F_o comparisons. Valid F_o measurements were clearly demonstrated in this preparation, making it a dependable approach to the study of qE.

Randomization of S states

What is the source of the difference between dark-adapted and S state-randomized F_o? It is known that different redox poises of the manganese cluster have different quenching effects on both the O_2 yield of PSII and the PSII fluorescence yield at F_o (F_m is not affected because saturation of PSII inherently randomizes the S states). Both O_2 and fluorescence can be observed in a period four oscillation of yields following single-turnover saturating flashes (Delrieu, 1998; Delrieu & Rosengard, 1993; Joliot & Joliot, 1973). However, the origin of the quenched states within the oscillations is an interesting phenomenon about which few conclusions have been drawn.

Yields of F_o and the absorption cross-sections both point to an effect of S states in the PSII antenna. The small increase in F_o (12%) in the randomized samples was closely accompanied by an increase in σ (11%). This pattern follows the

quantitative model prediction for PSII changes under conditions of affected antennae ($\Delta\sigma_{PSII}.\Delta F_o$), originally proposed by Butler (1984). Global target analysis of picosecond decay kinetics also suggested the best fit resulted from a major contribution of k_A, involving a lesser degree of antenna quenching in the randomized sample than in the dark-adapted sample. This conclusion is supported by the near identity of dark-adapted and qE-quenched decay curves, the latter of which was also reasonably modelled by a change in just k_A (compared to F_{RS}). The fits were of considerably higher quality when the k_A-affected solution for the randomized state was applied to modelling of qE at F_o (compared to that for a non-k_A-affected solution). Quantitative predictions of $\Delta\sigma_{PSII}$ were also much more reasonable assuming a change in k_A, with or without additional influence of a reaction centre mechanism. The validity of the choice to allow k_D to change along with k_A (in terms of fits and predicted $\Delta\sigma_{PSII}$) may reflect some small portion of closed reaction centres that caused k_D to decrease slightly. The same could be said had k_{PC} been allowed to change, permitting a small increase in radical pair recombination, although in both cases, the size of the change in the reaction centre-associated rate constant was almost negligible in light of the relatively large errors connected with them (Vasil'ev & Bruce, 1998). Report of electrochromic oscillations that behaved with a similar periodicity to fluorescence oscillations (Delrieu & Rosengard, 1993) and that fluorescence yield is susceptible to electrical fields (Dau & Sauer, 1991) could contribute to this antenna quenching. Creation of different local electrical fields by charge accumulation steps in the manganese cluster of the OEC could potentially alter the state of light harvesting via small structural reorganizations of the LHCII proteins, previously proposed to originate from cooperativity of proton binding (Delrieu, 1998).

Although an antenna quenching mechanism appears to operate in the dark-adapted state, this study is limited with respect to a full investigation of the effects of S states on fluorescence. First, the errors observed in the yields are too large compared to the small yield changes associated with the oscillation. This most likely originates from the relatively small number of repeats (n=4) and a limit to the resolution during collection of single-turnover flashes by the PAM fluorimeter. Second, and more importantly, the present study only illustrates data from two extremes of the phenomenon - full randomization and the dark-adapted state, which contains some

proportion of the S_0 and S_1 states only. A full investigation of the picosecond decays may be possible if these states could be achieved using the single-turnover flash protocol previously employed in our lab for studying the origins of the low yield of fluorescence during single turnovers (F_{sat} – Vasil'ev & Bruce, 1998). In any case, randomization of the S states remains useful for valid comparisons of F_o parameters, especially important since the F_o yields and picosecond decay curves of dark-adapted and qE-quenched samples at F_o were identical. This indicates that both are antenna-quenched with respect to the randomized states, although by different mechanisms.

Localization of qE

Does pH-dependent fluorescence quenching occur in the PSII antenna, in the PSII reaction centre, or both? To address this important question, spinach thylakoids with induced qE were measured by pump-probe and single photon counting techniques. The main strength of the approach was an effective comparison of qE with quenching by the known antenna quencher, 5-hydroxy-1,4-naphthoquinone, work repeated in the present study as had been previously reported (Vasil'ev & Bruce, 1998; Vasil'ev et al., 1998).

Contrary to the work from other groups (Gilmore, 1997; Mullineaux et al., 1994), qE quenching in spinach thylakoids is not the result of antenna quenching alone. Quenched thylakoids exhibited far too many differences between antenna quenching by 5-OH-NQ and light-induced qE. Quinone quenching displayed a significantly greater effect on F_o in all 3 techniques used, given the same extent of F_m quenching as that induced in qE-treated samples. Quinone quenching also induced a direct decrease in σ, while a decrease in σ during formation of qE could only be located within a larger overall increase that must be associated with some other accompanying process. Picosecond decay curves were both qualitatively and quantitatively different for quinone and qE. The qE samples had accelerated kinetics with respect to the control, but tended towards convergence with the control in the longer time frame, unlike 5-OH-NQ. Quinone-quenched kinetics at F_m and F_o could most reasonably be modelled with a variable k_A, while qE kinetics could not be sufficiently described by this adjustment alone. The hypothesis that antenna processes account for all of qE is therefore removed from consideration.

Despite elimination of antenna quenching as the sole source of qE in thylakoids, the reaction centre can also be ruled out as the basis for all of the observed quenching. Pronounced depressions in F_o detected in all three techniques point to the existence of at least a partial contribution by antenna processes. Reaction centre-based quenching cannot account for either a decreased F_o or a smaller effective absorption cross-section (Bruce et al., 1997), as was apparent within the large σ increase determined from flash saturation curves obtained in this report. Classically, reaction centre qE would not alter F_o yield or cross-section. Bruce et al. (1997) also reported no significant changes in the yield of the faster decay components associated with antenna processes, while a relatively slow component (~1.5 ns) associated with the reaction centre decreased as pH was reduced from 6.4 to 4.0. The present study demonstrates effects of quenching on most, if not all, of these decay components in qE quenched thylakoid samples. Kinetic modelling of the decay data demonstrated the necessity of allowing k_A to change, but also that others of the rate constants in the reaction centre must be variable along with it. It is therefore concluded that there are significant contributions from quenching mechanisms in both the antenna and in the reaction centre.

The unexpected overriding enhancement of σ during formation of qE presented a challenging deviation from the classical model of antenna quenching. Such an increase is not expected for reaction centre-based quenching either. A number of other measurements exhibited the classical Butler model for σ_{PSII}, such as post-quenching uncoupled cross-sections and the dark-adapted/S state-randomized transition, imparting validity in the form of positive controls to the new pump-probe setup applied to the measurement of σ. Without these appropriate checks on the calculation of σ, the overall increase observed during qE might have been discarded as unreliable. However, the expected model of antenna quenching is supported by three independent approaches to the problem. First, thylakoids were uncoupled with nigericin prior to treatment with qE-inducing light to prevent generation of a ΔpH. Second, they were treated with an inhibiting concentration of DTT to eliminate formation of zeaxanthin. Finally, thylakoids were circulated without the addition of ATP so that quenching was not maintained for a long enough period to allow detection. The increases in σ during the three experiments substantiated each other,

all resulting in approximately 60% increases. When compared pair-wise with the qE-quenched thylakoids (σ increased only 27%), each case revealed distinctly-diminished σ in the qE samples. The extent of the cross-section quenching is shown to be significant (~20%) compared to the 60% increases, yet it remains imprecise since the standard deviations became quite large within this analysis. These data strongly suggest a contribution to qE from antenna processes.

The likely source of the overall increase in absorption cross-section of PSII is related to the fundamental difference between F_m (PSII saturated by multiple turnovers) and F_{sat} (saturation with single turnover flashes). The F_{sat} level reached with single turnover flashes is quenched with respect to F_m, probably due to an antenna quenching mechanism that is separate from qE (Vasil'ev & Bruce, 1998). Cross-sections were measured with 300 ps laser pulses, constituting single turnovers of PSII. However, the qE-inducing light is continuous, and therefore provides multiple turnovers to PSII. Indeed, during exposure to light in the presence of the uncoupler nigericin, F_m was reached. Compared to this saturated level of fluorescence, the quenching exhibited during qE was quantitatively equal to that observed during F_m quenching on the PAM fluorimeter. Hence, it is probable that exposure to the multiple turnover light used to induce qE released the antenna quenching due to F_{sat}, allowing the cross-section to increase. The only requirement for this hypothesis is that the release of this form of quenching last longer than the 20 seconds of dark delay employed in the circulation system. This precludes the suggestion that oxidized PQ acts as the quencher (Vasil'ev & Bruce, 1998; Vernotte et al., 1979), since the 20 seconds of delay was shown to be sufficient to allow return to a true F_o level with fully oxidized PQ. The quenching species must either be an unidentified quencher like the alternative quencher Q_2 (Joliot & Joliot, 1979), or the mechanism involving PQ is more complicated than direct quenching of bulk antenna fluorescence by oxidized PQ (Vasil'ev & Bruce, 1998; Kolber et al., 1998). In any case, the magnitude of the increase still seems to be enhanced compared to what could be accounted for by a 60% increase in maximal fluorescence (F_m or F_{sat}). The source of the enhancement will be explored below.

All three of the approaches to distinguishing the antenna processes within the σ increase had elevated F_o levels during exposure to qE-inducing light, one of which

(pre-uncoupled) increased even further after removal of the light. A small and rapid rise in F_o was also reported by Gilmore and Yamamoto (1992) when DTT was added to inhibit de-epoxidation and antenna quenching. Bruce et al. (1997) observed a similar elevation of F_o in PSII-enriched membranes at low pH. The source of this elevation is unclear. It could be due to redox limitations of the PQ pool resulting in reaction centre closure, but it is not related directly to qE because it was revealed in thylakoids that were not competent for qE (pre-uncoupled), and in those without qE held during circulation (absence of ΔpH-maintaining ATP), unless some effect of reaction centre qE is long-lived ie greater than the 20 second delay. The elevated F_o will be explored further in the discussion of mechanisms of reaction centre quenching.

In regard to specific origins of the antenna quenching itself, a few reasonable conclusions can be drawn from the current study. The requirement for zeaxanthin is obligatory. Any quenching that remained when inhibiting concentrations of DTT were added displayed none of the typical aspects of antenna quenching: It showed no decline in F_o - in fact, F_o increased - and the absorption cross-section was not significantly different from the other unquenched states exposed to qE-inducing light (each had about a 60% increase). The presence of zeaxanthin was required to accomplish the changes in σ. Conversely, presence of zeaxanthin is insufficient to elicit qE, but requires a ΔpH. The post-qE presence of zeaxanthin was confirmed by 505 nm absorbance changes, and would be expected even were re-epoxidation possible since its timescale is on the order of minutes. Zeaxanthin alone in uncoupled thylakoids did not sustain any antenna quenching, as indicated by complete recovery of F_o and σ following uncoupling, eliminating the pH gradient. Similarly, in the case where quenching was not maintained by ATP, no cross-section or F_o quenching was observed, indicating that the zeaxanthin formed during light exposure was unable to maintain qE by itself (present study; Gilmore, 1997; Wagner et al., 1996). Aggregations occurring as a result of zeaxanthin-dependent effects of the ΔpH can not be ruled out, since there was no quenching of σ in DTT-treated thylakoids exposed to qE induction, when compared to pre-uncoupled and ATP-lacking samples. This does not eliminate an essential role of zeaxanthin in LHCII aggregations, in support of earlier reports (Härtel et al., 1996; Gilmore et al., 1995), but direct deactivation by zeaxanthin seems more likely. Formation of these efficient quenching

centres was considered briefly as the explanation for acceleration of the F_m decay curves in the qE state compared to the quinone-quenched state, since the static quinone quenching is most conceptually comparable to direct deactivation by zeaxanthin. However, the decay curves obtained here for 5-OH-NQ at F_m qualitatively resemble those found in Wagner et al. (1996) for qE and in Vasil'ev et al. (1997) for aggregated LHCII proteins. No other indications of protein aggregation are evident in the work completed here.

DTT inhibition of de-epoxidation clearly distinguished antenna- and reaction centre-based quenching. The quenching that persisted during qE induction in the presence of DTT did not have a depression in F_o or in σ when compared to the unquenched alternative trials (pre-uncoupled, absence of ATP). A similar situation with F_o decay kinetics was modelled without adjustment of the rate constant for decay in the antenna (Wagner et al., 1996). Could the relative contribution of antenna- and reaction centre-based quenching mechanisms be evaluated? In the absence of zeaxanthin-mediated antenna quenching, other qN processes - presumably reaction centre qE - make up 25% quenching of F_{sat} (~40% of F_v) compared to 36% quenching (~60% of F_v) during full qE. This appears to indicate a greater than 50% contribution from the reaction centre. However, compensatory increases in reaction centre quenching, or increased susceptibility to photoinhibition may contribute to overestimation of its role during qE. In addition, F_{sat} already involves antenna quenching of the F_m yield (Vasil'ev & Bruce, 1998) that may interfere with an estimation of its share of the photoprotective mechanism of qE. A comparison of F_m or F_o yields is more appropriate.

To test this hypothesis, one could compare the F_o yields and σ from the 5-OH-NQ experiments. Since accurate comparisons of σ do not appear possible due to the large errors associated with analysis of the overall σ increase, F_o will be examined. In this study and another (Vasil'ev et al., 1998), the amount of F_o quenching accompanying 60% F_m quenching when 5-OH-NQ was added was about 20%. That accompanying 60% F_m quenching during qE was closer to 10%, which corresponded to approximately 30% F_m quenching in 5-OH-NQ-quenched samples. This indicates that only about 50% of the total quenching of F_m can be attributed to antenna processes in qE under these experimental conditions. Although it seems to agree

with the calculation given by the DTT addition, both estimates of the antenna contribution seem low in light of the more extensive molecular machinery and structural reorganization required to elicit the response compared to putative effects associated with inhibited reaction centres. Such molecular effort might be expected to yield a more significant advantage *in vivo*. It could be that some aspect of thylakoid instability is making them more vulnerable to photoinhibition, which may, as will be discussed, involve reaction centre processes. A most effective method to pursue determination of the separate contributions from these processes will be to include modelling of low pH-quenched reaction centres to the effort. It will be possible to link reaction centre-quenched data with quinone-quenched antenna data in various proportions to ascertain how much of each is required together to model the quenching exhibited under qE conditions.

Concerning specific proposals for the origins of reaction centre quenching, conclusions are more difficult to reach. It has been established that there must be some changes in the reaction centre in order to describe the results portrayed in this study, a position that was especially strengthened by kinetic modelling. F_o is largely ignored in terms of modelling reaction centre processes, since these operate significantly only when reaction centres are closed. Are any of the proposed mechanisms evident in the F_m kinetics? It is expected that the main two proposals, charge recombination and cyclic electron transport, would be apparent in an increase in k_D, recombination possibly in an increase in k_{PC}^-. The quenching of the two longest decay components at F_m that are related to charge separation and charge stabilization seems to validate these ideas. But in reference to the RRP model (Figure L8, Schatz et al., 1988, Wasielewski et al., 1989), k_D includes any alternate pathway of electron transfer that does not include charge recombination of the primary radical pair (which is k_{PC}^-). None of the combinations examined consistently exhibited an increase in either of these rate constants when k_A was also variable. At least on the surface, neither of these mechanisms is obvious in these kinetic analyses, although on one occasion a large increase in both constants was found. Wagner et al. (1996) found that a combined increase in k_A and k_D could be used to sufficiently model qE, in agreement with the simulations from the present study which demonstrated this combination to be most effective in approximating qE at F_m. The major problem with

this solution is that k_D in the present study decreased in that example. It is probable that an inability to resolve the contributions from α and β centres caused the uncertainty in the directionality of the reaction centre rate constants.

The major difference between this study and Wagner et al. (1996) is the absence of continuous light in the latter. Induction of qE was accomplished in the dark using ATP hydrolysis after a short period of light activation. This was only possible in thylakoids isolated from light pre-treated leaves and not from dark-adapted leaves, explaining the failure of a similar protocol using the dark-adapted thylakoids in this study. The protocol of Wagner et al. (1996) should be adopted more closely, since it further limits any contributions of qI to the quenching.

One other hypothesis that could be tested with respect to reaction centre quenching is direct quenching by $P680^+$ (Bruce et al., 1997). Donor side-inhibited centres of that sort might be expected to completely dispel the reaction centre rate constants, since charge separation is not even permitted. The decrease in either k_D or k_{PC}^-, or in both, when modelled with increased k_A, supports this concept. Some centres may in fact form $P680^+$ as a quencher, in effect concealing charge recombinations or cyclic transport if they occur. The 100 μs timescale of measurement between pump and probe would allow detection of the $P680^+$ species. Furthermore, the slowest, reaction centre-associated decay component which appears at F_m and has been proposed to represent monoexponential decay from PSIIβ centres, almost completely disappeared in qE. It is realistic to conclude that its disappearance may in part be related to removal of certain centres from charge separation competence, as in $P680^+$ quenching. Whether or not these centres must absolutely be PSIIβ cannot be determined. The DAS for F_m in the qE state also illustrates a pronounced increase in the yield of the shorter PSII antenna component that is not so dramatic in quinone-quenched samples. The increase may represent increased yield of fluorescence from the antenna as a result of reduced trapping. However, $P680^+$ is suggested to quench fluorescence directly, implicating another form of reaction centre quenching in the enhancement of this component. The elevation of this component can be offset by antenna quenching represented in the longer PSII components (1.5 ns and 3.1 ns). It could also potentially account for the increased F_o when DTT was added. Without the presence of the antenna quenching,

the reaction centre component responsible for the partial elevation of F_o is no longer compensated. This is a logical result of reaction centre quenching when it is considered that these mechanisms can only operate assuming centres are closed. The 16 to 20% increase seen in this study may indicate the presence of some recombination, which makes some PSIIs look like closed centres. According to Bruce et al. (1997), $P680^+$ direct quenching would act like open centres.

The best estimation from these data suggests that multiple reaction centre processes affect fluorescence quenching. The complicated nature of the kinetics and cross-sections, along with the allusion to differential antenna quenching abilities in the k_A of the α and β PSII centres, and the multiple reaction centre mechanisms proposed here, all point to multi-state qE quenching. Most centres probably quench in the antenna, while only certain reaction centres are sensitized to alternate electron transfers. A 3- or even 4-state model of qE is concluded.

Can any of the reaction centre explanations account for any portion of the large increase in σ observed during qE induction? As discussed above, the majority of the increase can be attributed to the fluorescence quenching induced by single turnover saturation conditions at F_{sat}. Kinetic analysis also failed to correctly predict the cross-section increases measured during qE on its own. One solution at F_o appeared to do so, yielding an increase of 29% during qE. However, the dark-adapted sample that was quenched without first exposure to background light should have yielded a larger predicted increase of 54%. It only gave a 20% increase in the kinetic analysis. These results are difficult to interpret, especially since F_o and F_o in the qE state had identical kinetics. The overall increase in σ appears to be independent of the qE kinetics. It is only dependent on the presence of the red light used to induce qE. There is no pH-dependent effect since it occurs to the same extent in uncoupled samples as in DTT-treated samples - ie in the presence and absence of qE.

The only phenomenon remaining that can explain the magnitude of the cross-section increase is energetic connectivity of multiple antennae. A high degree of membrane stacking due to high Mg^{2+} concentrations supplied in the buffer should allow for optimized connectivity. There is most likely no connectivity with PSI, since there was little effect on the PSI decay component, and because PSI exists in the stroma lamellae, apart from PSII which is normally in the grana. Energetic

connectivity is validated in mathematical studies showing restricted energy transfer between photosynthetic units (Trissl & Lavergne, 1994), which themselves exist as dimers in higher plants *in vivo* (Jahns & Trissl, 1997; Boekema et al., 1995) that are almost fully excitonically coupled within the dimer. Fast exciton equilibration times have been found in these systems, indicating rapid exciton migration that is still far more rapid than overall trapping (Jahns & Trissl, 1997). Selective closing of one of a dimer?s reaction centres would allow exciton migration between antennae, possibly even inter-dimer, making the cross-section appear larger for the centres that remain open. However, the transient closing of a reaction centre implied here cannot account for the apparent connectivity present after the 21 seconds of delay after exposure to the red light. Reaction centre closure would have to be long-lived enough to see it that much later - normal Q_A^- saturation is an unlikely candidate because it re-oxidizes in a matter of a few hundred microseconds following a single turnover (Bruce et al., 1997). A long-lived closure due to extended effects of qE or photoinhibition, on the other hand, could prospectively accomplish closure on the timescale required. Photoinhibition, for example, occurs over many minutes, the time frame necessary for recycling of PSII proteins. Reaction centres knocked out by photoinhibition could contribute to exciton connectivity during the exposure to light.

Conclusions

Pulse Amplitude Modulated fluorescence measurements, absorption cross-sections, and picosecond decay kinetics with kinetic modelling were employed to elucidate the mechanism of pH-dependent non-photochemical quenching, qE, in thylakoid membranes isolated from spinach leaves. It appears that a multi-state model of quenching is most reasonable, in which most PSIIs make use of antenna quenching, while only a finite proportion are set to quench in the reaction centre. This model is quite likely complicated by exciton connectivity.

Comparing qE quenching with quenching induced by addition of a known antenna quencher, 5-OH-NQ, was a novel approach to the study of qE that allows us to conclude heterogeneous quenching mechanisms. Differences in susceptibility to F_o quenching, absorption cross-section changes, and in kinetic modelling contributed to the conclusion that qE cannot have its origin in antenna quenching alone. However, it did display some indicators that antenna quenching may constitute more than 50% of qE quenching, like a small but significant depression in F_o and cross-section, with acceleration of fast component kinetics that led to modelling that included a change in k_A, the rate constant of fluorescence decay in the antenna complex. The nature of this antenna quenching appears to be zeaxanthin-mediated LHCII aggregations.

The heterogeneity of qE localization is most evident in quenching that remained after addition of DTT to prevent the antenna quenching events. This is supported in the observation that variable reaction centre rate constants were necessary in order to best model the decay kinetics of qE quenching. The exact mechanisms which contribute to reaction centre-based qE are difficult to ascertain from this study, so no previous proposals are outright rejected.

The work accomplished in the present study will be most valuable in combination with further analysis of low pH quenching of the kind earlier suggested to elicit reaction centre quenching only (Bruce et al., 1997). Kinetic modelling of qE decays with a link of quinone and low pH decays is expected to yield a powerful approach to evaluating the extents of each of antenna and reaction centre-based quenching that contribute to the total qE effect in green plants.

References

Alberts,B., D. Bray, J.Lewis, M.Raff, K.Roberts, and J. Watson. 1989. *Molecular Biology of the Cell.* 2nd edition. Garland Publishing, Inc., New York.

Anderson,J. and E-M.Aro (1994) Grana stacking and protection of Photosystem II in thylakoid membranes of higher plant leaves under sustained high irradiance: An hypothesis. *Photosynthesis Research* 41:315-326.

Andréasson,L-E., I.Vass, and S.Styring (1995) Ca^{2+} depletion modifies the electron on both donor and acceptor side in Photosystem II from spinach. *Biochimica et Biophysica Acta* 1230:155-164.

Aro,E-M, I.Virgin, and B.Andersson (1993) Photoinhibition of Photosystem II. Inactivation, protein damage and turnover. *Biochimica et Biophysica Acta* 1143:113-134.

Barber,J. and J.De Las Rivas (1993) A functional model for the role of cytochrome b_{559} in the protection against donor and acceptor side photoinhibition. *Proceedings of the National Academy of Sciences, USA* 90:10942-10946.

Bassi,R., D.Sandonà, and R.Croce (1997) Novel aspects of chlorophyll *a/b*-binding proteins. *Physiologia Plantarum* 100:769-779.

Boekema,E.J., B.Hankamer, D.Bald, J.Kruip, J.Nield, A.F.Boonstra, J.Barber, M.Rögner (1995) Supramolecular structure of the Photosystem II complex from green plants and cyanobacteria. *Proceedings of the National Academy of Sciences, USA* 92:175-179.

Bracht,E. and A.Trebst (1994) Hypothesis on the control of D1 protein turnover by nuclear coded proteins in *Chlamydomonas reinhardtii. Z. Naturforsch* 49:439-446.

Briantais,J-M, C. Vernotte, G.Krause, and E.Weis (1986) Chlorophyll a fluorescence of higher plants: chloroplasts and leaves. *Academic Press Inc.* 539-583.

Bruce,D. and J.Miners (1993) Use of a pulsed laser diode to measure picosecond fluorescence lifetimes. *Photochemistry and Photobiology* 58:464-468.

Bruce,D., G.Samson, and C.Carpenter (1997) The origins of nonphotochemical quenching of chlorophyll fluorescence in photosynthesis. Direct quenching by $P680^{+}$ in Photosystem II-enriched membranes at low pH. *Biochemistry* 36:749-755.

Buser,C.A., B.A.Diner, and G.W.Brudvig (1992) Photooxidation of cytochrome b_{559} in oxygen-evolving Photosystem II. *Biochemistry* 31:11449-11459.
Butler,W. (1984) *Photochemistry and Photobiology* 40:513-518.

Casper-Lindley,C. and O.Björkman (1996) Nigericin insensitive post-illumination reduction in fluorescence yield in *Dunaliella tertiolecta* (chlorophyte). *Photosynthesis Research* 50:209-222.

Chylla,R.A. and J.Whitmarsh (1987) *Biochimica et Biophysica Acta* 894:562-571.

Crofts,A. and C.Yerkes (1994) A molecular mechanism for qE-quenching. *FEBS Letters* 352:265-270.

Dau,H. and K.Sauer (1991) *Biochimica et Biophysica Acta* 1098:49-60.

Delrieu,M.J. (1998) Regulation of thermal dissipation of absorbed excitation energy and violaxanthin de-expoxidation in the thylakoids of *Lactuca sativa*. Photoprotective mechanism of a population of Photosystem II carriers. *Biochimica et Biophysica Acta* 1363:157-173.

Delrieu,M.J., and F.Rosengard (1993) *Photosynthesis Research* 37:205-215.

Demeter,S., P.Neale, and A.Meirs (1987) Photoinhibition: Impairment of the primary charge separation between P680 and pheophytin in Photosystem II of chloroplasts. *FEBS Letters* 214:370-374.

Demmig-Adams,B. and W.W.Adams (1992) Operation of the xanthophyll cycle in higher plants in response to diurnal changes in incident sunlight. *Planta* 186:390-398.

Falkowski,P.F., Y.Fujita, A.Ley, and D.Mauzerall (1986) Evidence for cyclic electron flow around Photosystem II in *Chlorella pyrenoidosa*. *Plant Physiology* 81:310-312.

Färber,A., A.J.Young, A.V.Ruban, P.Horton, and P.Jahns (1997) Dynamics of xanthophyll-cycle activity in different antenna subcomplexes in the photosynthetic membranes of higher plants. *Plant Physiology* 115:1609-1618.

Frank,K. and A.Trebst (1995) Quinone binding sites on cytochrome b/c complexes. *Photochemistry and Photobiology* 61:2-9.

Frid,D., A.Gal, W.Oettmeier, G.Hauska, S.Berger, and I.Ohad (1992) The redox-controlled ligh-harvesting chlorophyll a/b protein kinase. *Journal of Biological Chemistry* 267:25908-25915.

Gilmore,A.M. (1997) Mechanistic aspects of xanthophyll cycle-dependent photoprotection in higher plant chloroplasts and leaves. *Physiologia Plantarum* 99:197-209.

Gilmore,A.M., T.Hazlett, and Govindjee (1995) Xanthophyll cycle-dependent quenching of Photosystem II chlorophyll a fluorescence: Formation of a quenching complex with a short fluorescence lifetime. *Proceedings of the National Academy of Science, USA* 92:2273-2277.

Gilmore,A.M. and H.Y.Yamamoto (1992) Dark induction of zeaxanthin-dependent nonphotochemical fluorescence quenching mediated by ATP. *Proceedings of the National Academy of Science, USA* 89:1899-1903.

Härtel,H., H.Lokstein., B.Grimm, and B.Rank (1996) Kinetic studies on the xanthophyll cycle in barley leaves. *Plant Physiology* 110:471-482.

Havir,E.A., S.L.Tausta, and R.B.Peterson (1997) Purification and properties of violaxanthin de-epoxidase from spinach. *Plant Science* 123:57-66.

Hodges,M., I.Moya, J-M.Briantais, and R.Remy (1987) in *Progress in Photosynthesis Research* 86 (Biggins,J., Ed.) Nijhoff, Dordrecht.

Horton,P., A.Ruban, and R.Walters (1994) Regulation of light harvesting in green plants. *Plant Physiology* 106:415-420.

Horton,P. and A.Ruban (1995) Regulation of non-photochemical quenching of chlorophyll fluorescence in plants. *Australian Journal of Plant Physiology* 22:221-230.

Huner,N., L.Lapointe, R.Carpentier, and C.Ottander (1991) Resistance to low temperature photoinhibition is not associated with isolated thylakoid membranes of winter rye. *Plant Physiology* 97:804-810.

Hurry,V., J.M.Anderson, W.S.Chow, and C.B.Osmond (1997) Accumulation of zeaxanthin in abscisic-acid deficient mutants of Arabidopsis does not affect chlorophyll fluorescence quenching or sensitivity to photoinhibition *in vivo*. *Plant Physiology* 113:639-648.

Jahns,P. and H-W.Trissl (1997) Indication for a dimeric organization of the antenna-depleted reaction centre core of Photosystem II in thylakoids of intermittent light grown pea plants. *Biochimica et Biophysica Acta* 1318:1-5.

Jansson,S., H.Stefánsson, U.Nyström, P.Gustafsson, and P-Å.Albertsson (1998) *Biochimica et Biophysica Acta* 1320:297-309

Johnson,G.N., A.J.Young, J.D.Scholes, and P.Horton (1993a) The dissipation of excess excitation energy in British plant species. *Plant, Cell, and Environment* 16:673-680.

Johnson,G.N., A.J.Young, J.D.Scholes, and P.Horton (1993b) Relationships between carotenoid composition and growth habit in British plant species. *Plant, Cell, and Environment* 16:681-686.

Joliot,P., and A.Joliot (1973) *Biochimica et Biophysica Acta* 305:302-316.

Joliot,P., and A.Joliot (1979) *Biochimica et Biophysica Acta* 546:93-105.

Klimov,V., A.Klevanik, A.Shuvalov, and A.Krasnovsky (1977) Reduction of pheophytin in the primary light reaction of Photosystem II. *FEBS Letters* 82:183-186.

Kolber,Z.S., O.Prasil, and P.G.Falkowski (1998) *Biochimica et Biophysica Acta*, in press

Krause,G. (1988) Photoinhibition of photosynthesis: An evaluation of damaging and protective mechanisms. *Physiologia Plantarum* 74:566-574.

Krause,G. and U.Behrend (1986) ΔpH-dependent chlorophyll fluorescence quenching indicating a mechanism of protection against photoinhibition of chloroplasts. *FEBS Letters* 200:298-302.

Krieger,A., I.Moya, and E.Weis (1992) Energy-dependent quenching of chlorophyll a fluorescence: Effect of pH on stationary fluorescence and picosecond relaxation kinetics in thylakoid membranes and Photosystem II preparations. *Biochimica et Biophysica Acta* 1102:167-176.

Krieger,A., A.W.Rutherford, and G.N.Johnson (1995) On the determination of redox midpoint potential of the primary quinone electron acceptor, Q_A, in Photosystem II. *Biochimica et Biophysica Acta* 1229:193-201.

Kyle,D.J. (1987) The biochemical basis for photoinhibition of Photosystem II. In *Topics in Photosynthesis. Photoinhibition*. (Kyle,D.J., C.B.Osmond, and C.J.Arntzen, Eds.) 9:197-226.

Laisk,A., V.Oja, B.Rasulov, H.Eichelmann, A.Sumberg (1997) Quantum yields and rate constants of photochemical and nonphotochemical excitation quenching. *Plant Physiology* 115:803-815.

Lee,J, W.Zipfel, and T.Owens (1992) Quenching of chlorophyll excited states in Photosystem I by quinones. *Journal of Luminescence* 51:79-89.

Mauzerall,D., N.L.Greenbaum (1989) The absolute size of a photosynthetic unit. *Biochimica et Biophysica Acta* 974:119-140.

McCormac,D., D.Bruce, and B.Greenberg (1994) State transitions, light-harvesting antenna phosphorylation and light-harvesting antenna migration *in vivo* in the higher plant *Spirodela oligorrhiza*. *Biochimica et Biophysica Acta* 1187:301-312.

Melis,A. (1985) *Biochimica et Biophysica Acta* 808:334-342.

Misuzawa,N., M.Ebina, and T.Yamashita (1995) Restoration of high potential form of cytochrome b_{559} through the photoreactivation of Tris-inactivated oxygen-evolving centres. *Photosynthesis Research* 45:71-77.

Mullineaux,C., A.Pascal, P.Horton, and A.Holzwarth (1993) Excitation energy quenching in aggregates of the LHCII chlorophyll-protein complex: a time-resolved study. *Biochimica et Biophysica Acta* 1141:23-28.

Mullineaux,C., A.Ruban, and P.Horton (1994) Prompt heat release associated with ΔpH-dependent quenching in spinach thylakoid membranes. *Biochimica et Biophysica Acta* 1185:119-123.

Niyogi,K.K., A.R.Grossman, and O.Björkman (1998) Arabidopsis mutants define a central role for the xanthophyll cycle in the regulation of photosynthetic energy conversion. *The Plant Cell* in press.

Niyogi,K.K., A.R.Grossman, and O.Björkman (1997) Chlamydomonas xanthophyll cycle mutants identified by video imaging of chlorophyll fluorescence quencing. *The Plant Cell* 9:1369-1380.

Olaizda,M., J.LaRoche, Z.Kolber, and P.Falkowski (1994) Non-photochemical fluorescence quenching and the diadinoxanthin cycle in a marine diatom. *Photosynthesis Research* 41:357-370.

Pospíšil,P. (1997) Mechanisms of non-photochemical chlorophyll fluorescence quenching in higher plants. *Photosynthetica* 34:343-355.

Rees,D. and P.Horton (1990) The mechanisms of changes in Photosystem II efficiency in spinach thylakoids. *Biochimica et Biophysica Acta* 1016:219-227.

Roelofs,T.A., C-H.Lee, and A.R.Holzwarth (1992) *Biophysical Journal* 61:1147-1163.

Ruban,A. and P.Horton (1994) Spectroscopy of non-photochemical and photochemical quenching of chlorophyll fluorescence in leaves; evidence for a role of the light harvesting complex of Photosystem II in the regulation of energy dissipation. *Photosynthesis Research* 40:181-190.

Ruban,A. and P.Horton (1998) The xanthophyll cycle modulates the kinetics of nonphotochemical energy dissipation in isolated light harvesting complexes, intact chloroplasts and leaves. Submitted to *Plant Physiology*, May 1998.

Ruban,A., P.Horton, and B.Robert (1995) Resonance Raman Spectroscopy of the Photosystem II light harvesting complex of green plants: A comparison of trimeric and aggregated states. *Biochemistry* 34:2333-2337.

Ruban,A.V., D.Phillips, A.J.Young, and P.Horton (1997) Carotenoid-dependent oligomerization of the major chlorophyll *a/b* light harvesting complex of Photosystem II of plants. *Biochemistry* 36:7855-7859.

Ruban,A., D.Rees, A.Pascal, and P.Horton (1992) Mechanism of ΔpH-dependent dissipation of absorbed excitation energy by photosynthetic membranes. The relationship between LHCII aggregation *in vitro* and qE in isolated thylakoids. *Biochimica et Biophysica Acta* 1102:39-44.

Ruban,A.V., A.J.Young, and P.Horton (1993) Induction of nonphotochemical energy dissipation and absorbance changes in leaves. *Plant Physiology* 102:741-750.

Samson,G. and D.Bruce (1995) Complementary changes in absorbance cross-section of Photosystem I and Photosystem II due to phosphorylation and magnesium depletion in spinach thylakoids. *Biochimica et Biophysica Acta* 1232:21-26.

Samson,G. and D.Bruce (1996) Origins of the low yield of chlorophyll *a* fluorescence induced by single turnover flash in spinach thylakoids. *Biochimica et Biophysica Acta* 1276:147-153.

Schatz,G.H., H.Brock, and A.R.Holzwarth (1988) A kinetic and energetic model for the primary processes in Photosystem II. *Biophysical Journal* 54:397-405.

Schreiber,U. and C.Neubauer (1990) O_2-dependent electron flow, membrane energization, and the mechanism of nonphotochemical quenching of chlorophyll fluorescence. *Photosynthesis Research* 25:279-293.

Šiffel,P. and F.Vàcha (1998) Aggregation of the light-harvesting complex in intact leaves of tobacco plants stressed by CO_2 deficit. *Photochemistry and Photobiology* 67:304-311.

Taiz,L. and E.Zeiger. 1991. *Plant Physiology*. The Benjamin/Cummings Pub. Co., Inc., Don Mills, Ont.

Terjung,F. and K.Maier (1998) Non-photochemical quenching of chlorophyll fluorescence in higher plant leaves studied by delayed fluorescence decay measurements. *Zeitschrift für Naturforschung* 53c:27-32.

Thompson,L.K. and G.W.Brudvig (1988) Cytochrome b_{559} may function to protect Photosystem II from photoinhibition. *Biochemistry* 27:6653-6658.

Trissl,H-W. and J.Lavergne (1994) Fluorescence induction from Photosystem II: Analytical equations for the yields of photochemistry and fluorescence derived from analysis of a model including exciton-radical pair equilibrium and restricted energy transfer between photosynthetic units. *Australian Journal of Plant Physiology* 22:183-193.

Vasil'ev,S. and D.Bruce (1998) Non-photochemical quenching of excitation energy in Photosystem II. A picosecond time-resolved study of the low yield of chlorophyll *a* fluorescence induced by single turnover flash in isolated spinach thylakoids. *Biochemistry* in press.

Vasil'ev,S., K-D.Irrgang, T.Schrötter, A.Bergmann, H-J.Eichler, and G.Renger (1997) Quenching of chlorophyll *a* fluorescence in the aggregates of LHCII: steady state fluorescence and picosecond relaxation kinetics. *Biochemistry* 36:7503-7512.

Vasil'ev,S., S.Wiebe, and D.Bruce (1998) Non-photochemical quenching of chlorophyll fluorescence in photosynthesis. 5-hydroxy-1,4-naphthoquinone in spinach thylakoids as a model for antenna based quenching mechanisms. *Biochimica et Biophysica Acta* 1363:147-156.

Verhoeven,A.S., B.Demmig-Adams, and W.W.Adams (1997) Enhanced employment of the xanthophyll cycle and thermal energy dissipation in spinach exposed to high light and N stress. *Plant Physiology* 113:817-824.

Vernotte,C., A.L.Etienne, and J.-M.Briantais (1979) *Biochimica et Biophysica Acta* 545:519-527.

Wraight,C., G.Kraan, and N.Gerrits (1972) The pH dependence of delayed and prompt fluorescence in uncoupled chloroplasts. *Biochimica et Biophysica Acta* 283:259-267.

Wagner,B., R.Goss, M.Richter, A.Wild, and A.R.Holzwarth (1996) Picosecond time-resolved study on the nature of high-energy-state quenching in isolated pea thylakoids. Different localization of zeaxanthin dependent and independent quenching mechanisms. *Journal of Photochemistry and Photobiology B:Biology* 36:339-350.

Walters,R.G. and P.Horton (1993) Theoretical assessment of alternative mechanisms for non-photochemical quenching of PSII fluorescence in barley leaves. *Photosynthesis Research* 36:119-139.

Walters,R., A.Ruban, and P.Horton (1994) Higher plant light-harvesting complexes LHCIIa and LHCIIb are bound by DCCD during inhibition of energy dissipation. *European Journal of Biochemistry* 226:1063-1069.

Wasielewski,M.R., D.G.Johnson, M.Seibert, and Govindjee (1989) *Proceedings of the National Academy of Sciences, USA* 86:524-528.

Weis,E. and J.Berry (1987) Quantum efficiency of PSII in relation to energy dependent quenching of chlorophyll fluorescence. *Biochimica et Biophysica Acta* 283:259-267.

Whitmarsh,J. and D.Ort (1984) *Arch. Biochemistry and Biophysics* 231:3378-3389.

Yamamoto,H. and N.Mohanty (1995) Mechanism of non-photochemical chlorophyll fluorescence quenching. I. The role of de-epoxidised xanthophylls and sequestered thylakoid membrane protons as probed by dibucaine. *Australian Journal of Plant Physiology* 22:231-238.

Young,A.J. and H.A.Frank (1996) Energy transfer reactions involving carotenoids: quenching of chlorophyll fluorescence. *Journal of Photochemistry and Photobiology B:Biology* 36:3-15.

Young,A.J., D.Phillips, A.V.Ruban, P.Horton, and H.A.Frank (1997) The xanthophyll cycle and carotenoid-mediated dissipation of excess excitation energy in photosynthesis. *Pure and Applied Chemistry* 69:2125-2130.

Ziegler,R. and K. Egle (1965) *Beitr. Biol. Pflanzen.* 41:11-37.

Zubay,G. 1993. *Biochemistry, Volume Two: Catabolism and Biosynthesis.* 3rd edition. Wm. C. Brown Publishers, Dubuque, IA.